AD-756 076

LONGITUDINAL VIBRATIONS OF ROCKETS WITH LIQUID FUEL ENGINES

K. S. Kolesnikov

Foreign Technology Division
Wright-Patterson Air Force Base, Ohio

4 January 1972

FTD-HC-23-1198-72

FOREIGN TECHNOLOGY DIVISION

LONGITUDINAL VIBRATIONS OF ROCKETS WITH LIQUID FUEL ENGINES

by

K. S. Kolesnikov

377

UNCLASSIFIED

Security Classification

DOCUMENT CONTROL DATA - R & D

(Security classification of title, body of abstract and indexing annotation must be entered when the overall report is classified)

1. ORIGINATING ACTIVITY (Corporate author) Foreign Technology Division Air Force Systems Command U. S. Air Force	2a. REPORT SECURITY CLASSIFICATION UNCLASSIFIED 2b. GROUP

3. REPORT TITLE

LONGITUDINAL VIBRATIONS OF ROCKETS WITH LIQUID FUEL ENGINES

4. DESCRIPTIVE NOTES (Type of report and inclusive dates)

Translation

5. AUTHOR(S) (First name, middle initial, last name)

K. S. Kolesnikov

6. REPORT DATE 1971	7a. TOTAL NO. OF PAGES 318	7b. NO. OF REFS 106
8a. CONTRACT OR GRANT NO. b. PROJECT NO. 782 c. d.	9a. ORIGINATOR'S REPORT NUMBER(S) FTD-HC-23-1198-72 9b. OTHER REPORT NO(S) (Any other numbers that may be assigned this report)	

10. DISTRIBUTION STATEMENT

Approved for public release; distribution unlimited.

11. SUPPLEMENTARY NOTES report	12. SPONSORING MILITARY ACTIVITY Foreign Technology Division Wright-Patterson AFB, Ohio

13. ABSTRACT

In the book, vibrations in the powered-flight phase of a liquid fuel rocket are examined as a closed mechanical-hydraulic system consisting of the elastic body of the rocket with liquid fuel in tanks, fuel lines, and liquid rocket engine. The dynamic characteristics of each of these elements of the system are examined. Methods of calculating the form and frequencies of inherent longitudinal vibrations of the body of the rocket are presented, taking into account the axi symmetrical vibrations of the elastic fuel tanks. The dynamic characteristics of the fuel lines are determined with a consideration of the local resistances and elastic properties of the turbo-drives and bellows, taking into account the compressibility and cavitation of the liquid fuel entering the centrifugal pumps. The low-frequency dynamic characteristics of the liquid propellant rocket engine are determined with closed and open feeding system. In the calculations, the combustion chamber of the engine, the turboprop unit, the supply lines, and the regulator are considered as elements of the system with lumped parameters. The amplitude-phase frequency characteristics of the rocket body, the fuel lines, and the engine are presented. On the basis of an analysis of the dynamic characteristics, methods are presented for evaluating and insuring the stability of the rocket in flight relative to the lingitudinal elastic vibrations.

DD FORM 1 NOV 1473

UNCLASSIFIED

Security Classification

14. KEY WORDS	LINK A		LINK B		LINK C	
	ROLE	WT	ROLE	WT	ROLE	WT
Liquid Rocket Fuel Liquid Rocket Engine Test Rocket Engine Fuel Tank Vibration Test						

ic

EDITED TRANSLATION

FTD-HC-23-1198-72

LONGITUDINAL VIBRATIONS OF ROCKETS WITH LIQUID FUEL ENGINES

By: K. S. Kolesnikov

English pages: 318

Source: Prodol'nyye Kolebaniya Rakety S Zhidkostnym Raketnym Dvigatelem, 1971, pp. 1-260.

Translated Under: F33657-72-D-0854

Requester: FTD/PDSL

TABLE OF CONTENTS

In the book, vibrations in the powered-flight phase of a liquid fuel rocket are examined as a closed mechanical-hydraulic system consisting of the elastic body of the rocket with liquid fuel in tanks, fuel lines, and liquid rocket engine. The dynamic characteristics of each of these elements of the system are examined.

Methods of calculating the form and frequencies of inherent longitudinal vibrations of the body of the rocket are presented, taking into account the axi symmetrical vibrations of the elastic fuel tanks. The dynamic characteristics of the fuel lines are determined with a consideration of the local resistances and elastic properties of the turbo-drives and bellows, taking into account the compressibility and cavitation of the liquid fuel entering the centrifugal pumps.

The low-frequency dynamic characteristics of the liquid propellant rocket engine are determined with closed and open feeding system. In the calculations, the combustion chamber of the engine, the turboprop unit, the supply lines, and the regulator are considered as elements of the system with lumped parameters.

The amplitude-phase frequency characteristics of the rocket body, the fuel lines, and the engine are presented. On the basis of an analysis of the dynamic characteristics, methods are presented for evaluating and insuring the stability of the rocket in flight relative to the longitudinal elastic vibrations.

The book is intended for scientific workers and engineers in the rocket construction industry, but may also be useful to teachers, graduate students, and students of higher technical education institutions.

Six tables, 136 illustrations, 104 bibliographic references.

Reviewed by M. S. Galking, candidate of physical and mathematical sciences.
Edited by A. F. Minayev, candidate for technical sciences.

PREFACE

The longitudinal elastic vibrations (expansion-compression vibrations) of a rocket as a closed mechanical-hydraulic system, consisting of an elastic body with liquid fuel in the tanks, the fuel lines, and in the liquid rocket engine, are low-frequency (50 Hz) vibrations. The stability of such a system is generally taken to designate the stability of a rocket with a liquid fuel engine relative to longitudinal elastic vibrations.

Recently, a great deal of attention has been devoted to the study of longitudinal elastic vibrations in rockets with liquid fuel rocket engines in flight. Such vibrations in the case of instability may lead to large amplitudes and cause destruction of the rocket.

The generalized results presented in the book of research in the indicated area may be useful both for mechanical engineers who are engaged in the development of rocket design and should, in planning, consider the influence of construction of parameters and dynamic properties of the rocket upon the stability of the closed system, as well as for specialists working in the area of creating liquid fuel rocket engines and regulating systems.

In the calculations of the form and frequencies of the intrinsic vibrations of the rocket body, the vibrations of the liquid fuel in the elastic tanks is simulated by the vibrations of mechanical oscillators. The cavitation characteristics of the pumps, exerting great influence upon the dynamic properties of the fuel lines, are simulated by the dynamic characteristics of a certain determined volume of a steam-gas mixture entering the pump.

In the derivation of the dynamic equations it is assumed that the system is linear in relation to small perturbations in the steady-state area (unperturbed) of the work regime. Structural block diagrams of all dynamic systems and of their separate parts are constructed, taking into account the connections between the separate physical elements of the system.

The book is a logical extension of the book 'Zhidkostnaya raketa kak ob'yekt regulirovaniya,' published by the 'Mashinostroyeniye' publishing house in 1969. In both books, the liquid fuel rocket is considered as a closed oscillation system taking into account both transfers and longitudinal elastic vibrations of the body as well as vibrations of the liquid fuel in the tanks and in the fuel lines.

The author expresses deep appreciation to A. E. Osherov , A. F. MinayeV , M. S. Balkin , and A. A. Pozhalostin for critical comments and advice, significantly improving the content of the book.

The author will be grateful to readers extending their critical comments and desires to the address: Moscow, B-66, 1-y Basmannyy per., 3, izdatel'stvo 'Mashinostroyeniye.'

Chapter 1

LONGITUDINAL VIBRATIONS OF ROCKETS WITH LIQUID PROPELLANT ROCKET ENGINES

1. The Perturbation Mechanism of Longitudinal Self-Oscillations of a Rocket with a Liquid Fuel Engine

Low-frequency vibrations in a direction of the longitudinal axis of the rocket (longitudinal vibrations) arise as a result of the interaction between the elastic construction of the rocket body, the liquid fuel, and the engine. The body of the rocket, the fuel lines, and the liquid fuel rocket engine are the three principal component parts of the closed oscillation system which is schematically shown in Fig. 1.1. Using this diagram, it is possible to explain the perturbation mechanism of the low-frequency longitudinal vibrations of the rocket.

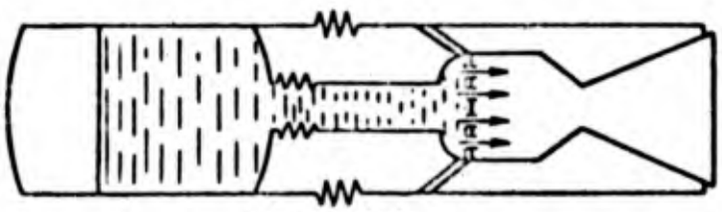

Figure 1.1

Let us assume that thrust perturbation forces have arisen in the rocket. These perturbations produce longitudinal vibrations in the body of the rocket, as a result of which fuel pressure oscillations arise in the fuel lines. The pressure oscillations, in turn, change the fuel supply in the combustion chamber, and, consequently, are the reason for the change in thrust. Changes in the thrust intensify the vibrations of the body and the fuel pressure oscillations in the fuel lines, and thus the original perturbations may be intensified according to the amplitude of vibration.

The dynamic processes of a real vibrational system of a rocket with a liquid fuel engine are described by nonlinear differential equations, of which the most complicated are differential equations describing the dynamic processes in the centrifugal pump and in the combustion chamber of the engine.

Also nonlinear are the dependence of pressure in the bottom of the tank upon the amplitude of the vibrations in the bottom, the forces of hydraulic resistance upon the speed of liquid flow, and the speed of fuel supply in the chamber upon the pressure transfer in the injectors.

With an increase in the amplitude of vibrations, the nonlinear properties of the system become more noticeable, and the increasing vibrations become generally a stationary self-oscillating process.

Self-oscillating systems differ from other vibrational systems principally in that stationary vibrations in them may take place in the absence of external periodic action. In each self-oscillating system, three elements may be distinguished--the vibration system, the energy source, and the feedback, through the oscillating system acts upon the energy source (Fig. 1.2).

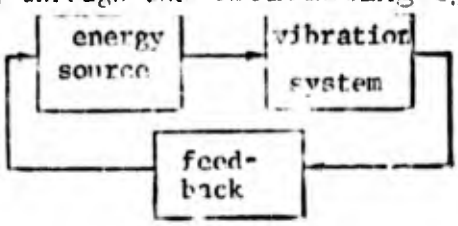

Figure 1.2

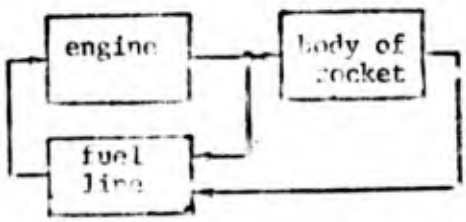

Figure 1.3

Auto-oscillations are self-influencing vibrations. In some systems the energy of perturbation should be not less than a determined quantity. Self-oscillations characterize nonlinear systems. The possibility of self-perturbation arising may in certain cases be determined with linearized equations describing the oscillations of the system.

Concerning longitudinal vibrations, a rocket with a liquid fuel engine is a typical self-oscillating system. We shall present a rocket with a one-component liquid fuel engine, a simplified block diagram of which is shown in Fig. 1.3. The vibrational system is the body of the rocket, the feedback is the fuel line, and the liquid fuel rocket serves as the energy source. Besides the external feedback between the body and the engine, which closes the system, there is an internal feedback between the engine and the fuel line. This feedback is accomplished by means of the influence of pressure

in the combustion chamber upon the velocity of fuel supply from the fuel lines through the injector.

The self-oscillations in the closed system, shown in Fig. 1.3, are generally called longitudinal self-oscillations of the rocket.

Vibrations in the fuel supply in the combustion chamber take place with the same freqeuncy with which the longitudinal vibrations of the body and the fuel in the turbo-drive take place; the thrust of the engine changes with the same frequency. In the self-oscillation process, all the members of the closed system vibrate with a frequency which is called the 'self-oscillation frequency.'

With such a powerful energy source as a liquid fuel rocket engine, self-oscillations may lead to large dynamic loads arising in the structure of the rocket housing which may cause damage to equipment and apparatus. It is also possible that damage to the rocket's structure may take place even before the self-oscillation process becomes stationary.

Longitudinal self-oscillations of rockets with liquid fuel engines do not always arise. Everything depends upon the properties of the oscillation system determined relative to its parameters. By a corresponding change of these parameters, the nominal work regime of the system may be made stable, and random occurring vibrations may be damped. A rocket with a liquid fuel engine should have just such properties.

Longitudinal vibrations should be considered as a potential problem inherent to rockets with liquid fuel.

2. Self-Oscillations of Separate Closed Systems of the Rocket

Besides the examined self-oscillation system there are in a liquid fuel rocket separate closed systems in which self-oscillations may arise. For example, the system of supplying the engine from a centrifugal pump is related

to such systems. During the operation of the pump cavitation (the formation of a vapor-gas mixture) may arise in its intake part, which causes a change in the velocity of the flow of the liquid in the fuel line, and a change in the pressure of the liquid in leaving the fuel line exerts an influence on the formation of the vapor-gas mixture; thus a closed system is formed in which the perturbation of self-oscillations is possible.

The fuel line, together with the combustion chamber of the engine, also forms a closed system in which self-oscillations are possible (see Fig. 1.3). It is formed by the engine, the internal feedback, and the feed line itself which in this scheme is the oscillating member.

The fuel tank with the fuel, together with the gas supercharge system, forms a closed oscillating system if between the tank and the supercharge system there is feedback. When longitudinal oscillations arise in the tank with the liquid, the volume of the gas cushion over the liquid and the pressure in it are changed. The regulator of the pressure may receive a signal from this pressure change and influence the supercharging system. In this closed system, self-oscillations may also arise.

In examining longitudinal oscillations of the body of the rocket together with the liquid fuel engine and the fuel lines, it is assumed that the body of the rocket performs expansion-compression longitudinal oscillations. But simultaneously with longitudinal vibrations, bending vibrations of the body may also arise. In bending oscillations, the thrust vector will be deflected by a certain angle, as also the tail section of the body, as a consequence of which the component of thrust in the direction of the non-perturbed longitudinal axis of the rocket will experience small perturbations with a frequency two times greater than the frequency of the bending vibrations of the body. If in this the characteristic frequency of the longitudinal oscillations of the body are twice as great as the frequency of the bending vibrations, then favorable conditions are created for the perturbation of simultaneous longitudinal-transverse oscillations of the rocket. A consideration of oscillations of this nature are beyond the scope of this book.

If the engine and its fuel line are not arranged in the axis of the rocket, then during the bending vibrations of the body, the fuel lines of one engine will be lengthened, and the fuel lines of the other engine will be shortened. A change in the length of the fuel lines causes a change in the fuel supply to the combustion chamber and a change in the pressure of this chamber. In this manner is accomplished the interaction of the bending vibrations of the body with the oscillations of the fuel in the fuel lines and with the change of the quantity of thrust of the engine. In this closed scheme self-oscillations are also possible.

3. A Closed Oscillating System

Let us examine an oscillating system consisting of three basic parts: the rocket body, the liquid fuel engine, and the fuel lines. Omitting several details, it may be considered that both the body and the fuel lines are mechanical-hydraulic oscillating systems. The body of the rocket is an elastic axisymmetrical structure of elongated shape. Longitudinal oscillations of the rocket are characterized first of all by the expansion-compression oscillations of the body. The liquid fuel in the tanks also takes part in these oscillations. Because the vibrations of the body and the fuel in the tanks are simultaneous and the weight of the fuel is usually many times greater than the weight of the body, the liquid in the tanks and the body are generally combined into one oscillating system in the study of low-frequency oscillations.

The weight of the liquid fuel is transmitted to the body through the elastic bottom of the tank; therefore the liquid, relative to the walls of the body, may be considered as if it were suspended on a spring. The liquid moves relative to the walls of the body in an axial direction not only due to the stretching of the bottom of the tank, but also due to the change in the diameter of the shell of the tank, caused by the hydraulic pressure. The elastic shell of the tank together with the liquid forms an independent oscillating system which may be separated from the overall oscillating system.

The engine is attached to the body with the aid of a frame, and in the first approximation for a calculation of the shape and frequency of the

characteristic vibrations, included in the mechanical oscillating system of the body as an elastic suspended mass. Special significance is attached to the motion of the bottom of the tank and the engine relative to the body of the rocket in the examined longitudinal vibrations, because upon the vibrations of the bottom of the tank and the engine depends the change of pressure of the liquid in the fuel line, and consequently the influence of the force on the longitudinal vibrations of the body.

The overall parameters of the body are the shape and the frequency of the characteristic vibrations. A calculation of the form and frequencies of the characteristic vibrations of the body, taking into the account the peculiarity of its construction, constitutes one of the major problems in the study of longitudinal rocket vibrations. Since the mass of the rocket decreases according to the degree of fuel combustion, from which the frequencies increase and the shape of the characteristic vibrations change, the calculation of the shape and frequencies should be conducted for variously filled levels of the fuel tanks.

The thin-walled shell of the rocket body has a series of stringers and formers. Methods for calculating the longitudinal vibrations of the body for the case where the length of the wave of the oscillations is many times greater than its radius, are sufficiently developed. The forms and frequencies of the inherent vibrations of the body may be sufficiently exactly calculated in a digital computer, and in this regard the rocket body is the simplest member of a closed vibrational system.

We shall consider the fuel supply system from the tanks into the combustion chamber of the two-component liquid fuel rocket engine to consist of two fuel lines--the fuel line and the oxidant line. The section of the line along which the fuel is delivered from the tank to the pump is called the low-pressure line (turbo-drive), or the discharge line. The section of the line from the pump to the combustion chamber is called the high-pressure line (turbo-drive), or the delivery line. The low-pressure line generally consists of comparatively long rectilinear sections of low rigidity. The high-pressure line consists of shorter and more rigid sections than the low-pressure line. Between the

low- and high-pressure lines are the centrifugal pumps. The fuel pump and the oxidant pump together with the turbine which mixes them are combined into one turbo-pump unit. Arising in the suction part of the pump, local cavitation cavities may appear even when the pressure before the intake in the pump satisfies the condition of non-cavitational pump operation. As a consequence of cavitation in the suction part of the pump, vapor-gas volumes are formed which make a more pliable liquid head in the low-pressure line and, consequently, reduce the frequency of the inherent liquid vibration. The influence of cavitation in the pump upon the frequency of the characteristic vibrations of the liquid in the fuel line is generally determined experimentally.

The fuel line forms an independent mechanical-hydraulic oscillating system, the analysis of which may be conducted separately. A change in the pressure of the fuel in the fuel line causes vibrations in the bottom of the tank, motion of the engine, and of the turbo-pump unit relative to the flow of the liquid by the oscillating pressure in the combustion chamber. For a study of the dynamic characteristics of the high-pressure line, it is convenient to combine them into one member with the engine. The pumps of both lines are generally mounted on one shaft and driven by the revolutions of the turbine. The interconnections between the lines may vary as a function of the means of supplying the gases from the liquid-gas generator.

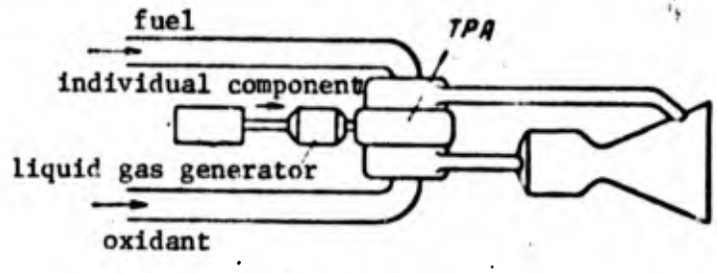

Figure 1.4

In Fig. 1.4 a diagram is shown of the supply of the fuel components in a liquid fuel engine and the individual components in the liquid-gas generator. Perturbations of the dynamic parameters of the fuel flow in one of the lines feeding the liquid fuel rocket engine causes a change in the dynamic parameters in the flow of the other line as a consequence of the change in the load transferred from the pumps in the shaft of the turbopump unit. In Fig. 1.5 a diagram is presented of the supply of the liquid fuel rocket engine with both of

the basic components of the fuel delivered in the liquid-gas generator. In this case the perturbations of the dynamic parameters of the flow in any line cause not only a change in the moment of resistance in the shaft of the turbopump unit, but also a change in the supply of the component to the liquid-gas generator, i.e., a change in the quantity of generated gas and, consequently, a change in the speed of revolution and torque in the shaft of the turbine.

From the point of view of dynamic processes, the most complex part of the closed system is the liquid fuel rocket engine. In its combustion chamber and nozzle, chemical, thermal, gas dynamic, and vibrational processes take place. However, it will be shown later that for an analysis of longitudinal self-oscillations, the frequencies of which do not exceed 100 Hz, the dynamic processes in the engine sometimes may be presented in the form of a comparatively simple model.

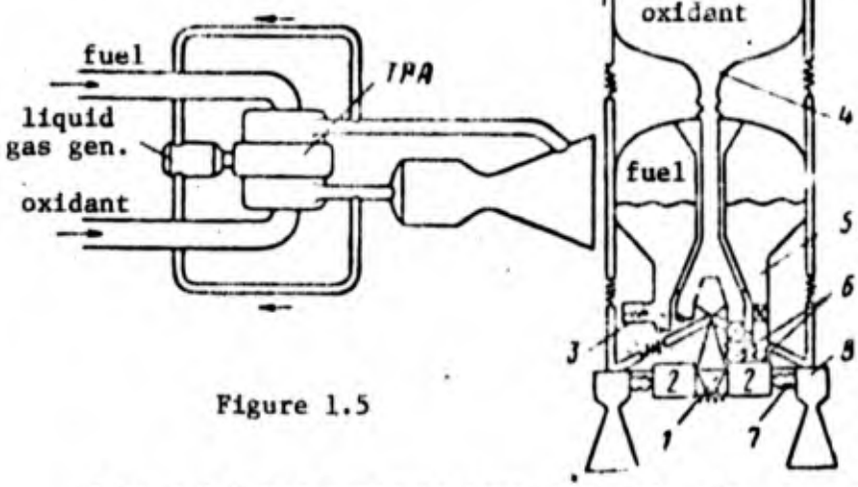

Figure 1.5

Figure 1.6

Figure 1.6 was borrowed from work [3]. It presents a dynamic scheme of the first stage of the American payload rocket Titan-2. In the diagram are shown the elastic body with two tanks, the supply system, and the engine. Here 1) is the joining connection of the turboprop unit, 2) are the fuel supply pumps, 4) and 5) are the initial part of the discharge line of the oxidant and the fuel, 6) is the outlet section of the discharge line, 7) is the fuel line, 8) is the liquid fuel rocket engine. In order to reduce the frequencies of the characteristic vibrations of the liquid in the fuel line and insure the stability of the supply system, hydraulic dampers are mounted in the fuel line.

Such a damper, 3), schematically shown in the discharge line of the fuel, is the oscillating member which changes the dynamic characteristics of the fuel lines. It is noted in [3] that with the aid of these dampers it was possible to eliminate longitudinal self-oscillations of the Titan-2.

4. A Simplified Mathematical Model

Let us examine a simplified mathematical model of a liquid fuel rocket with a one-component liquid fuel rocket engine. We shall write equations of motion for the divergence perturbation of the variable quantities from their values in the steady-state regime. Under the steady-state regime we shall understand the flight of the rocket without oscillations according to a rectilinear (or nearly rectilinear) trajectory. In small time intervals which are significantly greater than the examined periods of the characteristic longitudinal oscillations of the rocket, the fuel supply into the combustion chamber, the thrust of the engine, and the acceleration of all elements of the structure of the rocket in the standard regime are taken to be constant.

A calculation of the parameters of the system, the conclusion, and the analysis of the equations, a mathematical description of the interaction of the individual elements of the oscillating system, and an analysis of the properties of the closed dynamic system are basic problems of the present book. In section 4 a simplified equation is presented for the perturbed motion of the basic members of the examined system, in order to show the dynamic scheme of a rocket with a liquid fuel engine for the study of longitudinal vibrations.

The dynamic interaction of the oscillations of the liquid with the elastic shell of the fuel tank and the elastically suspended engine from the body of the rocket is taken into account in a calculation of the form and frequencies of the characteristic oscillations of the rocket body. As a result of this equation the forms $f_n(x)$ are determined and the frequencies ω_n of the characteristic oscillations of the rocket structure together with the liquid fuel in the tanks.

The body of the rocket vibrates longitudinally as a consequence of the divergence* of the thrust of the engine P(t) from the standard quantity and the divergence of the force $P_{1n}(t)$, caused by a divergence of the pressure of the liquid in the discharge line in the intake into the pump. If the shape $f_n(x)$ of the characteristic oscillations of the body of the n-th tone is known, then the equation of oscillations for the generalized coordinate $q_n(t)$ has the same structure as the equation of oscillation of a mechanical system with one degree of freedom.

We shall consider to be positive the motion of the body in the direction from the tip through the tail of the rocket. Then the reduced force acting upon the rocket body is equal to $(P_{1n}(t)f_{np} - P(t)f_{ne})$, where f_{np} is the coefficient of the shape of the elastic vibrations of the pump; f_{ne} is the coefficient of the shape of the elastic vibrations of the engine.

The equation of the forced oscillations for the generalized coordinate $q_n(t)$ will have the form

$$\ddot{q}_n + 2\xi_n\omega_n\dot{q}_n + \omega_n^2 q_n = \frac{1}{m_n}(P_{1n}(t)f_{np} - P(t)f_{ne}). \qquad (1.1)$$

Here m_n is the reduced mass of the rocket; ξ_n is the relative coefficient of damping of the characteristic oscillations; ω_n is the frequency of the characteristic oscillations.

The deflection of the pressure p_b of the liquid in the bottom of the tank (as the liquid goes out of the tank into the discharge line) may be assumed to be proportional to the acceleration of the bottom of the tank:

$$p_b = \rho_0 H \varkappa f_{nb} q_n, \qquad (1.2)$$

where ρ_0 is the density of the liquid;

H is the height of the liquid head in the tank;

*Here and later, small perturbations (increments) of forces and parameters of motion shall be called divergences from their respective standard values, not assigning them the usual symbols Δ or δ.

f_{nb} is the coefficient of the form of elastic vibrations of the bottom of the tank;

κ is a certain coefficient depending upon the relationship of the diameters of the tank and the discharge line and the shape of the bottom.

The relation between the divergence of the pressure p_b upon the discharge from the tank and the divergence of the pressure p_{1p} in the inlet of the pump, without taking into account the compressibility of the liquid and the elasticity of the walls of the discharge lines, is determined by the equation

$$p_{1p}(t) = p_b - \rho_0 l v_1(t) \tag{1.3}$$

where l is the length of the discharge line;

$v_1(t)$ is the acceleration of the liquid in the discharge line.

We shall evaluate the volume of the vapor-gas mixture in the liquid in the suction part of the pump using a linearized law for an ideal gas. Denoting the divergence of this volume as V_p and the elastic constant of k^*_{vg}, we shall have

$$V_p = -k^*_{vg} p_{1p}.$$

The divergence of the velocity of the liquid in being discharged from the discharge line, designated by the change of the volume of the vapor-gas mixture is:

$$v_{vg} = \frac{1}{F_T}\frac{dV_{vg}}{dt} = k_{vg}\dot{p}_{1n}\left(k_{vg} = \frac{k^*_{vg}}{F_T}\right). \tag{1.4}$$

Here F_T is the area of a section of passage of the turbodrive to the pump.

If we neglect the change in the speed of rotation of the shaft of the pump, then the divergence of the pressure p_{2p} in the discharge from the pump will be determined by the formula

$$p_{2p}(t) = \left(1 + \frac{\partial \hat{H}}{\partial p}\right) p_{1p}(t) + \left(\frac{\partial H_p}{\partial v}\right) v_p(t), \tag{1.5}$$

where H_p is the head of the liquid in the discharge from the tank;

$v_p(t)$ is the divergence of the velocity of the liquid going through the pump.

The values of the partial derivative in equation (1.5) may be obtained from an examination of the discharge and delivery characteristics of the pump. These values will be equal to the tangent of the angle of inclination of the tangents to the indicated characteristics in the working point.

Taking into account only the inertia of the head of the liquid and the hydraulic resistance including the resistance of the nozzles, the equation of motion of the liquid along the delivery line may take the form

$$\varrho_0 l \dot{v}_к(t) - \xi_\Phi v_к^* \varrho_0 v_к(t) = p_{2p}(t) - p_к(t), \tag{1.6}$$

where $v_c(t)$ is the divergence of the velocity of the fuel entering the combustion chamber of the engine ($v_c = v_p$);

$p_c(t)$ is the divergence of the pressure in the combusion chamber;

$\xi\Phi$ is the coefficient of resistance of the delivery line and the nozzle head;

v_c^* is the velocity of the fuel entering the combustion chamber in the standard stationary regime.

We may determine the divergence of the velocity of the liquid $v_1(t)$ in the discharge line from the equation of discontinuity of the flow through the vapor-gas mixture

$$v_1(t) = v_p(t) + v_{vg}(t) + f_{np}\dot{q}_n(t), \tag{1.7}$$

where $f_{np}\dot{q}_n(t)$ is the divergence of the velocity of the flow of the liquid in the turbodrive, caused by the oscillations of the pump.

For low frequencies and small perturbations the equation for determining the divergence of the pressure $p_c(t)$ in the combustion chamber of a single-component liquid fuel rocket engine with an open delivery system may take the form [2]

$$\eta_к \frac{dp_к(t)}{dt} + p_к(t) = kF_т\varrho_0 v_к(t). \tag{1.8}$$

Here θ_c is the relaxation time in the chamber; k is a proportionality constant between the divergence of the per-second entry of the mass of the fuel into the chamber and the divergence of the pressure.

If the liquid fuel rocket engine has a closed supply system, then in studying longitudinal self-oscillations of a turbopump unit, the liquid gas generator, the delivery line, and the combustion chamber are generally combined into one member (the engine), the dynamic properties of which may be expressed by one characteristic.

The divergence of the force P is proportional to F_T, the ratio between the divergence of the pressure $p_c(t)$ in the combustion chamber and the divergence of the thrust P(t) of the engine may be expressed by the coefficient k_T. Then we have

$$P(t) = k_T p_k^*(t),$$
$$P_{1\beta}(t) = F_T p_{1\beta}(t). \qquad (1.9)$$

Equations (1.1)-(1.9) express a simplified mathematical model of the oscillating system.

A block diagram showing the interaction between the different members of the model of a rocket with a liquid fuel engine with a two-component fuel is shown in Fig. 1.7. Here, 1) is the rocket body; 2) is the discharge line; 3) is the pump; 4) is the fuel supply line; 7), 8), and 9) are the oxidant supply lines; 5) is the combustion chamber; 6) is the thrust coefficient [the broken lines show the additional elements of the system not taken into account in equations (1.1)-(1.9)]; 10) is the liquid-gas generator; 11) is the turbine for driving the pump. The connection between the liquid-gas generator and the turbines with the lines are the same as they are for the liquid-gas generator, operating on the basic components (see Fig. 1.5). Through the liquid-gas generator and the turbine, the fuel line interacts with the oxidant line which significantly complicates the dynamic scheme.

From an analysis of the linearized equations (1.1)-(1.9) inferences may be drawn only on the stability of the system, i.e., to establish whether the

randomly arising small oscillations will die out. The amplitudes and frequencies of the self-oscillations may be determined only from nonlinear equations. Nevertheless, an analysis of the linearized equation may produce sufficiently complete information on the influence of various parameters and their combinations upon the stability of the system. Equations (1.1)-(1.9) do not take into account the wave vibrations of the liquid in the fuel lines and the elasticity of the walls of these lines. Meanwhile, if the fuel lines have a significant length and possess sufficient elasticity, then the frequency of the characteristic oscillations of the liquid in them may be communserate with the frequency of the characteristic oscillations of the rocket body. Not only the perturbations of the pressure of the liquid going out of the tank and into the combustion chamber are the sources of perturbation of the oscillations of the liquid in the fuel lines, but also the motion of the pump and the combustion chamber relative to the flow of the liquid due to the oscillations of the rocket body itself. These and other factors complicating the mathematical model will be examined later.

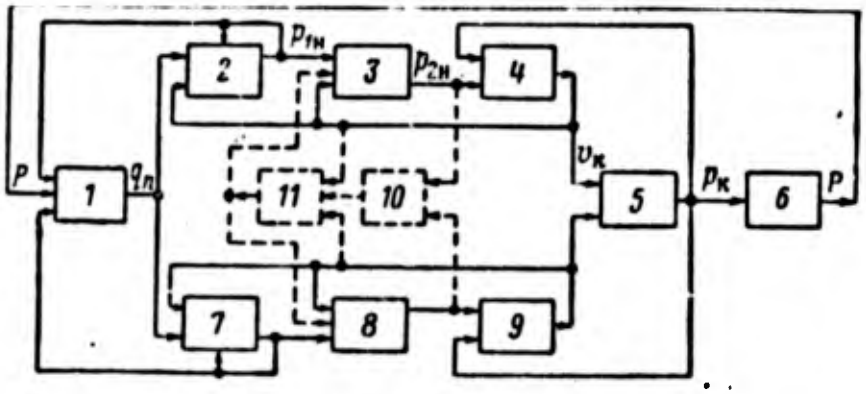

Figure 1.7

5. Methods of Analyzing the Dynamic Properties of the System

For the analysis of the dynamic properties of the system and its individual members, frequency methods of the theory of automatic regulation are widely used. Later, we shall use the Nyquist frequency criterion of stability, the concepts of a complex transmission number and amplitude-phase frequency characteristics. We shall derive their brief determination.

Let the equation of the first oscillations of the generalized coordinates y(t) have the form

$$\ddot{y}(t)+2\varepsilon\dot{y}(t)+\omega_0^2 y(t)=q(t), \tag{1.10}$$

where q(t) is the external influence;

ω_0, ε are the frequency and the damping coefficients, respectively, of the characteristic vibrations.

The quantities y(t) and q(t) are generally called the output and input coordinates of the system (element).

For $q(t) = q_0 e^{i\omega t}$, a partial solution of equation (1.10) may assume the form

$$y(t)=ye^{i\omega t}, \quad y=Kq_0, \quad K=\frac{1}{\omega_0^2-\omega^2+2i\varepsilon\omega}.$$

The number K, expressing the relation of the steady-state harmonic oscillations of the linear system in the output to the harmonic action in the input, is called the complex transmission number. Because in the system there may be certain members with varying input and output coordinates, then for differences in their complex transmission numbers, square brackets designating coordinates are attached to these numbers. For example, $K[y, q_0]$ designates that the coordinate y is the output coordinate (the first letter in the square brackets), and q_0 is the input coordinate (second letter).

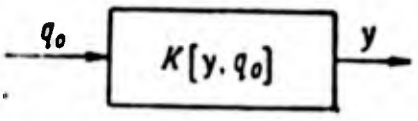

Figure 1.8

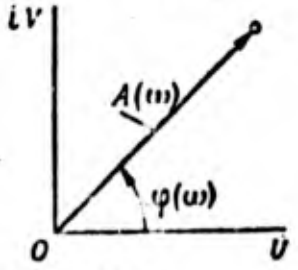

Figure 1.9

If the complex dynamic system may be separated into such elements, each of which is a member with one input and one output, then the interaction of the members of the system may be represented by the structural block diagram. Let us suppose that between the input and output member there exists a linear relation. Then for harmonic oscillations the output coordinate y is equal to a complex transmission number multiplied by the input coordinate q_0 (Fig. 1.8):

$$y = K[y, q_0]q_0.$$

In the plane of the complex transmission number $K[y, q_0]$ is the vector (Fig. 1.9)

$$K[y, q_0] = U(\omega) + iV(\omega) = A(\omega)e^{i\varphi(\omega)},$$

where

$$A(\omega) = \sqrt{U^2(\omega) + V^2(\omega)}, \quad \operatorname{tg}\varphi(\omega) = \frac{V(\omega)}{U(\omega)}.$$

In our example

$$U(\omega) = \frac{\omega_0^2 - \omega^2}{(\omega_0^2 - \omega^2)^2 + 4\varepsilon^2\omega^2}, \quad V(\omega) = \frac{-2\varepsilon\omega}{(\omega_0^2 - \omega^2)^2 + 4\varepsilon^2\omega^2}.$$

The modulus of the vector $A(\omega)$, equal to the model of the complex transmission number shows how many times greater is the amplitude of the forced harmonic oscillations of the output coordinate than the amplitude of the input coordinate.

The argument $\varphi(\omega)$ of the complex transmission number shows at what phase angle the force oscillation leads or lags (if the sign of $\varphi(\omega)$ is negative) relative to the activating force (the input coordinate). In other words, $\varphi(\omega)$ is the phase shift for the harmonic oscillations between the output and the input coordinate.

The modulus and the argument of the complex transmission number are a function of the frequency of the external influence. Therefore if we construct a hodograph of the vector $K[y, q_0]$ for frequency changes in the interval $0 \leq \omega \leq +\infty$ (Fig. 1.10) then according to the form of the hodograph we may obtain the complete representation of the dynamic properties of the member examined. Knowing the hodograph of the vector we may determine the amplitude and the phase of the forced oscillations in any given frequency of change of the input coordinate.

In the theory of automatic regulation, the hodograph of the vector $K[y, q_0]$ is called also the phase-amplitude frequency characteristic of the number (of the system). The phase-amplitude frequency characteristic is

equivalent to two characteristics: the phase-amplitude characteristic and the phase-frequency characteristic. The phase-amplitude characteristic (Fig. 1.11a) shows the relation of the amplitude of the forced oscillations (more exactly, the ratio of the amplitude of the forced oscillations to the amplitude of the external influence) to the frequency of the external influence. The phase-frequency characteristic (Fig. 1.11b) shows how the phase shift of the forced oscillations depends upon the frequency of the external force.

The complex transmission number of the closed chain of the successively included members of the directed action is equal to the derivative of the complex transmission numbers of the separate members (Fig. 1.12a):

$$K = K_1 K_2 \ldots K_n$$

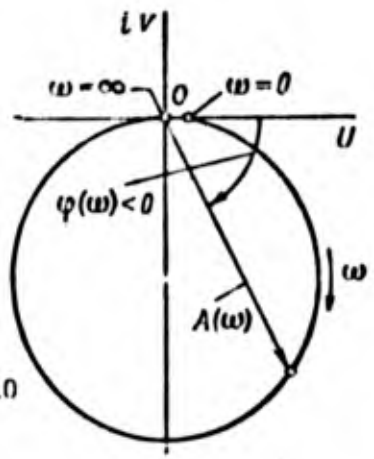

Fig. 1.10

The complex transmission number of the parallely included member of the directed action is equal to the sum of the complex transmission numbers (Fig. 1.12b):

$$K = K_1 + K_2 + \ldots$$

The closed chain shown in Fig. 1.11a corresponds to the closed system depicted in Fig. 1.12c. For a closed chain the output and the input coordinates should be equal to each other, i.e.,

$$y_n = \eta_0$$

The whole system of automatic regulation is closed. The dynamic system of a rocket with a liquid fuel engine, which we have examined, is also closed.

Conclusions on the stability of the motion of the closed system may be made if the values of the roots of its characteristic equation are known. For an analysis of the stability, sometimes on the complex surface, the trajectories are examined by which the points move forming the roots of the closed system during the change of any parameter of the system. The roots on the left of the

half-plane characterize the stability of the motion of the system, the roots on the right of the half-plane characterize the instability of the motion of the system.

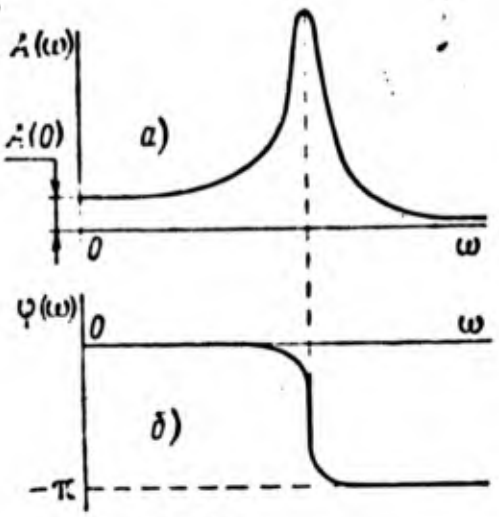

Figure 1.11

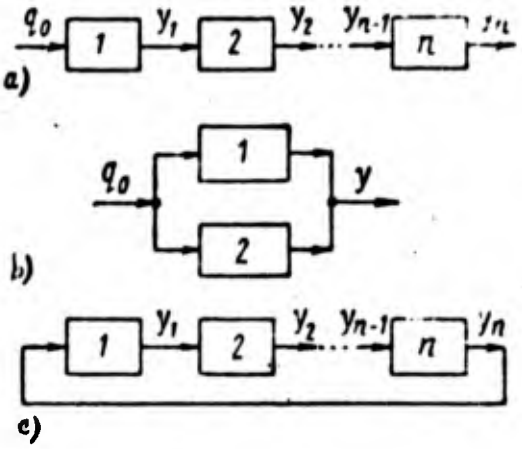

Figure 1.12

A determination of the roots is connected, however, to a large amount of computational work. The laboriousness of calculating the roots of the equation greatly increases with an increase in the degree of this equation. At the present time the calculation of the roots is performed on a digital computer. From the point of view of the expense of machine time, it is unprofitable to determine all the roots of a complex multistream system by means of expanding the characteristic equation into its factors. Instead, the separate roots of interest are obtained by the iteration matrix process.

Conclusions on the stability of the dynamic system may be drawn also without resorting to calculating the roots of its characteristic equation. Stability criteria are used for this. Several stability criteria exist [9]: the Routh-Duvrits algebraic criterion, the Mikhaylov frequency criterion, the Nyquist phase-amplitude criterion, the Vyshnegrad criterion for third-order systems, etc. We shall present without proof the Nyquist phase-amplitude frequency stability criterion, which permits conclusions to be drawn on the stability of a closed system by an outline of the phase-amplitude characteristic of the corresponding closed circuit. Let us assume that the degrees of the characteristic equation of the closed system and the closed circuit are the same.

For the stability of the closed linear automatic system, it is necessary and sufficient that for the motion of the point N along all of the phase-amplitude characteristics corresponding to the closed circuit for $0 \leq \omega \leq +\infty$, the vector CN (Fig. 1.13) turns through an angle $\varphi_{CN} = m_p$ (counterclockwise). Here, m is the number of roots with positive real parts in the characteristic equation of the closed circuit. For example: if m = 0 then the curve 1 confirms the stability of the closed system, and curve 3 confirms the instability. Curve 2 passes through the point C(+1, i0) and the closed system in this case is bordering on stability. The value of ω in this point of the phase-amplitude characteristic also determines the frequency of the oscillations arising in the closed system on the border of stability.

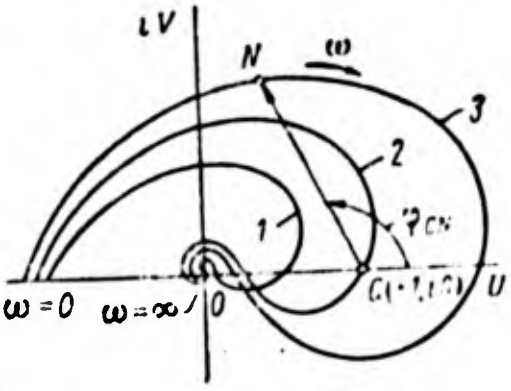

Figure 1.13

The proposition presented may be given a simple physical interpretation. The phase-amplitude frequency characteristic is the ratio of the output coordinate to the input coordinate for stable harmonic oscillations. The phase-amplitude characteristic at the point C(+1, i0) shows that the output is equal to the input, and if the system is closed, then the stable harmonic oscillations in the closed system will be the same as in the closed circuit. If the characteristic intersects the positive semi-axis left of the point C (curve 1), then the amplitude in the output is less than it is in the input. For closed systems this decreased amplitude for repeated oscillations passing in the chain is decreased even more. Consequently in this case the characteristic oscillations in the closed system will always die out. On the other hand, if the characteristic intersects the real semi-axis to the right of the point C (curve 3), then during the passage of a signal in the chain the amplitude of oscillations is increased and, consequently, for a closed system the amplitude of the free oscillations will increase. Such a closed system is unstable. For randomly arising oscillations in the closed system to die out more quickly, it is necessary that the phase-amplitude characteristic of the open circuit to intersect the positive real semi-axis as far left of the point C(+1, i0) as possible.

We note that in the work on the theory of automatic regulation, closing the system by the rule $q_0 = -y_n$ is the most widely used. For this rule, the frequency criteria of stability are formulated relative to the point C(-1, i0), lying on the negative real semi-axis.

For an analysis of the stability of a closed system, the D-partition method may also be used. This method is based on the fact that at the border of stability, the system performs harmonic oscillations. Placing in the characteristic equation of the closed system $D(p) = 0$ and $p = i\omega$, we obtain the relation between the parameters of the system and the frequency of oscillations at the border of stability. In the system of coordinates in which we are interested, we may construct for the parameters (the rest being fixed) a border of stability after which we may determine in what area the parameters examined lie--in the area of stability or in the area of instability.

Real systems and, in particular, the rocket system which we are examining, in the majority of cases have elements of nonlinearity. And for a study of the behavior of such systems for small perturbations, the differential equations describing them are linearized, i.e., members containing second and higher degree divergences of variables and their derivatives are thrown out. Judging to what degree the stability determined by the linearized equation corresponds to the stability of a real system may be obtained from the theorem of A. M. Lyapunov, the essence of which is included later [9].

1. If the characteristic equation of the linearized system has all roots with negative real parts, then the actual system will also be stable.

2. If the characteristic equation of the linearized system has but one root with a positive real part, then the actual system will also be unstable.

3. In the presence of but one zero or purely imaginary root in the characteristic equation of the linearized system, the behavior of the actual system remains undetermined. It depends upon the significance of the discarded nonlinear members.

The dynamic system of a rocket with a liquid fuel engine consists of interacting heterogeneous members. During the oscillation of the system, deviations of pressures, velocities, and acceleration take place in the members relative to the steady-state motion, and the members move relative to each other. An analysis of the dynamic properties of such a system is conducted in the following order.

1. The dynamic system is broken down into the individual members which are comparatively homogeneous according to the processes taking place in them. For each member, differential equations are formulated describing the connections of the deviations of the examined quantities (the differential equations of perturbed motion) with a consideration of the boundary (borderline) conditions arising from the separation of the system into individual members.

2. The equations are solved and an analysis is conducted of the characteristic and forced oscillations of each member individually. The analysis is conducted by the methods of the theory of oscillations and frequency method which have been widely used in the theory of automatic regulation.

3. On the basis of a structural block diagram of the closed system and the boundary conditions taken for the division of the system into its members, the members are 'joined' (unified) and a study is made of the stability of the motion of the whole system. The study is conducted with complex transmission numbers and phase-amplitude frequency characteristics. We shall examine this method of solving the problem in subsequent chapters.

REFERENCES

1. Колесников К. С. Низкочастотная неустойчивость номинального режима жидкостного ракетного двигателя. — ПМТФ, М., «Наука», 1965, № 2.

2. Крокко Л., Чжен Синь-И. Теория неустойчивости в жидкостных ракетных двигателях. М., ИИЛ, 1958.

3. Маккена, Уолкер, Виньи. Совместные колебания двигателя и конструкции ракеты на жидком топливе. — «Вопросы ракетной техники», 1966, № 1.

4. Мокшин Е. К. Динамические процессы в ЖРД. М., «Машиностроение», 1964.

5. Натанзон М. С. Влияние собственной частоты колебаний жидкости в топливоподающем тракте на продольную устойчивость корпуса ракеты. Изв. АН СССР, Энергетика и транспорт, 1969, № 3.

6. Натанзон М. С. Вынужденные разрывные колебания жидкости в трубопроводах. Изв. АН СССР, Механика и машиностроение, 1965, № 2.

7. Натанзон М. С., Сухих В. А. Экспериментальные исследования вынужденных разрывных колебаний жидкости в трубопроводах. Изв. АН СССР. Механика жидкости и газа, 1969, № 1.

8. Пинсон, Монард, Рейни. Исследование продольных колебаний ракеты-носителя «Сатурн-5». — «Вопросы ракетной техники», 1968. № 5.

9. Попов Е. П. Динамика систем автоматического регулирования. М., Гостехиздат, 1954.

10. Роуз. Анализ продольной устойчивости ракет на жидком топливе. — «Вопросы ракетной техники», 1967, № 5.

11. Харкевич А. А. Автоколебания. М., Гостехиздат, 1953.

12. Wick R. S. The Effect of Vehicle Structure on Propulsion System dynamics and Stability. —„Jet. Propulsion", 1956, vol. 24, 26

Chapter 2

AXISYMMETRICAL OSCILLATIONS OF THE TANK WITH THE LIQUID FUEL

1. Statement of the Problem

As has already been noted, the longitudinal vibrations of the rocket body are accompanied by oscillations of the liquid fuel in the tank. During the oscillations, the pressure of the liquid changes as a consequence of which additional deformation of the tank takes place. The cylindrical tank is a thin-walled structure. The structure of the tank is executed in the form of a thin-walled circular cylindrical shell. The bottom of the tank is a thin-walled axisymmetrical shell of revolution usually having the form of a spear segment. The tanks may also be conical, spherical, or take the shape of a torus.

The elastic shell of the tank oscillates together with the liquid, because the liquid and the shell form an oscillating system with an infinite number of degrees of freedom. It is expedient to separate the tank with the liquid from the problem of the longitudinal oscillations of the rocket body, and at first examine its oscillations separately from the oscillations of the body.

We shall consider the liquid to be ideal and incompressible. Under the concept of an ideal liquid we understand such a deformable continuum in which there are no friction forces. If in this liquid a certain volume is separated bounded by the surface S, then the action of the remaining part of the liquid on it leads to a standard pressure.

The motion of the ideal liquid is described by the Euler equations [7]:

$$\begin{aligned}
&\frac{\partial v_x}{\partial t} + v_x\frac{\partial v_x}{\partial x} + v_y\frac{\partial v_x}{\partial y} + v_z\frac{\partial v_x}{\partial z} = X - \frac{1}{\rho}\frac{\partial p}{\partial x},\\
&\frac{\partial v_y}{\partial t} + v_x\frac{\partial v_y}{\partial x} + v_y\frac{\partial v_y}{\partial y} + v_z\frac{\partial v_y}{\partial z} = Y - \frac{1}{\rho}\frac{\partial p}{\partial y},\\
&\frac{\partial v_z}{\partial t} + v_x\frac{\partial v_z}{\partial x} + v_y\frac{\partial v_z}{\partial y} + v_z\frac{\partial v_z}{\partial z} = Z - \frac{1}{\rho}\frac{\partial p}{\partial z}
\end{aligned} \qquad (2.1)$$

and the equation of discontinuity

$$\frac{\partial v_x}{\partial x} + \frac{\partial v_y}{\partial y} + \frac{\partial v_z}{\partial z} = 0. \tag{2.2}$$

Here v_x, v_y, v_z are the components of the velocity vector $\bar{v}$ of the liquid particles along the axis of the coordinate x, y, z, respectively; ρ is the density of the liquid which in the case of an incompressible liquid is assumed to be constant; p is the hydraulic pressure; and X, Y, Z are the components of the mass force vector. Consequently for the four unknowns v_x, v_y, v_z, p, there are four equations.

The three equations (2.1) written in scalar form may be substituted for one vector equation:

$$\frac{d\bar{v}}{dt} = \bar{F} - \frac{1}{\rho} \operatorname{grad} p, \tag{2.3}$$

where

$$\bar{v} = v_x\bar{i} + v_y\bar{j} + v_z\bar{k}; \quad \bar{F} = X\bar{i} + Y\bar{j} + Z\bar{k}.$$

We shall assume the steady-state motion of the liquid to be vortex-free and consequently irrotational. Then the velocity vector is the irrotational vector, i.e.,

$$\bar{v}(x, y, z, t) = \operatorname{grad} \varphi \tag{2.4}$$

or in scalar form,

$$v_x = \frac{\partial \varphi}{\partial x}, \quad v_y = \frac{\partial \varphi}{\partial y}, \quad v_z = \frac{\partial \varphi}{\partial z} \tag{2.5}$$

Here (x, y, z, t) is the velocity potential.

In the existence of a velocity potential (2.5) the equation of discontinuity (2.2) for an incompressible liquid becomes the Laplace equation:

$$\Delta\varphi = \frac{\partial^2 \varphi}{\partial x^2} + \frac{\partial^2 \varphi}{\partial y^2} + \frac{\partial^2 \varphi}{\partial z^2} = 0. \tag{2.6}$$

In the existence of a velocity potential the acceleration will also be the irrotational vector [5, 7]:

$$\frac{d\bar{v}}{dt} = \text{grad}\left(\frac{1}{2}v^2 + \frac{\partial \varphi}{\partial t}\right).$$

Inserting this expression in (2.3) and denoting the vector $\bar{F}$ as the mass force potential U, i.e.

$$\bar{F} = -\text{grad } U,$$

we obtain

$$\text{grad}\left(\frac{\partial \varphi}{\partial t} + \frac{1}{2}v^2 + U + \frac{p}{\rho}\right) = 0.$$

Hence,

$$\frac{p - p_0}{\rho} = -\left(\frac{\partial \varphi}{\partial t} + \frac{1}{2}v^2 + U\right) + F(t). \tag{2.7}$$

This integral of the equations of motion is called the Cauchy integral. Without a loss of generality, in the future we shall assume F(t) = 0.

If we find the velocity potential $\varphi(x, y, z, t)$ then the process of the motion of the liquid will be known.

The differential equation of the oscillations of the shell may be presented in the form [3, 9]

$$\begin{aligned} L_{11}u + L_{12}v + L_{13}w + \rho_0 h \frac{\partial^2 u}{\partial t^2} &= X, \\ L_{21}u + L_{22}v + L_{23}w + \rho_0 h \frac{\partial^2 v}{\partial t^2} &= Y, \\ L_{31}u + L_{32}v + L_{33}w + \rho_0 h \frac{\partial^2 w}{\partial t^2} &= Z. \end{aligned} \tag{2.8}$$

Here L_{11}, L_{12}, ... are certain differential operators; u, v, w are the components of the vector of the complete motion of the shell along the axes of the coordinates x, y, z, respectively; ρ_0 is the density of the shell material; h is the thickness of the shell; X, Y, Z are the components of the vector of external forces acting upon the shell.

The external forces for the shell are the force of the liquid pressure upon the wetted surface S, the pressure of the gases upon the unwetted surface, the axial compression or extension forces, acting upon the shell of the tank from the adjacent segments of the body. We shall assume that the axial forces

and the pressure of the supercharge of the gases are known. The pressure of the liquid upon the wetted surface S is determined by a formula analogous to (2.7):

$$\frac{p_S - p_0}{\rho} = -\left(\frac{\partial \varphi}{\partial t} + \frac{1}{2} v^2 + U\right)_S, \qquad ((2.9)$$

where p_0 is the pressure of the gases upon the free surface.

The solutions of equations (2.1), (2.6), and (2.8) should satisfy the boundary (bordering) and initial conditions. For the shell, the boundary condition is given in the form of geometrical or force conditions of the form:

$$Q_l(u, v, w) = 0 \qquad (2.10)$$

Because the tank shell is impenetrable, then on the boundary of the wetted surface S, the normal component of the velocity of the liquid should be equal to the normal component of the velocity of the motion of the shell

$$\left.\frac{\partial \varphi}{\partial n}\right|_S = \frac{\partial Q_n}{\partial t}, \qquad (2.11)$$

where Q_n is the motion of the shell normal to the surface.

On the free surface S' the pressure of the liquid is equal to the pressure of the gases, therefore

$$\left(\frac{\partial \varphi}{\partial t} + \frac{1}{2} v^2 + U\right)_{S'} = 0. \qquad (2.12)$$

The conditions (2.9) and (2.11) are the conditions of compatibility of the oscillations of the shell and the liquid.

The arbitrary constants of the general solution of the equations are determined from the initial conditions.

Later, we shall evaluate the stability of the motion of the system by frequency methods which are based upon an analysis of the dynamic properties of the system in steady-state harmonic influences. The motions caused by the initial conditions are not of interest, and we shall not ascertain them.

Thus the problem of the oscillations of the liquid in the elastic tank is reduced to finding a solution of the equation (2.8) satisfying the boundary condition (2.10) in the given line, and a solution of the equation (2.6) satisfying the boundary condition (2.12) on the free surface. Both solutions, moreover, should satisfy conditions (2.9) and (2.11) on the wetted surface.

Let us specify and simplify the problem, subjecting it to the objectives formulated in Chapter 1. The solution of the problem of the oscillations of the liquid in the elastic tank is important for two reasons: 1) for the determination of the shape and frequencies of the characteristic longitudinal oscillations of the rocket body, 2) for a determination of the perturbation of the pressure as the liquid leaves the tank. Let us introduce the following assumptions.

1. Let us assume that the rocket has the form of a straight axisymmetrical elongated body, so that in a cross-section the distribution of mass and rigidity in any radial direction is the same.

2. Let us assume that the rocket executes a rectilinear flight and the vector of the external forces acting upon the rocket is directed along the axis of the rocket. Then the surface of the liquid will be situated perpendicularly to the axis of the rocket and the pressure of the liquid upon the walls of the tank will possess the property of axial symmetry. If thrust vibrations arise in the flight, then the elastic tank and the liquid will oscillate with forced vibrations. The large diversity of forms of oscillations in the study of longitudinal vibrations of the system, we may examine only the axisymmetrical shape of oscillations which substantially simplify the study.

3. Longitudinal acceleration of the rocket in a small segment of the trajectory may be considered constant. Under reaction of the pressure of the pressurized delivery and the hydrostatic pressure, the tank and the liquid are in a position of statistical equilibrium. We note that the forced oscillations of the tank and liquid take place relative to this situation of statistical equilibrium.

4. We shall consider the oscillations of the rocket body, as with also the oscillations of the tank and the liquid, to be small; this means that the occurrence of small movements and velocities may be neglected in comparison with the quantities of the movements and velocities themselves.

In solving the problem on the oscillations with the liquid, it is sufficient to consider only the hydrodynamic pressure of the liquid. Then the formula (2.7) takes the form

$$p = -\varrho \frac{\partial \varphi'}{\partial t} . \qquad (2.13)$$

5. For longitudinal vibrations, generally speaking, the transverse dimensions of the body change also. The change in the radius of the tank, causing extension or compression of the shell in the axial direction, exerts a certain influence on the oscillations of the liquid in the tank. However, we shall neglect these influences. We shall consider that during the longitudinal oscillations of the body, only the length of the tank shell changes, and the radius of the tank is changed only by the hydrodynamic pressure of the liquid. This assumption makes it possible to study separately the axisymmetrical oscillations of the liquid in the elastic tank and to find a simple mechanical for them.

6. We shall not consider the oscillations of the free surface of the liquid. Calculations show that in the majority of cases these oscillations exert an insignificant influence upon the frequency of the oscillating system.

7. The forces of inertia of the shell of the tank are small in comparison to the inertial forces of the liquid in the tank, therefore we shall not take them into consideration. As will be seen later, these forces may be considered without changes the method of solution.

8. We shall consider the shell tank to be thin-walled and with a zero moment.

2. Determination of the Basic Frequency of the Characteristic Axisymmetrical Oscillations by the Rayleigh Method

If in the calculations, one may be restricted to a calculation only of one basic tone of the axisymmetric oscillations of the tank and the liquid, then it is advisable to determine the frequency of the characteristic oscillations by the Rayleigh approximation method. The idea behind the Rayleigh method is generally known and may be briefly reduced to the following. For oscillations of a conservative system, the sum of the kinetic energy T and the potential energy Π is constant. Because the oscillations in time occur by the harmonic law, then, given the assumed form of the oscillations from the equation $T_{max} = \Pi_{max}$, we may approximately (with a certain exaggeration) determine the frequency of the basic tone of the characteristic oscillations ω_1. The more accurately the accepted form of the oscillations coincides with the actual form, the more accurate will be the obtained value of the frequency of the characteristic of the oscillations. The form of the characteristic oscillations must be given in accordance with the boundary conditions. In particular, for the form of the oscillations of the basic tone, one may take the function of the motions for the statistical load.

In systems with distributed parameters, the potential energy is generally expressed as the coefficient of the reduced rigidity k_{cc}:

$$\Pi = \frac{1}{2} k_{cc} q^2(t),$$

and the kinetic energy of the coefficient of the reduced mass m_{cc}

$$T = \frac{1}{2} m_{cc} \dot{q}^2(t) = \frac{1}{2} m_{cc} \omega^2 q^2(t),$$

where q(t) is the generalized coordinate.

From the equality $T_{max} = \Pi_{max}$ we obtain the formula for determining the frequency of the characteristic oscillations of the system

$$\omega^2 = \frac{k_{cc}}{m_{cc}}. \qquad (2.14)$$

We shall derive an approximate determination of the frequency of the basic tone for the case where the tank shell is executed in the form of a circular

cylinder, and the bottom is executed in the form of a spherical segment with the height of the segment significantly smaller than the diameter of the sphere ($H_2 \leq 0.2D$), as assumed by V. Z. Vlasov [2]. Besides the assumptions formulated in the foregoing section, we shall consider that the kinetic energy of motion of the liquid is small in the radial direction relative to the kinetic energy of its motion along the axis of the cylinder and the velocity of the particles of the liquid in the direction of the axis of the cylinder does not depend upon the radius.

The geometry of the tank and its mounting scheme are shown in Fig. 2.1a; there are also shown the statistical motions of the fill on the bottom of the tank in the direction of the radius produced by the hydrostatic pressure.

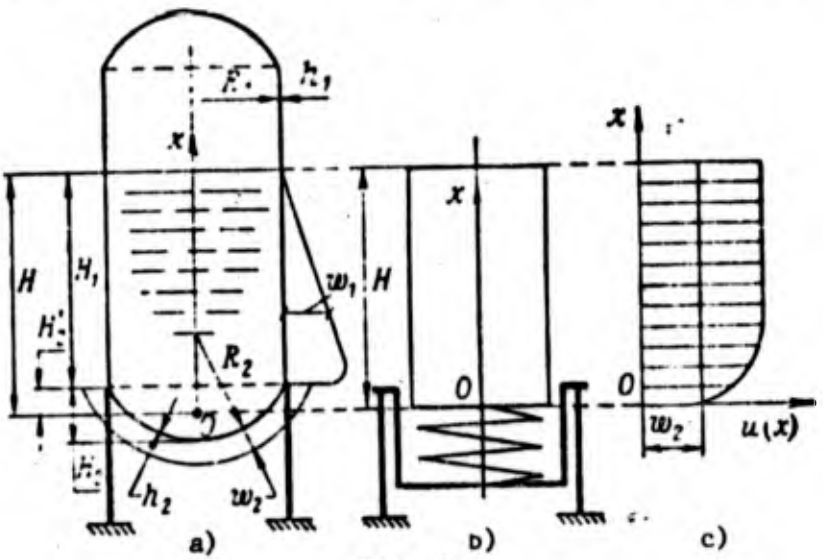

Fig. 2.1

We shall designate as R_1, h_1 the radius and thickness of the tank shell; as R_2, h_2, the radius and thickness of the spherical shell (the bottom of the tank); as H_1, the height of the wetted part of the tank shell; as H_2, the height of the segment of the spherical bottom; as H, the reduced height of the liquid head in the tank; and as γ, the specific weight of the liquid.

We shall calculate the potential energy of the shell and the bottom of the tank corresponding to deformation from hydrostatic pressure.

Under the action of the hydrostatic pressure, the shell of the tank is in a uni-axially directed position. The specific potential energy $\Pi_{1\varepsilon}$ and the

declination ε_1 in the peripheral direction is determined as

$$\Pi_{1\varepsilon} = \frac{1}{2} E\varepsilon_t^2, \quad \varepsilon_t = \frac{\gamma(H-x)R_1}{Eh_1},$$

where E is the modulus of elasticity of the first order.

We obtain the potential energy of the shell by integrating the quantity $\Pi_{1\varepsilon}$ throughout the volume. Setting R_1 = const, h_1 = const, we get

$$\Pi_1 = \int\int\int_V \Pi_{1\varepsilon} dV = 2\pi R_1 h_1 \int_{H_2}^{H} \Pi_{1\varepsilon} dx = \frac{\pi\gamma^2 R_1^3 H_1^3}{3Eh_1}. \qquad (2.15)$$

Because the height H_2 of the segment of the spherical bottom is small, for simplification we note that the pressure of the liquid in any part of the sphere is the same and equal to the hydrostatic pressure at depth H. For a spherical shell under the action of a constant pressure γH the specific potential energy is [3, 16]

$$\Pi_{2\varepsilon} = \frac{E\varepsilon_2^2}{1-\mu}, \quad \varepsilon_2 = \frac{w_2}{R_2} = \frac{\gamma H R_2}{2Eh_2}(1-\mu),$$

where μ is the Poisson coefficient.

The volume of part of the spherical shell is

$$V_2 = h_2 2\pi R_2 H_2,$$

where

$$H_2 = R_2 - \sqrt{R_2^2 - R_1^2}.$$

The complete potential energy for a declination of the bottom of the tank

$$\Pi_2 = \Pi_{2\varepsilon} V_2 = \frac{\pi R_2^3 \gamma^2 H^2 H_2}{2Eh_2}(1-\mu). \qquad (2.16)$$

We shall replace the volume of the liquid located in a segment of the spherical bottom with the equivalent volume of a cylindrical head of the liquid with a radius R_1. Then the complete reduced height of the cylindrical liquid head with radius R_1, taking into account the liquid in the bottom of the tank, will be

$$H = H_1 + H_2': \quad H_2' = \frac{1}{R_1^2} \int_{-(H_2 - H_2')}^{H_2'} (2R_2 x - x^2)\, dx = \frac{\pi H_2^2 (3R_2 - H_2)}{3R_1^2}.$$

To obtain the radial compressive forces in the place of the junction of the bottom with the shell of the tank, a former (force ring) is noted. The rate of the liquid head is counterbalanced by the meridian forces T_2 along the contour of the bottom (Fig. 2.2)

$$\pi R_1^2 H\gamma = 2\pi R_1 T_1 = 2\pi R_1 T_2 \sin\theta_0.$$

The force T_2, projected in the plane of the ring, produces a radial load on the ring

$$q_к = T_2 \cos\theta_0 = \frac{R_1 H\gamma}{2\sin\theta_0}\cos\theta_0.$$

The compressing force in a cross-section of the ring is

$$S_к = q_к R_1.$$

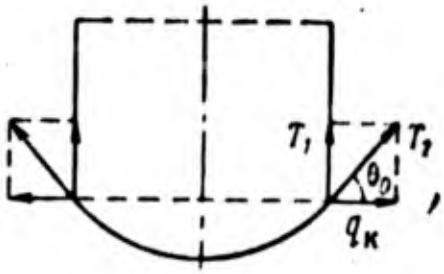

Figure 2.1

The potential energy of the declination of the ring is

$$\Pi_3 = \frac{1}{2}\,\frac{S_к^2}{EF_к}\,2\pi R_1 = \frac{\pi R_1^5 \gamma^2 H^2}{4EF_к}\operatorname{ctg}^2\theta_0 \qquad (2.17)$$

where F_k is the area of the cross-section of the ring.

Thus, the complete potential energy of declination is

$$\Pi = \Pi_1 + \Pi_2 + \Pi_3. \qquad (2.18)$$

The coefficient k_{cc} is numerically equal to twice the value of the potential energy of the system for q(t) = 1. Therefore for q(t) = 1

$$k_{cc} = 2\Pi_{max}.$$

Now we shall calculate the maximum value of the kinetic energy of the liquid, assuming that the liquid performs harmonic motion with a frequency ω_1 in the direction of the longitudinal axis of the tank. The shape of the oscillations corresponds to the motion of the shell of the tank under the action of the hydrostatic pressure.

For a visualization of the argument we note that the liquid head height H consists of a certain number of thin layers. The motion of any layer in the

direction of the axis of the cylinder may be considered to consist of two parts: 1) motion in the amount w_2 with the bottom, and 2) motion caused by a decrease in the thickness of the underlying layers of liquid as a consequence of an increase of the diameter of the shell.

An increase in the diameter of the shell and a decrease as a consequence of this of the thickness of the layer of liquid is proportional to the hydrostatic pressure. Because the second part of the motion of the liquid will be the same as the compressed head under the action of weight, then instead of an incompressible liquid and a pliable shell, in determining axial motions we may consider a certain equivalent compressible liquid head and an absolutely rigid shell. The cited modulus of elasticity E_{rr} of this head should be calculated from the condition of the equation of motion. For determination of E_{rr}, we shall examine a thin layer consisting of liquid and the shell. We shall take the height of the layer in the undeformed state to be unity. The increase of the radius of the shell due to hydrostatic pressure is

$$w_1 = \frac{\gamma (H - x) R_1^2}{E h_1}.$$

As a consequence of the increase of the radius, the height of the layer of the liquid is decreased by the amount

$$\Delta_1 = \frac{2\pi R_1 w_1}{\pi R_1^2} = \frac{2\gamma (H - x) R_1}{E h_1}.$$

If we now consider the layer of the liquid as compressible, then under the action of the axial compressing force, equal to $\gamma(H - x)\pi R_1^2$, the height of the layer is decreased by the amount

$$\Delta_2 = \frac{\gamma (H - x) \pi R_1^2}{E_{rr} \pi R_1^2} = \frac{\gamma (H - x)}{E_{rr}}.$$

Because a decrease in the height of the layer of the liquid as a consequence of an increase in the diameter of the shell from the pressure $\gamma(H - x)$ should be equal to the decrease in height of the same layer as a consequence of the compressibility of the height $\Delta_1 = \Delta_2$, then

$$E_{rr} = E \frac{h_1}{2R_1}, \qquad (2.19)$$

where E is the modulus of elasticity of the material of the tank shell.

In Fig. 2.1b, a model is presented of a compressible liquid head; a spring imitates the elasticity of the bottom. The complete motion of an arbitrary layer of liquid is

$$u(x)=w_2+\int_0^x \frac{\gamma(H-x)\,dx}{E_{rr}}=w_2+\frac{\gamma x\left(H-\frac{x}{2}\right)}{E_{rr}}, \qquad (2.20)$$

where

$$w_2=\frac{\gamma H R_2^2}{2Eh_2}(1-\mu). \qquad (2.21)$$

A graph of the function u(x), assuming the form of liquid oscillations, is shown in Fig. 2.1c.

The maximum value of the kinetic energy of the axial oscillations of the liquid head is

$$T_{\max}=\frac{1}{2}\int_0^H \frac{\pi R_1^2\gamma}{g}\omega_1^2 u^2(x)\,dx=\frac{1}{2}m_{rr}\omega_1^2, \qquad (2.22)$$

where

$$m_{rr}=\frac{\pi R_1^2\gamma H}{g}\left(w_2^2+\frac{2w_2\gamma H^2}{3E_{rr}}+\frac{2\gamma^2H^4}{15E_{rr}^2}\right).$$

If the tank is suspended and hung from the upper force rib (Fig. 2.3), then under the action of the hydrostatic pressure the stressed state of the shell will be bi-axial. The stress σ_1 in the direction of the axis of the shell and σ_t in the peripheral direction will be

$$\sigma_1=\frac{\gamma H R_1}{2h_1}, \quad \sigma_t=\frac{\gamma(H-x)R_1}{h_1}.$$

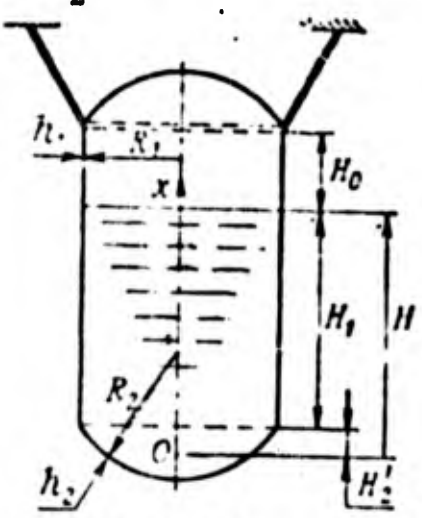

Figure 2.3

The potential energy of the shell in this case will be postulated from the formula [3, 16]:

$$\Pi_1=\frac{h_1}{2}\int\!\!\int_S(\sigma_1\varepsilon_1+\sigma_t\varepsilon_t)\,dS+\frac{h_1}{2}\int\!\!\int_{S_0}\frac{\sigma_1^2}{E}\,dS_0,$$

where S is the wetted surface of the shell, and S_0 is the unwetted surface of the shell. Since

$$\varepsilon_1=\frac{1}{E}(\sigma_1-\mu\sigma_t), \quad \varepsilon_t=\frac{1}{E}(\sigma_t-\mu\sigma_1),$$

then

$$\Pi_1 = \frac{h_1}{2E}\int_{H_2}^{H}(\sigma_1^2 + \sigma_t^2 - 2\mu\sigma_1\sigma_t)\,2\pi R_1 dx + \frac{\pi\gamma^2 H^2 H_0 R_1^3}{4Eh_1}. \qquad (2.23)$$

As a consequence of the stressing of the shell in the axial direction, additional motion arises of the entire liquid height by the amount

$$\Delta H = \int_0^H \varepsilon_1 dx + \frac{\sigma_1}{E} H_0 = \frac{\gamma H^2 R_1}{2Eh_1}(1-\mu) + \frac{\gamma H H_0 R_1}{2Eh_1}.$$

If we consider, as before, that the liquid head is compressible, then the reduced modulus of compression E (x) here will depend upon the coordinate x. We shall calculate it.

$$w_1 = \varepsilon_1 R_1, \quad \Delta_1 = \frac{2\pi R_1 w_1}{\pi R_1^2} = \frac{2\gamma R_1}{Eh_1}\left[(H-x) - \mu\frac{H}{2}\right],$$

$$\Delta_2 = \frac{\gamma(H-x)}{E_{rr}(x)}, \quad \Delta_1 = \Delta_2,$$

$$E_{rr}(x) = \frac{Eh_1}{R_1}\,\frac{(H-x)}{2(H-x)-\mu H}.$$

The complete motion of an arbirary layer of liquid is

$$u(x) = w_2 + \Delta H + \int_0^x \frac{\gamma(H-x)}{E_{rr}(x)}\,dx =$$

$$= w_2 + \Delta H + \frac{\gamma}{E_{np}}\left[Hx\left(1-\frac{\mu}{2}\right) - \frac{x^2}{2}\right]. \qquad (2.24)$$

Here w_2 is determined by the formula (2.21) and E is determined by formula (2.19). Thus, if the tank is suspended, then in formula (2.17) Π_1 should be substituted from (2.23), and for determination of the kinetic energy, the function u(x) should be taken in the form of (2.24)

The frequency of the characteristic oscillations will be determined as before by the formula (2.14).

3. An Approximate Determination of Forced Longitudinal Oscillations of the Elastic Tank and the Liquid

Let a forced ring, to which is attached the bottom of the tank, perform small oscillations in the direction of the axis of the tank according to the law

$$u_к(t)=u_0e^{i\omega t},$$

where u_0, ω are the amplitude and the frequency of the oscillations of the ring, be given. If the frequency ω of the forced oscillations is less than the frequency of the characteristic oscillations of the basic tone ω_1, then we may consider only the basic tone of the oscillations of the tank and the liquid and obtain an approximate solution of the problem on the assumption that the shape of the oscillations of the tank and the liquid are forced oscillations the same as they are under the influence of hydrostatic pressure.

As we did in section 2, we shall substitute the elastic tank and the incompressible liquid for a compressible liquid head with a modulus of elasticity E_{rr} (2.19). A diagram is shown in Fig. 2.4; here a spring imitates the elasticity of the bottom of the tank.

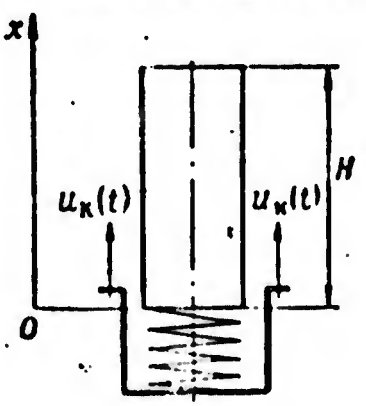

Figure 2.4

We shall set the motion of the arbitrary layer of the liquid in the direction of the axis of the liquid head, reckoned from the position of statistical equilibrium, in the form

$$u(x,\ t)=u_к(t)+f(x)q(t), \qquad (2.25)$$

where f(x) and q(t) are the coordinate of the function and the generalized coordinate of motion of the arbitrary liquid layer, respectively, of the force ring to the function f(x), which as in section 1 we shall select with regard to the motion of the tank shell under the influence of the hydrostatic pressure of the liquid. For the design of the tank shown in Fig. 2.1, on the basis of (2.20) and (2.21), we get

$$f(x)=1+a\left(\frac{x}{H}-\frac{x^2}{2H^2}\right), \quad a=\frac{4HR_1h_2}{(1-\mu)R_2^2h_1}, \qquad (2.26)$$

where x is the distance from the low section of the liquid head to an arbitrary section in the position of statistical equilibrium. In equation (2.26), the motion due to the deformation of the bottom of the tank (in Fig. 2.4 it is the deformation of the spring) is taken as equal to unity, i.e., f(0) = 1.

For the suspended tank, the function f(x) may be found from equation (2.24).

In order to obtain an equation of the forced oscillations, we shall write an expression of the kinetic and potential energy of the system and apply the Lagrange equation of the second kind

$$\frac{d}{dt}\left(\frac{\partial L}{\partial \dot{q}_n}\right)-\frac{\partial L}{\partial q_n}=P_n, \quad L=T-\Pi.$$

The kinetic energy of the liquid head is

$$T=\frac{1}{2}\pi R_1^2\frac{\gamma}{g}\int_0^H(\dot{u}_\kappa+f(x)\dot{q})^2dx=\frac{1}{2}m\dot{u}_\kappa^2+ \\ +\pi R_1^2\frac{\gamma}{g}\dot{u}_\kappa\dot{q}\int_0^H f(x)dx+\frac{1}{2}\pi R_1^2\frac{\gamma}{g}\dot{q}^2\int_0^H f^2(x)dx, \tag{2.27}$$

where m is the quantity of mass of the liquid in the tank.

The potential energy of the system consists of the potential energy of deformation of the spring, the liquid head, and the force ring, and may be calculated by the method expounded in section 1. We may express the potential energy of deformation as the coefficient of the reduced rigidity

$$\Pi=\frac{1}{2}k_{rr}q^2.$$

The potential energy and consequently k_{rr} need not be calculated, if the frequency of the characteristic oscillations ω_1 is known from the foregoing oscillations. Indeed, on the basis of (2.14),

$$k_{rr}=\omega_1^2 m_{rr}.$$

The coefficient of the reduced mass m_{rr} of the liquid head in the motions relative to the force ring is calculated by the formula

$$m_{rr}=\pi R_1^2\frac{\gamma}{g}\int_0^H f^2(x)dx. \tag{2.28}$$

The generalized force P_n in the problem examined is equal to zero.

Inserting the expressions for T and Π in the Lagrange equation, we get

$$m_{rr}\ddot{q} + k_{rr}q = -\ddot{u}_k \pi R_1^2 \frac{\gamma}{g}\int_0^H f(x)\,dx$$

or

$$\ddot{q} + \omega_1^2 q = -b\ddot{u}_k, \quad b = \frac{\int_0^H f(x)\,dx}{\int_0^H f^2(x)\,dx}. \tag{2.29}$$

We shall examine only the steady-state oscillations which are expressed by the partial solution of the equation (2.29):

$$q = \frac{b\omega^2}{\omega_1^2 - \omega^2} u_0 e^{i\omega t} \quad (\omega_1 \neq \omega). \tag{2.30}$$

Force oscillations of any layer of liquid agreeable to (2.25) may be written in the form

$$u(x, t) = \left[1 + f(x)\frac{b\omega^2}{\omega_1^2 - \omega^2}\right] u_0 e^{i\omega t}. \tag{2.31}$$

Forced oscillations of the lower section of the liquid head (the bottom of the tank) are expressed by the equation

$$u(t) = \left(1 + \frac{b\omega^2}{\omega_1^2 - \omega^2}\right) u_0 e^{i\omega t}. \tag{2.32}$$

Forced oscillations of any layer of the liquid occur relative to the force ring by the law

$$u_{отн}(x, t) = f(x)q(t) = \left[1 + a\left(\frac{x}{H} - \frac{x^2}{2H^2}\right)\right]\frac{b\omega^2}{\omega_1^2 - \omega^2} u_0 e^{i\omega t}.$$

Force oscillations of the bottom of the tank relative to the force ring are

$$u^{*}_{отн}(t) = \frac{b\omega^2}{\omega_1^2 - \omega^2} u_0 e^{i\omega t}.$$

The axial force arising in any cross-section of the liquid head during oscillations is equal to the sum of the inertial forces of all layers distributed above the section examined

$$N(x, t) = -\frac{\pi R_1^2 \gamma}{g} \int_x^H \frac{\partial^2 u(x,t)}{\partial t^2} dx. \qquad (2.33)$$

The inertial force of the whole liquid head is determined from the expression

$$N(t) = \frac{\pi R_1^2 \gamma}{g} u_0 \omega^2 e^{i\omega t} \int_0^H \left[1 + f(x) \frac{b\omega^2}{\omega_1^2 - \omega^2}\right] dx.$$

This is the dynamic force of influence on the liquid in the bottom of the cylindrical tank which is transmitted to the supporting shell through the force ring (see Fig. 2.1). When N(t) > 0, the spring is extended; when N(t) < 0, the spring is compressed. If the form of the oscillations f(x) is taken in the form (2.26), then the force N(t) may be calculated by the formula

$$N(t) = \frac{\pi R_1^2 H \gamma}{g} u_0 \omega^2 e^{i\omega t} \left[1 + \frac{\left(1 + \frac{a}{3}\right)^2}{1 + \frac{2a}{3} + \frac{2a^2}{15}} \frac{\omega^2}{\omega_1^2 - \omega^2}\right]. \qquad (2.34)$$

4. The Approximate Determination of the Velocity Potential of the Liquid in an Elastic Cylindrical Tank with a Rigid Bottom

The liquid velocity potential φ_1 should satisfy the Laplace equation (2.6) and the boundary conditions. The Laplace equation in cylindrical coordinates for axisymmetrical oscillations has the form [7]

$$\Delta \varphi_1 = \frac{\partial^2 \varphi_1}{\partial r^2} + \frac{1}{r} \frac{\partial \varphi_1}{\partial r} + \frac{\partial^2 \varphi_1}{\partial x^2} = 0. \qquad (2.35)$$

As the pattern of the first approximation, we shall examine the cylindrical tank of circular cross-section with elastic walls and a rigid bottom.

Later we shall also consider an elastic tank bottom: The tank diagram is presented in Fig. 2.5.

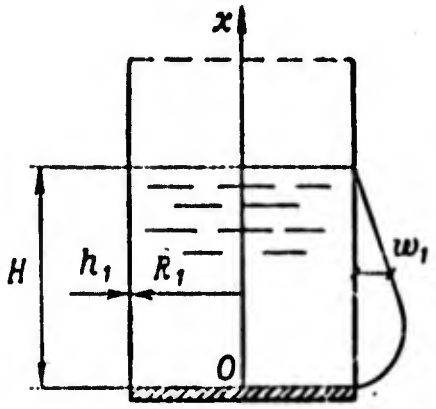

Figure 2.5

We shall write the boundary conditions on the wall and on the bottom of the tank:

$$\frac{\partial \varphi_1}{\partial r} = \frac{\partial w_1}{\partial t} \qquad \text{for} \quad r = R_1, \tag{2.36}$$

$$\frac{\partial \varphi_1}{\partial x} = 0 \qquad \text{for} \quad x = 0, \tag{2.37}$$

where $w_1 = w_1(x, t)$ is the radial motion of the cylindrical wall of the tank.

On the free surface the pressure of the liquid is equal to the pressure of the gases, therefore on the basis of (2.13) the boundary condition is written as

$$\left(\frac{\partial \varphi_1}{\partial t}\right)_{x=H} = 0. \tag{2.38}$$

We shall solve equation (2.35) by the Fourier method. We shall write the velocity potential in the form of the sum of the products of the function:

$$\varphi_1 = \sum_{(s)} D_s X_s(x) R_s(r) i\omega_s e^{i\omega_s t}.$$

Placing this expression in equation (2.35) and separating variables, we obtain the following equation for determining the function $X_s(x)$ and $R_s(r)$:

$$\frac{d^2X_s(x)}{dx^2} + k_s^2 X(x) = 0, \tag{2.39}$$

$$\frac{d^2R_s(r)}{dr^2} + \frac{1}{r}\frac{dR_s(r)}{dr} - k_s^2 R_s(r) = 0, \tag{2.40}$$

where k_s is a certain parameter not yet determined.

In order to satisfy the boundary condition (2.36), we shall write the function w_1 in the form

$$w_1 = \sum_{(s)} G_s X_s(x) e^{i\omega_s t},$$

wherein the function $X_s(x)$ should satisfy equation (2.39).

Here G_s is an undetermined coefficient.

Equation (2.40) for determining the function $R_s(r)$ is a linear differential equation with variable coefficients--a Bessel equation. Because the function $R_s(r)$ for $r = 0$ should be restricted, the solution of equation (2.40) should consist of a zero-order Bessel function of the first kind [14].

If the coefficient k_s in equations (2.39) and (2.40) is an imaginary number, then the function $R_s(r)$ will be a zero-order Bessel function of the first kind:

$$R_s(r) = J_0(k_s r).$$

Here k_s is the modulus of the imaginary number.

If in equations (2.39) and (2.40) k_s is a real number, then the functions $R_s(r)$ will be modified by the zero-order Bessel function of the first kind

$$R_s(r) = I_0(k_s r).$$

The modified Bessel functions are determined from the relation

$$I_0(k_s r) = J_0(ik_s r),$$

where k_s is a real positive number.

For imaginary values of k_s the solution of equation (2.39) is expressed as the hyperbolic functions sh $k_s x$ and ch $k_s x$, and for real values of k_s, as the trigonometric functions sin $k_s x$ and cos $k_s x$, whereupon

$$\sin ik_s x = i \operatorname{sh} k_s x, \qquad \cos ik_s x = \operatorname{ch} k_s x.$$

From the expression for the velocity potential φ_1 and equations (2.37) and (2.38) we find

$$\left(\frac{\partial X_s(x)}{\partial x}\right)_{x=0} = 0, \quad [X_s(x)]_{x=H} = 0. \tag{2.41}$$

Because equations (2.41) may be satisfied simultaneously only for real values of k_s, the solution of equation (2.39), satisfying the boundary conditions (2.41), will take the form

$$X_s(x) = \cos k_s x,$$

where

$$k_s = \frac{(2s-1)\pi}{2H} \qquad (s = 1, 2, \ldots).$$

For real values of k_s a solution of equation (2.40) may take the form

$$R_s(r) = I_0\left(\nu_s \frac{r}{R_1}\right), \tag{2.42}$$

where

$$\nu_s = k_s R_1 = \frac{(2s-1)\pi R_1}{2H} \qquad (s = 1, 2, \ldots)$$

Thus we get the following expression for the velocity potential of the liquid φ_1 and the function w_1:

$$\varphi_1 = \sum_{s=1}^{\infty} D_s' I_0\left(\nu_s \frac{r}{R_1}\right) \cos\left(\nu_s \frac{x}{R_1}\right) i\omega_s e^{i\omega_s t},$$

$$w_1 = \sum_{s=1}^{\infty} G_s \cos\left(\nu_s \frac{x}{R_1}\right) e^{i\omega_s t}. \tag{2.43}$$

For determining the coefficient D_s, C_s and the frequencies of the characteristic oscillations ω_s, it is necessary to examine the connection between the radial oscillations of the cylindrical wall of the tank and the radial oscillations of the liquid.

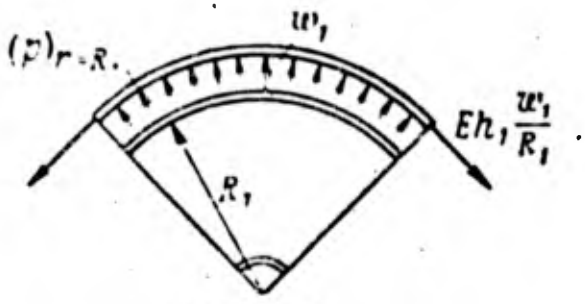

Figure 2.6

Let us examine a part of the ring cut away from the cylindrical wall of the tank (Fig. 2.6). For axisymmetrical oscillations, an increase or a decrease in the diameter of the ring takes place; expansion or contraction forces arise in the ring. We shall take the width of the ring as equal to unity. When the radius of the ring is increased by a quantity w_1 a stretching force equal to $Eh_1(w_1/R_1)$ arises in the ring. The liquid pressure

$$(p)_{r=R_1} = -\varrho\left(\frac{\partial \dot{w}_1}{\partial t}\right)_{r=R_1}. \qquad (2.44)$$

acts on the interior wall of the ring.

The equation of the radial oscillations of the ring may be presented in the form

$$\varrho_0 h_1 R_1 \frac{\partial^2 w_1}{\partial t^2} = R_1 (p)_{r=R_1} - Eh_1 \frac{w_1}{R_1}.$$

Dividing all members of this equation by $\rho_0 h_1 R_1$, we obtain

$$\frac{\partial^2 w_1}{\partial t^2} + \Omega_k^2 w_1 = \frac{1}{\varrho_0 h_1}(p)_{r=R_1}. \qquad (2.45)$$

Here, ρ_0 is the density of the material of the tank wall; Ω_k is the frequency of the characteristic radial oscillations of the ring with radius R_1:

$$\Omega_\kappa = \frac{1}{R_1}\sqrt{\frac{E}{\rho_0}}.$$

Inserting into equation (2.45) the value (p)r = R_1 from equation (2.44) and substituting for the functions w_1 and φ_1 their expressions from (2.43), we obtain

$$G_s\left(\Omega_\kappa^2 - \omega_s^2\right) = D_s' \frac{\rho}{h_1\rho_0} I_0(\nu_s)\omega_s^2 \qquad (s = 1, 2 \ldots). \tag{2.46}$$

From the boundary condition (2.46) we find

$$D_s'\left[\frac{d}{dr} I_0\left(\nu_s \frac{r}{R_1}\right)\right]_{r=R_1} = G_s.$$

Since

$$\frac{d}{dr} I_0(k_s r) = k_s I_1(k_s r),$$

then

$$D_s' = \frac{R_1 G_s}{\nu_s I_1(\nu_s)}. \tag{2.47}$$

Placing the expression for the coefficient D_s in equation (2.46), we obtain a formula for determining the frequency of the characteristic axisymmetrical oscillations of an elastic cylindrical tank and the liquid

$$\omega_s^2 = \frac{\Omega_\kappa^2}{1 + \frac{\rho R_1}{\rho_0 h_1}\frac{I_0(\nu_s)}{\nu_s I_1(\nu_s)}}. \tag{2.48}$$

Here ν_s is a real number determined by formula (2.42). If the mass of the wall of the tank is not taken into account, then the frequency of the characteristic oscillations of the tank is

$$\omega_s^2 = \frac{E h_1 \nu_s I_1(\nu_s)}{\rho R_1^3 I_0(\nu_s)}. \tag{2.49}$$

We shall now examine oscillations of the liquid in a cylindrical tank with rigid walls and an elastic bottom.

5. An Approximate Determination of the Velocity Potential of the Liquid in a Cylindrical Tank with Rigid Walls and an Elastic Bottom

The problem of determining the velocity potential of the liquid φ_2 in a cylindrical tank with a rigid wall and an elastic bottom is a part of the more general problem of determining the velocity potential in an elastic cylindrical tank. We shall take the cross-section of the tank to be in the form of a circle with a radius R_1, and the bottom of the tank to be in the form of a flat spherical shell with a radius R_2 and thickness h_2. A diagram of the tank is presented in Fig. 2.7. We shall designate the motion of any point in the bottom of the tank in the direction of the radius of the sphere as $w_2 = w_2(r, t)$.

At first we shall select the coordinates at a distance H from the free surface, where H is the reduced height of the liquid head

$$H = H_1 + H_2.$$

Because the depth of the liquid in the spherical shell of the tank is small, we shall take the pressure and velocity of the liquid at the boundary from the bottom for all points of the shell as being the same as at a depth H, i.e., for x = 0.

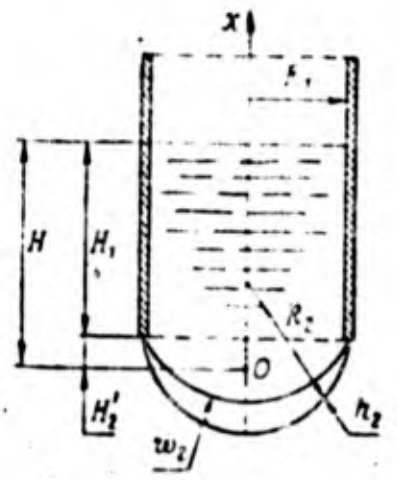

Figure 2.7

The velocity potential φ_2 should satisfy the Laplace equation (2.35) and the boundary conditions

$$\frac{\partial \varphi_2}{\partial r}=0 \quad \text{for } r=R_1, \tag{2.50}$$

$$\frac{\partial \varphi_2}{\partial x}=\frac{\partial w_2}{\partial t} \quad \text{for } x=0, \tag{2.51}$$

$$\frac{\partial \varphi_2}{\partial t}=0 \quad \text{for } x=H. \tag{2.52}$$

We shall take the form of the characteristic oscillations of the flat spherical shell of the bottom of the tank with the liquid as the same as for the dry shell. In the case of axisymmetrical oscillations, the form of the i-th tone of oscillations may be presented in the form [3, 10]:

$$f_i(r)=C_1 J_0\left(\mu_i \frac{r}{R_1}\right)+C_2 I_0\left(\mu_i \frac{r}{R_1}\right), \tag{2.53}$$

where

$$\mu_i^4=\frac{R_1^4}{D} Eh_2\left(\rho_0 \frac{\omega_i^2}{E}-\frac{1}{R_1^2}\right); \quad D=\frac{Eh_2^3}{12(1-\mu^2)};$$

with sufficient practical accuracy; where E, ρ_0 are the modulus of elasticity and the density of the shell material; w_i is the frequency of the characteristic oscillations of the dry shell. We shall consider the shell boundary to be confined, therefore the function $f_i(r)$ should satisfy the following boundary condition:

$$f_i(r)=0, \quad f_i'(r)=0 \qquad \text{при } r=R_1.$$

Placing the function $f_i(r)$ in these conditions, we obtain the characteristic equation for determining the coefficient μ_i

$$J_0(\mu_i) I_1(\mu_i)+I_0(\mu_i) J_1(\mu_i)=0 \tag{2.54}$$

and the relation between the coefficients C_1 and C_2

$$C_2=-C_1 \frac{I_0(\mu_i)}{I_0(\mu_i)}.$$

We shall write the motion of the bottom of the tank in the direction of the radius in the form

$$w_2(r, t) = \sum_{i=1}^{\infty} f_i(r) q_i(t),$$

where $q_i(t)$ is a generalized coordinate. Then, assuming in (2.53) the coefficient $C_1 = 1$, we obtain

$$w_2(r, t) = \sum_{i=1}^{\infty} q_i(t) \left[J_0\left(\mu_i \frac{r}{R_1}\right) - \theta_i I_0\left(\mu_i \frac{r}{R_1}\right) \right]. \tag{2.55}$$

Here

$$\theta_i = \frac{J_0(\mu_i)}{I_0(\mu_i)}.$$

We shall write the velocity potential in the form

$$\varphi_2 = \sum_{j=1}^{\infty} \frac{1}{\operatorname{ch}\left(\lambda_j \frac{H}{R_1}\right)} \dot{q}_j(t) J_0\left(\lambda_j \frac{r}{R_1}\right) \operatorname{sh}\left(\lambda_j \frac{x-H}{R_1}\right) + \dot{A}(t) \frac{x-H}{R_1}, \tag{2.56}$$

where $\dot{q}_j(t)$, $\dot{A}(t)$ are certain functions of time.

The function φ_2 satisfies the Laplace equation (2.35) and the boundary condition (2.52). Placing expression (2.56) in the boundary condition (2.50), we obtain an equation for determining λ_j

$$\left[\frac{d}{dr} J_0\left(\lambda_j \frac{r}{R_1}\right)\right]_{r=R_1} = -\frac{\lambda_j}{R_1} J_1(\lambda_j) = 0.$$

Solving this equation we find that $\lambda_0 = 0$; $\lambda_1 = 3.8317$; $\lambda_2 = 7.0156$; $\lambda_3 = 10.1735$. We shall select the functions $\dot{q}_j(t)$ and $\dot{A}(t)$ in such a manner as to satisfy the boundary condition (2.51). Inserting expressions (2.55) and (2.56) in condition (2.51), we obtain

$$\sum_{j=1}^{\infty} \frac{\lambda_j}{R_1} \dot{q}_j(t) J_0\left(\lambda_j \frac{r}{R_1}\right) + \frac{\dot{A}(t)}{R_1} = \sum_{i=1}^{\infty} \dot{q}_i(t) \left[J_0\left(\mu_i \frac{r}{R_1}\right) - \theta_i I_0\left(\mu_i \frac{r}{R_1}\right) \right]. \tag{2.57}$$

We multiply both parts of this equation by rdr and integrate through with reference to r in the limits from 0 to R_1. We obtain

$$\frac{\dot{\lambda}(t)}{R_1} = \sum_{i=1}^{\infty} a_i \dot{q}_i(t), \quad a_i = \frac{2}{\mu_i}\left[J_1(\mu_i) - \theta_i I_1(\mu_i)\right]. \tag{2.58}$$

We multiply both parts of equation (2.57) by $rJ_0(\lambda_j \frac{r}{R_1})$ and integrate through relative to r in the limits from 0 to R_1. We get

$$\int_0^{R_1} J_0^2\left(\lambda_j \frac{r}{R_1}\right) r\, dr = \frac{R_1^2}{2} J_0^2(\lambda_j).$$

According to the condition of orthogonality of the Bessel function,

$$\int_0^{R_1} J_0\left(\lambda_j \frac{r}{R_1}\right) J_0\left(\lambda_k \frac{r}{R_1}\right) r\, dr = 0. \qquad (k \neq j)$$

We may write the results of integration in the form

$$\frac{\dot{q}_j(t)}{\operatorname{ch}\left(\lambda_j \frac{H}{R_1}\right)} = \sum_{i=1}^{\infty} b_{ij} \dot{q}_i(t),$$

$$b_{ij} = \frac{2}{\lambda_j R_1 J_0^2(\lambda_j) \operatorname{ch}\left(\lambda_j \frac{H}{R_1}\right)} \int_0^{R_1} \left[J_0\left(\mu_i \frac{r}{R_1}\right) - \theta_i I_0\left(\mu_i \frac{r}{R_1}\right)\right] J_0\left(\lambda_j \frac{r}{R_1}\right) r\, dr =$$

$$= \frac{2R_1}{\lambda_j J_0(\lambda_j) \operatorname{ch}\left(\lambda_j \frac{H}{R_1}\right)} \left[\frac{\mu_i}{\lambda_j^2 - \mu_i^2} J_1(\mu_i) + \frac{\theta_i \mu_i}{\mu_i^2 + \lambda_j^2} I_1(\mu_i)\right]. \tag{2.59}$$

Finally, the expression for the velocity potential φ_2, taking into account formulas (2.58) and (2.59), may be written in the form

$$\varphi_2 = \sum_{i=1}^{\infty} \dot{q}_i(t) \left[\sum_{j=1}^{\infty} b_{ij} J_0\left(\lambda_j \frac{r}{R_1}\right) \operatorname{sh}\left(\lambda_j \frac{x - H}{R_1}\right) + a_i(x - H)\right]. \tag{2.60}$$

Now we shall move on to the solution of the more complicated problem--the determination of the velocity potential of the liquid in an elastic cylindrical container, i.e., in a tank with ealstic walls and an elastic bottom. For the solution, we shall use the results obtained in sections 4 and 5.

6. An Approximate Determination of the Velocity Potential of a Liquid in an Elastic Cylindrical Tank

Let us examine an elastic cylindrical tank of circular cross-section with radius R_1; the bottom of the tank is executed in the form of a flat spherical shell, the radius of curvature of which equals R_2. The velocity potential of the liquid φ should satisfy the Laplace equation and the boundary conditions

$$\frac{\partial \bar{\tau}}{\partial r} = \frac{\partial w_1}{\partial t} \quad \text{for} \quad r = R_1, \tag{2.61}$$

$$\frac{\partial \varphi}{\partial x} = -\frac{\partial w_2}{\partial t} \quad \text{for} \quad x = 0, \tag{2.62}$$

$$\frac{\partial \bar{\tau}}{\partial t} = 0 \quad \text{for} \quad x = H. \tag{2.63}$$

Here w_1, w_2 are the motion of the wall on the bottom of the tank in the direction of the radius of the cylinder and the radius of the sphere; H is the reduced height of the liquid head in the tank.

We shall write the form of the velocity potential in the form of the sum of two functions

$$\varphi = \varphi_1 + \varphi_2,$$

each of which is a solution to the Laplace equation. Moreover, the function φ_1 satisfies the boundary conditions (2.36)-(2.38) and the function φ_2 satisfies the boundary conditions (2.50)-(2.52). For such a selection of functions φ_1 and φ_2, the velocity potential φ will satisfy all the conditions (2.61)-(2.63).

The functions φ_1 and φ_2 are determined in sections 4 and 5. On the basis of expressions (2.43), (2.47), and (2.60), we obtain

$$\varphi_1 = \sum_{s=1}^{\infty} D_s I_0\left(\nu_s \frac{r}{R_1}\right) \cos\left(\nu_s \frac{x}{R_1}\right) \dot{w}_s(t) \quad \left(D_s = \frac{R_1}{\nu_s I_1(\nu_s)}\right),$$

$$\varphi_2 = \sum_{i=1}^{\infty} \dot{q}_i(t) \left[\sum_{j=1}^{\infty} b_{ij} J_0\left(\lambda_j \frac{r}{R_1}\right) \operatorname{sh}\left(\lambda_j \frac{x-H}{R_1}\right) + a_i(x-H)\right]. \tag{2.64}$$

Here in the expression for φ_1 in comparison with (2.43), it is assumed that

$$D_s \dot{w}_s(t) = D_s' i\omega_s e^{i\omega_s t}.$$

Knowing the velocity potential of the liquid, it is possible to determine the pressure at any point of the volume of the liquid, to find the kinetic energy, and to write the equation of the oscillations of the liquid in the elastic tank.

7. A Determination of the Kinetic Energy of the Liquid

The kinetic energy of the oscillating liquid is

$$T = \frac{1}{2} \varrho \iiint_V v^2 \, dV,$$

where V is the volume of the liquid.

According to Green's formula, the volume integral may be transformed to a surface integral. For the irrotational motion of an incompressible liquid, we obtain [5]

$$T = \frac{1}{2} \varrho \iint_S \varphi \frac{\partial \varphi}{\partial n} \, dS, \tag{2.65}$$

or

$$T = \frac{1}{2} \varrho \iint_S \left[\varphi \frac{\partial \varphi}{\partial x} \cos(n, x) + \varphi \frac{\partial \varphi}{\partial r} \cos(n, r)\right] dS, \tag{2.66}$$

where S is the surface of the liquid confining the volume V; n is the external normal to the surface to the liquid.

For the lateral surface of the cylindrical tank,

$$\cos(n, x)=0; \quad \cos(n, r)=1; \quad dS=2\pi R_1 dx.$$

For the bottom of the tank,

$$\cos(n, x)=-1; \quad \cos(n, r)=0; \quad dS=2\pi r dr.$$

On the free surface $(\varphi)_{x=H} = 0$; therefore

$$T=\frac{1}{2}2\pi\varrho\left[\int_0^H\left(\varphi\frac{\partial\varphi}{\partial r}\right)_{r=R_1}R_1\,dx-\int_0^{R_1}\left(\varphi\frac{\partial\varphi}{\partial x}\right)_{x=0}r\,dr\right]. \qquad (2.67)$$

The velocity potential of the liquid is

$$\varphi=\varphi_1+\varphi_2,$$

wherein the functions φ_1 and φ_2 are determined by the formula (2.64).

We calculate the auxilliary expressions entering into formula (2.67):

$$(\varphi)_{r=R_1}=\sum_{s=1}^{\infty}D_s\dot{w}_s I_0(\nu_s)\cos\left(\nu_s\frac{x}{R_1}\right)+$$

$$+\sum_{i=1}^{\infty}\dot{q}_i\left[\sum_{j=1}^{\infty}b_{ij}J_0(\lambda_j)\operatorname{sh}\left(\lambda_j\frac{x-H}{R_1}\right)+a_i(x-H)\right],$$

$$(\varphi)_{x=0}=\sum_{s=0}^{\infty}L_s\dot{w}_s I_0\left(\nu_s\frac{r}{R_1}\right)-$$

$$-\sum_{i=1}^{\infty}\dot{q}_i\left[\sum_{j=1}^{\infty}b_{ij}J_0\left(\lambda_j\frac{r}{R_1}\right)\operatorname{sh}\left(\lambda_j\frac{H}{R_1}\right)+a_iH\right],$$

$$\left(\frac{\partial \bar{\tau}}{\partial r}\right)_{r=R_1} = \sum_{s=1}^{\infty} D_s \dot{w}_s \frac{\nu_s}{R_1} I_1(\nu_s) \cos\left(\nu_s \frac{x}{R_1}\right),$$

$$\left(\frac{\partial \bar{\tau}}{\partial x}\right)_{x=0} = \sum_{i=1}^{\infty} \dot{q}_i \left[\sum_{j=1}^{\infty} b_{ij} \frac{\lambda_j}{R_1} J_0\left(\lambda_j \frac{r}{R_1}\right) \mathrm{ch}\left(\lambda_j \frac{H}{R_1}\right) + a_i\right].$$

Keeping in mind the function (2.42), we find

$$\int_0^H \cos^2\left(\nu_s \frac{x}{R_1}\right) dx = \frac{H}{2},$$

$$\int_0^H \mathrm{sh}^2\left(\lambda_j \frac{x-H}{R_1}\right) dx = \frac{R_1}{2\lambda_j} \mathrm{sh}\left(\lambda_j \frac{H}{R_1}\right) \mathrm{ch}\left(\lambda_j \frac{H}{R_1}\right) - \frac{H}{2},$$

$$\int_0^H \cos\left(\nu_s \frac{x}{R_1}\right) \mathrm{sh}\left(\lambda_j \frac{x-H}{R_1}\right) dx = -\frac{R_1 \lambda_j \mathrm{ch}\left(\lambda_j \frac{H}{R_1}\right)}{\lambda_j^2 + \nu_s^2},$$

$$\int_0^H \cos\left(\nu_s \frac{x}{R_1}\right) \cos\left(\nu_k \frac{x}{R_1}\right) dx = 0 \qquad (s \neq k),$$

$$\int_0^H (x-H) \cos\left(\nu_s \frac{x}{R_1}\right) dx = -\frac{R_1^2}{\nu_s^2},$$

$$\int_0^H (x-H) \mathrm{sh}\left(\lambda_j \frac{x-H}{R_1}\right) dx =$$

$$= -\frac{R_1^2}{\lambda_j^2}\left[\mathrm{sh}\left(\lambda_j \frac{H}{R_1}\right) - \lambda_j \frac{H}{R_1} \mathrm{ch}\left(\lambda_j \frac{H}{R_1}\right)\right].$$

The integrals on the Bessel functions entering into formula (2.67) have the following values:

$$\int_0^{R_1} J_0^2\left(\lambda_j \frac{r}{R_1}\right) r\,dr = \frac{R_1^2}{2} J_0^2(\lambda_j),$$

$$\int_0^{R_1} I_0\left(\nu_s \frac{r}{R_1}\right) r\,dr = \frac{R_1^2}{\nu_s} I_1(\nu_s),$$

$$\int_0^{R_1} J_0\left(\lambda_j \frac{r}{R_1}\right) r\,dr = \frac{R_1^2}{\lambda_j} J_1(\lambda_j) = 0, \tag{2.68}$$

$$\int_0^{R_1} I_0\left(\nu_s \frac{r}{R_1}\right) J_0\left(\lambda_j \frac{r}{R_1}\right) r\,dr = \frac{\nu_s R_1^2}{\nu_s^2 + \lambda_j^2} J_0(\lambda_j) I_1(\nu_s).$$

We write the final expression for determining the kinetic energy of the oscillating liquid in the form

$$T = \frac{1}{2}\left(\sum_{s=1}^{\infty} a_{w_s w_s} \dot{w}_s^2 + \sum_{l=1}^{\infty} a_{q_l q_l} \dot{q}_l^2 + \right.$$

$$\left. + \sum_{\substack{l=1 \\ l \neq k}}^{\infty} \sum_{k=1}^{\infty} a_{q_l q_k} \dot{q}_l \dot{q}_k + 2 \sum_{s=1}^{\infty} \sum_{l=1}^{\infty} a_{w_s q_l} \dot{w}_s \dot{q}_l \right), \tag{2.69}$$

where

$$a_{w_s w_s} = \pi H \varrho D_s^2 \nu_s I_0(\nu_s) I_1(\nu_s) = \frac{\pi R_1^2 H \varrho}{\nu_s} \frac{I_0(\nu_s)}{I_1(\nu_s)};$$

$$a_{q_l q_l} = \pi R_1^2 H \varrho \left\{ a_l^2 + \sum_{j=1}^{\infty} \frac{4R_1}{\lambda_j H} \operatorname{th}\left(\lambda_j \frac{H}{R_1}\right) \left[\frac{\mu_l J_1(\mu_l)}{\lambda_j^2 - \mu_l^2} + \right.\right.$$

$$\left.\left. + \frac{6_j \mu_l}{\mu_l^2 + \lambda_j^2} I_1(\mu_l) \right]^2 \right\},$$

$$a_{q_i q_k} = 2\pi R_1^2 H \varrho \left\{ \frac{a_i a_k}{2} + \sum_{j=1}^{\infty} \frac{2R_1}{\lambda_j H} \operatorname{th}\left(\lambda_j \frac{H}{R_1}\right) \left[\frac{\mu_i J_1(\mu_i)}{\lambda_j^2 - \mu_i^2} \right) + \right.$$

$$\left. + \frac{\theta_i \mu_i}{\mu_i^2 + \lambda_j^2} J_1(\mu_i) \right] \left[\frac{\mu_k J_1(\mu_k)}{\lambda_j^2 - \mu_k^2} + \frac{\theta_k \mu_k}{\mu_k^2 + \lambda_j^2} J_1(\mu_k) \right] \Bigg\},$$

$$a_{w_s q_i} = \pi R_1^3 \varrho \left\{ -\frac{2a_i}{\nu_s^2} + \right. \tag{2.70}$$

$$\left. + \sum_{j=1}^{\infty} \frac{4}{\nu_s^2 + \lambda_j^2} \left[\frac{\mu_i}{\lambda_j^2 - \mu_i^2} J_1(\mu_i) + \frac{\theta_i \mu_i}{\mu_i^2 + \lambda_j^2} J_1(\mu_i) \right] \right\}.$$

8. A Determination of the Potential Energy of Deformation of the Tank

In the potential energy of tank deformation enters the potential energy of deformation of the cylindrical shell, spherical bottom, and the force ring. In section 2, formulas are obtained for determining the potential energy on the assumption that the form of the oscillations coincides with the form of the statistical motion. These formulas may be used for calculating only the first (basic) cone of oscillations of liquid in the elastic tank. We shall determine the potential energy of deformation of the tank for the case where it is necessary to calculate several tones of the oscillations of the liquid.

We shall not consider the influence of the pressure of fuel injection and the hydrostatic pressure in the tank. This significantly simplifies the formulas; however, the quantity of the potential energy obtained this way is slightly underestimated. A determination of the potential energy, taking into account the fuel injection pressure, is examined in work [9].

We shall examine the potential energy of the cylindrical shell of the tank, which we shall consider to be without moment and thin-walled. For the supporting tank, we shall consider only the peripheral stresses arising as a consequence of the dynamic pressure of the liquid. Axial stresses shall be considered in calculating longitudinal oscillations of the entire body of the rocket.

The potential energy of deformation of the shell is

$$\Pi_1 = \frac{1}{2}\left(2\pi R_1 h_1 E \int_0^H \varepsilon_t^2 dx\right),$$

where E is the modulus of elasticity of the first kind; ε_t is the peripheral deformation of the shell; H is the filling height of the liquid. The deformation ε_t is related to the radial motion $w_1(x, t)$ by the relationship

$$\varepsilon_t = \frac{w_1(x,t)}{R_1},$$

whereupon in the basic expression (2.43), it may be assumed that

$$w_1(x, t) = \sum_{s=1}^{\infty} w_s(t)\cos\left(\nu_s \frac{x}{R_1}\right). \tag{2.71}$$

Inserting the quantity ε_t in the formula for Π_1 and integrating, we obtain

$$\Pi_1 = \frac{\pi H h_1 E}{2R_1} \sum_{s=1}^{\infty} w_s^2(t). \tag{2.72}$$

We shall determine the potential energy of the deformation of the bottom of the tank, which we shall consider to be a momentless thin-walled flat spherical shell. The shell is in a biaxially stressed situation. A diagram of the shell is presented in Fig. 2.8. The deformations as a function of the motion of the flat shell have the form [3, 16]

$$\varepsilon_t = \frac{v}{r} - \frac{w_2}{R_2}, \quad \varepsilon_r = \frac{dv}{dr} - \frac{w_2}{R_2},$$

where w_2, v are the motion of the shell in the radial and meridianal directions; ε_t, ε_r are the deformation of the shell in the directions around the circle and meridianally.

The quantity of potential energy of deformation of the shell may be calculated from the expression [3, 16]

$$\Pi_2 = \frac{\pi E h_2}{1-\mu^2} \int_0^{R_1} (\varepsilon_t^2 + \varepsilon_r^2 + 2\mu\varepsilon_t\varepsilon_r) r\, dr. \tag{2.73}$$

The radial motion of the shell is determined by the formula (2.55)

$$w_2 = \sum_{i=1}^{\infty} q_i(t)\left[J_0\left(\mu_i \frac{r}{R_1}\right) - \theta_i I_0\left(\mu_i \frac{r}{R_1}\right)\right].$$

The meridianal and radial motions are related by the function [16]

$$v = -\frac{R_2 D}{E h_2}(1+\mu)\frac{d}{dr}(\nabla^2 w_2)$$

$$\left(D = \frac{E h_2^3}{12(1-\mu^2)}\right).$$

Inserting in them the expression for w_2, we get

$$v = -\frac{R_2 h_2^2}{12(1-\mu)}\sum_{i=1}^{\infty} q_i(t) \times$$

$$\times\left(\frac{\mu_i}{R_1}\right)^3\left[J_1\left(\mu_i \frac{r}{R_1}\right) - \theta_i I_1\left(\mu_i \frac{r}{R_1}\right)\right].$$

We substitute into formula (2.73) the quantities ε_t and ε_r by their expressions w_2 and v. We introduce the dimensionless radius $\xi = r/R_1$. Then, for example

$$\int_0^{R_1} J_0\left(\mu_i \frac{r}{R_1}\right) r\, dr = R_1^2 \int_0^1 J_0(\mu_i \xi)\, \xi\, d\xi.$$

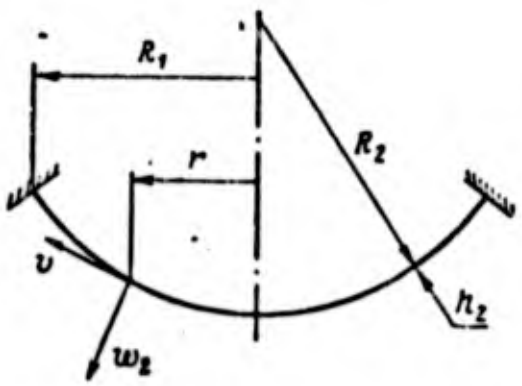

Figure 2.8

After integrating the right part of equation (2.73), we write the expression for the potential energy in the form

$$\Pi_2=\frac{1}{2}\sum_{i=1}^{\infty}b^{(2)}_{q_iq_i}q_i^2+\sum_{\substack{i=1\\ i\neq k}}^{\infty}\sum_{k=1}^{\infty}b^{(2)}_{q_iq_k}q_iq_k. \tag{2.74}$$

The coefficients $b^{(2)}_{q_1q_i}$ and $b^{(2)}_{q_1q_k}$ are determined by the following formula

$$b^{(2)}_{q_iq_i}=\frac{2\pi Eh_2}{1-\mu^2}\left\{\left[J_0^2(\mu_i)+J_1^2(\mu_i)\right]\left[\varkappa^2(1+\mu)+\frac{1}{2}\beta_i^2\mu_i^2-\right.\right.$$
$$\left.-\varkappa\beta_i\mu_i(1+\mu)\right]+2(1-\mu)\beta_i^2a_{ii}+\left[J_0^2(\mu_i)-J_1^2(\mu_i)\right]\left[\frac{1}{2}\beta_i^2\theta_i^2\mu_i^2+\right.$$
$$\left.+\varkappa\theta_i^2(1+\mu)(\varkappa-\beta_i\mu_i)\right]+2(1-\mu)\beta_i^2\theta_i^2b_{ii}-$$
$$-(1-\mu)\beta_i^2\left[1-J_0^2(\mu_i)\right]+2(1-\mu)(c_i-d_i)\beta_i^2\theta_i\mu_i- \tag{2.75}$$
$$-4(1-\mu)\beta_i^2\theta_if_i+(1-\mu)\beta_i^2\theta_i^2\left[1-J_0^2(\mu_i)\right]\},$$

where

$$\beta_i=-\left(\frac{\mu_i}{R_1}\right)^2\frac{R_2h_2^2}{12(1-\mu)},\quad \varkappa=\frac{R_1}{R_2},$$

$$a_{ii}=\int_0^1\frac{1}{\xi}J_1^2(\mu_i\xi)\,d\xi,\quad b_{ii}=\int_0^1\frac{1}{\xi}I_1^2(\mu_i\xi)\,d\xi,$$

$$c_i=\int_0^1J_0(\mu_i\xi)I_1(\mu_i\xi)\,d\xi,\quad d_i=\int_0^1I_0(\mu_i\xi)J_1(\mu_i\xi)\,d\xi,$$

$$f_i=\int_0^1\frac{1}{\xi}J_1(\mu_i\xi)I_1(\mu_i\xi)\,d\xi.$$

$$b_{q_i q_k} = \frac{\pi E h_2}{1-\mu^2}\left\{\frac{\mu_k J_1(\mu_k) J_0(\mu_i) - \mu_i J_1(\mu_i) J_0(\mu_k)}{\mu_k^2 - \mu_i^2}\left[2\varkappa^2(1+\mu) + \beta_{ik}\mu_{ik} - \right.\right.$$

$$\left. - 2\varkappa\gamma_k(1+\mu)\right] - \beta_{ik}\mu_i g_{ik} - \frac{\mu_k I_1(\mu_k) J_0(\mu_i) + \mu_i J_1(\mu_i) I_0(\mu_k)}{\mu_i^2 + \mu_k^2}\varepsilon_k\left[\mu_{ik}\beta_{ik} + \right.$$

$$+ 2\varkappa(1+\mu)(\varkappa - \gamma_k)\left] + \beta_{ik}\mu_i\varepsilon_k c_{ik} - \mu_k\beta_{ik} h_{ik}(1-2\mu) + 2\beta_{ik} a_{ik}(1-\mu) + \right.$$

$$+ \varepsilon_k\mu_k\beta_{ik} m_{ik}(1-2\mu) - 2\varepsilon_k\beta_{ik} f_{ik}(1-\mu) -$$

$$- \frac{\mu_i I_1(\mu_i) J_0(\mu_k) + \mu_k J_1(\mu_k) I_0(\mu_i)}{\mu_i^2 + \mu_k^2}\varepsilon_i\left[\mu_{ik}\beta_{ik} + 2\varkappa(1+\mu)(\varkappa - \gamma_k)\right] +$$

$$+ \varepsilon_i\mu_i\beta_{ik} d_{ik} - \varepsilon_{ik}\mu_i\beta_{ik} n_{ik} + \frac{\mu_i I_1(\mu_i) I_0(\mu_k) - \mu_k J_1(\mu_k) I_0(\mu_i)}{\mu_i^2 - \mu_k^2}\varepsilon_{ik}\left[\mu_{ik}\beta_{ik} + \right.$$

$$+ 2\varkappa(1+\mu)(\varkappa - \gamma_k)\left] + \beta_{ik}\varepsilon_i\mu_k(1-2\mu) p_{ik} - 2\beta_{ik}\varepsilon_i(1+\mu) t_{ik} - \right.$$

$$\left. - \varepsilon_{ik}\beta_{ik}\mu_k(1-2\mu) l_{ik} + 2(1-\mu)\beta_{ik}\varepsilon_{ik} b_{ik}\right\}, \qquad (2.76)$$

where

$$\beta_{ik} = \left(\frac{\mu_i}{R_1}\right)^3\left(\frac{\mu_k}{R_1}\right)^3\left[\frac{R_2 h_2^2}{12(1-\mu)}\right]^2, \quad \gamma_k = -\mu_k\left(\frac{\mu_k}{R_1}\right)^3\frac{R_2 h_2^2}{12(1-\mu)},$$

$$\mu_{ik} = \mu_i\mu_k, \quad \varepsilon_{ik} = \varepsilon_i\varepsilon_k,$$

$$\varepsilon_i = \theta_i = \frac{J_0(\mu_i)}{I_0(\mu_i)},$$

$$g_{ik} = \int_0^1 J_0(\mu_i\xi) J_1(\mu_k\xi)\, d\xi, \qquad c_{ik} = \int_0^1 J_0(\mu_i\xi) I_1(\mu_k\xi)\, d\xi,$$

$$h_{ik} = \int_0^1 J_1(\mu_i\xi) J_0(\mu_k\xi)\, d\xi, \qquad a_{ik} = \int_0^1 \frac{1}{\xi} J_1(\mu_i\xi) J_1(\mu_k\xi)\, d\xi,$$

$$m_{ik} = \int_0^1 J_1(\mu_i\xi) I_0(\mu_k\xi)\, d\xi, \qquad f_{ik} = \int_0^1 \frac{1}{\xi} J_1(\mu_i\xi) I_1(\mu_k\xi)\, d\xi,$$

$$n_{ik} = \int_0^1 I_0(\mu_i\xi) I_1(\mu_k\xi)\, d\xi, \qquad p_{ik} = \int_0^1 I_1(\mu_i\xi) J_0(\mu_k\xi)\, d\xi,$$

$$t_{ik} = \int_0^1 \frac{1}{\xi} I_1(\mu_i\xi) J_1(\mu_k\xi)\, d\xi, \qquad l_{ik} = \int_0^1 I_1(\mu_i\xi) I_0(\mu_k\xi)\, d\xi,$$

$$b_{ik} = \int_0^1 \frac{1}{\xi} I_1(\mu_i\xi) I_1(\mu_k\xi)\, d\xi, \qquad d_{ik} = \int_0^1 I_0(\mu_i\xi) J_1(\mu_k\xi)\, d\xi.$$

The potential energy of the deformation of expansion-compression of the ring is determined by the formula (2.17)

$$\Pi_3 = \frac{1}{2} \cdot \frac{S_к^2}{EF_к} 2\pi R_1 \qquad (S_к = q_к R_1),$$

where S_k is the force in the cross-section of the ring; q_k is the linear load acting upon the ring in a radial direction. The load may be expressed as the meridional force T_2 acting on the external boundary of the bottom of the tank (see Fig. 2.2):

$$|q_к| = |T_2| \cos \theta_0.$$

Here

$$T_2 = \frac{T_1}{\sin \theta_0}.$$

The force T_1 is determined from the equilibrium condition of the bottom of the tank

$$2\pi R_1 T_1 = 2\pi \int_0^{R_1} (p)_{x=0} r\, dr,$$

where $(p)_{x=0}$ is the dynamic pressure of the liquid in the bottom of the tank.

Now we shall write the formula for the calculation of the potential energy of the deformation of the ring in the form

$$\Pi_3 = \frac{\pi R_1}{EF_к} \operatorname{ctg}^2 \theta_0 \left[\int_0^{R_1} (p)_{x=0} r\, dr \right]^2. \qquad (2.77)$$

The dynamic pressure of the liquid in the bottom of the tank is

$$(p)_{x=0} = -\rho \left[\frac{\partial (\varphi_1 + \varphi_2)}{\partial t} \right]_{x=0}.$$

Taking into account the function (2.64), we find

$$\Pi_3=\frac{\pi R_1\varrho^2}{EF_\kappa}\operatorname{ctg}^2\theta_0\left\{\sum_{s=1}^{\infty}D_s\ddot{w}_s\int_0^{R_1}I_0\left(\nu_s\frac{r}{R_1}\right)r\,dr-\right.$$

$$\left.-\sum_{i=1}^{\infty}\ddot{q}_i\int_0^{R_1}\left[a_iH+\sum_{j=1}^{\infty}b_{ij}J_0\left(\lambda_j\frac{r}{R_1}\right)\operatorname{sh}\left(\lambda_j\frac{H}{R_1}\right)\right]r\,dr\right\}^2.$$

After integration and substituting the coefficient D_s by its values, we obtain

$$\Pi_3=\frac{\pi R_1\varrho^2}{EF_\kappa}\operatorname{ctg}^2\theta_0\left\{\sum_{s=1}^{\infty}\ddot{w}_s\frac{R_1^3}{\nu_s^2}-\frac{R_1^2H}{2}\sum_{i=1}^{\infty}a_i\ddot{q}_i\right\}^2.$$

For harmonic oscillations with frequency ω,

$$\ddot{w}_s=-\omega^2w_s,\quad \ddot{q}_i=-\omega^2q_i.$$

Finally, we write the expression for the potential energy of deformation of the ring in the following form

$$\Pi_3=\frac{1}{2}\sum_{s=1}^{\infty}b^{(3)}_{w_sw_s}w_s^2+\sum_{s=1}^{\infty}\sum_{\substack{k=1\\s\neq k}}^{\infty}b^{(3)}_{w_sw_k}w_sw_\kappa+$$

$$+\frac{1}{2}\sum_{i=1}^{\infty}b^{(3)}_{q_iq_i}q_i^2+\sum_{i=1}^{\infty}\sum_{\substack{k=1\\i\neq k}}^{\infty}b^{(3)}_{q_iq_k}q_iq_k+\frac{1}{2}\sum_{s=1}^{\infty}\sum_{i=1}^{\infty}b^{(3)}_{w_sq_i}w_sq_i, \tag{2.78}$$

where

$$b^{(3)}_{w_sw_s}=2b_0\frac{R_1^6}{\nu_s^4},\quad b_0=\omega^4\frac{\pi R_1\varrho^2}{EF_\kappa}\operatorname{ctg}^2\theta_0,\quad b^{(3)}_{w_sw_k}=b_0\frac{R_1^6}{\nu_s^2\nu_k^2},$$

$$b^{(3)}_{q_iq_k}=2b_0\frac{R_1^4H^2}{4}a_ia_k\quad b^{(3)}_{q_iq_i}=2b_0\frac{R_1^4H^2}{4}a_i^2\quad b^{(3)}_{w_sq_i}=-b_0^2\frac{R_1^5H}{2\nu_s^2}a_i. \tag{2.79}$$

The complete potential energy of deformation of the tank is

$$\Pi=\Pi_1+\Pi_2+\Pi_3$$

or, in the expanded form,

$$\Pi=\frac{1}{2}\left(\sum_{s=1}^{\infty} b_{w_s w_s} w_s^2+\sum_{s=1}^{\infty}\sum_{k=1}^{\infty} b_{w_s w_k} w_s w_k+\sum_{i=1}^{\infty} b_{q_i q_i} q_i^2+\right.$$

$$\left.+\sum_{\substack{i\ 1\\ i\neq k}}^{\infty}\sum_{k\ 1}^{\infty} b_{q_i q_k} q_i q_k+\sum_{\substack{s\ 1\\ s\neq l}}^{\infty}\sum_{l=1}^{\infty} b_{w_s q_l} w_s q_l\right), \tag{2.80}$$

where

$$b_{w_s w_s}=\frac{\pi H h_1 E}{R_1}+b^{(3)}_{w_s w_s},$$

$$b_{w_s w_k}=2b^{(3)}_{w_s w_k},\quad b_{q_i q_i}=b^{(2)}_{q_i q_i}+b^{(3)}_{q_i q_i}, \tag{2.81}$$

$$b_{q_i q_k}=2b^{(2)}_{q_i q_k}+2b^{(3)}_{q_i q_k},\quad b_{w_s q_l}=2b^{(3)}_{w_s q_l}.$$

9. Determination of the Shape and Frequencies of Characteristic Axisymmetrical Oscillations of a Liquid in an Elastic Tank

The expression for the kinetic energy and potential energy of the system may be written in matrix form

$$T=\frac{1}{2}\dot{\bar{Z}}'M\dot{\bar{Z}},\quad \Pi=\frac{1}{2}\bar{Z}'K\bar{Z}, \tag{2.82}$$

where M is the matrix of the inertial system; K is the matrix of rigidity of the system; $\bar{Z}$, $\dot{\bar{Z}}$ are the vectors of the generalized coordinate and the generalized velocity, characterizing the coincident motion of the liquid and the elastic walls of the tank; $\bar{Z}'$, $\dot{\bar{Z}}'$ are the corresponding vector rows.

Starting from expressions (2.69) and (2.80) and restricting in them the number of generalized coordinates $w_s(w_k)$ $s = 1, 2, \ldots, m^0$; $q_i(q_k)$ $i = 1, 2, \ldots, n^0$, we obtain the vectors of the generalized coordinates and the generalized velocities

$$\bar{Z}=\begin{bmatrix} w \\ q \end{bmatrix},\quad \dot{\bar{Z}}=\begin{bmatrix} \dot{w} \\ \dot{q} \end{bmatrix},$$

where

$$w=\begin{bmatrix} w_1 \\ w_2 \\ \cdot \\ \cdot \\ \cdot \\ w_{m^0} \end{bmatrix}, \quad q=\begin{bmatrix} q_1 \\ q_2 \\ \cdot \\ \cdot \\ \cdot \\ q_{n^0} \end{bmatrix}.$$

The matrix of the inertia of the system may be presented in the form

$$M=\begin{bmatrix} A_{11} & A_{12} \\ A_{21} & A_{22} \end{bmatrix},$$

where A_{11} is the diagonal matrix, the elements of which are on the diagonals $a_{w_s w_s}$, $s = 1, 2, \ldots, m^0$

$$A_{12}=\begin{bmatrix} a_{w_1 q_1} & a_{w_1 q_2} & \cdots & a_{w_1 q_{n^0}} \\ a_{w_2 q_1} & a_{w_2 q_2} & \cdots & a_{w_2 q_{n^0}} \\ \cdots & \cdots & \cdots & \cdots \\ a_{w_s q_1} & a_{w_s q_2} & \cdots & a_{w_s q_{n^0}} \end{bmatrix},$$

$$A_{21}=\begin{bmatrix} a_{w_1 q_1} & a_{w_2 q_1} & \cdots & a_{w_s q_1} \\ a_{w_1 q_2} & a_{w_2 q_2} & \cdots & a_{w_s q_2} \\ \cdots & \cdots & \cdots & \cdots \\ a_{w_1 q_{n^0}} & a_{w_2 q_{n^0}} & \cdots & a_{w_s q_{n^0}} \end{bmatrix},$$

$$A_{22}=\begin{bmatrix} a_{q_1 q_1} & a_{q_1 q_2} & \cdots & a_{q_1 q_{n^0}} \\ a_{q_2 q_1} & a_{q_2 q_2} & \cdots & a_{q_2 q_{n^0}} \\ \cdots & \cdots & \cdots & \cdots \\ a_{q_{n^0} q_1} & a_{q_{n^0} q_2} & \cdots & a_{q_{n^0} q_{n^0}} \end{bmatrix}.$$

The matrix of the rigidity of the system has the form

$$K=\begin{bmatrix} B_{11} & B_{12} \\ B_{21} & B_{22} \end{bmatrix},$$

where

$$B_{11}=\begin{bmatrix} b_{w_1 w_1} & b_{w_1 w_2} & \cdots & b_{w_1 w_s} \\ b_{w_2 w_1} & b_{w_2 w_2} & \cdots & b_{w_2 w_s} \\ \cdots & \cdots & \cdots & \cdots \\ b_{w_s w_1} & b_{w_s w_2} & \cdots & b_{w_s w_s} \end{bmatrix}.$$

The matrices B_{12}; B_{21}, B_{22} may be obtained respectively from the matrices A_{12}, A_{21}, A_{22} by substituting the elements $a_{w_s q_i}$ by the elements $b_{w_s q_i}$.

To derive the equations of motion of the system we use the Lagrange equations of the second kind

$$\frac{d}{dt}\left(\frac{\partial L}{\partial \dot{q}_n}\right)-\frac{\partial L}{\partial q_n}=0 \quad (L=T-\Pi)$$

The equation of motion of the system in matrix form has the following form:

$$M\ddot{\bar{Z}}+K\bar{Z}=0. \tag{2.83}$$

The squares of the frequencies of the characteristic oscillations of the system ω_s^2 may be determined from the characteristic equation

$$|M^{-1}K-\omega_s^2 E|=0, \tag{2.84}$$

where E is the unit matrix; M^{-1} is the inverse matrix to the matrix M.

The determination of the frequencies and forms of the characteristic oscillations of the liquid in the elastic tank amounts to finding the eigen-values and the eigen-vectors of the matrix $M^{-1}K$. Later we shall assume that the roots of equation (2.84) are simple.

Each frequency ω_s of the characteristic oscillations corresponds to an eigen-vector, the components of which are essentially the form of the oscillations in generalized coordinates. The connection between the generalized coordinate $\bar{Z}$ and the normal coordinates $\bar{\eta}$ in matrix form may be expressed as

$$\bar{Z}=R\bar{\eta}, \tag{2.85}$$

where

$$R=[\bar{\beta}_1 \quad \bar{\beta}_2 \quad \ldots \quad \bar{\beta}_s \quad \ldots \quad \bar{\beta}_{n^*+m^*}]$$

is the matrix of amplitude distribution;

$$\bar{\beta}_s = \begin{bmatrix} \nu^1_{\omega_s}(\omega_s) \\ \cdot \\ \cdot \\ \cdot \\ \nu_{\omega_{m^0}}(\omega_s) \\ \nu_{q_1}(\omega_s) \\ \cdot \\ \cdot \\ \cdot \\ \nu_{q_{n^0}}(\omega_s) \end{bmatrix}, \quad \bar{\eta} = \begin{bmatrix} r_1 \\ r_2 \\ \cdot \\ \cdot \\ \cdot \\ r_s \\ \cdot \\ \cdot \\ \cdot \\ \eta_{n^0+m^0} \end{bmatrix};$$

$\bar{\beta}_s$ is the characteristic normalized vector-column of equation (2.84);

$\bar{\eta}$ is the vector of the normal coordinates of the system. Here,

$$\eta_s = A_s(\omega_s)\lambda_s(t), \tag{2.86}$$

where $A_s(\omega_s)$ is a certain constant depending upon the frequency of the characteristic oscillations ω_s;

$\lambda_s(t)$ is the function of time of the s-th cone of oscillations.

We shall insert expression (2.85) in equation (2.82), using the condition of orthogonality of the eigen-vectors [6, 15]

$$\bar{\beta}_k' M\bar{\beta}_s = 0, \quad \bar{\beta}_k' K\bar{\beta}_s = 0, \tag{2.87}$$

where $\bar{\beta}_k$ is the vector-row obtained by transposing the vector-column $\bar{\beta}_k$, we find an expression for the kinetic and potential energy in normal coordinates.

$$T = \frac{1}{2}\sum_{s=1}^{n^0+m^0} A_s^2 \bar{\beta}_s' M\bar{\beta}_s \dot{\lambda}_s^2, \tag{2.88}$$

$$\Pi = \frac{1}{2}\sum_{s=1}^{n^0+m^0} A_s^2 \bar{\beta}_s' K\bar{\beta}_s \lambda_s^2. \tag{2.89}$$

Formulas (2.88) and (2.89) are suitable for deriving differential equations of motion of the liquid in an elastic tank.

10. Forced Axisymmetrical Oscillations of a Liquid in an Elastic Tank

Forced oscillations of a liquid in a tank arise as a consequence of longitudinal oscillations of the rocket body. The bottom of the tank oscillates in the direction of the longitudinal axis together with the body. Let us assume that the oscillations of the force ring in the direction of the longitudinal axis of the tank takes place according to the law

$$u_к(t) = u_0 e^{i\omega_n t},$$

where ω_n is the frequency of the n-th tone of the characteristic oscillations of the body.

The absolute motion of the liquid may consist of two parts: the migrational motion together with the force ring, and relative motion--motion relative to a sliding system of coordinates connected to the force ring. A diagram of the tank is shown in Fig. 2.9.

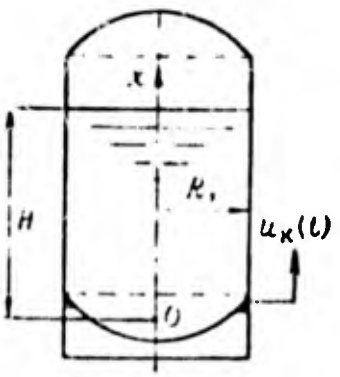

Figure 2.9

We may write the potential of the velocity of the liquid in migratory motion in the form

$$\varphi_e = \dot{u}_к(t)\,(x - H).$$

We may write the potential of velocity of the liquid in relative motion, taking into account expression (2.64) and the expression for the characteristic normalized vector column $\bar{\beta}_s$, in the form

$$\varphi_r = \sum_{s=1}^{s^0} \dot{\lambda}_s(t) \left\{ \sum_{k=1}^{m^0} \nu_{w_k}(\omega_s) I_0\left(\nu_k \frac{r}{R_1}\right) \cos\left(\nu_k \frac{x}{R_1}\right) + \right.$$
$$\left. + \sum_{l=1}^{n^0} \nu_{q_l}(\omega_s) \left[\sum_{(j)} b_{lj} J_0\left(\lambda_j \frac{r}{R_1}\right) \operatorname{sh}\left(\lambda_j \frac{x-H}{R_1}\right) + a_l(x-H) \right] \right\}$$
$$s^0 = m^0 + n^0, \tag{2.90}$$

where $\lambda(t)$ is a function of time; s^0 is the number of calculated tones of the characteristic oscillations. The expression between the braces may characterize the form of the characteristic normalized oscillations of the liquid in the elastic tank corresponding to the frequency ω_s. We introduce a symbolic notation for it

$$A_s R_s(r) X_s(x) = \sum_{k=1}^{m^0} \nu_{w_k}(\omega_s) I_0\left(\nu_k \frac{r}{R_1}\right) \cos\left(\nu_k \frac{x}{R_1}\right) +$$
$$+ \sum_{l=1}^{n^0} \nu_{q_l}(\omega_s) \left[\sum_{(j)} b_{lj} J_0\left(\lambda_j \frac{r}{R_1}\right) \operatorname{sh}\left(\lambda_j \frac{x-H}{R_1}\right) + a_l(x-H) \right]. \tag{2.91}$$

Then

$$\varphi_r = \sum_{s=1}^{s^0} A_s R_s(r) X_s(x) \dot{\lambda}_s(t). \tag{2.92}$$

The potential of the absolute velocities of the liquid may now be written in the form

$$\Phi = \ddot{u}_\kappa(t)(x-H) + \sum_{s=1}^{s^0} A_s R_s(r) X_s(x) \dot{\lambda}_s(t). \tag{2.93}$$

The kinetic energy of the liquid is

$$T = \frac{1}{2} \varrho \iiint_V (\operatorname{grad} \Phi)^2 dV.$$

Applying Green's theorem we obtain

$$T = \frac{1}{2} 2\pi\varrho \left[\int_0^H \left(\Phi \frac{\partial \Phi}{\partial r} \right)_{r=R_1} R_1 dx - \int_0^{R_1} \left(\Phi \frac{\partial \Phi}{\partial x} \right)_{x=0} r dr \right]. \tag{2.94}$$

Inserting expression (2.93) in formula (2.94) and assuming that $\lambda_s(t)$ is the generalized coordinate of the normal oscillations of the liquid in elastic tank, we obtain an expression for the kinetic energy

$$T=\frac{1}{2}\sum_{s=1}^{s^0} A_s^2 B_s \dot{\lambda}_s^2+\dot{u}_\kappa\sum_{s=1}^{s^0} A_s C_s \dot{\lambda}_s+\frac{m\dot{u}_\kappa^2}{2}, \tag{2.95}$$

where

$$m=\pi R_1^2 H\varrho,$$

$$B_s=2\pi R_1\varrho\int_0^H R_s(R_1)R_s'(R_1)X_s^2(x)\,dx-$$

$$-2\pi\varrho\int_0^{R_1} R_s^2(r)X_s(0)X_s'(0)\,r\,dr,$$

$$C_s=\pi R_1\varrho\int_0^H (x-H)R_s'(R_1)X_s(x)\,dx+ \tag{2.96}$$

$$+\pi H\varrho\int_0^{R_1} R_s(r)X_s'(0)\,r\,dr-\pi\varrho\int_0^{R_1} R_s(r)X_s(0)\,r\,dr.$$

The potential energy of deformation of the tank in normal coordinates may be presented thus:

$$\Pi=\frac{1}{2}\sum_{s=1}^{s_0} A_s^2 k_s^* \lambda_s^2. \tag{2.97}$$

Here $A_s^2 k_s^*$ is the coefficient of the reduced rigidity of the tank for the s-th tone of oscillations.

We shall derive an equation for the motion of the system. Using the Lagrange equation of the second kind, we obtain

$$A_s^2 B_s\ddot{\lambda}_s+A_s^2 k_s^*\lambda_s=-A_s C_s\ddot{u}_\kappa \quad (s=1,2,\ldots,s^0). \tag{2.98}$$

If we use the matrix notation method of transformation to the normal coordinates (section 9), then for the kinetic energy of the liquid the following formula may be obtained:

$$T=\frac{1}{2}\sum_{s=1}^{s^0}A_s\bar{\beta}_s'M\bar{\beta}_s\dot{\lambda}_s^2+\dot{u}_\kappa\sum_{s=1}^{s^0}A_s(\bar{\beta}_s'\bar{F})\dot{\lambda}_s+\frac{m\dot{u}_\kappa^2}{2}, \tag{2.99}$$

where

$$\bar{F}=\begin{bmatrix}
-\varrho\nu_{w_1}(\omega_s)2\pi\dfrac{R_1^2}{\nu_1}I_1(\nu_1)\\
-\varrho\nu_{w_2}(\omega_s)2\pi\dfrac{R_1^2}{\nu_2}I_1(\nu_2)\\
\cdots\cdots\cdots\cdots\\
\cdots\cdots\cdots\cdots\\
-\varrho\nu_{w_k}(\omega_s)2\pi\dfrac{R_1^2}{\nu_\kappa}I_1(\nu_\kappa)\\
\cdots\cdots\cdots\cdots\\
-\varrho\nu_{w_{m^0}}(\omega_s)2\pi\dfrac{R_1^2}{\nu_{m^0}}I_1(\nu_{m^0})\\
\varrho\nu_{q_1}(\omega_s)a_1\pi R_1^2H\\
\varrho\nu_{q_2}(\omega_s)a_2\pi R_1^2H\\
\cdots\cdots\cdots\cdots\\
\varrho\nu_{q_l}(\omega_s)a_l\pi R_1^2H\\
\cdots\cdots\cdots\cdots\\
\varrho\nu_{q_{n^0}}(\omega_s)a_{n^0}\pi R_1^2H
\end{bmatrix}$$

Here the components of the vector $\bar{F}$ are essentially the coefficients for the generalized coordinates of the following expression:

$$\varrho\iiint_V\frac{\partial\varphi}{\partial x}dV.$$

The equation of motion of the system, taking into account the expressions (2.93) and (2.99) may take the form

$$A_s\bar{\beta}_s'M\bar{\beta}_s\ddot{\lambda}_s+A_s\bar{\beta}_s'K\bar{\beta}_s\lambda_s=-A_s(\bar{\beta}_s'\bar{F})\ddot{u}_\kappa. \tag{2.100}$$

Equations (2.98) and (2.100) differ only in the notation of the coefficients. These are the equations of forced oscillations. For oscillations of the force ring the relative motion of the liquid in the elastic tank constitutes forced oscillations. Knowing the frequency and amplitude of the oscillations

of the ring by the equation (2.98) or (2.100), we may find the function of time $\lambda_s(t)$ and the potential of the absolute velocity will be considered determined.

Projections on the axis Ox of the dynamic force transmitted through the force ring to the body may be calculated as the sum of the pressures of the liquid in the bottom of the tank:

$$N(t)=2\pi\rho\int_0^{R_1}\left(\frac{\partial\phi}{\partial t}\right)_{x=0} r\,dr.$$

Taking into account expression (2.93) we find

$$N(t)=-\pi R_1^2 H\rho\ddot{u}_k+2\pi\rho\sum_{s=1}^{s^*} A_s\ddot{\lambda}_s\int_0^{R_1} R_s(r)X_s(0)r\,dr. \qquad (2.101)$$

11. A Mechanical Analog of Oscillations of the Liquid in an Elastic Tank

The axial dynamic force arising during forced longitudinal oscillations of the liquid are transmitted by the force ring to the body. Knowing the potential of the absolute velocities ϕ (2.93), we may calculate the pressure of the liquid in the bottom of the tank and determine the axial dynamic force. Such an algorithm of solving the problem may be introduced for calculating the forms and frequencies of the characteristic oscillations of the rocket body.

But for a calculation of the axial dynamic force from the oscillations of the liquid it is convenient to introduce a mechanical analog into the calculation of the forms and frequencies of the characteristic oscillations of the body. Since for any tone the equation (2.100), characterizing forced oscillations of the liquid in the tank, has the same structure as the formula for forced oscillations of the simplest mechanical system--a concentrated mass on a spring--then for determining the axial dynamic force of the oscillation of the liquid, we may substitute the oscillations of the concentrated masses on the springs. In such a substitution the quantity of the mass and rigidity of the spring should be selected so that the axial dynamic force from the oscillations of the liquid is equal to the dynamic force of the oscillations of the

mechanical system in any amplitude and frequency of the oscillations of the body.

Let us examine a mechanical system, the diagram of which is presented in Fig. 2.10. The concentrated mass m_s on a weightless spring with rigidity k_s is suspended from the rigid bottom of the tank, which together with the force ring oscillates along the axis of the tank by the law $u_k(t)$. We shall designate the motion of the mass m_s relative to the force ring as $\lambda_s(t)$. Each s-th tone of oscillations of the liquid corresponds to its mass m_s on the spring.

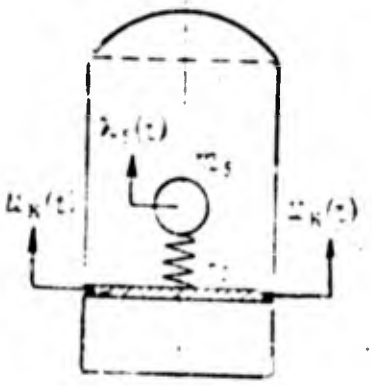

Figure 2.10

The equation of the forced oscillations of the concentrated mass may assume the form

$$m_s\ddot{\lambda}_s + k_s\lambda_s = -m_s\ddot{u}_k \tag{2.102}$$

or

$$\ddot{\lambda}_s + \omega_s^2\lambda_s = -\ddot{u}_k. \tag{2.103}$$

On the identity condition of equations (2.98) and (2.102), we find

$$m_s = A_s^2 B_s, \quad m_s = A_s C_s, \quad k_s = k_s^* A_s^2 = \omega_s^2 m_s$$

or

$$C_s = A_s B_s, \quad A_s = \frac{C_s}{B_s}.$$

Consequently, the rigidity of the spring and the concentrated mass of the mechanical system for the s-th tone of oscillation should be

$$k_s = \omega_s^2 m_s, \quad m_s = \frac{C_s^2}{B_s}. \tag{2.104}$$

Here C_s and B_s are determined by formula (2.96), and ω_s is the frequency of the characteristic oscillations of the s-th tone for the elastic tank and the liquid.

With such a selection of the quantities m_s and k_s the frequency of the characteristic oscillations of the concentrated mass on the spring will be equal to the frequency of the s-th tone of the characteristic oscillations of the liquid in the elastic tank and the function λ_s, found from a solution of the equation (2.103), will be the same as the function λ_s in equation (2.98).

We shall show that for a selected normalized eigen-vector $\overline{\beta}_s$ the sum of all concentrated masses suspended from the springs is equal to the mass of the liquid in the tank.

Let us insert equations (2.95) and (2.97) in the Lagrange equation, setting $q_n = u_k$ and $n^0 = \omega$. We obtain

$$m\ddot{u}_k + \sum_{s=1}^{\infty} A_s C_s \ddot{\lambda}_s = 0.$$

Since $A_s C_s = m_s$, then

$$m\ddot{u}_k + \sum_{s=1}^{\infty} m_s \ddot{\lambda}_s = 0. \tag{2.105}$$

We insert expression (2.102) in the Lagrange equation for $q_n = u_k$. We find

$$\ddot{u}_k \sum_{s=1}^{\infty} m_s + \sum_{s=1}^{\infty} m_s \ddot{\lambda}_s = 0. \tag{2.106}$$

From a comparison of equations (2.105) and (2.106), we obtain

$$m\ddot{u}_{\kappa}=\ddot{u}_{\kappa}\sum_{s=1}^{\infty}m_{s}.$$

Setting $\ddot{u}_k \neq 0$, we finally find

$$\sum_{s=1}^{\infty}m_{s}=m=\pi R_{1}^{2}H\varrho. \tag{2.107}$$

The mechanical system, the quantity of the concentrated mass of which is determined by formula (2.104), is suitable for combining with the body of the rocket in the calculation of the shapes and frequencies of the characteristic oscillations. If we consider a restricted number s^0 of tones of the oscillations of the liquid in the tank, then for $s > s^0$ it is necessary to set all $k_s = \infty$.

We shall verify that the axial dynamic force N, transferred to the body from the oscillations of the liquid, is the same as the axial force arising during the oscillations of the mechanical system. Since $(\phi)_{x=H} = 0$, then $X_s(H) = 0$, and

$$\int_{0}^{H}X_{s}'(x)\,dx=-X_{s}(0).$$

Taking into account this equation, we write the expression for the coefficient C_s in the form

$$C_{s}=-2\pi\varrho\int_{0}^{R_{1}}R(r)X_{s}(0)r\,dr.$$

The projection on the axis Ox of the dynamic force from the oscillations of the liquid may be calculated by formula (2.101). We write this formula as the coefficient C_s:

$$N(t)=-\pi R_{1}^{2}H\varrho\ddot{u}_{\kappa}-\sum_{s=1}^{\infty}A_{s}C_{s}\ddot{\lambda}_{s}.$$

Keeping in mind the relationship (2.107), and also the equation $m_s = A_s C_s$, we get

$$N(t) = -\sum_{s=1}^{\infty} m_s(\ddot{u}_k + \ddot{\lambda}_s). \tag{2.108}$$

The absolute acceleration of the mass m_s of the mechanical system in the direction of the axis Ox is equal to $(\ddot{u}_k+\ddot{\lambda}_s)$. The projection on the axis Ox of the dynamic force acting through the spring on the bottom of the tank, on the basis of the d'Alembert principle is equal to

$$N_s = -(\ddot{u}_k + \lambda_s)\, m_s.$$

The summation of the dynamic force transferred through the entire spring is equal to N(t) (2.108), i.e., equal to the dynamic force of the liquid. We shall now use matrix notation for determining the mass m_s of the mechanical system of the s-th tone of oscillations. From a comparison of the coefficient of equations (2.98) and (2.100) we find

$$B_s = \bar{\beta}_s' M \bar{\beta}_s, \quad C_s = (\bar{\beta}_s' \bar{F}).$$

On the basis of formula (2.104), we obtain

$$m_s = \frac{(\bar{\beta}_s' \bar{F})^2}{\bar{\beta}' M \bar{\beta}_s}. \tag{2.109}$$

Calculations show that the quantity of the mass m_s quickly decreases with an increase in the number of tones of oscillations. For example, for a tank with dimensions $R_2 = 2.25$ m, $R_1 = 1.5$ m, $H = 9$ m, $h_1 = 2.5$ mm, $h_2 = 3$ mm, $\mu = 0.3$, $\rho/\rho_0 = 0.364$, the quantities of mass of the mechanical system calculated for $n^0 = 4$ and $m^0 = 3$, are equal to [11]:

$$m_1 = 0.808\ m,\ m_2 = 0.084\ m;\ m_3 = 0.027\ m,\ m_4 = 0.0119\ m$$

Here m is the mass of all the liquid in the tank. The ratio m_s/m depends upon the level of filling H/R_1 of the tank.

References

1. Анисимов А. М. О колебаниях цилиндрической оболочки с жидкостью. Сб. «Прочность и устойчивость тонкостенных конструкций», МАИ, 1967.
2. Власов В. З. Избранные труды. Т. I, АН СССР, 1962.
3. Гонткевич В. С. Собственные колебания пластинок и оболочек, Киев, «Наукова Думка», 1964.
4. Колесников К. С. Жидкостная ракета как объект регулирования. М., «Машиностроение», 1969.
5. Кочин Е. Н. Векторное исчисление и начало тензорного исчисления. М., «Наука», 1965.
6. Курош А. Г. Курс высшей алгебры. М., Физматгиз, 1962.
7. Ламб Г. Гидродинамика. М., Гостехиздат, 1947.
8. Моисеев Н. Н., Петров А. А. Численные методы расчета собственных частот колебаний ограниченного объема жидкости. М., ВЦ АН СССР, 1966.
9. Онианашвили О. Д. Некоторые динамические задачи теории оболочек. М., изд-во АН СССР, 1957.
10. Пожалостин А. А. К расчету частот собственных колебаний полой сферической оболочки. Изв. ВУЗов, Машиностроение. Изд. МВТУ им. Баумана, 1965, № 10.
11. Пожалостин А. А. Определение параметров механического аналога для осесимметричных колебаний упругого цилиндрического сосуда с жидкостью. — Инженерный журнал МТТ, 1966, № 5.
12. Рабинович Б. И. О постановке задач динамики оболочек с жидким заполнением. Сб. V Всес. конф. по теории пластин и оболочек. М., «Наука», 1966.
13. Рапопорт И. М. Колебания упругих оболочек, частично заполненных жидкостью. М., «Машиностроение», 1967.
14. Смирнов В. И. Курс высшей математики, т. III, ч. 2. М., Гостехиздат, 1951.
15. Стрелков С. П. Введение в теорию колебаний. М., Физматгиз, 1964.
16. Тимошенко С. П., Войновский-Кригер С. Пластинки и оболочки, М., Физматгиз, 1963.
17. Шиманский Ю. А. Динамический расчет судовых конструкций. М., Судпромгиз, 1963.
18. Шмаков В. П. Об уравнениях осесимметричных колебаний цилиндрической оболочки с жидким заполнением. Изв. АН СССР, Механика и машиностроение, 1964, № 1.
19. Шклярчук Ф. Н., Осесимметричные колебания жидкости внутри упругой цилиндрической оболочки с упругим днищем. Изв вузов, Авиационная техника. Изд. Казанского авиационного института, 1965. № 4.
20. Шклярчук Ф. Н., О приближенном методе расчета осесимметричных колебаний оболочек вращения с жидким заполнением. Изв. АН СССР, Механика и Машиностроение, 1965, № 6.

Chapter 3

LONGITUDINAL VIBRATION OF A ROCKET BODY

1. Dynamic Scheme

We shall consider the construction of the rocket to be axisymmetrical. In the case of longitudinal vibrations, expansion and contraction stresses arise in cross-section of the body. Axial symmetry signifies that in a cross-section all radial directions are equivalent in relation to the distribution of masses, fluids, motions, velocities, stresses, and so forth.

A straight nonuniform rod may serve as the simplest scheme of a liquid propellant rocket for determining the forms and frequencies of longitudinal vibration. In this case, the mass of liquid in the tanks must be considered to be concentrated in a section of the body which corresponds to the location of the lower main frame of the tank. The scheme of a nonuniform rod may be used for approximate calculation in the case where the motion of the liquid fuel relative to the walls of the tank is small in the case of longitudinal vibrations and may be ignored.

In the majority of liquid fuel rockets, and firstly in large booster rockets with a pump feed system, the walls of the tank are comparatively thi. In the case of longitudinal vibrations, buckling of the bottom and bulging of the tank casings are significant, due to which the motion of the liquid relative to the tank wall in the direction of the rocket axis will also be significant. The scheme of a nonuniform elastic rod, in the mass of which is included the mass of liquid fuel, for such rockets may prove to be too crude, which will give an incorrect concept of the forms and frequencies of the eigen vibrations of the body, in particular with a large amount of fuel in the tank. The calculation of elastic longitudinal vibrations of the bodies of such rockets must be performed with regard to deformation of the bottom and radial deformations of tank casings.

In view of the structural complexity, in calculating the dynamic characteristics in first approximation it is possible to present a liquid propellant

rocket in the form of a spring-mass model, consisting of a system of elements with lumped values. It is necessary to give particular attention to the determination of such parameters of the model as the rigidity of the pump mounting and combustion chamber mounting, insofar as the attachment of the pump and engine to the body have a very strong influence on the form of the natural oscillations of the body.

For example, a spring-mass model of the two-stage rocket Titan-2 and the form of the first tone of the natural oscillations [9, 12] are given in Fig. 3.1. Localized masses are as follows: m_1 - payload mass, m_2 - mounting, bottom and 0.5 of the tank casing, m_3 - oxidizer, m_4 - bottom and 0.5 of tank casing, m_5 - section between tanks, m_6 - bottom and 0.5 of tank casing, m_7 - fuel, m_8 - bottom and 0.5 of tank casing, m_9 - rear flare of second-stage engine, m_{10} - engine, m_{11} - forward casing of first stage, m_{12} - bottom and 0.5 of tank casing, m_{13} - oxidizer, m_{14} - bottom, 0.5 of tank casing and 0.5 of section between tanks, m_{15} - bottom, 0.5 of tank casing and 0.5 of section between tanks, m_{16} - fuel, m_{17} - fuel tank cone and 0.5 of tank casing, m_{18} - turbine pump assembly, m_{19} - bottom flare of engine, m_{20} - engine.

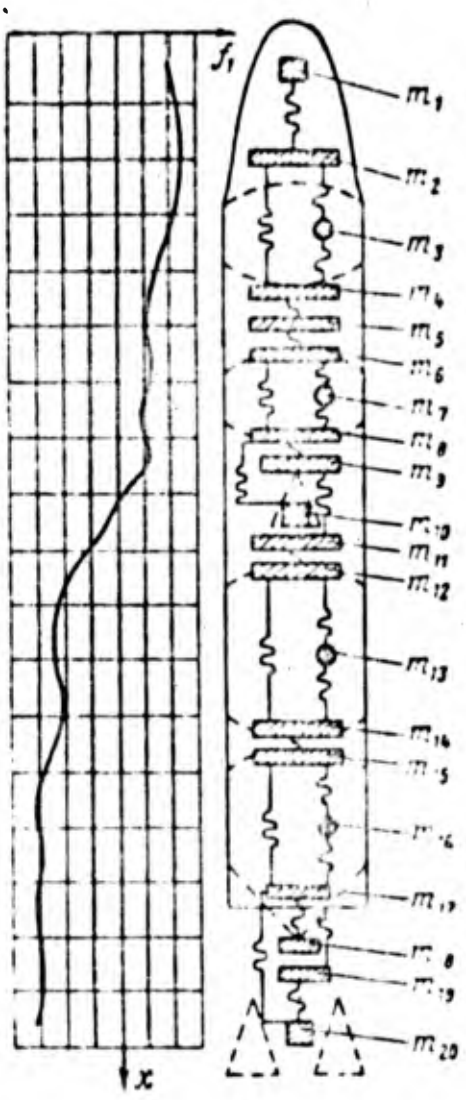

Figure 3.1

The spring-mass model gives satisfactory results in calculating the forms and frequencies of the natural oscillations of the lower tones.

In a scheme, considering the distribution of mass and rigidity longitudinally, it is necessary to more fully consider the oscillations of fluid in the elastic tanks. An elastic tank with incompressible liquid

in place of one oscillator mechanism must be replaced by a certain system of mechanical oscillators, the kinetic and potential energy of which in the case of oscillations are the same as in the case of the elastic tank with the liquid. The vibrations of each oscillator are a mechanical analog of the corresponding tone of axisymmetrical oscillations of the fluid in the elastic tank. The possibility for such a replacement is shown in Chapter 2. The total of the masses of all oscillators is equal to the mass of liquid in the tank, the frequency of natural oscillations of one oscillator is equal to the frequency of the natural oscillations of the corresponding tone of the liquid in the elastic tank. The springs of all oscillators are fixed onto the bottom of the tank, which, in an equivalent scheme, is assumed to be rigid.

The mass of an oscillator is equal to the reduced mass of an oscillating fluid of the corresponding tone of oscillations. The center of the elastic bottom of the tank is taken as the reduction point, therefore the motion of the oscillator mass in the case of oscillations of a relatively rigid bottom will characterize the motion of the center of the elastic bottom of the tank relative to the main frame. Such a selection of the reduction point simplifies the process of connecting the oscillations of the tank bottom with oscillations of the fuel in the pipes.

In the case of longitudinal oscillations in tank walls, expansion-contraction stresses arise, as in an ordinary rod. Together with the tank walls the main frame also moves in the direction of the longitudinal axis of the rocket, and the main frame excites vibrations of the oscillators through the bottom of the tank.

Since the engine and the turbine pump assembly are suspended from the body on a frame appearing as an elastic stretcher, then, in the case of longitudinal oscillations, motions of the engine and turbine pump assembly relative to the body may be replaced by motions of localized masses on springs. There is a corresponding oscillator for each tone of the elastic oscillations of the engine--a localized mass on a weightless spring.

An oscillatory system, equivalent to the elastic oscillations of an engine in the direction of the longitudinal axis of a rocket, is shown in Fig. 3.2.

Here m_{se} and k_{se} are the reduced mass and coefficient of reduced rigidity for the s-th tone of expansion-contraction oscillations of the engine.

The mass of the engine usually represents a small part of the mass of the rocket, therefore small movements of this mass relative to the rocket body can not have any significant influence on the form and frequency of the oscillations of the body. The influence of the elastic suspension of the engine will be significant only when the frequency of the oscillations of the body is close to the frequency of the natural oscillations of the engine on an elastic suspension.

A turbine pump assembly, suspended on a frame separate from the engine, in the case of longitudinal oscillations of the rocket body, may be considered as a localized mass on a spring. If the turbine pump assembly is placed in one block with the engine, then its mass must be included within the mass of the engine. In both cases it is necessary to add the mass of the liquid column included in the pipes (between the turbine pump assembly and the free surface in tanks) to the mass of the turbine pump assembly.

We shall now formulate recommendations to be used for making a dynamic diagram with distributed and localized parameters for determining the forms and frequencies of the natural longitudinal oscillations of a rocket.

The rocket body is presented in the form of a straight nonuniform rod with free ends. In cross-sections where the main frames of the tanks and engine are located, mechanical oscillators are suspended on the rod axis. These oscillators, in the case of longitudinal oscillations of the rod, imitate the axisymmetrical oscillations of liquid in the tanks and the mechanical oscillations of the engine.

In practical calculations of the forms and frequencies of the lower tones of the body oscillations it is necessary to consider only certain of the first tones of the oscillations of the liquid in a tank, therefore the number of oscillators may be small (2-3). The springs of the remaining oscillators may be considered to be rigid and the localized masses suspended on them to be coupled with the mass of the main frame of the tank.

The following are not included in the linear mass m(x) of the rod: the mass of the engine, the kind f liquid in the fuel pipes, and the basic part of the liquid of the fuel tanks, which is presented in the form of localized masses and springs. Thus, the mass of the entire rocket

$$m = \int_0^l m(x)\,dx + \sum_{(j,\,s)} m_{sj},$$

where m_{sj} is the mass of the s-th oscillator, the j-th section of the body.

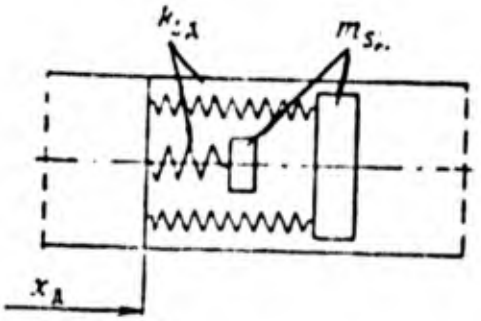

Figure 3.2

A diagram of a rocket with two fuel tanks is shown in Fig. 3.3; here the engine is represented by one oscillator.

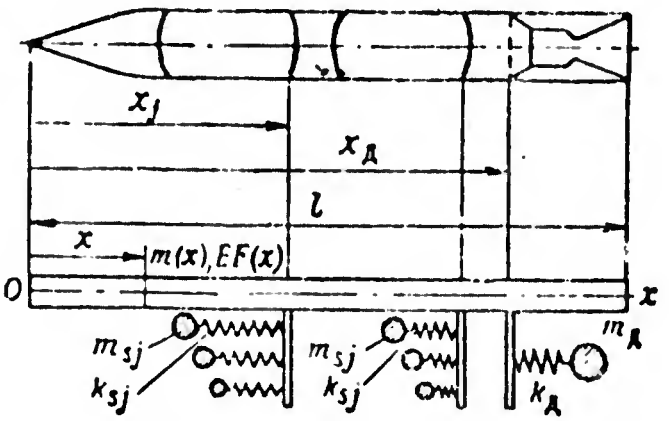

Figure 3.3

This chapter gives methods of calculating the natural and reduced longitudinal oscillations of a rocket on the basis of a nonuniform rod with elastically suspended localized masses. For methodological purposes we shall present a calculation first for a nonuniform rod, and then for a rod with elastically suspended localized masses.

2. Equation for the Longitudinal Oscillations of a Nonuniform Rod

Let the axis Ox correspond to the longitudinal axis of the rod. We shall use m(x) to designate the mass of a unit length of the rod; EF(x) to designate the expansion-contraction rigidity of the rod; q(x, t), the external distributed load; u(x, t), the motion of an arbitrary cross-section of the rod in the direction of the Ox axis.

Figure 3.4 shows an element of a rod of length dx. The left and right sections of the rod act on the separated elements with the forces N and N + (δN/δx)dx. Using d'Alembert's principle we compose an equilibrium equation of a rod element

$$\frac{\partial N}{\partial x}dx + \left[q(x, t) - m(x)\frac{\partial^2 u}{\partial t^2}\right]dx = 0.$$

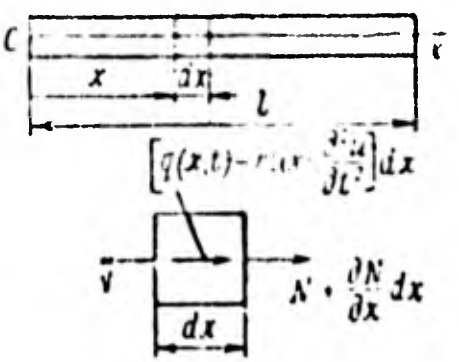

Figure 3.4

We shall apply Vogt's hypothesis [7], according to which stresses depend not only on the deformation δu/δx, but also on the rate of deformation (δ/δt)(δu/δx). Then the normal (axial) force in a cross-section is

$$N = EF(x)\frac{\partial u}{\partial x} + b(x)\frac{\partial^2 u}{\partial t\,\partial x},$$

where b(x) is the damping parameter.

The differential equation of the induced longitudinal oscillations of the rod will have the form

$$m(x)\frac{\partial^2 u}{\partial t^2} = \frac{\partial}{\partial x}\left[EF(x)\frac{\partial u}{\partial x} + b(x)\frac{\partial^2 u}{\partial t\,\partial x}\right] + q(x, t). \qquad (3.2)$$

We shall consider that

$$\frac{b(x)}{EF(x)} = 2\xi' = \text{const}.$$

We shall first examine the case where q(x, t) = 0. The general solution of equation (3.2) may be presented in the form:

$$u(x,\ t)=\sum_{n=1}^{\infty} f_n(x)\,q_n(t), \tag{3.3}$$

where $f_n(x)q_n(t)$ are the partial solutions of equation (3.2), which may be determined by Fourier's method. Having substituted the partial solution (3.3) into equation (3.2) and having separated the variables, we obtain

$$\frac{[EF(x)\,f_n']'}{m(x)\,f_n}=\frac{\ddot{q}_n}{q_n+2\xi'\dot{q}_n}=-\omega_n^2$$

or

(3.4)

$$\ddot{q}_n+2\xi_n\omega_n\dot{q}_n+\omega_n^2 q_n=0, \tag{3.5}$$

$$[EF(x)\,f_n']'=-\omega_n^2 m(x)\,f_n,$$

where $\frac{d}{dx}(\quad)=(\quad)'$; $\xi_n=\xi'\omega_n$.

The arbitrary integration constants of equation (3.4) must be determined from the initial conditions, while the arbitrary integration constants of equation (3.5) are determined from the boundary conditions, that is from the conditions of the attachment of the ends of the rod.

On each end of a free rod the force N is equal to zero. Therefore, with regard to the equalities (3.1) and (3.3) the function $f_n(x)$ must satisfy the following boundary conditions:

$$f_n'(0)=0,\quad f_n'(l)=0. \tag{3.6}$$

If one end of the rod is attached and the second is free (the rocket is located on the launch pad) then the function $f_n(x)$ must satisfy the boundary condition

$$f_n'(0)=0,\quad f_n(l)=0.$$

(3.7)

Equation (3.5) is an ordinary differential equation for the expansion of a rod under the influence of a distributed load $\omega_n^2 m(x) f_n$. Equation (3.4) shows that the natural oscillations of a rod in the presence of damping are always damped.

Energy scattering in the case of elastic oscillations of a structure takes place primarily due to friction between contiguous portions of structural units. Such friction is usually called structural. In order to calculate structural friction in differential equations, Ye. S. Sorokin [7] proposed a hypothesis according to which internal friction in the case of elastic harmonic oscillations is proportional to the elastic restoring force, but shifted in phase relative to this force at an angle of $\pi/2$. If a complex presentation of simple harmonic oscillatory motion is to be used, then instead of (3.1) the normal force may be expressed thus

$$N = \left(1 + i\frac{\psi}{2\pi}\right) EF(x)\frac{\partial u}{\partial x}, \qquad (3.1a)$$

where ψ is the coefficient of energy adsorption in the case of oscillations, equal to the ratio of energy adsorbed after one cycle ΔW to the total energy of the system W.

In the case of harmonic oscillations the absorption coefficient is equal to double the value of the decrement of free oscillations δ, so that

$$\psi = \frac{\Delta W}{W} = 2\delta.$$

Formula (3.1a) is sufficiently precise when ψ is a small value.

The differential equation of longitudinal oscillations of a rod with regard to Sorokin's hypothesis, instead of (3.2), will have the form

$$m(x)\frac{\partial^2 u}{\partial t^2} = \left(1 + i\frac{\psi}{2\pi}\right)\frac{\partial}{\partial x}\left[EF(x)\frac{\partial u}{\partial x}\right] + p(x)e^{i\omega t}. \qquad (3.2a)$$

All forms of natural oscillations $f_n(x)$ are mutually orthogonal with the weight function m(x). The orthogonality condition has the form

$$\int_0^l m(x) f_n f_m dx = 0 \qquad (n \neq m). \tag{3.8}$$

If the rod is uniform, that is, $m(x) = m_0 = \text{const}$, $EF(x) = EF_0 = \text{const}$, then equation (3.5) is simplified, and it will have the constant coefficient

$$f_n'' + a_n^2 f_n = 0, \qquad a_n^2 = \omega_n^2 \frac{m_0}{EF_0}. \tag{3.9}$$

When parameter a_n is found, the natural frequency of oscillations ω_n may be calculated according to formula

$$\omega_n = a_n \sqrt{\frac{EF_0}{m_0}} = a_n a \qquad a = \sqrt{\frac{E}{\rho}}, \tag{3.10}$$

where ρ is the density of the rod material, a is the propagation velocity of an elastic wave (the velocity of sound propagation) in the rod material.

The solution of equation (3.9), as is known, has the form

$$f_n(x) = C_1 \cos a_n x + C_2 \sin a_n x.$$

If one end of the rod is fixed and the second is free, then with regard to the boundary conditions (3.7) we find

$$a_n = \left(\frac{2n-1}{2}\right)\frac{\pi}{l} \qquad (n = 1, 2, \ldots).$$

The frequency of the natural oscillations of the n-th tone is

$$\omega_n = \frac{(2n-1)\pi}{2}\frac{a}{l}. \tag{3.11}$$

In the case of an unattached rod we have

$$a_n = \frac{n\pi}{l} \qquad (n = 1, 2, 3, \ldots) \text{ and } \quad a_n = 0.$$

The frequency of natural oscillations where $a_n \neq 0$ is

$$\omega_n = \frac{n\pi}{l} a. \tag{3.12}$$

In the case of an identical length of an unattached rod the frequency $_n$ of the first tone of the oscillations is two times greater than in the case of a rod with one fixed end. If the function $f_n(x)$ is normalized so that $f_n(0) = 0$, then $C_1 = 1$ and the form of the oscillations, corresponding to the value of $\omega_n \neq 0$ is:

$$f_n(x) = \cos \alpha_n x. \tag{3.13}$$

The first three forms of the natural oscillations of a rod are given in Fig. 3.5. We shall conditionally consider that a positive value of $f_n(x)$ corresponds to a displacement of a cross-section of the rod to the right, and a negative one to a displacement to the left. In nodal sections, displacements are absent, and the maximum contraction or expansion of the material takes place.

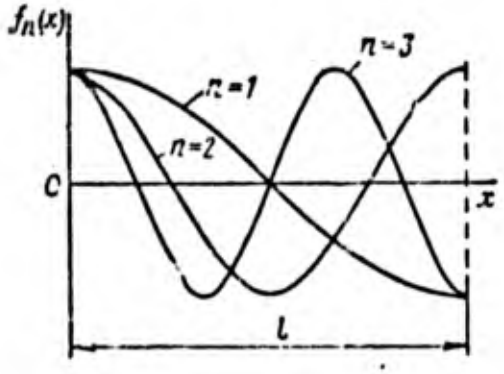

Figure 3.5

To the value $\alpha_n = 0$ correspond the frequency of the natural oscillations $\omega_n = 0$ and the form of the natural oscillations, the normalized value of which is equal to unity (3.13). This is inherent to the motion of a rod as a solid body.

Thus, for an unattached rod the complete system of natural functions will consist of a great number of functions $[f_n(x) = \cos \alpha_n x] (n = 0, 1, 2, \ldots)$. The displacement of an unattached rod along the longitudinal axis may be presented in the form

$$u(x, t) = u_M(t) + \sum_{n=1}^{\infty} f_n(x) q_n(t). \tag{3.14}$$

Here $u_M(t)$ is the displacement of the center of mass of the rod or the displacement of the rod as a rigid body; $f_n(x)q_n(t)$ is the displacement relative to the center of mass, taking place due to expansion or contraction of the rod.

We shall now turn to a calculation of forms and frequencies of the natural oscillations of a nonuniform rod.

3. Determination of the Forms and Frequencies of the Natural Oscillations of a Nonuniform Rod by Means of Successive Approximations

In order to determine the forms and frequencies of natural oscillations it is necessary to integrate equation (3.5) with the variable coefficient

$$[EF(x)f_n']' = -\omega_n^2 m(x) f_n.$$

In the case of an unattached rod the solution obtained must satisfy the boundary conditions of (3.6). With regard to these conditions we obtain

$$EF(x)f_n' = -\omega_n^2 \int_0^x m(x) f_n dx, \tag{3.15}$$

$$f_n = -\omega_n^2 \left(\int_0^x \frac{N_{1x}}{EF(x)} dx + D \right) = -\omega_n^2 \bar{f}_n, \tag{3.16}$$

where $N_{1x} = \int_0^x m(x) f_n dx$ is the axial force in a section with coordinate x.

The coefficient D may be obtained from formula

$$D = -\frac{1}{m} \int_0^l m(x) \int_0^x \frac{N_{1x}}{EF(x)} dx^2, \quad m = \int_0^l m(x) dx. \tag{3.17}$$

From equation (3.15) where $x = l$

$$\int_0^l m(x) f_n dx = 0. \tag{3.18}$$

The physical sense of this equation is given by the fact that the resultant of all inertial forces in the case of oscillations of a free rod, according to the form f_n of any tone, is equal to zero.

The method of successive approximations for determining the form of the natural oscillations of the first tone consists of the following. Any self

equilibrated form of oscillations f(x) is taken as an initial function and the following function is calculated from the distributed load m(x)f(x):

$$\bar{f}_1 = \int_0^x \frac{N_{1x}}{EF(x)}\,dx + D.$$

If the ratio $f(x)/\bar{f}$ is not a value invariable for all cross-sections of the rod, then the calculation must be repeated, taking f_1 as a new initial function. Continuing the calculation in the same order, it is possible to obtain a small difference between the functions of the two successive approximations as is desired and to obtain the desired function with the necessary degree of accuracy. The closer the initial function was to the form sought, the smaller will be the number of approximations necessary for obtaining the given degree of accuracy. In a majority of cases the solution may be obtained most readily by using the known eigen form f_1^0 of oscillations of the first tone of a corresponding uniform rod as an initial form.

In order to improve the process of convergence to the form f_1^0 it is useful to introduce correction, although the initial form of the oscillations was self-equilibrated:

$$f_1 = f_1^0 + D.$$

The coefficient D is determined from equation (3.18)

$$D = -\frac{1}{m}\int_0^l m(x) f_1^0\,dx. \qquad (3.19)$$

Using this method it is possible to determine only the form of the natural oscillations of the first tone. In order to determine the form of the natural oscillations of the second and higher tones, it is necessary to additionally fulfill the condition of orthogonality (3.18).

Let us first consider the order of calculation of the form of the natural oscillations of the second tone f_2. We shall use the function f_2, the form of a total of two functions

$$f_2 = f_2^0 + \Delta_{21} f_1 + D, \qquad (3.20)$$

where f_2^0 is the form of the natural oscillations of the second tone for a uniform free rod; and Δ_{21} is an as yet unknown coefficient, with which the function f_1, already known from the preceeding calculation, is introduced.

We substitute equation (3.20) into condition (3.8) and find the value of the following coefficient from it:

$$\Delta_{21} = -\frac{1}{m_1}\int_0^l m(x) f_1 f_2^0 dx, \qquad m_1 = \int_0^l m(x) f_1^2 dx. \tag{3.21}$$

The specific integrals, entering (3.21), are easily calculated by the tabular method, since the sub-integral functions are known. In many cases the accuracy obtained is sufficient for solving practical problems. However, if necessary, the function f_2 found according to equation (3.20) and (3.21) may be more precisely determined by the method of successive approximations examined above. In order that the condition of orthogonality not be disturbed, after each approximation it is necessary to again introduce correction according to equation (3.20), using the function f_2 instead of f_2^0 obtained in the last approximation in order to calculate the coefficient Δ_{21}. Having determined the values of the functions f_1 and f_2 with the accuracy required, it is possible to approach a determination of the function f_3, for which it is necessary that this function be given in the form of a total of functions

$$f_3 = f_3^0 + \Delta_{31} f_1 + \Delta_{32} f_2 + D. \tag{3.22}$$

Here f_3^0 is the form of the natural oscillations of the third tone for a uniform free rod.

The unknown coefficients Δ_{31} and Δ_{32} are determined from the conditions of orthogonality (3.8)

$$\int_0^l m(x) f_3 f_1 dx = 0, \qquad \int_0^l m(x) f_3 f_2 dx = 0.$$

We obtain

$$\Delta_{31} = -\frac{1}{m}\int_0^l m(x) f_1 f_3^0 dx, \quad \Delta_{32} = -\frac{1}{m_2}\int_0^l m(x) f_2 f_3^0 dx,$$

$$m_2 = \int_0^l m(x) f_2^2 dx.$$

A more precise determination of the function f_3 is made in the same order as was the case for the functions f_1 and f_2.

Now we obtain a formula for determining the frequency of natural oscillations. If the ratio $f_n/\bar{f}_n$ is constant for all cross-sections of the rod, then on the basis of equation (3.16)

$$\omega_n^2 = -(f_n/\bar{f}_n).$$

The frequency of natural oscillations may also be determined from the condition that for a conservative system in the case of natural oscillations the maximum value of kinetic energy is equal to the maximum value of potential energy. We have $T_{max} = P_{max}$. Where $q_{max} = 1$

$$T_{n\,max} = \frac{1}{2}\int_0^l m(x)(\omega_n f_n)^2 dx = \frac{1}{2}\omega_n^2 m_n,$$

$$\Pi_{n\,max} = \frac{1}{2}\int_0^l \frac{N^2}{EF(x)} dx = \frac{1}{2} k_n = \frac{1}{2}\omega_n^4 k_n',$$

where

$$m_n = \int_0^l m(x) f_n^2 dx, \quad k_n = \int_0^l EF(x) f_n'^2 dx, \quad k_n' = \int_0^l \frac{N_{1x}^2}{EF(x)} dx. \tag{3.23}$$

Here m_n is the reduced mass of the rod; k_n is the reduced rigidity of the rod. From the equality $T_{n\,max} = P_{n\,max}$ we obtain Rayleigh's formula

$$\omega_n^2 = \frac{k_n}{m_n}, \quad \omega_n^2 = \frac{m_n}{k_n'}. \tag{3.24}$$

We shall illustrate this method numerically. Curves (tables) of the distribution of mass m(x) and rigidity EF(x) along the length of the rod and f_1^0—the form of the natural oscillations of the first tone of a uniform free rod—are used as initial data for the calculation.

For convenience of calculation the scales of rigidity and mass are usually introduced:

$$EF(x)=\overline{EF}\cdot EF_0, \qquad m(x)=\bar{m}\cdot m_0.$$

The linear mass $\bar{m}$ and rigidy $\overline{EF}$ of a rod are shown in Fig. 3.6, where N = 0, 1, 2, ...—the number of the cross-section of the rod; the length of the rod l = 22.5 m. We assume that in sections N = 11, 23, and 25 there are located localized masses $\bar{m}$ of fuel in the tanks and the mass of the engine, respectively equal to 67.5, 135, and 10.5. In order that the calculation table not be too cumbersome, we shall assume the number of sections k = 15, the length of the section Δ = 1.5 m.

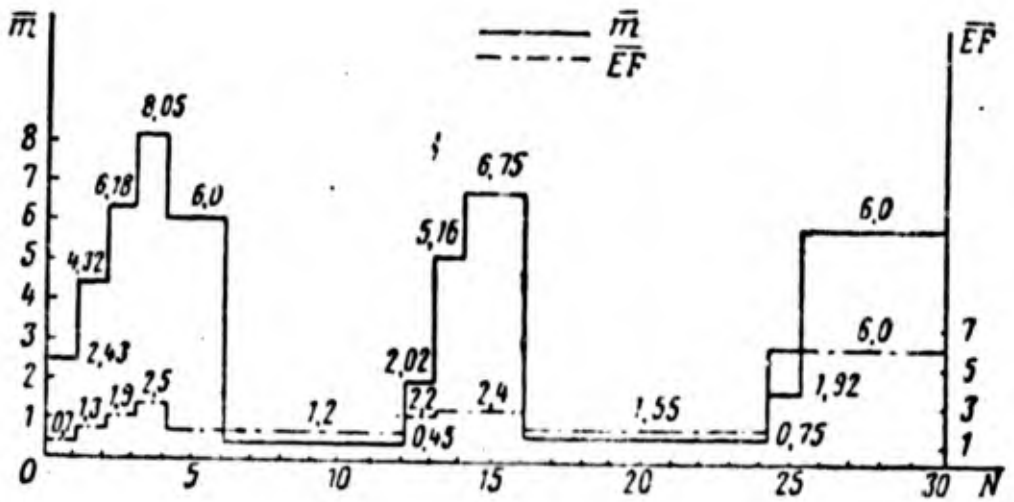

Figure 3.6

The entire calculation is given in Table 3.1. The initial data, the ordinates of the function $\overline{EF}$ and $\bar{m}$ taken from the graph of Fig. 3.6 for each section. In sections N = 6, 12, and 13 to the values of $\bar{m}$, taken from the graph, are added the values of the localized masses, distributed along the section Δ. These values are respectively equal to 45, 90, and 7. If in any section the ordinate $\overline{EF}$ or $\bar{m}$ has two extreme values, then it is necessary to take the mean value of the ordinate. Calculation of specific integrals with the use of Table 3.1 is performed by the trapezium method.

Correction in column 8 is $D' = -\dfrac{\sum_0^k \bar{m} f_1^0}{\sum_0^k \bar{m}}$.

Table 3.1

Rod Section N	$\overline{EF}$	$\bar{m}$	f_1^0	$\sum_0^N \bar{m}$	mf_1^0	$\sum_0^N \bar{m}f_1^0$	f_1^0+D'	$-\frac{f_1-f_{(8)}^*}{(8)\ N-0}$	$\bar{m}f_1$	$\sum_0^N$(10)	Correction ΔN	$N_{1,r}=$ (11) + (12)
(1)	(2)	(3)	(4)	(5)	(6)	(7)	(8)	(9)	(10)	(11)	(12)	(13)
0	0,70	2,43	1,000	2,43	2,430	2,430	1,334	1,000	2,430	0	0	0
1	1,60	5,25	0,978	10,1	5,134	9,994	1,312	0,983	5,163	7,593	0,166	7,759
2	1,85	7,02	0,913	22,4	6,409	21,538	1,247	0,935	6,562	19,318	0,332	19,650
3	1,20	3,60	0,809	33,0	2,912	30,860	1,143	0,857	3,085	28,965	0,497	29,462
4	1,20	0,45	0,669	37,0	0,301	34,073	1,003	0,752	0,338	32,388	0,663	33,051
5	1,20	0,45	0,500	37,9	0,225	34,599	0,834	0,625	0,281	33,097	0,828	33,835
6	1,70	46,23	0,309	84,6	14,285	49,109	0,643	0,482	22,285	55,578	0,994	56,567
7	2,40	5,95	0,104	136,8	0,619	64,013	0,438	0,328	1,954	79,812	1,160	80,972
8	2,00	4,15	—0,104	146,9	—0,432	64,200	0,230	0,172	0,716	82,482	1,325	83,807
9	1,55	0,75	—0,309	151,8	—0,232	63,537	—0,025	—0,019	—0,014	83,184	1,491	84,675
10	1,55	0,75	—0,500	153,3	—0,375	62,930	—0,166	—0,124	—0,093	83,077	1,656	84,733
11	1,55	0,75	—0,669	154,8	—0,502	62,054	—0,335	—0,251	—0,188	82,796	1,822	84,618
12	3,77	91,33	—0,809	246,9	—73,886	—12,334	—0,475	—0,356	—32,511	50,096	1,988	52,084

Table 3.1 (continued)

13	6,00	13,00	−0,913	351,2	−11,869	−98,089	−0,579	−0,434	−5,641	11,943	2,153	14,096
14	6,00	6,00	−0,978	370,2	−5,868	−115,826	−0,644	−0,483	−2,896	3,406	2,319	5,726
15	6,00	6,00	−1,000	382,2	−6,000	−127,694	−0,666	−0,499	−2,995	−2,485	2,485	0

N	$\frac{N_{1r}}{EF}$	$\sum_0^N$(14)	(3)·(15)	$\sum_0^N$(16)	$\bar{f}_1$=(15)+D	f_1	f_1	f_1	$\bar{m}f_1^2$	$\sum_0^N \bar{m}f_1^2$	$\frac{N_{1r}^2}{EF}$	$\sum_0^N \frac{N_{1r}^2}{EF}$
(1)	(14)	(15)	(16)	(17)	(18)	(19)	(20)	(21)	(22)	(23)	(24)	(25)
0	0	0	0	0	−528,1	1,000	1,000	1,000	2,430	2,430	0	0
1	4,849	4,849	25,4	25,4	−523,3	0,991	0,992	0,992	10,000	10,030	37,6	37,6
2	10,622	20,321	142,6	193,4	−507,8	0,961	0,994	0,965	6,540	21,740	208,7	284,0
3	24,552	55,495	199,8	535,8	−472,6	0,895	0,902	0,904	2,940	31,220	723,3	1216,6
4	27,543	107,590	48,4	784,0	−420,5	0,796	0,810	0,814	0,300	34,460	910,3	2819,7
5	28,198	163,331	73,5	905,9	−364,8	0,691	0,712	0,717	0,230	34,990	951,0	4711,0
6	33,276	224,805	10392,7	11372,1	−303,3	0,574	0,599	0,605	16,920	52,140	1882,2	7550,2
7	33,739	291,820	1736,3	23501,1	−236,3	0,447	0,471	0,476	1,340	70,400	2734,9	12164,4
8	41,904	367,463	1525,0	26762,4	−160,6	0,304	0,323	0,327	0,440	72,180	3511,9	18408,0
9	54,630	463,996	348,0	28635,4	−64,1	0,121	0,132	0,135	0,013	72,630	4625,7	26545,5
10	54,667	573,293	430,0	29413,4	45,2	−0,085	−0,084	−0,083	0,005	72,650	4632,0	35803,3
11	54,592	682,552	511,9	30355,6	154,4	−0,292	−0,300	−0,302	0,068	72,720	4619,5	45054,8
12	13,815	750,959	68585,1	99452,3	222,8	−0,422	−0,435	−0,437	17,440	90,230	719,6	50393,9
13	2,349	767,123	9972,6	178010,0	239,0	−0,453	−0,465	−0,468	2,850	110,520	33,1	51146,6
14	0,954	770,427	4622,6	192605,0	242,3	−0,459	−0,471	−0,474	1,350	114,720	5,5	51185,1
0	0	771,381	4628,3	201856,0	243,3	−0,461	−0,472	−0,475	1,360	117,420	0	51190,6

The law of the distribution of axial force along sections of the rod is obtained in column 11. At the right end of the rod (in section N = k = 15), due to the accumulation of errors, the value $\sum_0^k$ (10) differs from zero; therefore in order to complete the conditions on the right end of the rod it is necessary that correction be introduced. This correction may be considered to be linearly dependent on the length and determined according to the formula

$$\Delta_N = -\frac{N}{k}\sum_0^k (10).$$

The correction is introduced into column 13, Table 3.1.

According to formula (3.17), the coefficient is

$$D = -\frac{\sum_0^k (16)}{\sum_0^k \bar{m}}.$$

Columns 20 and 21 give the values of the function f_1 obtained in second and third approximations. We shall consider provisionally that the third approximation satisfies the required degree of accuracy.

We use the function f_1 of column 21 in order to determine the frequency of natural oscillations of the first tone. According to formulas (3.23) and (3.24) with regard to scales of mass m_0, rigidity EF_0 and the length of the rod section Δ we obtain

$$\omega_1^2 = \frac{m_0\Delta_1\sum_0^k \bar{m} f_1^2}{\frac{(m_0\Delta_1)^2\Delta_1}{EF_0}\sum_0^k \frac{N_{1x}^2}{\overline{EF}}} = \frac{EF_0}{m_0\Delta_1^2}\frac{\sum_0^k \bar{m} f_1^2}{\sum_0^k \frac{N_{1x}^2}{\overline{EF}}} =$$

$$= \frac{EF_0}{0{,}75^2 m_0}\cdot\frac{117{,}43}{51190{,}6} \approx 0{,}00408\frac{EF_0}{m_0}.$$

If we assume

$$m_0 = 15\ кГ \cdot сек^2/м,\ а\ EF_0 = 10^8\ кГ,$$

then

$$\omega_1^2 \approx 27\,000\ 1/сек^2\ (\omega_1 \approx 165\ 1/sec)$$

4. Determining the Forms and Frequencies of Natural Oscillations of a Nonuniform Rod by Means of the Initial Parameters

Beside the method of successive approximations, there are other methods for a numerical solution of the differential equations of boundary problems. Let us examine the method of initial parameters, which is suitable for a numerical solution of boundary problems on a digital computer.

The basic idea of the initial parameter method is that values of a function and its derivatives are given for one end of a rod, which, together with the differential equation, completely determine the behavior of the elastic system. In these calculations the initial parameters are given in the form of numbers and, in order to satisfy the boundary conditions on the other end, it is necessary to make some approximations. The initial parameter method is used in structural mechanics in the form of different modifications, presented at various times by Klebsch, A. N. Krylov, Sh. Ye. Mikeladze, N. I. Bezukhov, and others [4, 5, 6].

As opposed to statistical problems, in calculating elastic oscillations, it is necessary also to establish the frequency of natural vibrations, in order to know the coefficients of the differential equation.

We shall divide the rod into k sections, for each of which the coefficient

$$EF(x) = EF(x)_i, \qquad m(x) = m(x)_i$$

are considered as constant.

The differential equation (3.5) for any i-th section will have the constant coefficients

$$f''_{nl} + \alpha^2_{nl} f_{nl} = 0, \tag{3.25}$$

where

$$\alpha^2_{nl} = \frac{m(x)_l}{EF(x)_l} \omega^2_n, \tag{3.26}$$

ω_n is an arbitrary initial parameter.

As is known, equation (3.25) has a precise solution

$$f_{nl} = C_i \sin \alpha_{nl} x_i + D_i \cos \alpha_{nl} x_i \tag{3.27}$$

and its arbitrary constants may be determined by the arbitrary integration constant of the preceeding section from the conjugation conditions where $x_i = l_i$ and $x_{i+1} = 0$ (here l_i is the length of the i-th section of the rod).

At the boundary of the i-th and the i+1-th sections we have the conjugation conditions:

$$\begin{aligned} f_{nl} &= f_{n(l+1)}, \\ EF_l f'_{nl} &= (EF f'_n)_{l+1}. \end{aligned} \tag{3.28}$$

Having here substituted the equations (3.27) for the i-th and the i+1-th sections, we obtain two equations, from which we find the dependence of the constants of the i+1-th section on the constants of the i-th section:

$$\begin{aligned} C_{i+1} &= \gamma_i (C_i \cos \alpha_{nl} l_i - D_i \sin \alpha_{nl} l_i), \\ D_{i+1} &= C_i \sin \alpha_{nl} l_i + D_i \cos \alpha_{nl} l_i, \end{aligned} \tag{3.29}$$

where

$$\gamma_i = \frac{(\alpha_n EF)_i}{(\alpha_n EF)_{i+1}} = \sqrt{\frac{(mEF)_i}{(mEF)_{i+1}}}$$

Using the boundary condition on the left end of the first section $(f_{n1})_{x_1=0} = 0$ and having assumed, moreover, $(f_{n1})_{x_1=0} = 1$, we find $C_1 = 0$ and $D_1 = 1$. According to formulas (3.29) the coefficients C_i and D_i will be obtained for all sections.

The boundary condition present on the right end of the last section

$$f'_{nk}(l_k)=0 \tag{3.30}$$

is used to control the given frequency ω_n. If the frequency ω_n used in the calculation is a frequency of the natural oscillations of the rod, then the condition (3.30) will be fulfilled and the calculation of the form of the elastic oscillations may be considered to be finished.

In practical calculation, the frequency ω_n is first given approximately, therefore condition (3.30) is usually not fulfilled. In this case the calculation is repeated for several values of the frequency and $f'^{*}_{nk}(l_k)$ is calculated as a function of ω_n:

$$f'^{*}_{nk}(l_k)=C_k\cos a_{nk}l_k-D_k\sin a_{nk}l_k. \tag{3.31}$$

The value of ω_n, turning the value of $f'^{*}_{nk}(l_k)$ into zero and responding to condition (3.30), will be equal to the desired frequency of natural oscillations.

After the frequency of the natural oscillations is found, it is still impossible to say to which tone it corresponds. In order to establish the number of the tone of the oscillations, it is necessary, according to equation (3.27), to construct the function $f_n(x)$ and to determine the number of nodes, that is, the number of sections in which $f_n(x) = 0$. For longitudinal oscillations of a rod the number of the tone corresponds to the number of nodes ($n = 1, 2, \ldots$).

5. Determining the Form and Frequencies of Natural Oscillations of a Nonuniform Rod by the Finite Difference Method

One of the simplest and most universal methods for numerical solution of a boundary problem is by reducing it to a system of finite difference equations. The finite difference method is widely used for numerical solution of boundary problems on digital computers, since it reduces to a simple calculation

algorithm, and the necessary accuracy is reached by increasing the number of sections into which the basic integration segment is divided.

In order to convert from a differential equation (3.5) to a system of finite difference equations, it is necessary to divide the integration segment l into k equal portions of a length $h = l/k$. We shall designate the abscissa of the points of rod division by x_i ($i = 0, 1, 2, \ldots, k$).

We integrate equation (3.5) for x within the limits from $x_1 = x_{i-0.5}$ to $x_2 = x_{i+0.5}$, where $i > 0$:

$$\int_{x_1}^{x_2} [EF(x) f_n']' dx = -\omega_n^2 \int_{x_1}^{x_2} m(x) f_n dx.$$

We shall calculate the integral in the first member of the equality approximately and give this equality in the form

$$EF(x) f_n'|_{x_2} - EF(x) f_n'|_{x_1} = -\omega_n^2 h m(x_i) f_{ni}, \qquad (3.32)$$

where $m(x_i)$, f_{ni} is the value of the distributed mass and the value of the form of the natural oscillations of the rod at a point with the abscissa x_i.

The values of the derivatives $f_n'(x)$ at points, the abscissas of which are $x_{i+0.5}$ and $x_{i-0.5}$, will be replaced by their finite difference expressions:

$$f_n'(x)|_{x_i+0,5} = \frac{f_n(x_{i+1}) - f_n(x_i)}{h},$$

$$f_n'(x)|_{x_i-0,5} = \frac{f_n(x_i) - f_n(x_{i-1})}{h}.$$

Substituting these expressions into equation (3.32), we obtain

$$EF(x_{i+0,5})[f_n(x_{i+1}) - f_n(x_i)] - EF(x_{i-0,5})[f(x_i) - f_n(x_{i-1})] = -\omega_n^2 h^2 m(x_i) f_n(x_i).$$

After transformation we obtain

$$f_n(x_{i+1}) = f_n(x_i)\left[1 + \frac{EF(x_{i-0,5})}{EF(x_{i+0,5})} - \frac{\omega_n^2 h^2 m(x_i)}{EF(x_{i+0,5})} - \right.$$

$$\left. - \frac{EF(x_{i-0,5})}{EF(x_{i+0,5})} f_n(x_{i-1}) \right. \qquad (i = 1, 2, \ldots, k-1) \qquad (3.33)$$

Having set the value of ω_n^2, according to equation (3.33), it is possible to calculate the coefficient of the form of the natural oscillations for any point x_{i+1} according to the values of the coefficient in the preceeding two points x_i and x_{i-1}. The calculation must be performed from the point x_0 to the point x_k.

The values of the coefficients of the form in the first two points are obtained from the boundary condition where $x = x_0$ and the scale selected for the function $f_n(x)$. We select the scale for $f_n(x)$ so that $f_n(x_0) = 1$, and from boundary condition (3.6)

$$f_n'(x_0) = \frac{f_n(x_1) - f_n(x_0)}{h} = 0$$

we obtain $f_n(x_1) = 1$.

Further solution reduces to a variation of the parameter ω_n^2 in order that the boundary condition (3.6) at the point x_k be satisfied:

$$f_k'(x_k) = \frac{f_{nk} - f_n(k-1)}{h} = 0. \qquad (3.34)$$

For this it is necessary to calculate the numbers $(\omega_n) = f_{nk} - f_{n(k-1)}$ and $(\omega_n + \Delta\omega_n)$ and, observing $(\omega_n)\ (\omega_n + \Delta\omega_n)$ for the sign of the product, to select ω_n in such a sequence as was recommended in the preceeding section.

The sequence of solving equation (3.5) by means of transformation to equations with constant coefficients and the application of the initial parameter method is essentially identical with calculation according to the finite difference method. In both methods it is necessary to establish the initial parameter—the frequency ω_n and to seek a value of ω_n whereby the boundary condition on the right end of the rod is satisfied. In the case of the application of the initial parameter method, the number of sections may be small,

that is, it is determined by the properties of the functions m(x) and EF(x). However, in the process of calculation it is necessary to calculate the function $\sin \alpha_{ni} l_i$ and $\cos \alpha_{ni} l_i$. Calculation by the finite difference method is simpler, but the number of sections is much greater.

If the rigidity of EF(x) or a linear mass m(x) of the rod in certain sections with abscissas x_i, $x_{i-\frac{1}{2}}$, and $x_{i+\frac{1}{2}}$ varies gradually, then in calculation by the finite difference method the values EF(x) and m(x) in these sections must be considered to be equal to half totals of the corresponding ordinates.

6. Oscillations of the Engine as a Mechanical System

The engine is a source of tractive force, which is transmitted through the frame to the rocket body. With all other conditions being equal, the induced oscillations of the rocket will be the greater, the greater the operation of tractive force is on displacements of the point of application of this force, arising during oscillations. The engine as a mechanical system, possessing a mass and elasticity, oscillates together with the body and, consequently, influences the form and frequency of the natural oscillations of the body. Therefore, an analysis of the mechanical oscillations of the engine is of important significance, both in regards to a calculation of the influence of these oscillations on the form and frequency of the natural oscillations of the body, as well as in regard to a determination of displacements of the engine relative to the body, on which the operation of the tractive force depends.

The simplest scheme for calculating the mechanical oscillations of the engine may be given by one mechanical oscillator, the localized mass of which m_e is equal to the reduced mass of the engine and frame. In this scheme the engine is considered to be a solid body, and the suspension of the engine to be a weightless spring. The frequency of the natural oscillations of the engine relative to the rocket body is determined by Rayleigh's method. We shall consider that the engine frame is made of elastic rods (beams), whereby the engine is suspended on the frame symmetrically relative to the supports.

Due to the elasticity of the rocket body shell the frame supports, fixed on the body, are elastic with a total coefficient of rigidity k. The scheme of the elastic system for determining the frequencies of the natural oscillations is given in Fig. 3.7. Static displacement of the engine consists of two parts: static sag of the supports x_0 and static deflection of the frame from the elastic line $f(y_1)$. The scale of static displacement η is expressed so that the total displacement of the mass of the engine is equal to unity, that is,

$$\eta\left[f\left(\frac{l_1}{2}\right)+x_0\right]=1. \tag{3.35}$$

The reduced mass of the engine and frame are

$$m_e=m_e'+\eta^2\int_0^{l_1} m(y_1)[f(y_1)+x_0]^2 dy_1. \tag{3.36}$$

Here $m(y_1)$ is the linear mass of the engine frame, m_e is the mass of the engine. In the case of the scale selected, the coefficient of reduced rigidity k_e is numerically equal to twice the value of the potential energy of the system:

$$k_e=\eta^2 k x_0^2+\eta^2\int_0^{l_1} EJ(y_1) f''^2(y_1) dy_1. \tag{3.37}$$

The potential energy may be calculated also by the operation of the force of gravity. We shall have

$$k_e=gm_e'+g\eta\int_0^{l_1} m(y_1)[x_0+f(y_1)]dy_1, \tag{3.38}$$

where g is the acceleration of terrestrial gravity.

The frequency of the natural oscillations of an elastically suspended engine will be calculated according to Rayleigh's formula

$$\omega_e=\frac{k_\Sigma}{m_\Sigma}. \tag{3.39}$$

In the case of longitudinal oscillations of the body, expansion-contraction oscillations of the engine as an elastic body may be observed. They will

be significant if the natural frequencies of such oscillations are close to the frequencies of the rocket body oscillations. An analysis of these oscillations is of interest for evaluating the stability of the engine and for more precisely determining the reduced thrust.

Selection of a scheme for determining the form and frequencies of expansion-contraction oscillations of the engine depends on the construction of the engine and the method of its attachment to the frame, and also on the purposes of the calculation. For example, the frame together with the engine may be considered to be an elastic system in the form of a nonuniform rod. The form of the natural oscillations of the first and second tones of such a system are given in Fig. 3.8. For each tone of the natural oscillations an equivalent system may be presented by one oscillator.

If the mass of the frame is small in comparison with the mass of the engine, and the rigidity of the frame is great, then the natural expansion-contraction oscillations of the engine may be analyzed individually, assuming the region where the engine is attached to the frame to be immobile. In such a scheme the frame may be presented in the form of an individual oscillatory system with one degree of freedom.

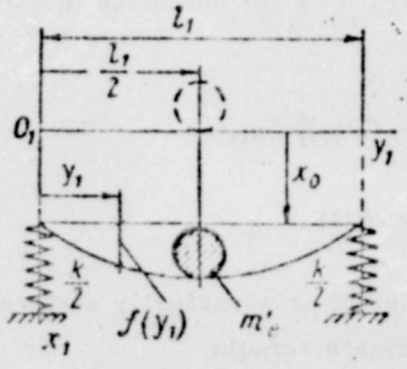

Figure 3.7

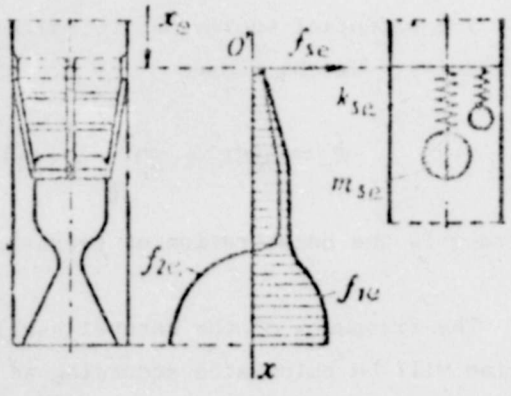

Figure 3.8

In the case of longitudinal oscillations of the body the oscillations of the engine as a mechanical system may be considered to be forced oscillations caused by the displacement of the suspension point. The amplitude of

induced oscillations of a concentrated mass of an oscillatory (we assume $\eta_n = 1$)

$$f_{nse} = f_n(x_e) \frac{1}{1 - \left(\frac{\omega_n}{\omega_{se}}\right)^2} \qquad (\omega_n \neq \omega_{se}), \tag{3.46}$$

where $f_n(x_e)$, ω_n are the amplitude and frequency of oscillations of the suspension point of the engine; ω_{se} is the frequency of natural oscillations of the s-th numbered oscillator.

The coefficient f_{nse} will significantly differ from the coefficient $f_n(x_e)$ if the frequency of natural oscillations of the s-th numbered tone of the engine ω_{se} is close to the frequency of the natural oscillations of the rocket body. In analyzing the stability of a closed rocket system with a liquid propellant engine, both the value and the sign of the coefficient f_{nse} are of great significance. If the frequency of the natural oscillations of the engine is significantly greater than the frequency of oscillations of the rocket body, that is, ω_{se} is much greater than ω_n, and the mass of the engine is small in comparison with the mass of fuel in the tanks, then in the case of calculating the longitudinal oscillations of the rocket body, the elasticity of the engine suspension cannot be considered. In this case the masses of the engine and frame must be considered to be localized in a cross-section of the body with the coordinate x_e.

For the first tone of natural oscillations of the body the ratio of frequencies $\omega_e \gg \omega_n$ usually is fulfilled. However, for higher tones the frequencies ω_{se} and ω_n may be close, and then it is necessary to consider the elasticity of the engine suspension in order to study longitudinal oscillations.

7. Determining the Forms and Frequencies of the Natural Oscillations of a Rocket Body

The model of a straight nonuniform rod with elastically suspended localized masses is used to determine the forms and frequencies of the natural longitudinal oscillations of a rocket body. These masses on springs, appearing as the mechanical analog of the oscillations of the engine and liquid in elastic tanks,

are suspended on the axis of symmetry in cross-sections of the rod corresponding to the location of the main frames of the bottom of the tanks and engine (see Fig. 3.2). A mechanical oscillator with a mass m_{sj} and a spring rigidity k_{sj} corresponds to each s-th numbered tone of the oscillations of the fluid. The supplementary index j designates a cross-section with abscissa x_j. For example, if for a one-stage rocket the upper tank is labelled A and the lower B, then for the upper tank j = A, and for the lower j = B. The localized masses m_{sj} and the frequencies of their natural oscillations are determined by the method presented in Chapter 2.

We replace the engine as a mechanical system with one mechanical oscillator which is suspended in a section with abscissa x_e (j = E). If it becomes necessary to consider several tones of the elastic oscillations of the engine, then it is necessary to place several oscillators in this section. We consider that the turbine pump assembly is rigidly connected with the engine and is included in the mass m_e: the mass of the engine, the mass of the turbine pump assembly, and the mass of the liquid fuel located in the conduits below the bottom of the tanks. The method of successive approximations may be successfully used for determining the forms and frequencies of the lower tones of the natural oscillations of a nonuniform rod with elastically suspended localized masses; for high tones of the oscillations the solution is derived very slowly.

We will use the initial parameter method, which was presented in section 4, in order to calculate the forms and frequencies of the natural oscillations of a nonuniform rod. We divide the rod into sections of constant rigidity EF(x) and linear mass m(x). The length of the sections l_i may be different.

If between uniform sections i and i+1 there is a section with elastically suspended localized masses, then on the transition from the i-th to the i+1-th section a jump in the normal (axial) force will be observed equal to the total of the reactions of the oscillator springs (Fig. 3.9). The conjugation conditions of such sections are

$$f_{ni}(l_i) = f_{n(i+1)}(0),$$

$$EF(l_i) f'_{ni}(l_i) = [EF(0) f'_n(0)]_{i+1} + \sum_{s=1}^{s^0} \Delta N_{sj}, \tag{3.41}$$

where N_{sj} is the normal force, applied to a cross-section through the spring of the s-numbered oscillator; s^0 is the number of oscillators.

The force N_{sj} is numerically equal to the inertial force of the s-numbered localized mass. In order to make the signs of the projections of the forces EFf_n' and N_{sj} agree, we turn to equation (3.15). If the function f_n is known, then according to this equation it is possible to calculate the axial force in any cross-section. On the basis of (3.15) it is possible to establish that where $\int_0^x m(x) f_n dx > 0$ the following pressing force arises in a cross-section

$$EF(x) f_n' = -\omega_n^2 \int_0^x m(x) f_n dx. \tag{3.42}$$

Since all localized masses are displaced with a frequency of body oscillations $_n$, then the force is

$$N_{sj} = -\omega_n^2 m_{sj} f_{nsj}, \tag{3.43}$$

where f_{nsj} is the value of the coefficient of the form of the oscillations of mass m_{sj}, suspended in the j-th section with the n-th tone of the body oscillations.

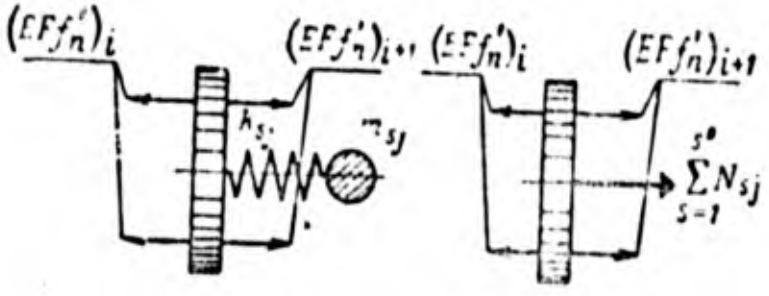

Figure 3.9

The value f_{nsj} is determined according to formula (3.38)

$$f_{nsj} = f_n(x_j) \frac{1}{1 - \left(\frac{\omega_n}{\omega_{sj}}\right)^2}, \tag{3.44}$$

where $f_n(x_j)$ is the value of the coefficient of the form of body oscillations in a section with abscisse x_j; ω_{sj} is the frequency of the natural oscillations of the s-th numbered oscillator in the j-th section.

We obtain formulas for calculating coefficients D_{i+1} and C_{i+1} of the section i+1 through the coefficient D_i and C_i of the i-th section, when the j-th section with s^0 oscillators is located between these sections. Bearing in mind that

$$f_{ni}(l_i) = f_{n(i+1)}(0) = f_n(x_j),$$

on the basis of equations (3.27) and (3.41)-(3.44) we find

$$\begin{aligned} D_{i+1} &= C_i \sin \alpha_{ni} l_i + D_i \cos \alpha_{ni} l_i, \\ C_{i+1} &= (C_i \zeta_i + \zeta_{nj} D_i) \cos \alpha_{ni} l_i + (\zeta_{nj} C_i - \zeta_i D_i) \sin \alpha_{ni} l_i, \end{aligned} \tag{3.45}$$

where

$$\zeta_i = \sqrt{\frac{(mEF)_i}{(mEF)_{i+1}}},$$

$$\zeta_{nj} = \frac{\omega_n^2}{(EF\alpha_n)_{i+1}} \sum_{s=1}^{s^0} \frac{m_{sj}}{1 - \left(\frac{\omega_n}{\omega_{sj}}\right)^2}. \tag{3.46}$$

Only one localized mass m_e is suspended in the section with abscissa $x_j = x_e$. Therefore for the coefficient β_{ne}, formula (3.46) acquires the form

$$\zeta_{ne} = \frac{\omega_n^2}{(EF\alpha_n)_{i+1}} \frac{m_e}{1 - \left(\frac{\omega_n}{\omega_e}\right)^2} \qquad (\omega_n \neq \omega_e). \tag{3.47}$$

Calculation of the form of the oscillations proceeds from the left end of the rod to the right. Having selected the scale of the form of oscillations so that at the left end of the rod the value of the coefficient of the form was equal to unity, that is, $f_{n1}(0) = 1$, and bearing in mind that at the left free end $f'_{n1}(0) = 0$, we find the coefficients of the first section $D_1 = 1$ and $C_1 = 0$. Then according to formula (3.29), we calculate the coefficient D_{i+1} and C_{i+1} for the subsequent sections. Transition through the j-th section, in which the localized masses are suspended, is performed according to formulas (3.45)-(3.47). The boundary condition at the right end of the last k-th section

$$f'_n(l_k)=0$$

is used for verifying the correctness of selecting the frequency ω_n. The sequence of selecting the frequency is given in section 4.

After determining the frequency of the natural oscillations ω_n from equation (3.27) we obtain the form of the natural oscillations for all sections of the rod, and from formula (3.44), the value of the coefficients of the form for all elastically suspended localized masses.

For an unattached rod without elastically suspended masses the number of oscillations corresponds to the number of nodal sections of the rod (see Fig. 3.5). For a rod with elastically suspended masses where ω_n is not equal to zero, forms of natural oscillations may exist whereby the rod does not have nodal sections.

For illustration we shall examine the simplest example—longitudinal oscillations of a free straight uniform rod with one elastically suspended localized mass on the right end (Fig. 3.10).

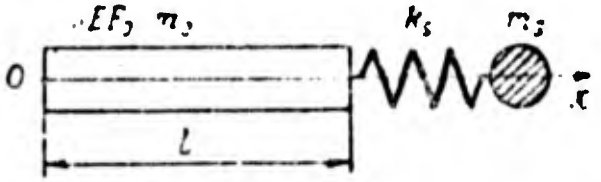

Figure 3.10

The value of the coefficient of the form of the natural oscillations of mass m_s is determined according to formula (3.44) and

$$f_{ns}=f_n(l)\frac{1}{1-\left(\frac{\omega_n}{\omega_s}\right)^2} \qquad (\omega_n \neq \omega_s),$$

where ω_n is the frequency of the natural oscillations of the system; ω_s is the frequency of the natural oscillations of the mass m_s with an immobile suspension point of the spring; $f_n(l)$ is the value of the coefficient of the form of oscillations on the right end of the rod.

The elongation of the spring is equal to the difference of displacements

$$f_{ns} - f_n(l) = f_n(l)\frac{1}{\left(\frac{\omega_s}{\omega_n}\right)^2 - 1}. \qquad (\omega_s \neq \omega_n)$$

The boundary condition at the right end of the rod may be presented in the form

$$EF_0 f_n'(l) = k_s f_n(l)\frac{1}{\left(\frac{\omega_s}{\omega_n}\right)^2 - 1},$$

where k_s is the stiffness factor of the spring.

From equation (3.27) and the boundary condition $f_n'(0) = 0$ we find

$$f_n = D\cos\alpha_n x.$$

Substituting this expression into the boundary condition at the right end of the rod, we obtain the following transcendental equation for determining the frequencies of the natural oscillations of the system:

$$-EF_0\alpha_n \sin\alpha_n l = k_s \frac{1}{\left(\frac{\omega_s}{\omega_n}\right)^2 - 1}\cos\alpha_n l.$$

Since $\omega_n^2 = \alpha_n^2 a^2$, $a^2 = \frac{EF_0}{m_0}$, then the equation of the frequencies may be presented in the form

$$\operatorname{tg}\alpha_n l = -\frac{k_s}{m_0}\frac{\alpha_n}{\omega_s^2 - a^2\alpha_n^2}.$$

Here the values l, k_s, ω_s, a, and m_0 are considered to be known.

The roots of the frequency equation may be determined using a trigonometrical tables. Figure 3.11 graphically illustrates determination of the roots using graphs of the functions. Here solid lines are used to show a graph of the function found in the left member of the frequency equation, and dotted lines to indicate the functions in the right member of the equation. The intersections of the lines give the values of the roots of the equation. If the stiffness factor of the spring k_s is equal to zero (a rod without a localized mass), then the dotted line coincides with the axis of abscissas, and

the roots of the equation, corresponding to non-zero frequencies will be

$$\alpha_n l = np \quad (n = 1, 2, \ldots).$$

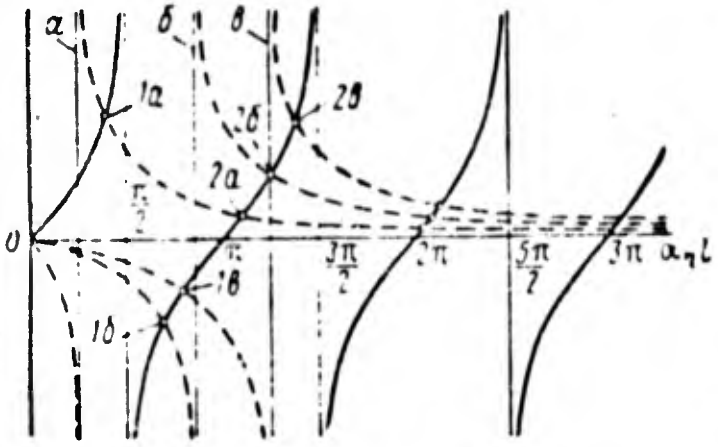

Figure 3.11

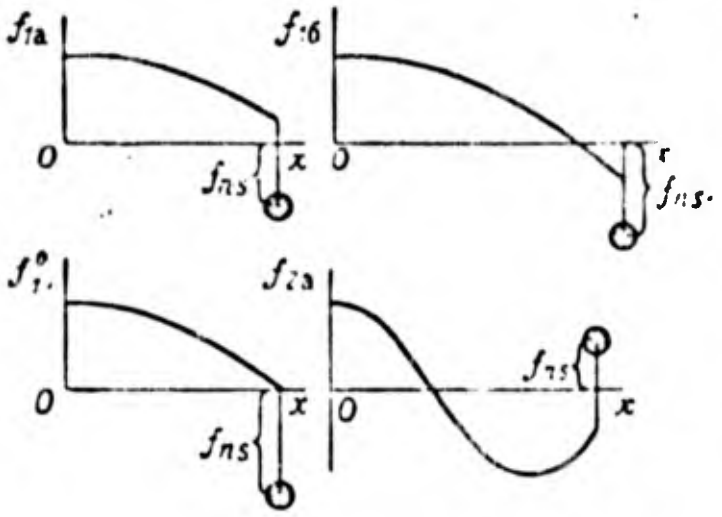

Figure 3.12

Where $k_s \neq 0$, the graphs of the functions for the right member of the equation are given in Fig. 3.11 for three different ratios:

$$1)\ 0 < \omega_s < \frac{\pi a}{2l}, \quad 2)\ \frac{\pi a}{2l} < \omega_s < \frac{\pi a}{l}, \quad 3)\ \frac{\pi a}{l} < \omega_s < \frac{3\pi a}{2l}.$$

The first root of the equation, corresponding to a non-zero frequency of the system, is determined respectively by the intersections 1a, 1b, and 1c, the second root by the points 2a, 2b, and 2c. The forms of the natural oscillations of the system, corresponding to frequencies determined by the intersections 1a, 1b, and 2a are shown in Fig. 3.12.

If a localized mass on a spring and an unattached rod are considered as separate oscillatory systems, the frequencies of the natural oscillations of these partial systems will be respectively equal to ω_s, $\pi a/l$, $2\pi a/l$, $3\pi a/l$,...

Where $$\frac{\pi a}{2l} < \omega_s < \frac{3\pi a}{2l},$$

then the first frequency of the system, consisting of a rod with an elastically suspended localized mass, is below the lowest partial frequency, and the

second frequency of the system is higher than the second partial frequency. With an increase in the number of the tone of oscillations, the frequency of the system will differ even less from the partial frequency of the rod.

Where $$\omega_s < \frac{\pi a}{2l},$$

then the first and second frequency of the system are higher than the corresponding partial frequencies (in Fig. 3.11, the intersections 1a and 2a). The forms of the natural oscillations of the first and second tones, corresponding to such a ratio of partial frequency is given in Fig. 3.12 by the graphs f_{1a} and f_{2a}. In the case of oscillations of the first tone in the rod there will be no nodal section and in the case of oscillations of the second tone in the rod there will be one nodal section.

If $\omega_s << \pi a/2l$, then the form of the natural oscillations will correspond to the lowest frequency of the system, then the entire rod as a rigid body is displaced in the direction opposite the direction of displacement of the localized mass m_s. The system appears as two masses connected with a spring. The frequency of the natural oscillations of such a system, as is known, is higher than any of the partial frequencies

$$\sqrt{\frac{k_s}{m_s}} \text{ and } \sqrt{\frac{k_s}{m_0 l}}.$$

Several peculiarities arise when

$$\omega_s = \frac{n\pi a}{2l} \quad (n = 1, 3, \ldots),$$

and are explained by the fact that the numbers $n\pi/2$ are eigen values of the system. The form of the natural oscillations of the first tone f_1^0 is shown in Fig. 3.12. For a rod it corresponds to the form of its natural oscillations in the case of an attached right end. Here we have a case where both partial oscillatory systems have the same immobile point and perform oscillations relative to it with the same frequency independently. The frequency of the system is equal to the partial frequency of the oscillations of a rod, one end of which is fixed. The value of the coefficient of the form f_{ns} of

elastic oscillations of a localized mass in this case cannot be calculated according to formula (3.44). It may be determined from the condition that the center of mass of the system is not displaced in the case of natural oscillations:

$$m_0 \int f_n^0 dx + f_{ns} m_s = 0.$$

Since,

$$f_n^0 = \cos \frac{n\pi}{2l} x,$$

then

$$f_{ns} = -\frac{m_0 l}{m_s} \frac{2}{n\pi} \sin \frac{n\pi}{2} \quad (n = 1, 3, 5, \ldots).$$

Analogous peculiarities in calculation may arise even in the case of a nonuniform rod with elastically suspended localized masses if the frequency of the system proves to be equal to one of the partial frequencies of elastically suspended localized masses. In this case we assume $\omega_n = \omega_{s*j}$ and determine the form of the oscillations, eliminating the term with index s*j in formula (3.46) under the sign of the total, whereby $\omega_n = \omega_{s*j}$. The value of the coefficients of the forms of oscillations of localized masses for which $\omega_n \neq \omega_{sj}$ is calculated according to formula (3.44). The value of the coefficient of the form of oscillations f_{ns*j} for the localized mass m_{s*j} is determined from the condition that the center of mass of the system is not displaced in the case of natural oscillations:

$$\int_0^l m(x) f_n dx - \sum_{(s,j)} m_{sj} f_{ns*j} + m_{s*j} f_{ns*j} = 0.$$

After determining f_{ns*j} we more accurately determine the form of the natural oscillations. In formula (3.46) for β_{nj} under the sign of the total we exclude the term with the index s*j, and the influence of axial force

$$N_{s*j} = -\omega_n^2 m_{s*j} f_{ns*j}$$

from the mass m_{s*j} on the form of the natural oscillations may be considered by means of altering the structure of the second equality (3.45):

$$C_{i+1} = (\beta_i C_i + \gamma_{nj} D_i) \cos \alpha_{ni} l_i + (\gamma_{nj} C_i - \beta_i D_i) \sin \alpha_{ni} l_i + \frac{\omega_n^2}{(EF\alpha_n)_{i+1}} m_{s*j} f_{ns*j}.$$

Having determined the form of the natural oscillations of the rod, according to formula (3.44), we calculate the new values of the coefficients of the form of the elastic oscillations of the localized masses m_{sj} (except for m_{s*j}) and we find a second approximation for f_{ns*j}. Further approximation is performed in the same order.

If several localized masses with different partial frequencies ω_{sj} are suspended from a nonuniform rod, then in order to determine the forms of the natural oscillations as first approximation for the frequency ω_n it is necessary to assume a value less than the lowest of the partial frequencies ω_{sj}, and approximation in frequency is made with the small $\Delta\omega_n$.

We shall now examine a determination of the forms and frequencies of the natural oscillations of a rod by the finite difference method, whereby the linear mass m(x) and rigidity EF(x) of a rod may be variable along the length of a section. For a nonuniform rod the method of calculation is given in section 5. Here we turn our attention only to peculiarities introduced by the presence of elastically suspended localized masses. The values of the coefficient of the form of natural oscillations in the i+1-th section, if the values of the coefficients of this form in the i-th and the i-1-th sections are known, may be calculated according to formula (3.33), obtained after integrating the differential equation (3.5) and replacement of the derivatives by finite differences:

$$f_{n(i+1)} = f_{ni}\left[1 + \frac{EF_{i-1/2}}{EF_{i+1/2}} - \frac{\omega_n^2 m_i h^2}{EF_{i+1/2}}\right] - \frac{EF_{i-1/2}}{EF_{i+1/2}} f_n(i-1) \quad (i = 1, 2, \ldots, k-1) \tag{3.48}$$

For the purposes of calculation we divide the length of the rod into k equal sections: the length of a section of rod between two neighboring sections is $h = l/k$. Among the k sections of rod will be those to which localized masses are suspended on springs. For these sections equations (3.5) and (3.48) are unacceptable.

Let, for example, the localized masses m_{sj} be suspended on the j-th section between the i-th and the i+1-th points of the rod, similar to that as is shown in Fig. 3.9. The values of the function f_{ni} at the i-th and all preceding points of the rod are calculated according to equation (3.48). Having assumed d'Alembert's principle, we write the equilibrium equation for the section of rod located between the i-th and the i+1-th points. We obtain

$$EF_i f'_{ni} = EF_{i+1} f'_{n(i+1)} + m_i h \omega_n^2 f_{ni} + \sum_{(s)} N_{sj}.$$

Having replaced the derivatives in this equation by finite differences

$$f'_{ni} = \frac{f_{n(i+1)} - f_{n(i-1)}}{2h}, \quad f'_{n(i+1)} = \frac{f_{n(i+2)} - f_{ni}}{2h}, \tag{3.49}$$

we obtain

$$EF_i \frac{f_{n(i+1)} - f_{n(i-1)}}{2h} = EF_{i+1} \frac{f_{n(i+2)} - f_{ni}}{2h} + m_i h \omega_n^2 f_{ni} + \sum_{(s)} N_{sj}.$$

The

The value of the function $f_{n(i+2)}$ is calculated according to equation (3.48), considering $f_{n(i+1)}$ to be known:

$$f_{n(i+1)} = \frac{a}{b} f_{ni} + c f_{n(i-1)} + d \sum_{(s)} N_{sj},$$

Eliminating $f_{n(i+2)}$ from the last two equations, we find

(3.50)

where

$$a = 1 + \frac{EF_{i+1/2}}{EF_{i+3/2}} - \frac{2h^2 \omega_n^2 m_i}{EF_{i+1}},$$

$$b = 1 + \frac{EF_{i+1/2}}{EF_{i+3/2}} - \frac{h^2 \omega_n^2 m_{i+1}}{EF_{i+3/2}},$$

$$c = -\frac{1}{b}\frac{EF_i}{EF_{i+1}},$$

$$d = -\frac{1}{b}\frac{2h}{EF_{i+1}}.$$

The value of the axial force N_{sj} is calculated according to formulas (3.43) and (3.44). Since in this calculation the integration step h is usually taken as small, then in these formulas, instead of the coefficient f_{nj}, it is possible to use the coefficient f_{ni}. Then we obtain

$$N_{sj} = -\frac{\omega_n^2 m_{sj} f_{ni}}{1 - \left(\frac{\omega_n}{\omega_{sj}}\right)^2} \qquad (\omega_n \neq \omega_{sj}). \tag{3.51}$$

The following sequence of calculations is recommended for determining the forms and frequencies of the natural oscillations of a nonuniform rod with elastically suspended localized masses. We shall assign the frequency of oscillations of the system ω_n, and for each point on the rod shall find the values m_i, $EF_{i+\frac{1}{2}}$. We shall select the scale of the form of natural oscillations so that at the left end of the rod $f_{n0} = 1$. From the boundary condition on the left end of the rod we find $f_{n1} = 1$.

According to equation (3.48) we calculate the coefficient f_{ni} sequentially for all points of the rod, preceeding the first j-th section with elastically suspended localized masses. The transition from the i-th to the i+1-th point, between which the j-th section with localized masses is located, is made according to formulas (3.50) and (3.51). And thus up to the point when we reach the right end of the rod. Further solution leads to finding such a value of ω_n whereby the boundary condition at the right end of the rod is satisfied (3.34). The sequence of determining ω_n is shown in the preceeding section.

For the value of the frequency of natural oscillations obtained ω_n, we find the values of the coeficients of the form of the natural oscillations at all points in the rod. Values of the coefficient of the form f_{nsj} for the

s-numbered localized mass is determined according to formula (3.44), in which we assume $f_n(x_j) = f_{ni}$:

$$f_{nsj} = \frac{f_{ni}}{1 - \left(\frac{\omega_n}{\omega_{sj}}\right)^2} \qquad (i < j < i + 1).$$

We shall illustrate the method of determining the forms and frequencies of the natural oscillations of a rocket body with a numerical example. We shall consider only the first tone of the axisymmetrical oscillations of the liquid in an elastic tank and the first tone of the oscillations of the engine relative to the rocket body. For a single-stage rocket we shall use a straight nonuniform rod with free elastically suspended masses (Fig. 3.13) as a calculation model. The localized masses m_A, m_B, and m_E are equal, respectively, to the masses of liquid in the tanks A and B and the mass of the engine.

We assume the length of the body l, the distribution of rigidity EF(x) and the mass m(x) to be the same as in the numerical example in section 3. Such a selection of initial data gives the possibility of comparing results of calculations for two systems: for the model of a nonuniform rod and for the model of a nonuniform rod with elastically suspended localized masses. For calculation we assume

$$l = 22{,}5\ м; \quad EF(x) = EF_0\overline{EF}; \quad m(x) = m_0\overline{m};$$
$$\overline{m}_A = 67{,}5; \quad \overline{m}_B = 135; \quad \overline{m}_E = 10{,}5; \quad m_1 = m_0\overline{m}_A;$$
$$m_B = m_0\overline{m}_B; \quad m_2 = m_0\overline{m}_E; \quad m_0 = 15\ кГ\ сек^2/м;$$
$$EF_0 = 10^8\ кГ.$$

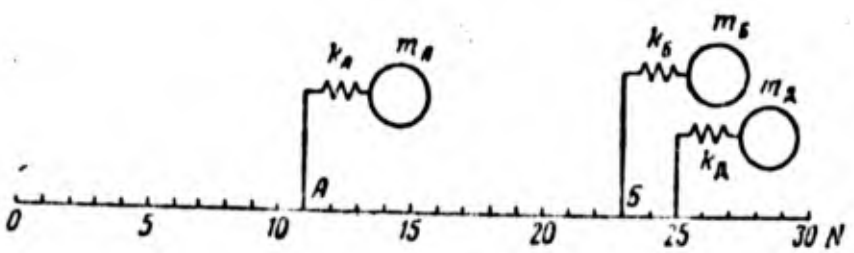

Figure 3.13

We divide the rod into 30 sections (k = 30, h = l/k = 0.75 m).

The distribution of rigidity $\overline{EF}$ and mass $\bar{m}$ along the length of the body is shown in Fig. 3.6 and in columns 2 and 3 of Table 3.1. We shall consider the localized masses m_A, m_B, and m_E to be suspended in the rod sections N = 11, 23, and 25, respectively. We assume, moreover, the following values of partial frequencies:

$$\omega_A^2 = \frac{k_A}{m_A} = 30\,000 \ 1/sec^2; \quad \omega_B^2 = \frac{k_B}{m_B} = 12\,000 \ 1/sec^2;$$

$$\omega_e^2 = \frac{k_e}{m_e} = 25\,000 \ 1/sec^2.$$

Results of calculating the forms and frequencies of natural oscillations for the first five tones are given in Table 3.2 and shown in Figs. 3.14 and 3.15. Table 3.2 also shows the values of the reduced masses m_n; the values of the coefficients of the forms of the oscillations for the localized masses m_A, m_B, and m_E are indicated after the line for the sections N = 12, 24, and 26, respectively.

The frequency of the first tone of the natural oscillations of a rod with elastically suspended localized masses ω_1 = 103.37 1/sec. This same frequency for the model of a rod on which localized masses m_A, m_B, and m_E are rigidly fixed is 1.6 times greater (ω_1 = 165 1/sec), therefore in the example under consideration the model with attached masses must be considered to be unsatisfactory.

The partial frequencies ω_A, ω_B, and ω_E are higher than the frequency of the system ω_1; therefore in the case of oscillations according to form f_1, the masses m_A, m_B, and m_E perform motion in phase with oscillations of the suspension points. In the case of oscillations according to the form of the second tone, where $\omega_A < \omega_2$, $\omega_B < \omega_2$, and $\omega_E > \omega_2$, the mass m_B performs motion in counterphase to the suspension point. In the case of the third, fourth, and higher tones of oscillations all the masses oscillate in counterphase to the suspension points.

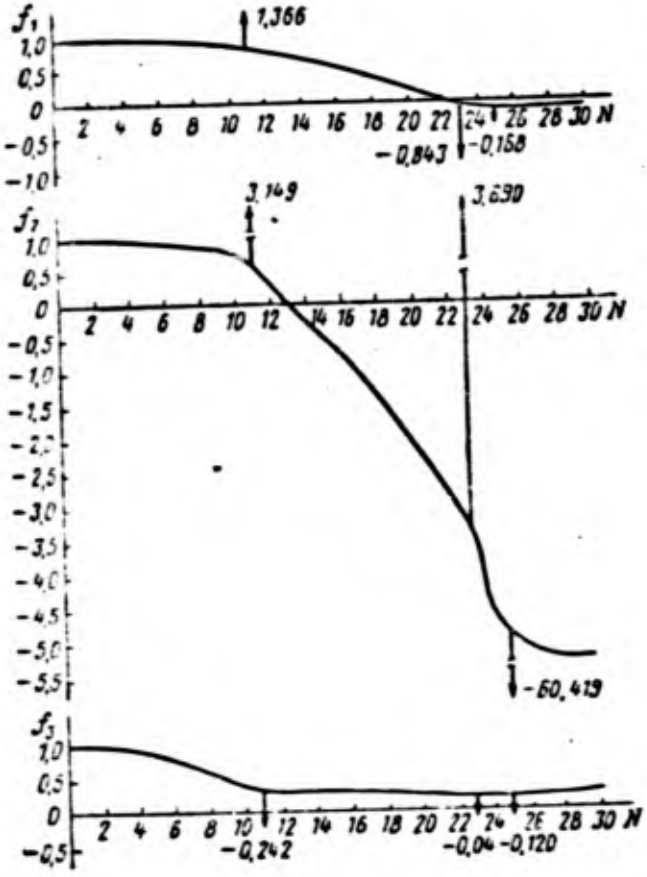

Figure 3.14

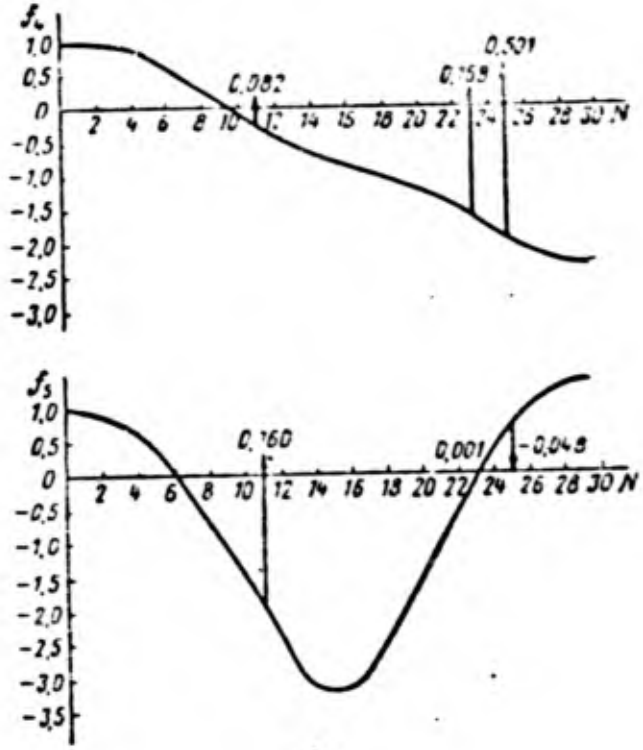

Figure 3.15

Table 3.2

Rod Section N	Form of oscillations				
	f_1	f_2	f_3	f_4	f_5
0	1,0000	1,0000	1,0000	1,0000	1,0000
2	0,9968	0,9932	0,9805	0,9631	0,8882
4	0,9897	0,9779	0,9369	0,8819	0,6571
6	0,9829	0,9210	0,7778	0,5930	—0,0388
8	0,9298	0,8511	0,5856	0,2523	—0,8293
10	0,8958	0,7796	0,3901	—0,0910	—1,5628
12	0,7685	0,2495	0,2937	—0,4989	—2,6386
	1,3659	3,1491	—0,2416	0,0823	0,1605
14	0,7685	—0,2445	0,2932	—0,7248	—3,2073
16	0,6574	—0,7350	0,2826	—0,9023	—3,1336
18	0,5426	—1,4869	0,2559	—1,1182	—2,3479
20	0,3516	—2,2351	0,2274	—1,3189	—1,4636
22	—0,0015	—2,9777	0,1972	—1,5016	—0,5179
24	—0,0949	—4,5402	0,1971	—1,8699	0,4453
	—0,8427	3,6902	—0,0403	0,1677	0,0011
26	—0,0967	—5,2155	0,2037	—2,1578	0,9185
	—0,1679	—60,4188	—0,1197	0,5008	—0,0476
28	—0,0974	—5,2974	0,2132	—2,3585	1,2502
30	—0,0977	—5,3248	0,2164	—2,4266	1,3675

ω_n в 1/sec	103,37	151,27	257,08	354,21	621,90
$\overline{m}_n$	3650	619860	300	1760	2250

If the frequency of the system is close to the partial frequencies ω_A, ω_B, or ω_E, then the value of the coefficient of the form of oscillations of the respective elastically suspended masses becomes large. This peculiarity appeared in the example under consideration in the case of the second tone of oscillations. The value of the coefficient of the form of the natural oscillations for the mass m_E (see Fig. 3.14)

$$f_{2E} = -60{,}419,$$

since for a nonuniform rod with rigidly fixed masses m_A, m_B, and m_E in the section N = 25 the value of the coefficient of the form $|f_2| < 1$. The great difference in the values of the coefficients of the forms of the elastic oscillations of the engine causes a great difference in the values of the reduced forces in the case of calculating induced oscillations. This comparison serves as additional confirmation of the fact that in the example under consideration the model of a rod with rigidly fixed masses of liquid and engine is unsatisfactory.

8. Perturbations from Fluctuations of Gas Pressure in the Tanks

During longitudinal oscillations the casing and bottom of a tank are deformed under the influence of the dynamic pressure of the liquid. This is accompanied by a change in the volume of the tank and, consequently, by a change in the volume of the gas cushion which leads to a change in the gas pressure on the free surface of the liquid and the top of the tank. Change in the gas pressure may also take place due to variations in the pressure feeding system. Such a change in gas pressure causes supplementary axial forces in the rocket body and therefore influences its longitudinal oscillations.

If the mass of gas in a tank at a given moment is considered to be constant, then in calculating the forms and frequencies of the natural oscillations of the body, the gas cushion may be replaced by a weightless spring, one end of which is attached to the top of the tank and the other to an equivalent mass m_{sj} (Fig. 3.16). The stiffness factor of the spring may be calculated from the expression

$$k_V = -F_b^2\left(\frac{\partial p}{\partial V}\right)_{V=V_0},$$

where F_b^2 is the area of effective tank surface (for a cylindrical tank $F_b = R_1^2$); p, V are the pressure and volume of the gas cushion in the tank; and V_0 is the nominal volume. For the n-th tone of oscillations of the body the force of the spring is

$$N_{sja} = k_V(f_{nsj} - f_n(x_{ja}))q_n,$$

where f_{nsj} is the coefficient of the form of the elastic oscillations of the localized mass m_s; $f_n(x_{ja})$ is the coefficient of the forms of the oscillations of the top of the tank; and q_n is a generalized coordinate.

A spring with a stiffness factor k_V somewhat elevates the frequency of natural oscillations of the mass m_{sj} so that

$$\omega_{sj}^2 = \frac{k_{sj} + k_V}{m_{sj}}.$$

Since the stiffness factor k_V does not depend on the number of the tone of the oscillations, and the stiffness factor k_{sj} increases with an increase in the number of the tone, then the influence of the spring attached to the top of the tank, on the frequency of the natural oscillations of the mass m_{sj}, decreases with an increase in the number of the tone. The value of the stiffness factor k_V is significant with a small V_0 and a large F_b.

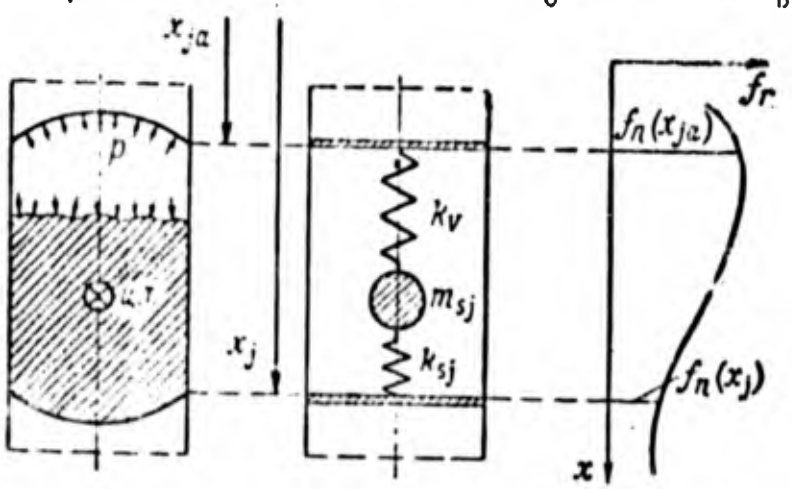

Figure 3.16

It is not difficult to calculate a spring with a stiffness factor of k_V in calculating the forms and frequencies of the natural oscillations of a rocket body. In order to do this the conjugation condition (3.41) must be used and even with transition through the section with abscissa $x = x_{ja}$ corresponding to the top of the tank.

We find the coefficient f_{nsj} of the form of the elastic oscillations of the localized mass m_{sj}. We calculate the force of the upper and lower springs (see Fig. 3.17) according to the following formulas:

$$N^*_{sja} = k_V [f_{nsj} - f_n(x_{ja})],$$
$$N^*_{sj} = k_{sj} [f_{nsj} - f_n(x_j)].$$

From the equilibrium condition of the localized mass m_s

$$-m_{sj}\omega_n^2 f_{nsj} = -k_V [f_{nsj} - f_n(x_{ja})] - k_{sj} [f_{nsj} - f_n(x_j)]$$

we obtain

$$f_{nsj} = f_n(x_j) \frac{\omega_{sj}^2}{\omega_{sj}^{*2} - \omega_n^2} + f_n(x_{ja}) \frac{\omega_{sV}^2}{\omega_{sj}^{*2} - \omega_n^2},$$

where

$$\omega_{sj}^2 = \frac{k_{sj}}{m_{sj}}, \quad \omega_{sV}^2 = \frac{k_V}{m_{sj}}.$$

Variation in the gas supply from the nominal value takes place due to perturbations in the pressure feeding system. These perturbations may not depend on the longitudinal oscillations of the rocket body, and then the change in the force of gas pressure on the top of the tank and the surface of the liquid will be external in relation to oscillations of the body. If the perturbations on the pressure feeding systems arise from the longitudinal oscillations of the body, then a supplementary feedback will exist in the closed dynamic system of the rocket, the character of which depends on the dynamic properties of the pressure feeding system. The pressure feeding system, consisting of a volume of gas, a regulator with a pressure sensor for feedback, and a gas cushion in the tank, is closed. The parameters of the system must be such that no unstable operating conditions arise in it.

9. Induced Oscillations of the Rocket Body

Longitudinal oscillations of a rocket with a liquid propellant engine are oscillations of a closed system, the basic physical members of which are the rocket body, the engine, and the main fuel lines. If one link is isolated from the closed system, in the given case, the rocket body, then it is possible to examine its induced isolations under the influence of a variation in engine thrust.

It is methodologically worthwhile to study the induced oscillations by beginning with an examination of the simpler problem, that is, the induced oscillations of a straight nonuniform unattached rod. Let us represent the external force q (x, t) in equation (3.2) in the form of the product

$$q(x, t) = q(t)p(x).$$

We present the deflection of the rod u(x, t) in the case of induced oscillations in the form of a series expansion (3.14) according to the form of the natural oscillations

$$u(x, t) = u_M(t) + \sum_{n=1}^{\infty} f_n(x) q_n(t), \tag{3.52}$$

where $u_M(t)$ is the deflection of the center of mass of the rod or the deflection of the rod as a rigid body; $f_n(x)$ is the form of the natural oscillations of the rod, corresponding to a non-null natural frequency; $q_n(t)$ is the generalized coordinate of the elastic oscillations of the rod

Having substituted into equation (3.2), instead of u(x, t), its expression from (3.52), we obtain

$$m(x)\left(\ddot{u}_M + \sum_{n=1}^{\infty} f_n \ddot{q}_n\right) = \left[EF(x)\sum_{n=1}^{\infty} f_n'(q_n + 2\xi\dot{q}_n)\right]' + q(t)p(x). \tag{3.53}$$

We shall integrate equation (3.53) for x within the limits from 0 to l, then we multiply this equation by the function f_n, where n is an arbitrary

fixed natural number, and we integrate for x within the limits from 0 to l. With regard to equations (3.53) to (3.7) and (3.18) we obtain the following system of ordinary differential equations with constant coefficients for determining the generalized coordinates $q_M(t)$ and $q_n(t)$:

$$\ddot{q}_M = \frac{1}{m} q(t) \int_0^l p(x)\,dx,$$

$$\ddot{q}_n + 2\xi_n \omega_n \dot{q}_n + \omega_n^2 q_n = \frac{1}{m_n} P_n(t) \qquad (n = 1, 2, \ldots), \tag{3.54}$$

where

$$m_n = \int_0^l m(x) f_n^2\,dx, \quad \omega_n^2 = \frac{k_n}{m_n};$$

$$2\xi_n \omega_n = 2\xi' \omega_n^2 = \frac{k_n 2\xi'}{m_n}; \tag{3.55}$$

$$P_n(t) = q(t) \int_0^l p(x) f_n\,dx.$$

The first equation is an equation of motion of the center of mass of an absolutely solid rod. From the second equation, in the case of the given external force q(t)p(x), it is possible to find the generalized coordinate $q_n(t)$ of the longitudinal oscillations of the rod relative to its center of mass. The total displacement of any cross-section of the rod is determined according to equation (3.52).

The value of $P_n(t)$, standing in the right term of the second equation (3.54), is the reduced force for the n-th tone of the oscillations. When the localized forces $q_r(t)P_r$ (r = 1, 2, ...) act on a rod, in addition to the distributed external force q(t)p(x), then the formula for determining the reduced force will have the form

$$P_n(t) = q(t) \int_0^l p(x) f_n\,dx + \sum_{(r)} q_r(t) P_r(x_r) f_n(x_r), \tag{3.56}$$

where $f_n(x_r)$ is the value of the coefficient of the form of the natural oscillations for that section of the rod in which the localized force $q_r(t)P_r$ is applied.

We shall now examine the calculations of a rocket body, using a nonuniform rod with elastically suspended localized masses (see Fig. 3.3) as a model. The equation of the induced longitudinal oscillations of the rocket body will differ from equation (3.2) by the additional terms in the right member

$$m(x)\frac{\partial^2 u}{\partial t^2}-\frac{\partial}{\partial x}\left[EF(x)\frac{\partial u}{\partial x}+b(x)\frac{\partial^2 u}{\partial x\,\partial t}\right]=q(t)\,p(x)+ \\ +\sum_{(j,\,s)}N_{sj}\delta(x-x_j), \tag{3.57}$$

where $(x-x_j)$ is Dirac's function, possessing the following property:

$$\int_0^l \varphi(x)\delta(x-x_j)\,dx=\varphi(x_j). \tag{3.58}$$

The localized force N_{sj}, transmitted to the rod through the spring, is numerically equal to the inertial force of the mass m_{sj}

$$N_{sj}=-m_{sj}\frac{d^2u_{sj}}{dt^2}, \tag{3.59}$$

where u_{sj} is the displacement of the mass m_{sj}.

In order to determine the induced oscillations of a rod with elastically suspended localized masses we shall introduce a new function $u^*(x, t)$, which will unite the function $u(x, t)$ and all the functions $u_{sj}(t)$

$$u^*(x,t)=u_M^*(t)+\sum_{n=1}^{\infty}f_n^*(x)q_n(t). \tag{3.60}$$

Here $u_M^*(t)$ is the displacement of the center of mass of the system; $f_n^*(x)$ is the form of the natural oscillations of the n-th tone of the rod with elastically suspended localized masses; and $q_n(t)$ is the generalized coordinate of the elastic oscillations.

$$f_n^*(x)=\begin{cases}f_n(x) & 0\leqslant x\leqslant l, \text{ furthermore,}\\ f_{nsj} & x=x_j \quad (s=1,2,\ldots,s^0)\end{cases} \tag{3.61}$$

In the case where $x = x_j$ the function $f_n^*(x)$ will be multivalent with values $f_n(x_j)$, f_{nsj} $(s = 1, 2, \ldots, s^0)$. For all remaining x this function will have one value $f_n(x)$.

On the basis of (3.61) we shall have

$$\frac{\partial u^*(x,t)}{\partial x}=\frac{\partial u(x,t)}{\partial x};\quad f_n^{*\prime}(x)=f_n'(x). \tag{3.62}$$

We also introduce the function

$$m^*(x)=m(x)+\sum_{(j,s)} m_{sj}\delta(x-x_j) \tag{3.63}$$

and the following rule for the integration of functions

$$\int_0^l u^*(x,t)m^*(x)\,dx=\int_0^l m(x)u(x,t)\,dx+\sum_{(j,s)} m_{sj}u_{sj}(t). \tag{3.64}$$

Now with regard to relations (3.60)-(3.64) equation (3.57) may be put

$$\begin{aligned} m(x)\frac{\partial^2 u^*(x,t)}{\partial t^2}-\frac{\partial}{\partial x}\left[EF(x)\frac{\partial u^*(x,t)}{\partial x}+b(x)\frac{\partial^2 u^*(x,t)}{\partial x\,\partial t}\right]=\\ =q(t)p(x). \end{aligned} \tag{3.65}$$

Where $b(x)/EF(x) = 2\xi'$ and $q(t)p(x) = 0$ the variables in (3.65) may be separated out and an equation obtained for determining the forms and frequencies of the natural oscillations

$$[EF(x)f_n^{*\prime}(x)]'=-\omega_n^2 m^*(x)f_n^*(x)\quad (n=1,2,\ldots) \tag{3.66}$$

The function $f_n^*(x)$, satisfying equation (3.66) and the boundary conditions

$$f_n^{*\prime}(0)=0,\quad f_n^{*\prime}(l)=0$$

are orthogonal with the weight function $m^*(x)$

$$\int_0^l m^*(x)f_n^*f_m^*\,dx=0\qquad (n\neq m). \tag{3.67}$$

The condition of orthogonality with regard to (3.61) and (3.64) may be put in the form

$$\int_0^l m(x)f_n(x)f_m(x)+\sum_{(l,s)} m_{sj}f_{nsj}f_{msj}=0. \tag{3.68}$$

The method of determining the functions $f_n^*(x)$ and the frequency ω_n was given in section 6; we shall consider them to be known and move to an examination of the problem of induced oscillations. Having substituted the expression from (3.60) instead of $u^*(x, t)$ into equation (3.65), we obtain

$$m^*(x)\left(\ddot{u}_M^* + \sum_{n=1}^{\infty} f_n^* \ddot{q}_n\right) - \left[b(x)\sum_{n=1}^{\infty} f_n^{*\prime}\dot{q}_n\right]' - \left[EF(x)\sum_{n=1}^{\infty} f_n^{*\prime} q_n\right]' = q(t)\,p(x). \tag{3.69}$$

We integrate equation (3.69) for x on the section $[0, l]$. Then we multiply equation (3.69) by $f_n^*(x)$, where n is an arbitrary fixed number and we integrate it for x on the section $[0, l]$. With regard to equations (3.61)-(3.64) and, bearing in mind that

$$\int_0^l m^*(x)\, f_n^*(x) = 0$$

we obtain the following system of ordinary differential equations for determining the generalized coordinates $u_M^*(t)$ and $q_n(t)$:

$$\ddot{u}_M^* = q(t)\frac{1}{m}\int_0^l p(x)\,dx,$$
$$\ddot{q}_n + 2\xi_n\omega_n\dot{q}_n + \omega_n^2 q_n = q(t)\frac{P_n(t)}{m_n}, \tag{3.70}$$

where

$$m = \int_0^l m^*(x)\,dx = \int_0^l m(x)\,dx + \sum_{(j,s)} m_{sj},$$
$$m_n = \int_0^l m^*(x)\, f_n^{*2}\,dx = \int_0^l m(x)\, f_n^2\,dx + \sum_{(j,s)} m_{sj} f_{nsj}^2, \tag{3.71}$$
$$P_n = \int_0^l p(x)\, f_n^*\,dx.$$

In the future the function $u_M^*(t)$ will be written without the index (*).

Despite the complex oscillatory system, such a simple structure of equations (3.70) is obtained because the forms and frequencies of the natural oscillations of the body are found with regard to the oscillations of the liquid in the elastic tanks as a single oscillatory system.

Induced longitudinal oscillations of a rocket may take place under the influence of external forces, that is, variations in engine thrust and variations in aerodynamic drag. Variation in the engine thrust has significantly greater influence on the longitudinal oscillations of the rocket body than a variation in drag. Therefore in practical calculations variation in drag is usually not considered. When the discharge main is put into a separate unit, variation in the pressure of the liquid in front of the pump intake will also create an external force in relation to the body. This force is transmitted onto the rocket body through the pump suspension.

According to the accepted model (see Fig. 3.3) and the symbols introduced in section 5, the coefficient of the form of the natural oscillations, the point of application of engine thrust is designated by f_{ne}. The coefficient of the form of the elastic oscillations of the pump is designated by f_{np}. On the basis of the last formula (3.71) the reduced force is

$$P_n(t) = -P(t) f_{ne} + P_{1p}(t) f_{np}, \tag{3.72}$$

where P(t) is the variation in engine thrust; and $P_{1p}(t)$ is the variation in the force of fluid pressure in front of the pump intake.

The minus sign in front of the force P(t) signifies that the displacement of the body from the top to the tail section of the rocket is assumed to be a positive variable, that is, opposite the direction of thrust. If the pump is rigidly connected with the engine, then $f_{np} = f_{ne}$ and equation (3.72) will have the form

$$P_n(t) = [-P(t) + P_{1p}(t)] f_{ne}. \tag{3.73}$$

For the first equation (3.70) the external force is

$$q(t)\int_0^l p(x)\,dx = -P(t) + P_{1p}(t).$$

10. Determining the Form of Induced Oscillations

Determining induced oscillations by means of representing them in the form of a series according to eigen functions has several advantages. The solution is graphic and simple to interpret. The induced oscillations of a system are presented in the form of the sum of the oscillations of simple oscillators.

Using this method it is possible to visually evaluate the influence of the distribution of m(x) and EF(x) on the frequency and form of natural oscillations, and in analyzing stability, their influence on the stability of the system, which is very important at the planning stage. The method is even more convenient when the frequencies of the natural oscillations of the rocket body significantly differ from one another and it is possible to make an analysis of stability for each tone of the oscillations individually.

It is also possible to use another method. The external harmonic force may be included in the boundary conditions and induced oscillations may be determined in the form of the function $\phi(x, \omega)e^{i\omega t}$ without expanding them in series according to eigen-functions. Here, instead of a series, only one function $\phi(x, \omega)$ characterizes the induced oscillations. The method gives an accurate solution, characterized by one function, which has advantages in analyzing the stability of motion, when the frequencies of several forms of body oscillations are very close. Application of this method is also very convenient at the final stages when the rocket is already constructed and it is necessary to perform tests of stability and to obtain certain quantitative evaluations.

The function $\phi(x, \omega)$ may be called the form of the induced oscillations. It is useful to first determine the function $\phi(x, \omega)$ and analyze its properties for the model of a nonuniform rod.

Let us assume that an external localized force $P(t) = P_0 e^{i\omega t}$ and an external distributed force $q(x, t) = 0$ acts on the right end of a rod ($x = l$) along its axis.

We give a partial solution of equation (3.2) in the form

$$u(x, t) = \varphi(x, \omega) e^{i\omega t}. \tag{3.74}$$

Having substituted equation (3.74) into (3.2) and having assumed $q(x, t)=0$ in it, we obtain

$$-\omega^2 m(x)\varphi = \frac{\partial}{\partial x}\left[EF(x)\varphi' + b(x) i\omega\varphi'\right] \quad (\varphi = \varphi(x, \omega)).$$

We use the finite difference method to integrate this equation. Having integrated the equation for x within the limits from $x_{i-0.5}$ to $x_{i+0.5}$ and having replaced the derivatives with finite difference ratios,

$$\varphi'\Big|_{x_{i+0,5}} = \frac{\varphi_{i+1} - \varphi_i}{h}; \quad \varphi'\Big|_{x_{i-0,5}} = \frac{\varphi_i - \varphi_{i-1}}{h},$$

where h is the length of the integration section, we find

$$-\omega^2 h^2 m(x_i)\varphi_i = (EF_{i+0,5} + i\omega b_{i+0,5})(\varphi_{i+0,5} - \varphi_i) - (EF_{i-0,5} + i\omega b_{i-0,5})(\varphi_i - \varphi_{i-1}).$$

We shall solve this equation relative to φ_{i+1}. We obtain

$$\varphi_{i+1} = (a_i^* + id_i^*)\varphi_i - (a_i + id_i)\varphi_{i-1}, \tag{3.75}$$

where

$$a_i^* = 1 + a_i - r_i,$$

$$d_i^* = d_i + p_i,$$

$$a_i = \frac{1}{A_{i+0,5}^2}(c_{i-0,5}^2 c_{i+0,5}^2 + 4\omega^2 \xi_{i-0,5}\xi_{i+0,5}),$$

$$d_i = \frac{2\omega}{A_{i+0,5}^2}(c_{i+0,5}^2 \xi_{i-0,5} - c_{i-0,5}^2 \xi_{i+0,5}),$$

$$r_i = \frac{\omega^2 h^2 c_{i+0,5}^2}{A_{i+0,5}^2}, \tag{3.76}$$

$$p_l = \frac{2h^2\omega^3\varepsilon_{l+0,5}}{A^2_{l+0,5}},$$

$$A^2_{l+0,5} = c^4_{l+0,5} + 4\omega^2\varepsilon^2_{l+0,5},$$

$$c^2_{l+0,5} = \frac{EF_{l+0,5}}{m_l}; \quad c^2_{l-0,5} = \frac{EF_{l-0,5}}{m_l},$$

$$\varepsilon_{l-0,5} = \frac{b_{l+0,5}}{2m_l}; \quad \varepsilon_{l-0,5} = \frac{b_{l-0,5}}{2m_l}.$$

In equation (3.75) Φ_{i+1}, Φ_i, and Φ_{i-1} are complex numbers

$$\varphi_{l+1} = U_{l+1} + iV_{l+1}, \quad \varphi_l = U_l + iV_l, \quad \varphi_{l-1} = U_{l-1} + iV_{l-1},$$

therefore this equation may be put in the form

$$\varphi_{l+1} = U_{l+1} + iV_{l+1}, \tag{3.77}$$

where

$$\begin{aligned} U_{l+1} &= a_l U_l - d_l V_l - a_l U_{l-1} + d_l V_{l-1}, \\ V_{l+1} &= a_l V_l + d_l U_l - a_l V_{l-1} - d_l U_{l-1}. \end{aligned} \tag{3.78}$$

Since the left end of the rod is free, and the external force $P_0 e^{i\omega t}$ is applied to the right end, then the boundary condition for the function $\Phi(x, \omega)$ will be the following:

$$\varphi'(0, \omega) = 0, \quad \varphi'(x_k, \omega)[EF(x_k) + i\omega b(x_k)] = P_0,$$

where x_k is the abscissa of the rod end of the rod.

Having replaced the derivatives in these equations with finite differences and having divided the second equation by m_k, where m_k is the value of the function m(x) in a section with abscissa x_k, we present the boundary conditions in the form

$$\begin{aligned} \varphi_1 - \varphi_0 &= 0, \\ (\varphi_k - \varphi_{k-1})(c_k^2 + i2\omega\varepsilon_k) &= \frac{P_0 h}{m_k}. \end{aligned} \tag{3.79}$$

We shall determine the complex numbers ϕ_{i+1} according to formulas (3.77) in a scale of $A_M e^{i\varphi_M}$. On the left end of the rod we assume $U_0 = 1$, $V_0 = 0$. Then from the first equation (3.79) we find $U_1 = 1$, $V_1 = 0$. Further, according to formulas (3.78) we calculate U and V for each section of the rod, including the section on the end. The second equation (3.79) is used for determining the scale. The left member of the second equation (3.79) is given in the form

$$[U_k - U_{k-1} + i(V_k - V_{k-1})](c_k^2 + i2\omega\varepsilon_k) = U\phi_k + iV\phi_k.$$

Hence we find

$$\begin{aligned} U\phi_k &= (U_k - U_{k-1})c_k^2 - 2\omega\varepsilon_k(V_k - V_{k-1}), \\ V\phi_k &= 2\omega\varepsilon_k(U_k - U_{k-1}) + c_k^2(V_k - V_{k-1}). \end{aligned} \tag{3.80}$$

We give the scale of the complex number ϕ_1 in the form

$$A_M e^{i\varphi_M} = U_M + iV_M.$$

Since all the numbers U_1 and V_1, including U_k and V_k, are calculated in the scale $A_M e^{i\varphi_M}$, then the second equation (3.79) may now be written thus:

$$(U_M + iV_M)(U_{\phi_k} + iV_{\phi_k}) = \frac{P_0 h}{m_k}.$$

Having divided the real and imaginary parts, we obtain

$$\begin{aligned} U_M U_{\phi_k} - V_M V_{\phi_k} &= \frac{P_0 h}{m_k}, \\ V_M U_{\phi_k} + U_M V_{\phi_k} &= 0. \end{aligned}$$

From these equations we find the value of the scale

$$\begin{aligned} U_M &= \frac{1}{D}\frac{P_0 h}{m_k} V_{\phi_k}, \\ V_M &= -\frac{1}{D}\frac{P_0 h}{m_k} U_{\phi_k}, \end{aligned} \tag{3.81}$$

$$D = U_{\phi_k}^2 + V_{\phi_k}^2, \quad A_M = \sqrt{U_M^2 + V_M^2}, \quad \operatorname{tg}\varphi_M = \frac{V_M}{U_M}.$$

From equations (3.77) and (3.78) it is possible to determine the real and imaginary parts of the following complex number for any section of the rod:

$$\phi_i = U_i + iV_i = A\phi_i e^{i\varphi\phi_i},$$

which in the scale $A_M e^{i\varphi_M}$ characterizes the induced oscillations of the i-th section of the rod.

The form of the induced oscillations for a nonuniform rod may be represented by the total number of vectors (complex coefficients of the form) for all sections of the rod. For the derivative of the i-th section of the rod the complex coefficient of the form

$$\Phi(x_i, \omega) = A(x_i, \omega) e^{i\varphi(x_i, \omega)}, \tag{3.82}$$

where

$$A(x_i, \omega) = A_{\Phi_i} A_M,$$
$$\varphi(x_i, \omega) = \varphi_{\Phi_i} + \varphi_M. \tag{3.83}$$

The form of the induced oscillations may be presented also as the sum of the real and imaginary parts

$$\Phi(x, \omega) = U(x, \omega) + iV(x, \omega), \tag{3.84}$$

where

$$U(x, \omega) = U_i U_M - V_i V_M,$$
$$V(x, \omega) = U_i V_M + V_i U_M. \tag{3.85}$$

Irrespective of whether the external force varies as $P_0 \cos \omega t$ or as $P_0 \sin \omega t$, in conversion to the trigonometrical form of writing in equation (3.82) it is necessary to preserve the real and imaginary parts.

The form of the induced oscillations $\Phi(x, \omega)$ in the coordinates x, U, and iV is a spatial curve. In order to represent this curve, it is necessary in each section i = 0, 1, 2, ... k from the axis of the rod in a plane parallel to the plane Z = U + iV, to construct the vector $\Phi(x_i, \omega)$ and to connect the ends of all vectors with the curve (Fig. 3.17). This curve will also be the form of the induced oscillations with the frequency ω. The higher the frequency of the induced oscillations ω is, the greater the angle will be at which the vector $\Phi(x_i, \omega)$ revolves around the 0x axis with motion of the vector beginning along this axis ($0 \leq i \leq k$). Thus, a spiral shaped curve with variable radius is obtained. The modulus $A(x_i, \omega)$ of the vector characterizes the amplitude, and the angle $\varphi(x_i, \omega)$, the phase shift of the induced oscillations of the i-th section of the rod.

The mutual disposition of the vector A_{Φ_i}, the vector $A_M e^{i\varphi_M}$, characterizing the scale, and the vector $A_i e^{i\varphi_i}$, preceding the coefficient of the form of the induced oscillations, is shown in Fig. 3.18. According to the number of half-turns of the vector $\Phi(x_i, \omega) = A_i e^{i\varphi_i}$ around the Ox axis, it is possible to determine the frequency of which tone of the natural oscillations ω_n is

closest to the frequency of the external force ω: the closer these frequencies are the greater is the amplitude of the form of the induced oscillations.

An analysis of the total angle $\varphi(x, \omega)$ of rotation of the vector is necessary only for representation of the form of the induced oscillations. In order to investigate the oscillations of any i-th numbered section of the rod it is sufficient to know the phase shift within the limits $0 \leqslant \varphi(x_1, \omega) \leqslant 2\pi$.

For the function $\phi(x, \omega)$ in the case of a uniform rod it is possible to obtain an analytical expression. If the left end of the rod is free, and an external $P(t) = P_0 e^{i\omega t}$ is applied to the right end, then where $b(x) = 0$

$$\phi(x, \omega) = -\frac{P_0}{aEF_0 \sin al} \cos ax \qquad \left(a \neq \frac{n\pi}{l},\ n = 1, 2\ldots\right),$$

where $$a = \omega \sqrt{\frac{m_0}{EF_0}}.$$

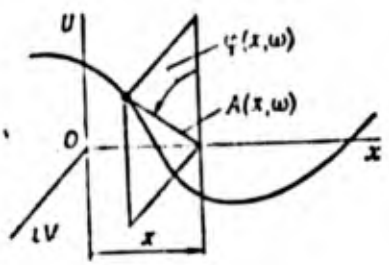

Figure 3.17

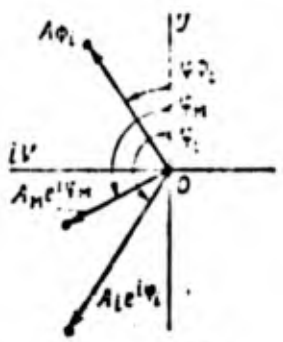

Figure 3.18

Graphs of the functions $\phi(x, \omega)$ for different values of a for a uniform rod are given in Fig. 3.19. These are plane curves which are plotted with

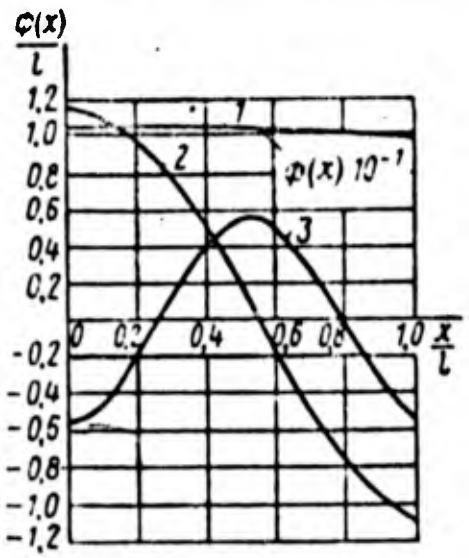

Figure 3.19

the assumption that $P_0/EF_0 = 1$. Curve 1 corresponds to $\alpha_1 = 0.1\ \pi/l$, curve 2 to $\alpha_2 = 0.9\ \pi/l$, curve 3 to $\alpha_3 = 1.9\ \pi/l$.

Where $\alpha \ll \pi/l$ the form of their oscillations varies little over the length of the rod. The rod performs harmonic oscillations almost as a solid body. Expansion-contraction oscillations, which are characterized by different displacement of sections of the rod, are almost absent since the frequency of the variation of the external force is significantly less than the frequency of the first tone of the natural oscillations of the rod. Where $\alpha_2 = 0.9\ \pi/l$ and $\alpha_3 = 1.9\ \pi/l$ the form of the induced oscillations is close to the form of the natural oscillations of the first and second tones, respectively. This is explained by the fact that the frequency of the external force is close to the frequency of the natural oscillations of the first and second tones (for the first tone $\alpha_1 = \pi/l$, for the second tone $\alpha_2 = 2\pi/l$).

11. An Algorithm for Calculating the Forms of the Induced Oscillations of a Rocket Body

As in the case of calculating the forms and frequencies of natural oscillations, we use a straight nonuniform rod with elastically suspended localized masses as a dynamic analog for the rocket body.

We shall first solve two auxiliary problems: 1) we shall find the rule for the transition through the j-th section, to which the localized force from the elastically suspended masses, simulating the liquid, is transmitted, and 2) we shall find the rule for the transition through the section with abscissa $x_j = x_e$, to which the engine is elastically suspended.

We shall begine with the first problem. Let the j-th section be located between the sections i and i+1. Assuming the displacements of the adjacent sections x_i and x_j to be equal, i.e., $u(x_j, t) = u(x_i, t)$, we determine the displacement $u_{sj}(t)$ of the mass m_{sj} in a stationary coordinate system (Fig. 3.20). This is a problem of the induced oscillations of the mass m_{sj}, caused by the harmonic displacement of the suspension point

$$u(x_j, t) = u(x_i, t) = \varphi(x_i, \omega)e^{i\omega t} = \varphi_i e^{i\omega t}.$$

On the basis of Newton's second law, the equation of motion for the mass m_{sj} may be put in the form

$$m_{sj}\frac{d^2u_{sj}}{dt^2}=\left(k_{sj}+h_{sj}\frac{\partial}{\partial t}\right)[u(x_j,\ t)-u_{sj}(t)],$$

where k_{sj} and h_{sj} are the stiffness factor of the spring and the coefficient of friction of the localized mass m_{sj}, respectively. Having assumed

$$u_{sj}=\phi_{sj}(\omega)e^{i\omega t}=\phi_{sj}e^{i\omega t}$$

and having substituted this expression into the preceeding equation, we obtain

$$-m_{sj}\omega^2\phi_{sj}=(k_{sj}+i\omega h_{sj})(\phi_j-\phi_{sj}).$$

Having solved this equation relative to ϕ_{sj}, we find

$$\phi_{sj}=\phi_j\frac{\omega_{sj}^2+i2\varepsilon_{sj}\omega}{\omega_{sj}^2-\omega^2+i2\varepsilon_{sj}\omega}, \tag{3.86}$$

where

$$\omega_{sj}^2=\frac{k_{sj}}{m_{sj}},\qquad \varepsilon_{sj}=\frac{h_{sj}}{2m_{sj}}.$$

The complex coefficient of the form ϕ_{sj}, expressing the induced oscillations of the mass m_{sj}, on the basis of (3.86) is finally put in the form

$$\begin{aligned}\phi_{sj}&=U_{sj}+iV_{sj},\\ U_{sj}&=U_j[\omega_{sj}^2(\omega_{sj}^2-\omega^2)+4\varepsilon_{sj}^2\omega^2]+V_j2\varepsilon_{sj}\omega^3,\\ V_{sj}&=V_j[\omega_{sj}^2(\omega_{sj}^2-\omega^2)+4\varepsilon_{sj}^2\omega^2]-U_j2\varepsilon_{sj}\omega^3.\end{aligned} \tag{3.87}$$

Here U_j and V_j are the real and imaginary parts of the complex coefficient of the form ϕ_j, respectively.

In the section of the rod, the abscissa of which is equal to x_j, from each mass m_{sj} a localized force $N_{sj}(\omega)$ is transmitted to the rod, which may be determined according to the formula

$$N_{sj}(t)=-m_{sj}\frac{d^2u_{sj}}{dt^2}$$

or

$$N_{sj}(\omega)=N_{sj}=m_{sj}\omega^2\phi_{sj}. \tag{3.88}$$

We shall now examine the equilibrium of the section located between the i and i+1 sections of the rod (Fig. 3.21) From the left side of the rod, the following tensile force acts upon this section:

$$N_i = \varphi'(x_i)(EF_i + i\omega b_i). \tag{3.89}$$

The following tensile force acts from the right:

$$N_{i-1} = \varphi'(x_{i+1})(EF_{i-1} + i\omega b_{i+1}). \tag{3.90}$$

Also the forces N_{sj} from the elastically suspended localized masses, the number of which is s^0, act on this particular section of the rod. For the sake of simplicity we shall ignore the frictional forces arising within this section of the rod.

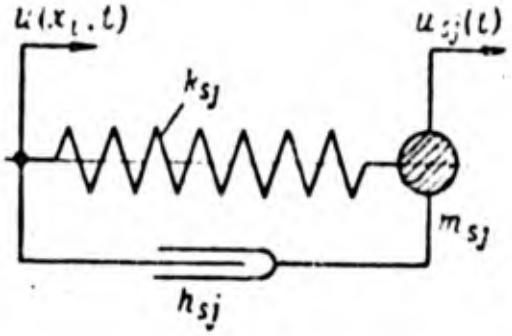

Figure 3.20

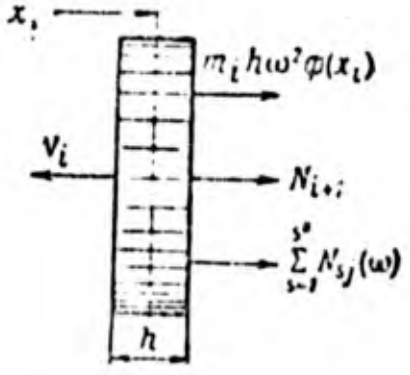

Figure 3.21

The equilibrium condition of the section of rod under examination at any moment of time will have the form

$$N_i = N_{i+1} + \sum_{(s)} N_{sj} + m_i h\omega^2 \varphi_i. \tag{3.91}$$

According to (3.49)

$$\varphi_i' = \frac{\varphi_{i+1} - \varphi_{i-1}}{2h}, \quad \varphi_{i+1}' = \frac{\varphi_{i+2} - \varphi_i}{2h}. \tag{3.92}$$

On the basis of equation (3.75), we obtain

$$\Phi_{l+2}=(a^*_{l+1}+id^*_l)\Phi_{l+1}-(a_{l+1}+id_{l-1})\Phi_l. \tag{3.93}$$

Having substituted equations (3.87)-(3.90) and (3.92), (3.93) into equation (3.91) and having solved this equation relative to Φ_{l+1} we obtain

$$\Phi_{l+1}=U_{l+1}+iV_{l+1},$$

$$U_{l+1}=\frac{1}{a_l'^2+b_l'^2}[a_l'U_l-b_l'V_l+e'_{l-1}U_{l-1}-d_{l-1}V_{l-1}+$$
$$+2h\omega^2\sum_{(s)}\frac{m_{sj}}{m_l}(a_l'U_{sj}-bV_{sj}),$$

$$V_{l+1}=\frac{1}{a_l'^2+b_l'^2}[a_l'V_l+b_l'U_l+e'_{l-1}V_l+d_{l-1}U_{l-1}+$$
$$+2h\omega^2\sum_{(s)}\frac{m_{sj}}{m_l}(a_l'V_{sj}-U_{sj})],$$

where

$$\begin{aligned}
a_l'&=-a_l(c_l^2+c_l^2a_l-2\varepsilon_l\omega\gamma_l)+b_l(2\varepsilon_l\omega+2\varepsilon_l\omega a_l+c_l^2d_l),\\
b_l'&=-b_l'(c_l^2+c_l^2a_l-2\varepsilon_l\omega\gamma_l)-a_l'(2\varepsilon_l\omega+2\varepsilon_l\omega a_l+c_l^2d_l),\\
e'_{l-1}&=c_l^2a_l'+2\varepsilon_l\omega b_l',\\
d_{l-1}&=-c_l^2b_l'+2\varepsilon_l\omega a_l',\\
a_l'&=c_l^2-\frac{m_{l+1}}{m_l}c_{l+1}^2a^*_{l+1}+\frac{m_{l+1}}{m_l}2\varepsilon_{l+1}\omega d^*_{l+1},\\
b_l'&=2\varepsilon_l\omega-\frac{m_{l+1}}{m_l}c_{l+1}^2d^*_{l+1}-\frac{m_{l+1}}{m_l}a^*_l2\varepsilon_{l+1}\omega,\\
c_l^2&=\frac{EF_l}{m_l},\quad c_{l+1}^2=\frac{EF_{l+1}}{m_{l+1}},\\
\varepsilon_l&=\frac{b_l}{2m_l},\quad \varepsilon_{l+1}=\frac{b_{l+1}}{2m_{l+1}}.
\end{aligned} \tag{3.95}$$

Since the values U_l, V_l, U_{l-1}, V_{l-1}, U_{sj}, and V_{sj} are known, then according to equation (3.94) it is possible to calculate the complex coefficient of the form Φ_{l+1}.

We shall now examine the second problem and find the rule for the transition through the section with abscissa $x_j = x_e$, from which the engine is elastically suspended. Let x_i be less than x_j be less than x_{i+1}, where x_i is the abscissa of the section of the body, preceeding the section x_j. We shall consider that the external force $P(t) = P_0 e^{i\omega t}$, the displacement of the engine thrust (Fig. 3.22), acts on the localized mass m_e.

We shall first find the induced oscillations of the mass m_e

$$u_e = \varphi_e(\omega) = \varphi_e e^{i\omega t},$$

caused by the external force P(t) and the displacement of the suspension point

$$u(x_i, t) = \varphi_i e^{i\omega t}.$$

Having assumed Newton's second law, we obtain

$$-m_e\omega^2\varphi_e = (k_e + i\omega h_e)(\varphi_i - \varphi_e) + P_0.$$

From this equation we find

$$\varphi_e = \frac{P_0}{m_e(\omega_e^2 - \omega^2 + i2\varepsilon_e\omega)} + \varphi_i \frac{\omega_e^2 + i2\varepsilon_e\omega}{\omega_e^2 - \omega^2 + i2\varepsilon_e\omega}. \quad (3.96)$$

The force transmitted to the rod is:

$$N_e = (k_e + i\omega h_e)(\varphi_e - \varphi_i).$$

Having substituted the expression φ_e from (3.96) here, we obtain

$$N_e = (P_0 + m_e\omega^2\varphi_i)\frac{\omega_e^2 + i2\varepsilon_e\omega}{\omega_e^2 - \omega^2 + i2\varepsilon_e\omega}, \quad (3.97)$$

or

$$N_e = [P_0 + m_e\omega^2\varphi_i](U_e' + iV_e'), \quad (3.98)$$

where

$$U_e' = \frac{\omega_e^2(\omega_e^2 - \omega^2) + 4\varepsilon_e^2\omega^2}{(\omega_e^2 - \omega^2)^2 + 4\varepsilon_e^2\omega^2},$$

$$V_e' = \frac{2\varepsilon_e\omega(\omega_e^2 - \omega^2) - \omega^2 2\varepsilon_e\omega}{(\omega_e^2 - \omega^2)^2 + 4\varepsilon_e^2\omega^2}.$$

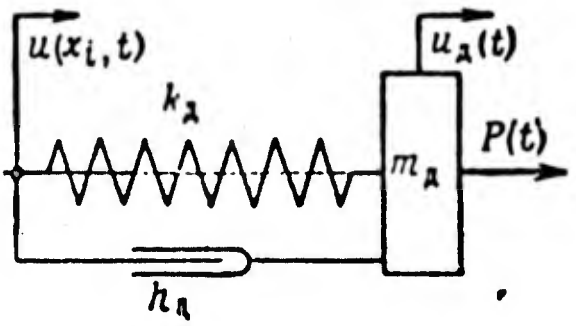

Figure 3.22

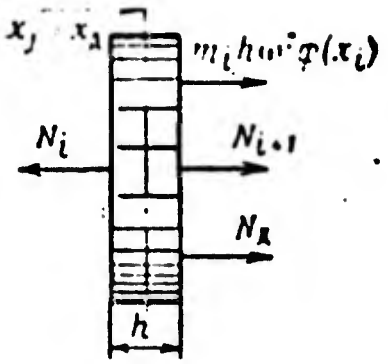

Figure 3.23

We shall examine the equilibrium of the section located between the sections i and i+1 of the rod. The forces acting on this section are shown in Fig. 3.23. From the equilibrium condition of the rod section we find

$$N_{i+1} = N_i - N_e - m_i h\omega^2 \varphi_i. \tag{3.99}$$

Let us now move to a discussion of the algorithm for calculating the form of induced oscillations of a rocket body. We shall use the finite difference method.

We divide the length of the body into k sections of equal length h = /k. The numbers of the cross-sections directly preceeding the j-th section with elastically suspended localized masses will in the future be written with the index j, i.e., they will be designated as i_j. For a model corresponding to a rocket body with two sequentially placed tanks, the symbols of the characteristic numbers of the sections are shown in Fig. 3.24. Roman numerals are also used there to show the four sections of the rod, within which it is possible to use the finite difference method in the 'pure' form.

The calculation algorithm is the following.

1. Knowing the values EF(x), m(x), and b(x) in each section of the rod, according to formula (3.76), we calculate the coefficients a_1, d_1, a_1^*, and d_1^* for all sections.

2. The as yet unknown scale for the form of the induced oscillations of the section 1 is designated by $A_{1M}e^{i\varphi_{1M}}$. We shall assume $\varphi_0 = 1$ at the left

end of the rod. Considering this end of the rod to be free, from the boundary condition we find $\phi_1 = 1$. Further, according to formulas (3.78) we calculate the real and imaginary parts of the complex numbers for all sections up to number i_A inclusively.

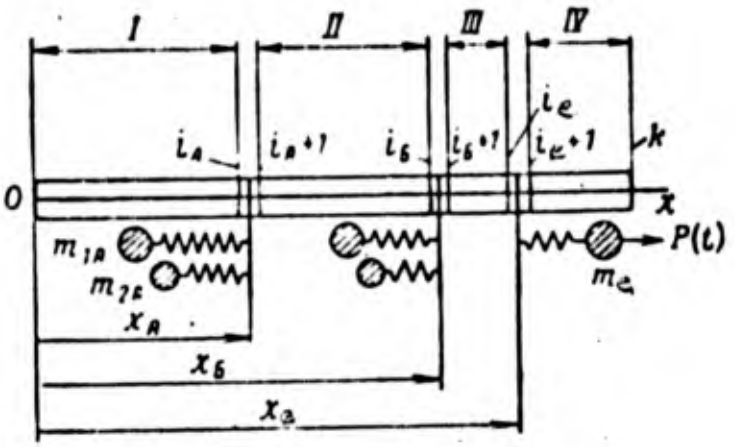

Figure 3.24

3. The localized masses m_{sA} are elastically suspended between sections i_A and i_{A+1}. Transition from section i_A to i_{A+1} is performed on the basis of equations (3.94) and (3.95). In these equations the indexes i and j must be replaced by the indexes i_A and A. The values of U_{sA} and V_{sA} are calculated ahead of time according to formulas (3.87) with replacement of the indexes i and j by the indexes i_A and A, respectively. The scale for the complex number ϕ_{i_A+1} in these calculations remains the same as for section I, i.e., $A_{IM}e^{i\varphi_{IM}}$. This same scale is preserved for the complex numbers ϕ_{sA}, characterizing the induced oscillations of the elastically suspended localized masses m_{1A} and m_{2A}.

4. Calculation of the form of the induced oscillations for the section II in the case of $i_A + 1 < i \leq i_B$ is performed according to formulas (3.78). The scale of the complex numbers in this case remains the same as for the number ϕ_{i_A+1}, i.e., $A_{IM}e^{i\varphi_{IM}}$.

5. Transition from section i_B to section i_{B+1} is performed on the basis of equations (3.94) and (3.95), in which the indexes i and j are replaced by the indexes i_B and B, respectively. The values of U_{sB} and V_{sB} are calculated

according to formulas (3.87) with replacement of the indexes i and j by the indexes i_B and B. The scale for the complex number ϕ_{i_B+1}, and also for the numbers $_{sB}$ remains as before.

6. Calculation of the complex numbers for section III where $i_B + 1 < i \leqslant i_e$ is performed according to formulas (3.78). The scale of the numbers remains as before, i.e., $A_{IM}e^{i\varphi IM}$.

7. Calculation of the complex numbers for the sections of part IV where $i_e + 1 < i \leqslant k$ is performed from the right (free) end of the rod. We shall obtain the corresponding formulas for this. The equation preceeding (3.75) is solved relative to ϕ_{i-1}. We obtain

$$\begin{gathered}\phi_{i-1}=(r_i^{\cdot}+ip_i^{\cdot})\phi_i-(r_i^{\prime}+ip_i^{\prime})\phi_{i+1}\\(i=k-1,\ldots,i_A+2,\ i_A+1,\ i_A),\end{gathered}\tag{3.100}$$

where

$$\begin{aligned}r_i^{\cdot}&=\frac{1}{D_i^{\prime}}\left[c_{i-0,5}^2\left(c_{i-0,5}^2-\omega^2h^2+c_{i+0,5}^2\right)+4\omega^2\varepsilon_{i-0,5}\left(\varepsilon_{i-0,5}+\varepsilon_{i+0,5}\right)\right],\\p_i^{\cdot}&=\frac{2\omega}{D_i^{\prime}}\left[c_{i-0,5}^2\left(\varepsilon_{i-0,5}+\varepsilon_{i+0,5}\right)-\varepsilon_{i-0,5}\left(c_{i-0,5}^2-\omega^2h^2+c_{i+0,5}^2\right)\right],\\r_i^{\prime}&=\frac{1}{D_i^{\prime}}\left(c_{i+0,5}^2c_{i-0,5}^2+4\omega^2\varepsilon_{i+0,5}\varepsilon_{i-0,5}\right),\\p_i^{\prime}&=\frac{1}{D_i^{\prime}}\left(\varepsilon_{i+0,5}c_{i-0,5}^2-\varepsilon_{i-0,5}c_{i+0,5}^2\right),\\D_i^{\prime}&=c_{i-0,5}^4+4\omega^2\varepsilon_{i-0,5}^2,\\c_{i+0,5}^2&=\frac{EF_{i+0,5}}{m_i},\quad c_{i-0,5}^2=\frac{EF_{i-0,5}}{m_i},\\\varepsilon_{i+0,5}&=\frac{b_{i+0,5}}{2m_i},\quad \varepsilon_{i-0,5}=\frac{2b_{i-0,5}}{2m_i}.\end{aligned}\tag{3.101}$$

Having substituted the complex coefficients of the form ϕ_{i-1}, ϕ_i, and ϕ_{i+1} in equation (3.100) by their real and imaginary parts, we find

$$\phi_{i-1} = U_{i-1} + iV_{i-1},$$
$$U_{i-1} = r_i^* U_i - p_i^* V_i - r_i' U_{i+1} + p_i' V_{i+1}, \qquad (3.102)$$
$$V_{i-1} = r_i^* V_i + p_i^* U_i - r_i' V_{i+1} - p_i' U_{i+1}.$$

We assume a coefficient of the form $\phi_k = 1$ at the free right end of the rod. From the boundary condition on this end we find $\phi_{k-1} = 1$. Further calculation is performed according to formulas (3.102). First we find U_{k-2} and V_{k-2}, then all the remaining numbers up to U_{i_e+1} and V_{i_e+1} inclusively.

Since calculation of the complex numbers for section IV is made independent of the calculations for the rest of the sections, then a scale $A_{IV\,M} e^{i\varphi_{IVM}}$ peculiar to this section must be introduced.

8. The two unknown scales $A_{I\,M} e^{i\varphi_{IM}}$ and $A_{IV\,M} e^{i\varphi_{IVM}}$ are determined from the conjugation conditions of sections III and IV. We give the force conjugation condition according to (3.99) in the form

$$N_{i_e+1} = N_{i_e} - N_e - m_{i_e} h\omega^2 \phi_{i_e}. \qquad (3.103)$$

The geometrical conjugation condition must express the compatibility of displacement and may be given by the following approximate formula:

$$\phi_{i_e+1} = \phi_{i_e} + h\phi'_{i_e}.$$

Having assumed the following ratio of finite differences,

$$\phi'_{i_e} = \frac{\phi_{i_e+1} - \phi_{i_e-1}}{2h},$$

we obtain

$$\phi_{i_e+1} = 2\phi_{i_e} - \phi_{i_e-1}.$$

With regard to the scales assumed the geometrical conjugation condition will have the form

$$A_{IV\,M} e^{i\varphi_{IV\,M}} \phi_{i_e+1} = A_{I_M} e^{i\varphi_{I\,M}} (2\phi_{i_e} - \phi_{i_e-1}). \qquad (3.104)$$

From this condition one scalar coefficient is expressed by the other. Replacing the complex numbers ϕ_{i_e+1}, ϕ_{i_e}, and ϕ_{i_e-1} by their real and imaginary

components, we find

$$A_{IV\,M}e^{i\varphi_{IV\,M}} = A_{I\,M}e^{i\varphi_{I\,M}}(U'_M + iV'_M), \tag{3.105}$$

where

$$U'_M = \frac{1}{D'}[U_{i_e+1}(2U_{i_e} - U_{i_e-1}) + V_{i_e+1}(2V_{i_e} - V_{i_e-1})],$$

$$V'_M = \frac{1}{D'}[-V_{i_e+1}(2U_{i_e} - U_{i_e-1}) - U_{i_e+1}(2V_{i_e} - V_{i_e-1})], \tag{3.106}$$

$$D' = U^2_{i_e+1} + V^2_{i_e+1}.$$

The force condition (3.103) is used for determining the last unknown--the scale $A_{I\,M}e^{i\,IM}$. The forces N_{i_e} and N_{i_e+1}, entering equation (1.103), is expressed by the inertial forces of the part of the rod located to one side of the section. We will have

$$N_{i_e+1} = h\omega^2 A_{I\,M}e^{i\varphi_{I\,M}}(U'_M + iV'_M)\sum_{i=i_e+1}^{i=k-1} m_i\phi_i,$$

$$N_{i_e} = -\omega^2 A_{I\,M}e^{i\varphi_{I\,M}}\left(h\sum_{i=0}^{i_1-1} m_i\phi_i + \sum_{j=A,\,B}^{(s)} m_{sj}\phi_{sj}\right). \tag{3.107}$$

On the basis of (3.98) the force N_e with regard to the scale is determined from the following equation:

$$N_e = (P_0 + m_e\omega^2\phi_{i_e}A_{I\,M}e^{i\varphi_{I\,M}})(U'_e + iV'_e). \tag{3.108}$$

Substituting into the force condition (3.103), instead of N_{i_e+1}, N_{i_e}, and N_e, their expressions in the form of (3.106) and (3.107) and considering the scale for ϕ_{i_e}, we obtain

$$h\omega^2 A_{I\,M}e^{i\varphi_{I\,M}}(U'_M + iV'_M)\sum_{i=i_e+1}^{i=k-1} m_i\phi_i =$$

$$= -\omega^2 A_{I\,M}e^{i\varphi_{I\,M}}\left(h\sum_{i=0}^{i=i_1} m_i\phi_i + \sum_{j=A,\,B}^{(s)} m_{sj}\phi_{sj}\right) -$$

$$-(P_0 + m_e\omega^2\phi_{i_e}A_{I\,M}e^{i\varphi_{I\,M}})(U'_e + iV'_e).$$

Having replaced all complex numbers by their real and imaginary components and having solved this equation relative to the desired scale, we find

$$A_{I\,M}e^{i\varphi_{I\,M}}=(U_{I\,M}+iV_{I\,M})P_0, \tag{3.109}$$

where

$$U_{I\,M}=-\frac{a_M U_K^{\cdot}+b_M V_K^{\cdot}}{a_M^2+b_M^2},$$

$$V_{I\,M}=-\frac{a_M V_K^{\cdot}-b_M U_K^{\cdot}}{a_M^2+b_M^2}, \tag{3.110}$$

$$a_M=h\left(\sum_{i=0}^{i-i_1} m_i U_i+U_M^{\cdot}\sum_{i-i_e+1}^{i-k-1} m_i U_i-V_M^{\cdot}\sum_{i-i_e+1}^{i-k-1} m_i V_i\right)+$$

$$+\sum_{j-A,\,B}^{(s)} m_{sj}U_{sj}+m_e(U_{i_e}U_e^{\cdot}-V_{i_e}V_e^{\cdot}),$$

$$b_M=h\left(\sum_{i=0}^{i-i_1} m_i V_i+V_M^{\cdot}\sum_{i-i_e+1}^{i-k-1} m_i U_i+U_M^{\cdot}\sum_{i-i_e+1}^{i-k-1} m_i V_i\right)+$$

$$+\sum_{j-A,\,B}^{(s)} m_{sj}V_{sj}+m_e(U_{i_e}U_e^{\cdot}+V_e^{\cdot}V_{i_e}).$$

All the values entering the formulas for the coefficient (3.110) are known, and the scale $A_{I\,M}e^{i\varphi_{IM}}$ can be considered to be determined.

9. We obtain the form of the induced oscillations with regard to the scales.

For the sections of the rod I, II, and III ($0 \leq i \leq i_e$) we will have

$$\varphi(x_i,\omega)A_{I\,M}e^{i\varphi_{I\,M}}=P_0[(U_iU_{I\,M}-V_iV_{I\,M})+i(U_iV_{I\,M}+U_{I\,M}V_i)].$$

The values U_i and V_i are calculated according to formulas (3.78) and the values U_{IM} and V_{IM} according to formulas (3.110).

For section IV where $i_e+1 < i \leq k$, with regard to equation (3.104), we find

$$\phi(x_i, \omega) A_{IV\,M} e^{i\varphi_{IV\,M}} = P_0 \{[(U_i U_{IM} - V_i V_{IM}) U'_M - V'_M (U_i V_{IM} + U_{IM} V_i)] + i [V'_M (U_i U_{IM} - V_i V_{IM}) + U'_M (U_i V_{IM} + U_{IM} V_i)]\}.$$

The values of U_i and V_i for section IV are calculated according to formula (3.102), the values of U_M and V_M, according to formulas (3.106), and the values of U_{IM} and V_{IM}, according to formulas (3.110). The form of the induced oscillations depends on the frequency of the external force and the scale of the form is proportional to the external force P_0.

In conclusion let us briefly examine how many elastically suspended localized masses m_s must be located in the j-th section for a practical calculation of the forms of the induced oscillations of a body. In other words, how many tones of natural oscillations of a liquid in an elastic tank must be considered in calculating the forms of the elastic oscillations of a body? Such a question also arises in calculating the forms and frequencies of the natural oscillations of a body.

The ratio between the coefficients of the form of induced oscillations for the suspension point $\phi(x_j, \omega)$ and the elastically suspended mass $\phi_{sj}(\omega)$ where $h_{sj} = 0$ is determined from the formula

$$\phi_{sj}(\omega) = \phi(x_j, \omega) \frac{\omega_{sj}^2}{\omega_{sj}^2 - \omega^2},$$

where ω_{sj} is the frequency of the natural oscillations of the elastically suspended mass m_{sj} and ω is the frequency of the induced oscillations. If the mass m_{sj} is rigidly attached to the body, then the amplitude of its oscillations is equal to $\phi(x_j, \omega)$, and the inertial force is equal to $m_{sj}\omega^2 (x_j, \omega)$. The difference between the inertial forces of an elastically suspended and a fixed mass is

$$a_{sj} m_{sj} \omega^2 \phi(x_j, m), \text{ and } a_{sj} = \frac{\omega^2}{\omega_{sj}^2 - \omega^2}.$$

A difference of inertial forces may be considered to be an error, which appears when calculating the axial forces N(x), if the mass m_{s0} is rigidly

attached. This difference is great if the frequency of induced oscillations is close to the frequency of the natural oscillations of the mass. In order that the error in calculation be insignificant the localized masses must be attached, beginning with such a number s^0 where $\omega_{s^0 j} \gg \omega$. For example, if $\omega/\omega_{sj} = 1.5$; 2, then the coefficient $\alpha_{sj} m_{sj}$, characterizing the difference of inertial forces, will be equal to $-(1.8; 1.33)\ m_{sj}$. This coefficient may be compared with the mass of the rod section ($m_i h$). The error from attaching a localized mass is equivalent to the decrease in the j-th section of the rod of some mass $m_{sj}\alpha_{sj}$. With an increase in the number s the value of the mass m_{sj} rapidly decreases, therefore the size of the error decreases not only due to the decrease in the coefficient α_{sj}, depending on the ratio of frequencies, but also due to the decrease in the mass m_{sj}. A more precise estimate may be obtained from a comparison of the forms of the induced oscillations (forms and frequencies of the natural oscillations) of the body, determined for the elastically suspended and attached mass m_{sj}.

Let us examine a numerical example. We shall determine the form of the induced longitudinal oscillations of the body of an imaginary rocket, a dynamic diagram of which is given in Fig. 3.13. Localized masses of fuel in tanks and an engine are elastically suspended in the cross-section i = N = 11, 23, and 25. The parameters of the system for purposes of calculation will be assumed to be the same as in section 7, namely:

$$\overline{m}_A = 67{,}5; \quad \overline{m}_Б = 135; \quad \overline{m}_e = 10{,}5; \quad m_0 = 15\ кГ \cdot сек^2/м;$$

$$EF_0 = 10^8\ кg; \quad \omega_A^2 = \frac{k_A}{m_A} = 30\,000\ 1/сек^2;$$

$$\omega_Б^2 = \frac{k_Б}{m_Б} = 12\,000\ 1/сек^2; \quad \omega_e^2 = \frac{k_e}{m_e} = 25\,000\ 1/сек^2.$$

The frequencies of the natural oscillations of such a rocket (see Table 3.2) are as follows: ω_1 = 103.37/sec; ω_2 = 151.27/sec; ω_3 = 257.08/sec; ω_4 = = 354.21/sec; and ω_5 = 621.9/sec.

In numerical calculation we assume the logarithmic decrement of oscillations for mechanical oscillators $\delta = 0.1$, i.e., $c_{sj} = 0.1\ \omega_{sj}/2\pi$. We shall

consider the external force $P(t) = 1 \cdot e^{i\omega t}$ to be applied to the section of the body N = 30.

A hodograph of the vector $\Phi(x, \omega)$ (amplitude-phase frequency characteristic) for the section of the rocket body $x_0 = 0$ is shown on the complex plane in Fig. 3.25. Calculation is completed for the frequencies of induced oscillations $50 \leq \omega \leq 800$/sec. The hodograph of the vector $\Phi(x_0, \omega)$ in Fig. 3.25 is shown by five seemingly independent curves. Each curve represents the

Section 0

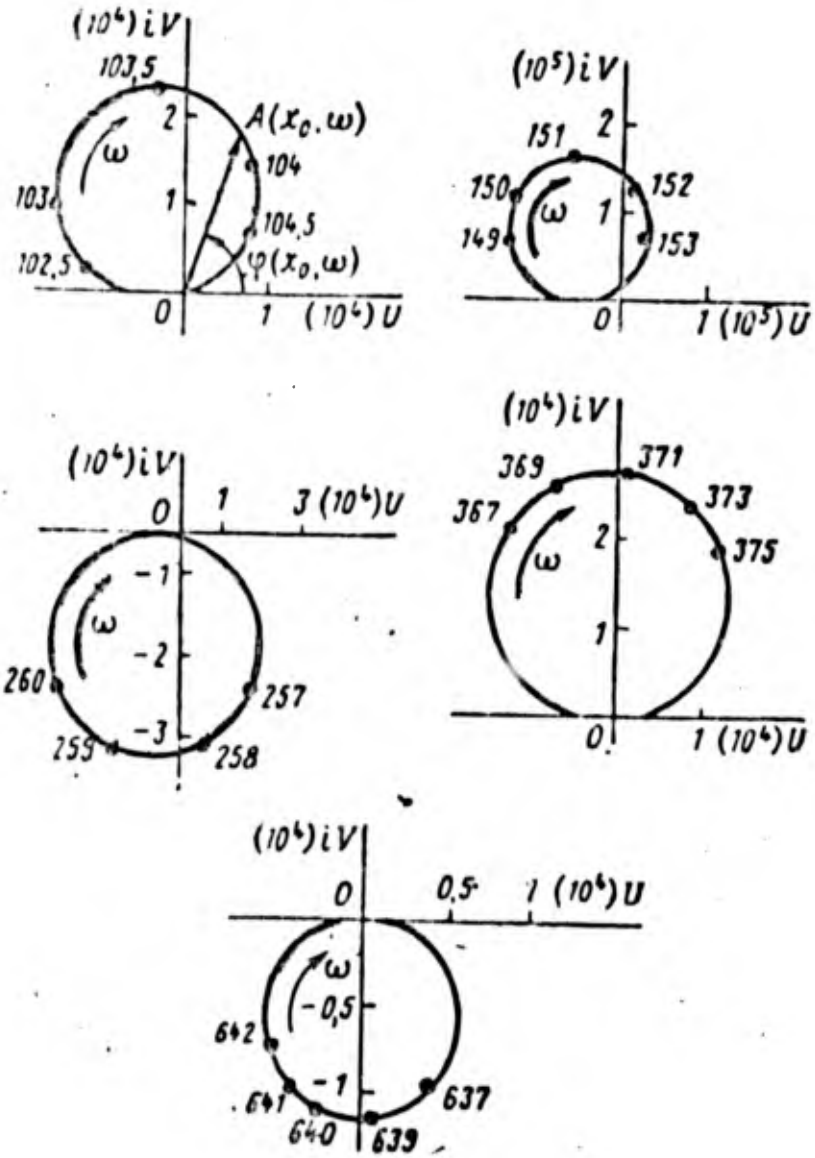

Figure 3.25

Section A

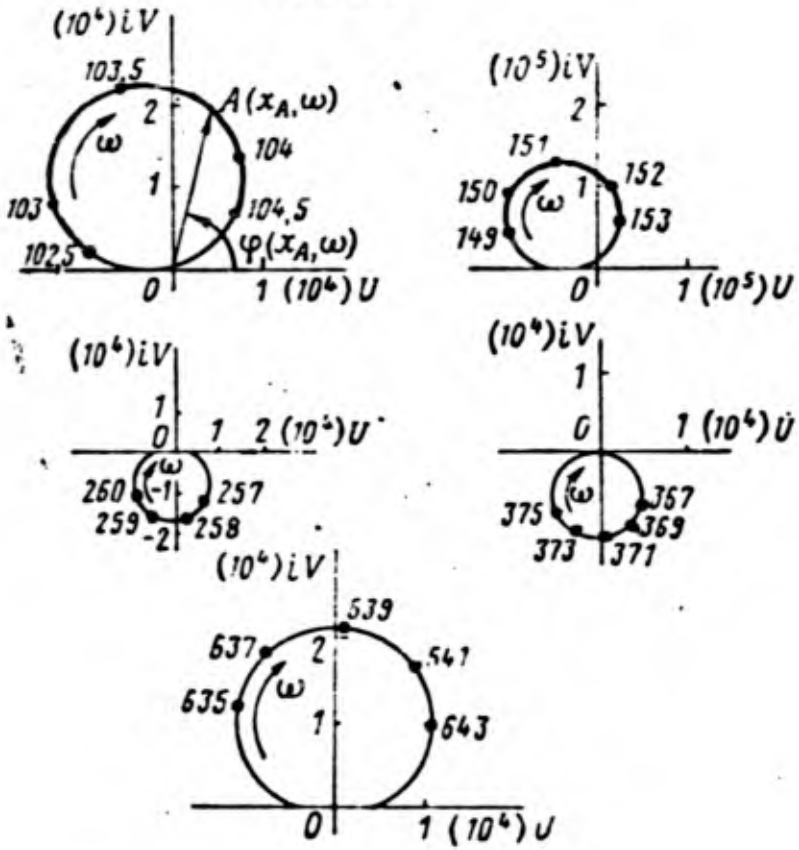

Figure 3.26

Elastically suspended localized mass m_A

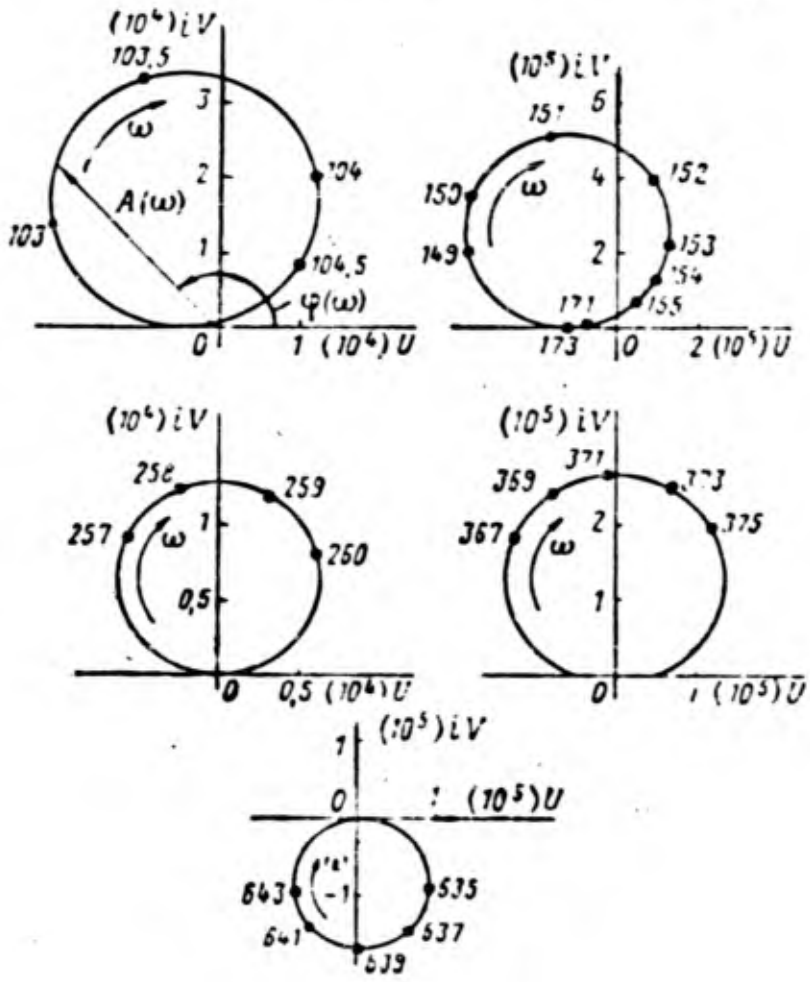

Figure 3.27

amplitude-phase characteristic close to the frequency of the natural oscillations ω_n of the body. In the vicinity of each of the frequencies of the natural oscillations the amplitude of the induced oscillations $A(x_0, \omega)$ rapidly increases and rapidly diminishes with an increase in ω and the phase shift $\varphi(x_0, \omega)$ varies by the value π. Beyond the immediate vicinity of the frequency of the natural oscillations the amplitude of induced oscillations is low. The values of the frequencies of induced oscillations ω/sec are given on the amplitude-phase characteristic.

Figure 3.26 shows the amplitude-phase characteristic for the section of the body $x_1 = x_A$, from which the localized mass m_A is elastically suspended, and Fig. 3.27 shows the amplitude-phase characteristic of the localized mass m_A. From a comparison of the characteristics it is apparent that where $\omega > \omega_A$ the localized mass m_A performs oscillations in counterphase to the oscillations of the suspension point.

The real U and imaginary V parts of the complex forms of the induced oscillations of the body at the fixed frequencies of ω = 103.5, 257, and 637 per second are shown in Figs. 3.28-3.30. These figures also give the real

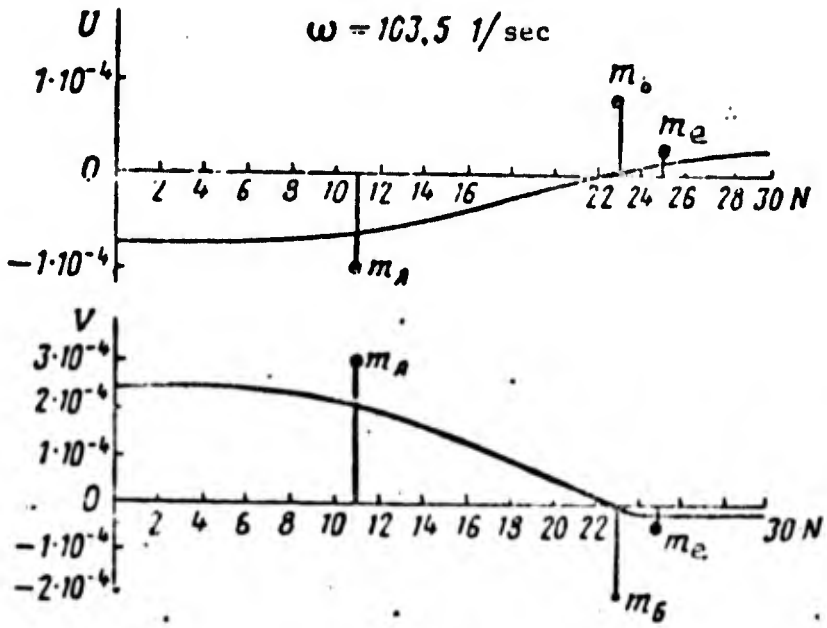

Figure 3.28

and imaginary parts of the coefficients of the form of induced oscillations for the elastically suspended masses m_A, m_B, and m_D. The forms of the induced oscillations are given in Table 3.3 in which, moreover, are shown the coordinates of the points of the forms of induced oscillations where ω = 151/sec and ω = 369/sec. The coordinates of the elastically suspended masses with their corresponding frequencies of induced oscillations are given in Table 3.4.

The amplitude-phase characteristics and forms of oscillations, similar to those depicted in Figs. 3.25-3.30, give a complete presentation of the induced oscillations of any cross-section of the rod.

We shall now examine the dynamic properties of fuel lines.

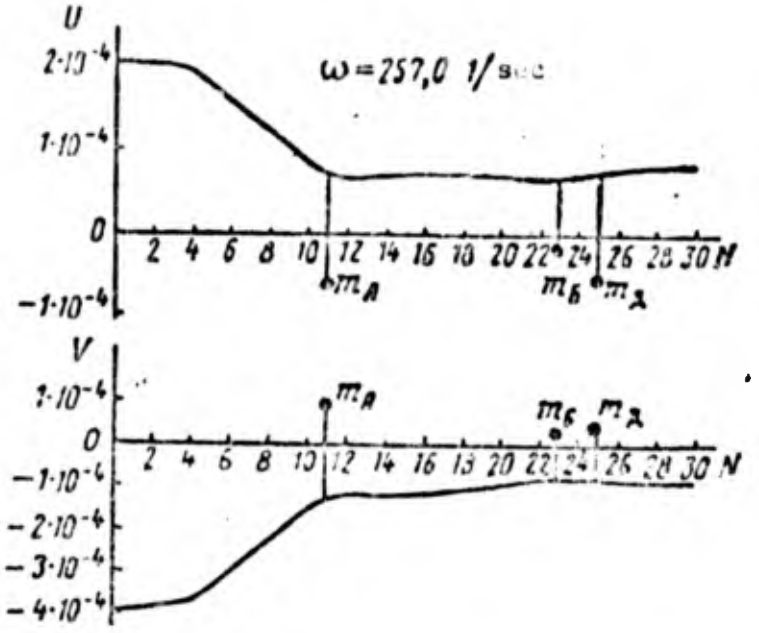

Figure 3.29

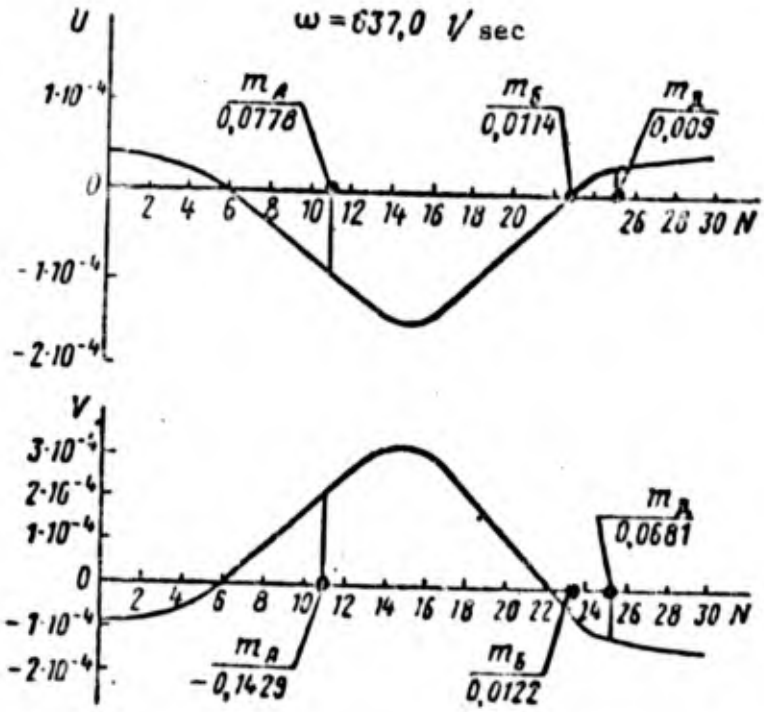

Figure 3.30

Table 3.3

No. section	Frequency of oscillations														
	ω=103,5 1/sec			ω=151 1/sec			ω=257 1/ sec			ω=369 1/ sec			ω=637 1/sec		
	$V\cdot10^4$	$U\cdot10^4$	$A\cdot10^4$	$V\cdot10^5$	$U\cdot10^5$	$A\cdot10^5$	$V\cdot10^4$	$U\cdot10^4$	$A\cdot10^4$	$V\cdot10^4$	$U\cdot10^4$	$A\cdot10^4$	$V\cdot10^4$	$U\cdot10^4$	$A\cdot10^4$
0	2,467	−0,728	2,572	1,669	−0,633	1,785	−3,917	2,028	4,412	2,709	−0,756	2,812	−0,951	0,414	1,036
2	2,464	−0,726	2,569	1,664	−0,631	1,780	−3,853	1,994	4,338	2,618	−0,731	2,718	−0,857	0,374	0,935
4	2,449	−0,722	2,553	1,642	−0,623	1,756	−3,694	1,912	4,159	2,395	−0,669	2,487	−0,640	0,279	0,698
6	2,399	−0,707	2,501	1,571	−0,596	1,680	−3,085	1,598	3,474	1,570	−0,439	1,630	0,070	−0,029	0,076
8	2,317	−0,683	2,416	1,455	−0,552	1,557	−2,334	1,209	2,629	0,580	−0,164	0,602	0,812	−0,352	0,885
10	2,234	−0,659	2,329	1,366	−0,507	1,429	−1,568	0,814	1,766	−0,415	0,114	0,430	1,527	−0,663	1,664
12	1,916	−0,567	1,998	0,428	−0,218	0,481	−1,192	0,651	1,358	−1,625	0,464	1,690	2,557	−1,150	2,804
14	1,593	−0,474	1,662	0,562	0,094	0,570	−1,192	0,684	1,374	−2,305	0,668	2,400	3,108	−1,428	3,421
16	1,309	−0,392	1,367	−1,404	0,359	1,449	−1,152	0,693	1,345	−2,824	0,825	2,942	3,027	−1,415	3,341
18	0,907	−0,276	0,948	−2,547	0,721	2,647	−1,045	0,680	1,247	−3,406	1,003	3,551	2,151	−1,048	2,396
20	0,455	−0,146	0,478	−3,822	1,124	3,984	−0,930	0,662	1,141	−3,938	1,166	4,108	1,157	−0,636	1,316
22	0,238	−0,015	0,239	−5,087	1,525	5,310	−0,809	0,640	1,032	−4,411	1,312	4,602	0,167	−0,195	0,257
24	−0,230	0,102	0,251	−7,730	2,435	8,104	−0,784	0,709	1,058	−5,401	1,661	5,651	−0,902	0,263	0,940
26	−0,235	0,164	0,286	−9,194	3,205	9,737	−0,805	0,755	1,104	−5,795	1,808	6,070	−1,171	0,380	1,231
28	−0,236	0,215	0,319	−9,314	3,754	10,04	−0,824	0,797	1,147	−6,062	1,918	6,358	−1,349	0,467	1,428
30	−0,236	0,266	0,356	−9,338	4,264	10,27	−0,829	0,828	1,171	−6,145	1,969	6,453	−1,405	0,512	1,495

Table 3.4

	ω=103,5 1/sec			ω=151 1/sec			ω=257 1/sec			ω=369 1/sec			ω=637 1/ sec		
	$V\cdot10^4$	$U\cdot10^4$	$A\cdot10^4$	$V\cdot10^4$	$U\cdot10^4$	$A\cdot10^4$	$V\cdot10^4$	$U\cdot10^4$	$A\cdot10^4$	$V\cdot10^4$	$U\cdot10^4$	$A\cdot10^4$	$V\cdot10^4$	$U\cdot10^4$	$A\cdot10^4$
m_A	2,9899	—0,9835	3,1475	0,5445	—0,1685	0,5700	0,9483	—0,5630	1,1050	0,2526	—0,0868	0,2671	—0,1429	0,0778	0,1627
$m_Б$	—1,9526	0,7817	2,1030	0,6222	—0,2295	0,6632	0,1573	—0,1439	0,2166	0,4264	—0,1673	0,4674	0,0122	0,0114	0,0167
m_A	—0,4113	0,2365	0,4744	—10,422	0,3580	10,460	0,4549	—0,4744	0,6572	0,1232	—0,4751	1,320	0,0681	0,0089	0,0687

BIBLIOGRAPHY

1. Белов В. Д., Колесников К. С., Короб В. И. О применении метода конечных разностей к задаче о собственных продольных колебаниях прямых стержней переменного сечения. — «Инженерный журнал МТТ», 1969. № 1.

2. Бидерман В. Л. Применение метода прогонки для численного решения задач строительной механики. — «Инженерный журнал МТТ», 1967, № 5.

3. Демидович Б. П., Марон И. А., Шувалова Э. З. Численные методы анализа. М., Физматгиз, 1963.

4. Крылов А. Н. О расчете балок, лежащих на упругом основании М., изд-во АН СССР, 1930.

5. Микеладзе Ш. Е. Новые методы интегрирования дифференциальных уравнений. М., ГТТИ, 1951.

6. Папкович П. Ф. Строительная механика корабля, ч. II. М., Судпромгиз, 1941.

7. Пановко Я. Г. Внутреннее трение при колебаниях упругих систем. М., Физматгиз, 1960.

8. Пенгелли. Нормальные формы и частоты продольных колебаний ракет на жидком топливе. — «Вопросы ракетной техники», 1969, № 4.

9. Пономарев С. Д., Бидерман В. Л., Лихарев К. К., Макушин В. М., Малинин Н. Н., Феодосьев В. И. Расчеты на прочность в машиностроении. М., Машгиз, т. 3, 1959.

10. Роуз. Анализ продольной устойчивости ракет на жадком топливе. — «Вопросы ракетной техники», 1967, № 5.

11. Тимошенко С. П. Колебания в инженерном деле. М., Физматгиз, 1959.

12. Шиманский Ю. А. Динамический расчет судовых конструкций. М., Судпромгиз, 1963.

13. Makenna K. J., Walker J. H., Winje R. A. A Model for Studying the Coupled Engine-Airframe Longitudinal Instability of Liquid Rocket Systems, AIAA, Aerospace Sci. Meeting, January, 1964.

Chapter 4

INDUCED OSCILLATIONS OF THE LIQUID IN THE FUEL LINES

1. Structure of Fuel Lines

The fuel components are delivered from the tanks to the combustion chambers of the engines along the fuel lines which are pipes of special construction. A characteristic feature of pressure lines is the presence of devices with great hydraulic resistance, such as valves, regulators, discharge collars, nozzles, the cooling track (for the cooling component), and so forth. The pressure in high-pressure lines reaches tens and even hundreds of atmospheres, therefore high-pressure lines are made rigid and relative short. With regard to these characteristics, in studying low-frequency oscillations it is possible to examine a high-pressure line as a hydraulic system with lumped values. Since the dynamic properties of the flow of liquid in a high-pressure line and units of a liquid propellant engine are interconnected, it is convenient to include this line in the dynamic scheme of the liquid propellant engine.

As opposed to the force mains, the discharge mains are made of comparatively great length. In order to provide a given cavitation pump reserve at an acceptable boost pressure in the tanks the hydraulic resistance in the discharge mains must be insignificant, and hence the flow rate of the liquid must be small. Low-pressure lines are of large diameter and have thin walls, due to which the rigidity of the lines and their junction is insignificant. The fundamental part of pressure losses in the discharge mains is due to local resistances—bends, joints, branching, pyrovalves, and so forth.

In order to compensate for variation in the length of the lines, to remove the influence of technological and temperature misalignments, and to remove the influence of vibrations, bellows, possessing low (in comparison with the pipe) axial and angular rigidity, are located at various points of the discharge main. The use of a system of silphons of special construction to provide for a constant volume of pipeline during revolutions of the engine is also known.

An important factor determining the significant pliability of the column of liquid in the input main is the presence of a vapor-gas mixture, appearing as a consequence of cavitation in those sections where the local static pressure is less than the pressure of the liquid and the equilibrium pressure of gases dissolved in the liquid. Cavitation is particularly developed in the jet ejectors and at the inlet to the screw pumps, which are present to increase the pressure at the inlet to the centrifugal pumps. In the presence of a vapor-gas mixture at the inlet to the pump the column of liquid in the input main is under the influence of a localized vapor pressure, similar to the action of a spring, as a consequence of which the frequency of its natural longitudinal oscillations is significantly lower than in the absence of a vapor-gas mixture.

In order to provide for stable operating conditions of a closed rocket system with a liquid propellant engine, the designers sometimes consciously strive to lower the frequency of the natural oscillations of the column of liquid, artificially decreasing the volumetric rigidity of the input main. This problem will be examined in detail below. At this point we shall only mention the methods which are known to be suitable for this purpose [1, 13, 30]: lowering the radial rigidity of the pipe introducing bubbles of an insoluble gas into the liquid, and including hydraulic accumulators (hydraulic dampers) in several sections, for example at the pump inlet.

In an analysis of the dynamic properties of the fuel mains consideration of the boundary conditions, which express the connection between pressure oscillations and the flow rate are of important significance. The nature of this connection may be established from a consideration of the hydrodynamic properties of the units and apparatus with which the pipeline is connected. They may be tanks, collars, throttles, receivers, collectors, sections of pipe with other parameters, and, finally, a liquid propellant engine. In dynamic conditions the presence of elasticity, hydraulic resistance, and inertia usually determines a complex relationship between the pressure and flow rate at the end of the pipe.

Figure 4.1 gives a diagram of the fuel lines of a Thor-Agena rocket [19] with one sustainer, 3. The fuel and oxidizer mains have the same structure; fuel tank 1 is located in the upper, and oxidizer tank 2 in the lower part of the rocket. The input fuel main consists of a long low-pressure pipe, 4, which is united with fuel pump 7 through an elbow and section of pipe, located in the plane of the cross-section. The low-pressure pipe passes through the oxidizer tank into conduit 5. The diagram also shows: the oxidizer input main (short) 6, the oxidizer pump 8, turbine 9, ZhGG [expansion unkwnown] 10. Both mains are provided with silphons 11, installed near the turbine pump assembly and funnel damper 12 at the outlet from the tanks.

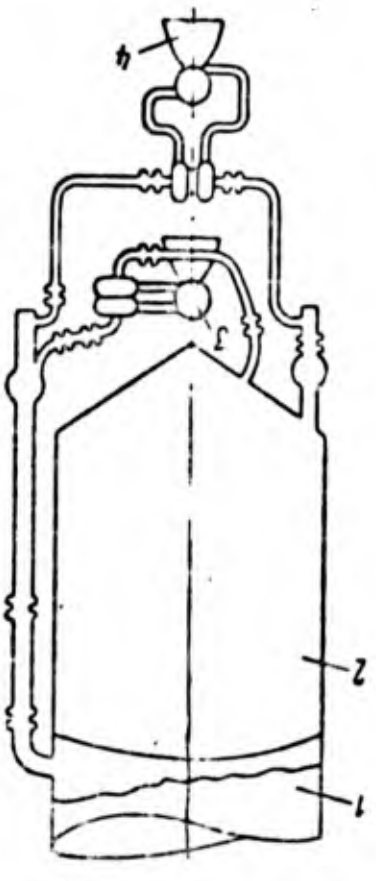

Figure 4.1

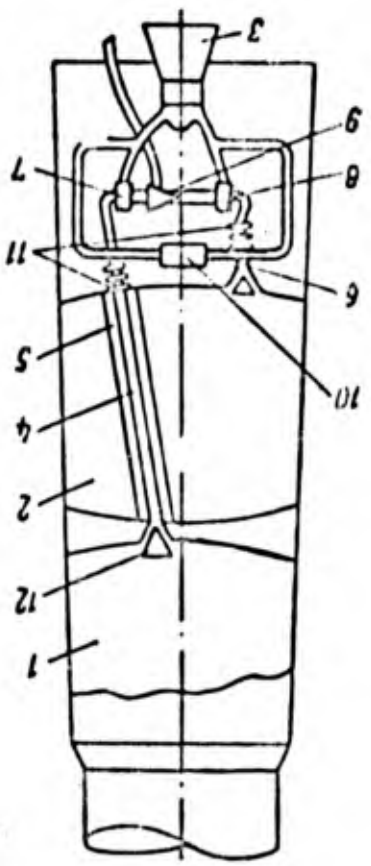

Figure 4.2

The fuel system of the Titan-2 [1, 3] with two sustainers is shown in Fig. 1.6. The fuel is fed from the tanks along two comparatively short, equally long input mains 5, which are provided with hydraulic dampers 3. The oxidizer input main branches into two branches in front of the turbine pump assembly, the structural parameters of which branches differ from the parameters of the

main before its branching. Between the branching unit (collector) and the turbine pump assembly there is a silphon and stresses on the collector from the pressure of the liquid are transmitted directly to the rocket body.

Still more complex are the fuel mains of an Atlas rocket [13] with one sustainer and two boosters (Fig. 4.2).

Here 1 is the oxidizer tank, 2 is the fuel tank, 3 is the sustainer, and 4 is the booster. The feeding system of the second booster is not shown. As is apparent, the oxidizer main in the engine section branches in the direction of the sustainer, and then divides into two monotypical branches, feeding the boosters. The fuel main for the boosters also divides into two branches. All the mains are provided with silphons and funnel dampers, and bends in the lines are extensively used.

The examples given are sufficient to show the structural complexity of the input mains of liquid propellant rockets. For convenience of further investigation we shall divide the input mains into the following typical elements possessing the specific properties:

— relatively long sections of pipe with constant diameters and wall thickness;

— silphons;

— elements of pipe, in which the flow of liquid on a short section undergoes such changes as bends, branching, and change in diameter;

— hydraulic accumulators (hydraulic dampers of longitudinal oscillations);

— local sections of the main with cavitating fuel;

— elements possessing localized hydraulic resistance.

Let us examine the dynamic characteristics of each of these elements in particular. We shall begin with a long straight pipe.

2. Equations of the Disturbed Motion of a Compressible Liquid in a Long Straight Pipe

In the case of a long pipe (with a diameter small in comparison with its length) a detailed analysis of the complex phenomena occurring at the ends of the pipe may be omitted and it may be considered that the dynamic processes on these sections are described by the same equations which describe the processes in the pipe itself.

We shall consider the internal friction in the liquid filling the pipe in a simplified way, considering that the motion speed of the particles of the liquid v is equal along the entire section, i.e., assuming a plane wave. We shall assume the force of friction to be proportional to the value of the wetted perimeter and speed v. In the case of low viscosity the speed of the liquid is almost constant along the entire section and decreases rapidly only in a narrow boundary layer near the wall. If, moreover, we only consider low frequencies of oscillations (the wavelength of which is large in comparison with the diameter of the pipe), then it is possible to consider that in each cross-section of the flow of the liquid in the pipe all values (speed, pressure, and so forth) are constant, and the flow of liquid is uniform.

Let us direct the axis Ox along the axis of the pipe. Linearized equations of the disturbed motion of the liquid in the pipe may be given in the form [18]

$$\frac{\partial v}{\partial t}+v_0\frac{\partial v}{\partial x}+\frac{1}{\varrho_0}\frac{\partial p}{\partial x}+\frac{8\nu_ж}{r_0^2}v=0, \tag{4.1}$$

where ρ_0 and a_0 are the density and speed of the liquid in an undisturbed flow; $v = v(x, t)$, $p = p(x, t)$ are small disturbances of the speed and pressure of the liquid; $\nu_ж$ is the kinematic coefficient of viscosity of the liquid; and r_0 is the radius of the pipe.

We shall put the linearized continuity equation of the liquid in the form

$$\frac{\partial \varrho}{\partial t}+v_0\frac{\partial \varrho}{\partial x}+\varrho_0\frac{\partial v_x}{\partial x}=0. \tag{4.2}$$

We shall introduce the dimensionless values

$$M=\frac{v_0}{a_0},\quad \tau=\frac{a_0}{l}t,\quad \xi=\frac{x}{l},\quad \tilde{v}(\xi,\tau)=\frac{v}{a_0},$$
$$p(\xi,\tau)=\frac{p}{a_0^2\varrho_0}, \tag{4.3}$$

where l is the length of the pipe; a_0 is the speed of sound in an undisturbed flow.

Equations (4.1) and (4.2) in dimensionless form will be

$$\begin{aligned}&\frac{\partial\tilde{v}(\xi,\tau)}{\partial\tau}+M\frac{\partial\tilde{v}(\xi,\tau)}{\partial\xi}+\frac{\partial\tilde{p}(\xi,\tau)}{\partial\xi}+\beta\tilde{v}(\xi,\tau)=0,\\&\frac{\partial\tilde{p}(\xi,\tau)}{\partial\tau}+M\frac{\partial\tilde{p}(\xi,\tau)}{\partial\xi}+\frac{\partial\tilde{v}(\xi,\tau)}{\partial\xi}=0,\end{aligned} \tag{4.4}$$

where

$$\beta=\frac{8\nu_{\text{ж}}l}{a_0r_0^2}.$$

We reduce these equations to one second order equation relative to the variable $v(\xi,\tau)$. Assuming $\beta M \approx 0$, we obtain

$$(1-M^2)\frac{\partial^2\tilde{v}(\xi,\tau)}{\partial\xi^2}-2M\frac{\partial^2\tilde{v}(\xi,\tau)}{\partial\xi\partial\tau}-\frac{\partial^2\tilde{v}(\xi,\tau)}{\partial\tau^2}-\beta\frac{\partial\tilde{v}(\xi,\tau)}{\partial\tau}=0. \tag{4.5}$$

Knowing the velocity disturbance $\tilde{v}(\xi,\tau)$, from the first equation (4.4) we find the pressure disturbance

$$\tilde{p}(\xi,\tau)=-M\tilde{v}(\xi,\tau)-\int\frac{\partial\tilde{v}(\xi,\tau)}{\partial\tau}d\xi-\beta\int\tilde{v}(\xi,\tau)d\xi. \tag{4.6}$$

Solutions of equations (4.4) or equation (4.5) must satisfy the boundary and initial conditions.

In the simplest case the boundary conditions may be reduced to linear uniform ratios between the variable $\tilde{p}(\xi,\tau)$ and $\tilde{v}(\xi,\tau)$, which must be satisfied at the ends of the pipe. We locate the origin of coordinates $\xi = 0$ at

the left end of the pipe, then for the right end of the coordinate $\xi = 1$. Under this condition the boundary conditions may be put in the form

$$b_{11}\tilde{v}(\xi, \tau) + b_{12}\tilde{p}(\xi, \tau) = 0 \quad \text{where} \quad \xi = 0,$$
$$b_{21}\tilde{v}(\xi, \tau) + b_{22}\tilde{p}(\xi, \tau) = 0 \quad \text{where} \quad \xi = 1.$$

Here b_{11}, b_{12}, ... are certain differential operators.

The initial conditions must give the velocity and pressure distribution along the length of the pipe. However, in the discussion below we shall be interested only with stationary oscillations of the liquid for which the initial conditions do not have value.

In the simplest cases the boundary conditions will be the following:
for the open end of the pipe $\tilde{p}(\xi, \tau) = 0$,
for the closed end of the pipe $\tilde{v}(\xi, \tau) = 0$.

The open and closed ends of the pipe must be understood in the acoustical sense. Pressure at the open end of the pipe remains constant and equal to p_0, i.e., the pressure disturbance $\tilde{p} = 0$. At the closed end of the pipe the velocity is constant ($v_0 = \text{const}$), i.e., the velocity disturbance $\tilde{v} = 0$. In the particular case the end of the pipe may be hydraulic closed, then $v_0 = 0$, $\tilde{v} = 0$.

Dispersion of energy almost always takes place at the inlet to the pipe and at the outlet to the pipe, which has primary significance in an analysis of the resonance conditions and in studying the stability of motion.

On the basis of equation (4.6) it is possible to establish that in any cross-section of the flow of the liquid the ratio between the pressure disturbance and the velocity disturbance during oscillations is expressed by a complex number. Therefore, for the boundary section, the ratio $\tilde{p}(\xi, \tau)/\tilde{v}(\xi, \tau)$ may be represented in the form

$$\frac{\tilde{p}(\xi, \tau)}{\tilde{v}(\xi, \tau)} = z = M\tilde{\psi} + ia. \tag{4.7}$$

The complex number z (complex resistance) is usually called the boundary impedance. By analogy with an electrical line it is possible to consider that the real part of this number characterizes the 'active' and the imaginary part characterizes the 'reactive' resistance. In equation (4.7) $\tilde{\psi}$ is the coefficient of the 'active' resistance, relative to the flow rate, and α is the coefficient of the 'reactive' resistance. Sometimes, instead of the complex resistance, the opposite value, the complex conductivity z*, is considered. Then, instead of ratio (4.7) we will have

$$\frac{\tilde{v}(\xi, \tau)}{\tilde{p}(\xi, \tau)} = z^*.$$

'Reactive' resistance or 'reactive' conductivity arise, for example, due to the presence of localized elasticity at the ends of the flow of the liquid caused by the presence of silphons or certain amounts of a vapor-gas mixture in the suction part of the pump. We shall obtain solutions for equation (4.5) under various boundary conditions.

3. The Natural Oscillations of a Liquid in a Uniform Pipe

We shall solve equation (4.5) by the Fourier method [14]. We shall represent the functions $\tilde{v}(\xi, \tau)$ and $\tilde{p}(\xi, \tau)$ in the form

$$\tilde{v}(\xi, \tau) = \tilde{v}(\xi) e^{is\tau}, \qquad \tilde{p}(\xi, \tau) = \tilde{p}(\xi) e^{is\tau}, \tag{4.8}$$

where s is a dimensionless oscillation frequency.

Having substituted the function expressions $\tilde{v}(\xi, \tau)$ and $\tilde{p}(\xi, \tau)$ into equations (4.5) and (4.6), and having eliminated the factor $e^{is\tau}$, we obtain the following equations for determining the functions $\tilde{v}(\xi)$ and $\tilde{p}(\xi)$:

$$(1 - M^2)\frac{d^2\tilde{v}(\xi)}{d\xi^2} - is2M\frac{d\tilde{v}(\xi)}{d\xi} + (s^2 - is\alpha)\tilde{v}(\xi) = 0, \tag{4.9}$$

$$\tilde{p}(\xi) = -M\tilde{v}(\xi) - (is + \alpha)\int \tilde{v}(\xi)\, d\xi. \tag{4.10}$$

Assuming $\tilde{v}(\xi) = Ce^{k\xi}$, and (4.9) we find

$$k_1 = n_1 + im_1, \qquad k_2 = n_2 + im_2. \tag{4.11}$$

Having solved this equation relative to k, we obtain

$$(1 - M^2)\, k^2 - is2Mk + s^2 - is^3 = 0. \tag{4.12}$$

In the particular case where $\beta = 0$

$$k_1 = \frac{is}{1 - M}, \quad k_2 = -\frac{is}{1 + M}. \tag{4.13}$$

Additionally considering the ratio (4.10), we obtain equations of the forms of the oscillations of velocity $\tilde{v}(\xi)$ and pressure $\tilde{p}(\xi)$:

$$\begin{aligned} \tilde{v}(\xi) &= C_1 e^{k_1 \xi} + C_2 e^{k_2 \xi}, \\ \tilde{p}(\xi) &= C_2 e^{k_2 \xi} - C_1 e^{k_1 \xi}. \end{aligned} \tag{4.14}$$

The arbitrary constants C_1 and C_2 may be determined from the boundary conditions.

On the basis of (4.14) the velocity and pressure at the ends of the pipe may be calculated according to the following formulas

$$\begin{aligned} \tilde{v}(0) &= C_1 + C_2, \quad \tilde{v}(1) = C_1 e^{k_1} + C_2 e^{k_2}, \\ \tilde{p}(0) &= C_2 - C_1, \quad \tilde{p}(1) = C_2 e^{k_2} - C_1 e^{k_1}. \end{aligned}$$

From these formulas we obtain the relationship between the parameters of the flow $\tilde{v}(1)$, $\tilde{p}(1)$ and the parameters of the flow $\tilde{v}(0)$, $\tilde{p}(0)$ at the beginning of the pipe:

$$\begin{aligned} \tilde{v}(1) &= v(0)\, \frac{1}{2}(e^{k_2} + e^{k_1}) + \tilde{p}(0)\, \frac{1}{2}(e^{k_2} - e^{k_1}), \\ \tilde{p}(1) &= \tilde{v}(0)\, \frac{1}{2}(e^{k_2} - e^{k_1}) + \tilde{p}(0)\, \frac{1}{2}(e^{k_2} + e^{k_1}). \end{aligned} \tag{4.15}$$

Relationships of the type (4.15), by analogy with electrical diagrams, are usually called quadrupole equations. If any two boundary conditions are known, then it is possible to determine the desired flow parameters at the ends of the pipe from these equations. For example, having established the harmonic influence on a flow at one of the ends of the pipe, it is possible to determine the harmonic oscillations of the flow at the other end and to obtain an expression for the amplitude-phase frequency characteristic.

We shall use equation (4.15) in order to determine the frequencies of the natural oscillations of a flow of liquid in a pipe, limiting ourselves to an analysis of the case where the coefficient $\beta = 0$ characterizes the friction of the liquid on the wall. Let us now examine several boundary conditions.

1. $\tilde{p}(0) = 0$, $\tilde{v}(1) = 0$ — the pipe is open at one end.

Having substituted these conditions into equation (4.15) and considering that $e^{k_2} \neq 0$, we obtain the characteristic equation in the form

$$e^{k_1 - k_2} = 1. \tag{4.16}$$

The frequency of the natural oscillations, generally speaking, is a complex number; therefore we assume

$$s = i\nu + \Omega, \tag{4.17}$$

where ν and Ω are real numbers.

With consideration of equations (4.13) and (4.17) we obtain

$$k_1 - k_2 = -\frac{2\nu}{1 - M^2} + i\frac{2\Omega}{1 - M^2}.$$

We shall write equation (4.16) in trigonometric form, having set its real and imaginary parts equal to zero separately:

$$\exp\left(\frac{-2\nu}{1 - M^2}\right)\cos\frac{2\Omega}{1 - M^2} = -1,$$

$$\exp\left(\frac{-2\nu}{1 - M^2}\right)\sin\frac{2\Omega}{1 - M^2} = 0.$$

Insofar as $\exp(-2\nu/1-M^2) > 0$, both equations will be realized simultaneously if

$$\nu=0 \text{ и } \frac{2\Omega_n}{1-M^2}=(2n-1)\pi \qquad (n=1, 2, \ldots).$$

The natural oscillations of the flow of an ideal liquid in a pipe are harmonic; the dimensionless frequencies of these oscillations are calculated according to the following formula

$$s_n=\Omega_n=\frac{(2n-1)\pi}{2}(1-M^2) \qquad (n=1, 2\ldots). \tag{4.18}$$

The dimensional frequency is

$$\omega_n=s_n\frac{a_0}{l}=\frac{(2n-1)\pi(1-M^2)a_0}{2l}. \tag{4.18a}$$

If $\tilde{v}_0 = 0$ (M = 0), then there will be an immobile column of liquid instead of a flow; the frequency of the natural oscillations of the column of liquid is expressed by the same formula as is used to express the frequency of the natural oscillations of a straight uniform rod (3.10).

When oscillations appear in the flow of a fluid ($M \neq 0$), the frequency of the natural oscillations of the flow is less than that of an immobile column of liquid. The difference will be greater the greater the number M is. As is known, in a supersonic flow (M > 1) the particle motion speed is greater, the greater the propagation speed of the elastic wave is; therefore where $M \geq 1$ natural oscillations cannot exist.

The motion speed of the fuel along the pipes from the tanks to the pump in liquid propellant rockets is small, since the number M is much less than 1. For such flows, the factor $(1 - M^2)$ practically does not differ from unity; therefore in the case of low values of M it is possible to consider $M^2 \approx 0$.

2. $\tilde{p}(0) = 0$, $\tilde{p}(1) = 0$ -- the pipe is closed from both ends.

Having performed analogous calculations, we obtain

$$\nu=0, \quad \frac{2\Omega}{1-M^2}=2n\pi \qquad (n=0, 1, 2, \ldots).$$

Or, paying attention to only the non-trivial values of the frequencies of the natural oscillations, we find

$$s_n = n(1-M^2)\pi,$$
$$\omega_n = s_n \frac{a_0}{l} = n(1-M^2)\frac{\pi a_0}{l}. \tag{4.19}$$

The natural oscillations of the flow of a liquid in a pipe with closed ends may be compared with the natural oscillations of a straight elastic unattached rod. The motion of a liquid flow without oscillations corresponds to a zero frequency, which takes during the transition of a flow to a new stationary flow speed at the same pressure.

3. $\tilde{p}(0) = -M\tilde{\psi}_1\tilde{v}(0)$, $\tilde{p}(1) = M\tilde{\psi}_2\tilde{v}(1)$ — the pipe has grids at the ends—hydraulic resistances. Here $\tilde{\psi}_1$ is the coefficient of resistance referred to the flow speed at the entrance to the pipe; and $\tilde{\psi}_2$ is the same at the outlet from the pipe (Fig. 4.3).

Having substituted these conditions into equation (4.15), we obtain the characteristic equation

$$3.\ \tilde{p}(0) = -M\tilde{\psi}_1\tilde{v}(0),\ \tilde{p}(1) = M\tilde{\psi}_2\tilde{v}(1) -$$

Having solved this, we find the neutral values of the frequencies of the natural oscillations

$$s_n = (1-M^2)n\pi \quad (n = 1, 2, \ldots) \tag{4.20}$$

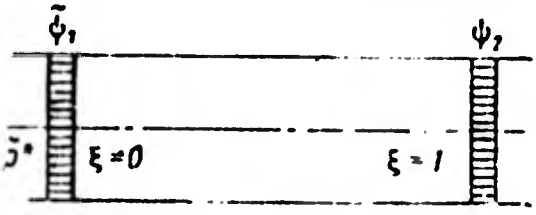

Figure 4.3

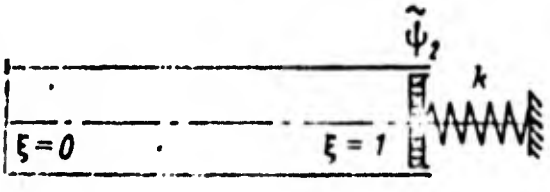

Figure 4.4

and the dimensionless damping coefficient of the oscillations

$$\nu = \frac{1-M^2}{2}\ln\frac{(1+\tilde{\psi}_1 M)(1+\tilde{\psi}_2 M)}{(1-\tilde{\psi}_1 M)(1-\tilde{\psi}_2 M)}. \tag{4.21}$$

The frequency of the natural oscillations of the flow of a liquid in a pipe with localized resistances at the ends is the same as in the case of a pipe with both ends closed without resistances (4.19).

Since $is = -\nu + i\Omega$, then the natural oscillations of the flow of a liquid in a pipe with resistances at its ends is damped.

4. $\tilde{p}(0) = 0$, $\tilde{v}(1) = z_2^*\tilde{p}(1)$ — one end of the pipe is closed, and the other end has the complex conductivity $z_2^* = (1/\tilde{\psi}_2 M) + i\alpha_2^*$. Such a boundary condition, for example, will take place if the hydraulic grid is elastically fixed in relation to the flow of the liquid (Fig. 4.4).

Since

$$\tilde{v}(1) = \frac{1}{\tilde{\psi}_2 M}\tilde{p}(1) + is\frac{F_T a_0^2 \rho_0}{kl}\tilde{p}(1),$$

where k is the stiffness factor of the spring and F_T, l is the area of the flow section and the length of the pipe, then for the diagram shown in Fig. 4.4 the coefficient $\alpha_2^* = s(F_T a_0^2 \rho_0/kl)$. If there is a weightless piston instead of the hydraulic grid, then $\tilde{\psi}_2 = \infty$ and $z_2^* = is\,(F_T a_0^2 \rho_0/kl$, if $\tilde{\psi}_2 \neq \infty$ and $k = \infty$, then $z_2^* = (1/\tilde{\psi}_2 M)$.

Having substituted the boundary condition equations into relationships (4.15), we obtain the following characteristic equation:

$$\frac{1 + e^{k_1 - k_2}}{1 - e^{k_1 - k_2}} = z_2^*.$$

Having assumed s in the form (4.17) and having assumed $M^2 \approx 0$, we transform the characteristic equation to the form

$$\operatorname{cth}(\nu - i\Omega) = z_2^*.$$

Having equated the real and imaginary parts of this equation, we obtain

$$\frac{\operatorname{sh}\nu \operatorname{ch}\nu}{\operatorname{sh}^2\nu + \sin^2\Omega} = \frac{1}{\tilde{\psi}_2 M},$$
$$\frac{\cos\Omega \sin\Omega}{\operatorname{sh}^2\nu + \sin^2\Omega} = \Omega\alpha_2^*. \qquad (4.22)$$

It is possible to determine the dimensionless damping coefficient ν and the frequencies of natural oscillations Ω_n by a numerical solution of the transcendental equations (4.22).

Let us examine the particular case where $\tilde{\psi}_2 = \infty$. Then from the first equation (4.22) it follows that $\nu = 0$ (there is no damping). From the second equation we obtain

$$\operatorname{tg}\Omega = \frac{1}{\Omega a_2^*}.$$

A solution of the last equation by the graphic method is schematically shown in Fig. 4.5. The intersection point of the curve tan Ω with the hyperbola $1/\Omega a_2^*$ gives the values of the roots of this equation. The greater a_2^* is (the less the stiffness factor of the spring k is), the lower the frequencies of the natural oscillations of the column of liquid will be. This has important significance for analyzing the dynamic properties of fuel lines since the frequency of the natural oscillations of the first tone of a column of liquid, one end of which rests on a 'spring', proves to be lower than the frequency of the first tone of the oscillations of a column of liquid 'without a spring'.

When $a_2^* = 0$ (i.e., $k = \infty$), then

$$\Omega_n = s_n = \frac{(2n-1)\pi}{2}.$$

This result was already obtained in (4.18) for the natural oscillations of a column of liquid in a pipe with one end closed.

The forms of the natural oscillations of velocity $\vartheta(\xi)$ and pressure $\mathfrak{p}(\xi)$ are determined from equations (4.14). Since $C_1' = C_2$ for a pipe closed at one end, then on the basis of (4.14)

$$\tilde{v}_n(\xi) = C_1(e^{k_{1n}\xi} + e^{k_{2n}\xi}),$$
$$\tilde{p}_n(\xi) = C_1(e^{k_{2n}\xi} - e^{k_{1n}\xi}).$$

Graphs of the functions $\tilde{v}_n(\xi)$ and $\tilde{p}_n(\xi)$ for the first two tones of the natural oscillations are given in Fig. 4.6. The form of the natural oscillations

of velocity $\tilde{v}_n(\xi)$ has the same appearance as the form of the natural oscillations of an elastic rod with one fixed end.

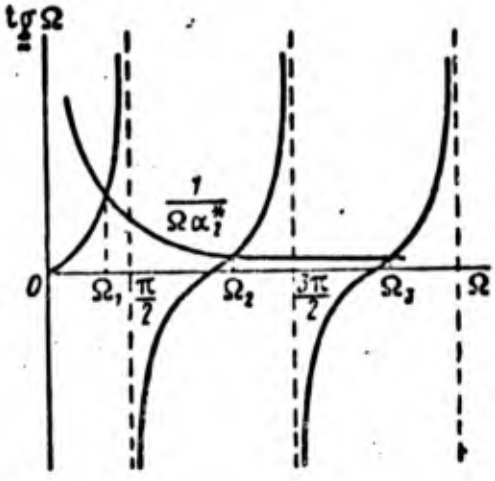

Figure 4.5

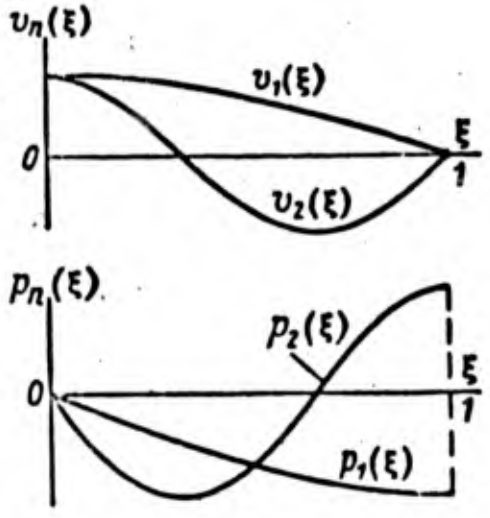

Figure 4.6

The forms of the natural oscillations $\tilde{v}_n(\xi)$ and $\tilde{p}_n(\xi)$ are standing waves, since the amplitude distribution of the oscillations of velocity and pressure longitudinally at any moment of time remains the same.

Besides standing waves, sometimes traveling waves are considered, which in our example characterize motion along the pipe of acoustical impulses $\tilde{u}_1(\xi, \tau)$ and $\tilde{u}_2(\xi, \tau)$ [12]:

$$\tilde{u}_1(\xi, \tau) = \frac{\tilde{v}(\xi, \tau) + \tilde{p}(\xi, \tau)}{2}, \quad \tilde{u}_2(\xi, \tau) = \frac{\tilde{v}(\xi, \tau) - \tilde{p}(\xi, \tau)}{2}. \tag{4.23}$$

From these equations we shall determine v and p and substitute them into equations (4.4). Then having taken the sum and difference of the equations obtained, we obtain the two following equations instead of (4.4) in the case where $\beta = 0$:

$$\frac{\partial \tilde{u}_1}{\partial \tau} + (1 + M)\frac{\partial \tilde{u}_1}{\partial \xi} = 0,$$

$$\frac{\partial \tilde{u}_2}{\partial \tau} + (1 - M)\frac{\partial \tilde{u}_2}{\partial \xi} = 0.$$

Each of these equations is integrated individually. Having used d'Alambert's method [14], we give the solution of the first equation in the form

$$\tilde{u}_1(\xi, \tau) = F_1[\xi - (1+M)\tau],$$

where F_1 is an arbitrary differential function.

In the case of ratios of moments of time τ and coordinates ξ, which satisfy the condition

$$\xi - (1+M)\tau = \xi_1 = \text{const},$$

the value $\tilde{u}_1(\tau, \xi)$ will be equal to $F_1(\xi_1)$ and it may be presented visually by an instantaneous photograph of a wave. Let us examine the motion of the crest of this wave. If at the moment $\tau = 0$ the crest had the coordinate ξ_1, then the section corresponding to it (in which F_1 reaches the maximum) will be displaced according to the law

$$\xi = \xi_1 + (1+M)\tau.$$

By analogous reasoning, for the function $\tilde{u}_2(\xi, \tau)$ we find that

$$\tilde{u}_2(\xi, \tau) = F_2[\xi - (M-1)\tau],$$

$$\xi = \xi_2 + (M-1)\tau.$$

Consequently, the solutions found for $\tilde{u}_1(\xi, \tau)$ and $\tilde{u}_2(\xi, \tau)$ describe the motion of the wave u_1 and the wave u_2 without changing their form in the positive direction of the axis with the velocities (1+M) and (M-1), respectively. This signifies that the wave $\tilde{u}_1$ is propogated only in the positive direction at the velocity (1+M), and the wave $\tilde{u}_2$, only in the negative direction (opposite the flow) at the velocity (1-M). Acoustical impulses move along the flow at the speed of sound plus the speed of the flow, and opposite the flow with the speed of sound minus the speed of the flow. According to this principle $\tilde{u}_1$ and $\tilde{u}_2$ are called traveling waves. In the case of motion along the axis ξ, the amplitude (crest height) of the traveling waves remains constant. For illustration Figs. 4.7 and 4.8 show standing ($\tilde{v}$, $\tilde{p}$) and traveling ($\tilde{u}_1$, $\tilde{u}_2$) waves at various moments of time τ.

The boundary conditions for the functions $\tilde{u}_1$ and $\tilde{u}_2$ are the following. For the open end of the pipe p = 0; on the basis of (4.23) we have $\tilde{u}_1 - \tilde{u}_2 = 0$ or $\tilde{u}_1 = \tilde{u}_2$. For the closed end of the pipe, $v = 0$. From (4.23) we obtain $\tilde{u}_1 + \tilde{u}_2 = 0$ or $\tilde{u}_1 = -\tilde{u}_2$.

The traveling wave from the open end of the pipe is reflected for motion in the opposite direction with the same sign ($\tilde{u}_1 = \tilde{u}_2$), from the closed end, with the opposite sign ($\tilde{u}_1 = -\tilde{u}_2$). If there is 'active' resistance with the coefficient M_2 at the end of the pipe, then at this end $p_2 = \psi_2 M v_2$. From equation (4.23) we find

$$\tilde{u}_2 = \frac{1 - \tilde{\psi}_2 M}{1 + \tilde{\psi}_2 M}\tilde{u}_1 \quad \text{and} \quad p_2 = \tilde{\psi}_2 M \tilde{v}_2. \tag{4.24}$$

In the presence of resistance the law of wave reflection is expressed by formula (4.24). From the formula it is apparent that where $\tilde{\psi}_2 M < 1$ the wave is reflected from the open end, and where $\tilde{\psi}_2 M > 1$, from the closed end of the pipe. The intensity of the reflected wave where $\tilde{\psi}_2 M < 1$ decreases (the damping

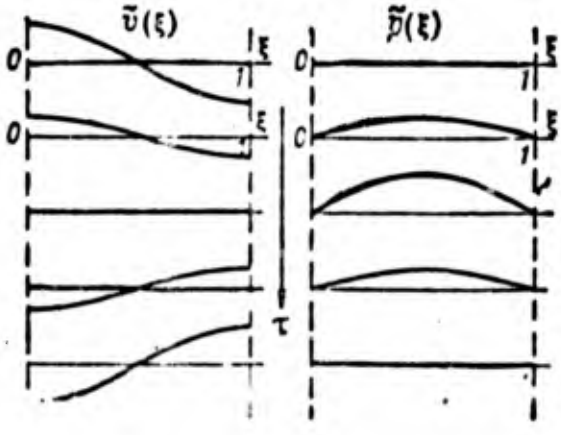

Figure 4.7

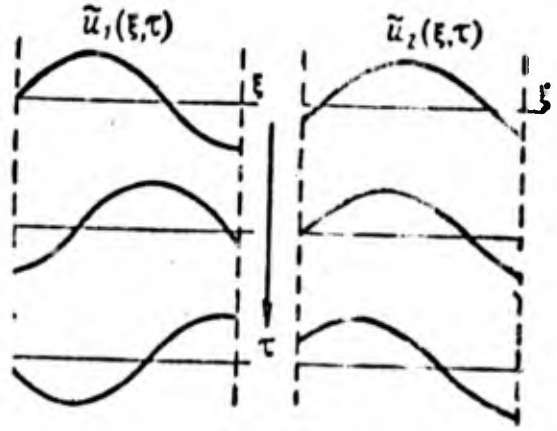

Figure 4.8

of the oscillations increases) with an increase in $\tilde{\psi}_2 M$. When $\tilde{\psi}_2 M = 1$, a sound wave is not reflected and the system does not have a natural frequency. We shall consider below that $\tilde{\psi}_2 M < 1$.

4. Induced Oscillations of a Liquid in a Uniform Pipe

In Chapter 3 the problem of the induced oscillations of a rocket body was solved by two methods. According to one method the induced oscillations are presented in the form of a series according to eigen functions and according to the second method, the induced oscillations are determined without presenting them in the form of a series. The type of solution obtained according to the second method is more convenient for the analysis of the dynamic properties of a system in which the rocket body is only a component. Therefore, we shall determine the induced oscillations of a liquid in a pipe according to the second method.

Induced oscillations of the liquid in fuel lines may arise due to such causes as: pressure disturbance during the entrance of the liquid into the pipe due to oscillations of the bottom of the tank, pressure disturbance in the engine chamber, velocity disturbance of the liquid at the outlet from the pipe due to displacement of the pump in relation to the flow of the liquid. In order to investigate the stability of a closed system we must know the oscillations of velocity and pressure of the liquid at the outlet from the pipe depending on the disturbance which gives rise to these oscillations.

In order to determine the induced oscillations we shall use quadrapole equations (4.15). We shall ignore the influence of small numbers M on the distribution of velocity and pressure along the length of the pipe in the case of induced oscillations, but we shall consider the influence of M numbers on the ends of the pipe where there are hydraulic resistances. Assuming M = 0 in (4.15), we obtain

$$\begin{aligned} \tilde{v}(1) &= \tilde{v}(0)\operatorname{ch} k + \tilde{p}(0)\operatorname{sh} k, \\ \tilde{p}(1) &= \tilde{v}(0)\operatorname{sh} k + \tilde{p}(0)\operatorname{ch} k, \end{aligned} \tag{4.25}$$

where $k = k_2 = -is$.

We shall determine the induced oscillations of pressure and velocity at the outlet from the pipe caused by a change in pressure in front of the inlet

to the pipe. We shall assume that there are the complex resistances z_1 and z_2 at the inlet and outlet of the pipe, respectively. Then

$$\tilde{p}^* = \tilde{p}(0) + z_1 \tilde{v}(0), \tag{4.26}$$

$$\tilde{v}(1) = z_2^* \tilde{p}(1), \tag{4.27}$$

where p* is the pressure disturbance before the inlet to the pipe, $\tilde{p}(0)$, $\tilde{v}(0)$, $\tilde{p}(1)$, and $\tilde{v}(1)$ are disturbances of pressure and flow velocity at the beginning and end of the pipe; z_2^* is the complex conductivity at the outlet from the pipe. Having substituted the values $\tilde{v}(1)$ from (4.27) and $\tilde{v}(0)$ from (4.26) into equation (4.25) and having eliminated $\tilde{v}(0)$, after uncomplicated transformations we obtain the following expression of the complex transmission ratio:

$$K[\tilde{p}_2, \tilde{p}^*] = \frac{\tilde{p}_2}{\tilde{p}^*} = \frac{1}{(1 + z_1 z_2^*)\cos s + i(z_1 + z_2^*)\sin s}, \tag{4.28}$$

where $\tilde{p}_2 = \tilde{p}(1)$. This complex transmission ratio expresses the ratio of the induced pressure oscillations $\tilde{p}_2$ at the end of the pipe, depending on the frequency s, to the amplitude of pressure oscillations p* before the inlet to the pipe.

A complex transmission ratio corresponds to each frequency value s (in the case of induced oscillations s has a real value). The set of complex numbers K, in the case of variation of frequency s in the interval $0 \leq s \leq +\infty$ on the complex plane Z, forms a hodograph of the vector K—an amplitude-phase frequency characteristic--which gives a full presentation of the induced harmonic oscillations of pressure at the outlet from the pipe.

Let us examine the properties of the amplitude-phase characteristic in several actual cases. Let $z_2^* = 0$, $z_1 = \tilde{\psi}_1 M$. The amplitude-phase characteristic is shown in Fig. 4.9. With an increase in the frequency s the vector K rotates clockwise, and the maximum value of its modulus, equal to $1/\tilde{\psi}_1 M$, corresponds to the frequencies s, which are equal to the frequencies of the natural oscillations of a flow of liquid in a pipe with one closed end (4.18). With an increase in the coefficient $\tilde{\psi}_1 M$ the maximum values of the modulus of the vector K decrease.

The minimum value of the modulus of the complex transmission ratio is equal to unity and corresponds to frequencies $s = 0, \pi, 2\pi, \ldots$ Where $s = 0$ the phase lag $\varphi = 0$, where $s = \pi$, we obtain $|\varphi| = \pi$. When $s = s_1$, then the absolute value of φ equals $\pi/2$, and if $s = s_2$, then $|\varphi| = 3/2\pi$.

Now let $z_2^* = 1/\tilde{\psi}_2 M$, $z_1 = \tilde{\psi}_1 M$. The amplitude-phase characteristic $K[p_2, p^*]$ for this case is shown in Fig. 4.10. The maximum values of the modulus of the vector $\tilde{\psi}_2/\tilde{\psi}_1+\tilde{\psi}_2$ correspond to $s = 0, \pi, 2\pi, \ldots$, i.e., to the frequencies of the natural oscillations of a column of liquid in a tube, both ends of which are closed. The minimum values of the modulus of the vector $\tilde{\psi}_2 M$ correspond to the frequencies $s = \pi/2, 3\pi/2, \ldots$ The phase lag in the case of resonace at the frequency of the natural oscillations of the first tone $|\varphi| = \pi$, and at the frequency of the natural oscillations of the second tone $\varphi = 0$.

In order to obtain the complex transmission ratio $K[p_2, p^*]$ we use equation (4.27). We shall have

$$K[\tilde{v}_2, \tilde{p}^*] = \frac{z_2^*}{(1 + z_1 z_2^*)\cos s + i(z_1 + z_2^*)\sin s}. \qquad (4.29)$$

The amplitude-phase characteristic $K[\tilde{v}_2, \tilde{p}^*]$ for the flow of a liquid in a tube closed at both ends and having a resistance and conductivity at the end, respectively equal to $z_1 = \tilde{\psi}_1 M$ and $z_2^* = 1/\tilde{\psi}_2 M$, is shown in Fig. 4.11; where $z_2^* = 1/\tilde{\psi}_2 M$ it differs from the characteristic given in Fig. 4.10, but only in scale.

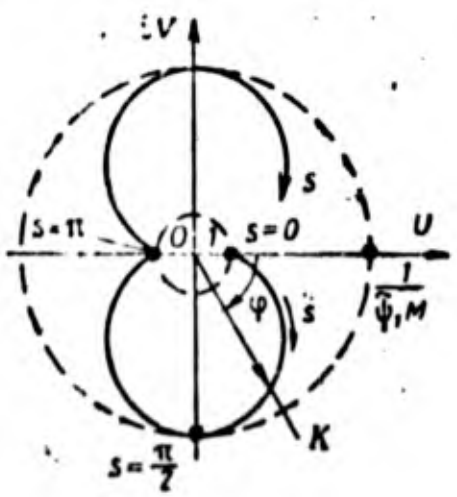

Figure 4.9

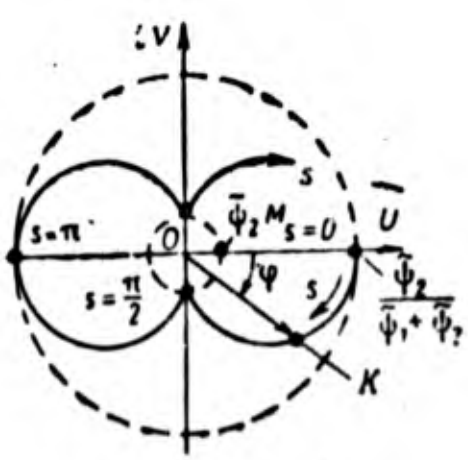

Figure 4.10

The form of the amplitude-phase characteristic $K[\tilde{p}_2, \tilde{p}^*]$ for the flow of a liquid in a tube, at the right end of which there is complex conductivity (see Fig. 4.4):

$$z_2^* = \frac{1}{\tilde{\psi}_2 M} + i a_2^*, \qquad \text{где } a_2^* = s \frac{F_т a_0^2 \varrho_0}{kl},$$

depends on the values and ratio of the real and imaginary part z_2^*. The graphs in Figs. 4.9 and 4.10 may be considered as particular cases in which $z_2^* = 0$ and $z_2^* = 1/\psi_2 M$. In the first case resonance oscillations arise at the frequencies of the natural oscillations of the column of liquid in a tube, closed at one end, and in the second, at the frequencies of the natural oscillations of the column of liquid in a tube closed at both ends.

If $\tilde{\psi} = \infty$, then resonance oscillations of pressure $\tilde{p}_2$ will arise at the frequencies Ω_1, Ω_2, ..., shown in Fig. 4.5. The amplitude of the pressure oscillations p_2 where $s_2 = \Omega_2$ will be less than where $s_1 = \Omega_1$, since the conductivity z_2^* is proportional to the frequency of oscillations. The amplitude-phase characteristic $K[\tilde{p}_2, \tilde{p}^*]$ for the case $z_2^* = ia_2^*$ is shown in Fig. 4.12 by the dotted line.

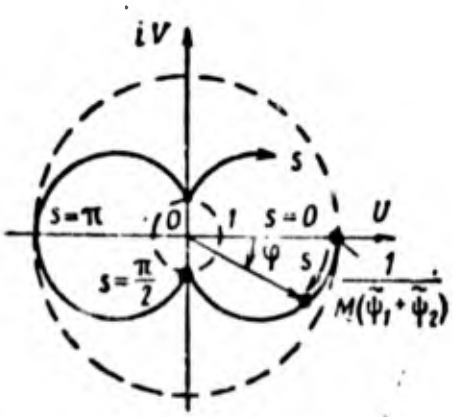

Figure 4.11

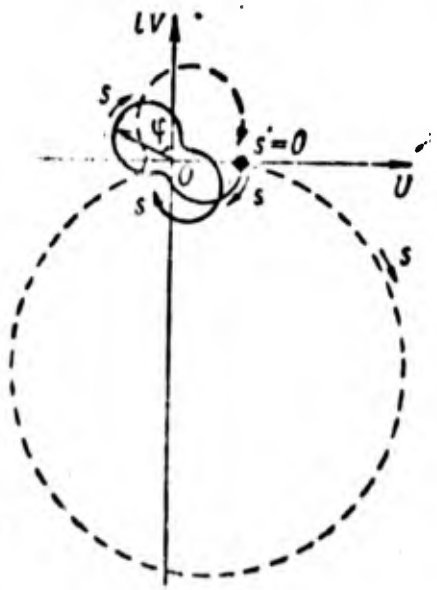

Figure 4.12

One of the variants of the amplitude-phase characteristic $K[p_2, p^*]$ for the case when

$$z_2^* = \frac{1}{\tilde{\psi}_2 M} + i a_2^* \quad (\tilde{\psi}_2 \neq \infty,\ a_2^* \neq 0),$$

is shown in Fig. 4.12 by the solid line. Resonance oscillations arise at the frequencies of the natural oscillations of the system, which differ from the frequencies determined according to formulas (4.18) and (4.19). At the frequency s_2 the amplitude of oscillations is less than at the frequency s_1. A characteristic feature of the oscillations of pressure $\tilde{p}_2$ where $\tilde{\psi}_2 \neq \infty$ and $\alpha_2^* \neq 0$ is the fact that the phase in the case of resonances is not equal to $(2n-1)\pi/2$ or $n\pi$ ($n = 1, 2, \ldots$), as takes place in the case of oscillations where $\alpha_2^* = 0$ (see Figs. 4.9 and 4.10).

Induced oscillations of the liquid in a tube may arise also due to mechanical oscillations of the pump relative to the flow of liquid. In the case of mechanical oscillations of the pump in the direction of the axis of the rocket the boundary of the flow at the outlet from the pipe performs induced oscillations; therefore the boundary conditions where $\xi = 1$ may be presented in the form

$$\tilde{v}(1) = \tilde{v}_p + z_2^* \tilde{p}(1), \tag{4.30}$$

where $\tilde{v}_p$ is the dimensionless motion speed of the pump. Substituting the expression $\tilde{v}(1)$ from (4.30) into equation (4.25) and assuming $\tilde{p}(0) = z_1 \tilde{v}(0)$ at the left end of the pipe, we obtain a complex transmission ratio, expressing the dependence of the pressure at the outlet from the pipe on the motion speed of the pump, in the form

$$K[\tilde{p}_2, \tilde{v}_n] = \frac{z_1 \cos s - i \sin s}{(1 - z_1 z_2^*)\cos s + i(z_2^* - z_1)\sin s}. \tag{4.31}$$

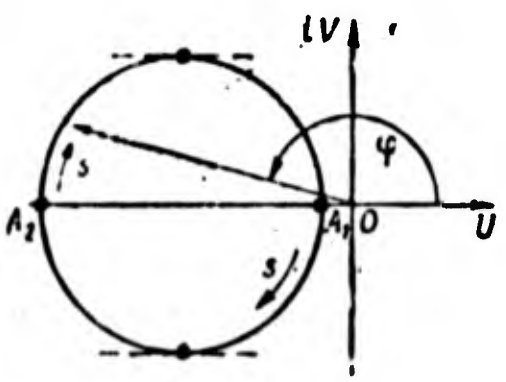

Figure 4.13

The amplitude-phase characteristic $K[\tilde{p}_2, \tilde{v}_p]$ where $z_2^* = 0$ and $z_1 = \tilde{\psi}_1 M$ is shown in Fig. 4.13 and appears as overlapping curves. The coordinates of the characteristics points A_1 and A_2 and the frequency corresponding to these points have the following values:

$$A_1(-\tilde{\psi}_1 M,\ i0), \quad s_1 = \frac{n_1\pi}{2}\ (n_1 = 0, 2, 4, \ldots),$$

$$A_2\left(-\frac{1}{\tilde{\psi}_1 M},\ i0\right), \quad s_2 = \frac{n_2\pi}{2}\ (n_2 = 1, 3, 5, \ldots).$$

Resonance oscillations arise at the frequencies s_2, which are equal to the frequencies of the natural oscillations of a column of liquid in a tube with one end closed. The maximum amplitude of induced oscillations, relative to the velocity of the mechanical oscillations of the pump $\tilde{v}_p$:

$$\left(A_{\tilde{p}_2\tilde{v}_p}\right)_{max} = \frac{1}{\tilde{\psi}_1 M},$$

in this case the phase lead is $\varphi_{\tilde{p}_2\tilde{v}_p} = -\pi$.

5. Calculation of the Elastic Properties of a Pipe

The problem of the oscillations of a flow of an ideal compressible liquid in a long straight pipe is solved in sections 2 and 3 with the assumption that the walls of the pipe are rigid. In the case of rigid walls, the form of the cross-section of the pipe for determining the frequencies and forms of oscillations of the liquid is not significant, and it is only important that the form not vary along the length of the pipe. Such a conclusion is justified, certainly, even for uniform straight rods.

The results of the solution of the uniform problem may also be extended to the motion of a flow of a liquid in an elastic pipe. This was first done by N. Ye. Zhukovskiy [5]. His idea is that the motion of a flow of a compressible liquid in a long elastic pipe can be replaced by the motion of a compressible flow (of the same density, but with a lower modulus of compression) in a rigid pipe. In the case of such a substitution the equivalent modulus of compression of the liquid will be less than the modulus of compression of the liquid due to the elasticity of the pipe wall. For a round pipe with a constant

wall thickness the equivalent modulus of compression of the liquid may be found quite simply. If we consider a pipe consisting of a series of rings, subjected to expansion-contraction, then the modulus of elasticity of a column of liquid E_1, caused by the elasticity of the walls, is determined according to formula (2.19).

$$E_1 = E\frac{h}{2r_0},$$

where E is the modulus of elasticity of the material of the pipe; h, r_0 are the thickness of the wall and the radius of the pipe.

An equivalent modulus of compression of the liquid E_e with regard to the elasticity of the pipe walls may be determined according to the formula

$$E_e = \frac{E_1 E_l}{E_1 + E_l} = E_l \frac{1}{1 + \frac{E_e}{E}\frac{2r_0}{h}},$$

where E_l is the modulus of compression of the liquid.

Substituting expressions for the moduluses of compression in the form

$$E_l = a_0^2\rho_0 \text{ и } E_1 = a_1^2\rho_0,$$

into this formula, where a_t is the equivalent speed of sound, we obtain

$$a_t = \frac{a_0}{\sqrt{1+a_1^2}}, \quad a_1^2 = \frac{2\rho_0 a_0^2 r_0}{hE}. \tag{4.32}$$

Since the equivalent modulus of compression of the liquid is less than the modulus of compression of the same liquid, then the equivalent speed of sound will also be less than the speed of sound of the liquid, i.e., $a_t < a_0$.

In order to lower the frequencies of the natural oscillations of liquid in pipes, sometimes pipes with a cross-section in the form of an ellipse is used instead of round pipes. In the case of a change in the pressure of the liquid the ratio between the dimensions of the semi-axis of the ellipse changes, due

to which the area pipe of elliptical cross-section varies more than that of a pipe of round cross-section. The equivalent modulus of compression of the liquid and, consequently, the equivalent speed of sound in the liquid in an elastic pipe of elliptical cross-section is less than that in a pipe of round cross-section with walls of equal thickness and equal cross-sectional area, corresponding to an undisturbed pressure.

The equivalent speed of sound in the liquid in an elastic pipe with a cross-section in the form of an ellipse may be determined according to the following formula [4]

$$a_t = \frac{a_0}{\sqrt{1+a_t^2}},$$

where

$$a_t^2 = \frac{2\varrho_0 a_0^2 r_0 (1-\mu^2)}{hE}\left[1+3\frac{(a-b)^2}{h^2}\right];$$

a and b are the lengths of the semi-axes of the ellipse; μ is Poisson's coefficient; h is the thickness of the pipe wall; r_0 is the radius of a circle, the area of which is equal to the area of the ellipse.

It is possible to significantly lower the frequency of the natural oscillations of liquid fuel in a pipe by means of injecting a small amount of an insoluble gas into the flow of the fuel. A uniform distribution of gas along the flow in cryogenic and non-cryogenic liquids is made using a single jet injector [1]. If the surface tension of the liquid is ignored (which is justified in the case of a relatively large diameter of gas bubbles) and the appearance of mass exchange between the gas and the liquid is not considered, then the equivalent speed of sound a_t of the gas-liquid mixture may be determined according to the following formula [1]

$$a_t^2 = \frac{E_r E_{np.l}}{[\beta E_{np.l} + (1-\beta) E_g][\beta \varrho_g + (1-\beta)\varrho_0]},$$

where E_g is the modulus of elasticity of the gas; E_{rl} is the reduced modulus of elasticity of the liquid (with regard to the elasticity of the pipe wall); β is the volumetric ratio of gas and liquid; ρ_G and ρ_0 are the density of the gas and the liquid.

Let us determine, for example, the equivalent speed of sound of a gas liquid mixture with the following initial data: $E_{rl} = 10^8$ kg/m^2;

$$E_r = 1{,}2 \cdot 10^4 \text{ kg/m}^2 \quad \rho_0 = 100 \text{ kg} \cdot \text{sec}^2/\text{m}^4$$
$$\rho_r = 0{,}1 \text{ kg} \cdot \text{sec}^2/\text{m}^4 \quad \beta = 0{,}01.$$

Having substituted these values into the formula given above, we find $a_t \approx 111$ m/sec. This speed is less than the speed of sound in a vapor-gas mixture (340 m/sec). Even a small amount of insoluble gas in a liquid (in our example 1%) leads to a significant decrease in the equivalent speed of sound.

The dimensional frequency of natural oscillations (4.18a) is proportional to the speed of sound, therefore the frequency of the natural oscillations of a flow of compressible liquid in an elastic pipe, with all other conditions being equal, will be less than that in a rigid pipe.

With an increase in the ratio of the radius of the pipe to the length, more precisely to the length of an elastic wave, the energy of the radial oscillations increases, therefore a unidimensional formulation of the problem may prove to be very crude. We shall give a solution of the problem with regard to radial oscillations of the liquid in the pipe.

We shall examine small axi-symmetrical oscillations of the liquid and the walls of the pipe; we shall assume the pipe to be a thin-walled momentless cylindrical shell of round cross-section. We shall designate small radial axi-symmetrical displacements of the pipe wall by $w(x, t)$; ρ^*, E are the density and modulus of elasticity of the material of the pipe; h, r_0 are the thickness of the wall and the radius of the pipe ($h \ll r_0$); $p(r, x, t)$ is the dynamic pressure of the liquid in the pipe.

Let us examine the radial motion of an elementary section of the pipe, separated from two adjacent sections perpendicular to the axis of the pipe and two adjacent radial sections. The forces acting on the isolated section of pipe are shown in Fig. 4.14. Having assumed Newton's second law, we obtain an equation for the oscillations of the isolated section of pipe in the direction of the radius

$$hr_0\varrho^* \frac{\partial^2 w(x, t)}{\partial t^2} = r_0 p(r_0, x, t) - E \frac{w(x, t)}{r_0} h.$$

We shall introduce the following dimensionless parameters

$$\eta = \frac{r}{r_0}, \quad \varkappa = \frac{\varrho^*}{\varrho_0}, \quad \tilde{h} = \frac{h}{r_0}, \quad a = \frac{r_0}{l}, \quad \gamma^2 = \frac{E}{\varrho_0 a_0^2},$$

$$\tau = \frac{a_0}{l} t, \quad \xi = \frac{x}{l}, \quad w(\xi, \tau) = \frac{w(x, t)}{r_0},$$

$$\tilde{p}(\xi, \tau)\Big|_{r_1=1} = \frac{p(r_0, x, t)}{a_0^2 \varrho_0}.$$

Here l is the length of the pipe; ρ_0 and a_0 are the density of an undisturbed column of liquid and the speed of sound in it.

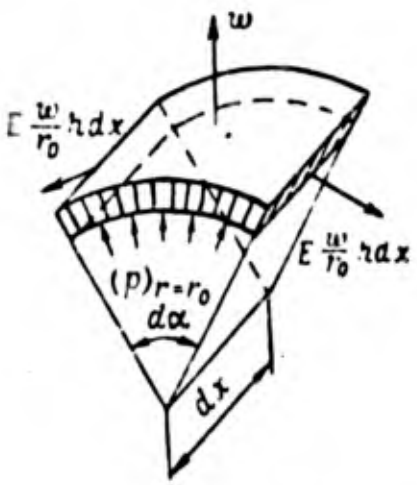

Figure 4.14

We now present an equation for the radial axi-symmetrical oscillations in dimensionless form

$$\varkappa \tilde{h} a^2 \frac{\partial^2 w(\xi, \tau)}{\partial \tau^2} + \gamma^2 \tilde{h} w(\xi, \tau) = \tilde{p}(\xi, \tau)\Big|_{r_1=1}. \qquad (4.33)$$

This equation is the third equation of the system (2.8). Due to the axial symmetry and the absence of longitudinal oscillations of the pipe the differential operators $L_{31} = 0$, $L_{32} = 0$, the differential operator L_{33} is

given in equation (4.33) by the real number $\gamma^2 h$ and the intensity of external forces Z is equal to the pressure of the liquid on the wall.

The velocity potential $\zeta(\eta, \xi, \tau)$ for a compressible liquid may be determined from an equation which, in cylindrical coordinates, has the form [9]:

$$\frac{\partial^2\varphi}{\partial t^2}=\frac{\partial^2\varphi}{\partial r^2}+\frac{1}{r}\frac{\partial\varphi}{\partial r}+\frac{\partial^2\varphi}{\partial x^2}.$$

In dimensionless form this equation will be

$$\frac{\partial^2\varphi}{\partial\eta^2}+\frac{1}{\eta}\frac{\partial\varphi}{\partial\eta}+\alpha^2\left(\frac{\partial^2\varphi}{\partial\xi^2}-\frac{\partial^2\varphi}{\partial\tau^2}\right)=0, \tag{4.34}$$

The pressure at any point in the volume of liquid, in correspondence with (2.13), in dimensionless form will be expressed by the formula

$$\tilde{p}(\eta, \xi, \tau)=-\frac{\partial\varphi}{\partial\tau}. \tag{4.35}$$

If the pipe is open at one end, then the boundary conditions for the function φ will be the following

$$\frac{\partial\varphi}{\partial\tau}=0 \text{ where } \xi=0, \quad \frac{\partial\varphi}{\partial\xi}=0 \text{ where } \xi=1, \tag{4.36}$$

For a pipe open at both ends:

$$\frac{\partial\varphi}{\partial\tau}=0 \text{ where } \xi=0, \ \xi=1. \tag{4.37}$$

Moreover, the kinematic boundary condition (2.11) is usually fulfilled on the walls of the pipe. In dimensionless form it may be expressed by the equation

$$\alpha^2\frac{\partial w}{\partial\tau}=\frac{\partial\varphi}{\partial\eta} \quad (\eta=1). \tag{4.38}$$

Thus the problem comes down to the following: to find the solution of equation (4.34), satisfying boundary conditions (4.36) or (4.37), to find the solution of equation (4.33), the right member of which is determined by the potential according to (4.35); in this case the solution of equations (4.33) and (4.34) must additionally satisfy condition (4.38).

We give the solution of equation (4.34) in the form

$$\varphi = \sum_{n=1}^{\infty} i\Omega_n D_n R_n(\eta) X_n(\xi) e^{i\Omega_n \tau}, \tag{4.39}$$

where D_n is an arbitrary constant; Ω_n is the frequency of the natural oscillations of the system, consisting of an elastic pipe and a liquid; $R_n(\eta)$, $X_n(\xi)$ are the desired functions.

Radial oscillations of the pipe, described by equation (4.33), must also be performed with the frequency Ω_n, therefore we give the function w in the form

$$w = \frac{1}{a^2} \sum_{n=1}^{\infty} X_n(\xi) e^{i\Omega_n \tau}. \tag{4.40}$$

The coefficient $1/a^2$ is here taken for the convenience of satisfying equation (4.38).

Having substituted the expression for the velocity potential (4.39) into equation (4.34) and having eliminated the variables, we obtain the following two equations to determine the function $X_n(\xi)$ and $R_n(\eta)$:

$$\frac{d^2 X_n(\xi)}{d\xi^2} + a_n^2 X_n(\xi) = 0, \tag{4.41}$$

$$\frac{d^2 R_n(\eta)}{d\eta^2} + \frac{1}{\eta} \frac{dR_n(\eta)}{d\eta} + \mu_n^2 R_n(\eta) = 0, \tag{4.42}$$

where

$$\mu_n^2 = a^2 \Omega_n^2 \sigma_n, \quad \sigma_n = 1 - \frac{a_n^2}{\Omega_n^2}. \tag{4.43}$$

Since the function $R_n(\eta)$ where $\eta = 0$ must be limited, then the solution of equation (4.42) must consist of Bessel functions of the first kind of zero order $R_0(\mu_n \eta) = J_0(\mu_n \eta)$.

Having replaced the functions w and φ in equation (4.38) by their expressions from (4.40) and (4.39), we dtermine the arbitrary constant

$$L_n = \frac{1}{J_0'(\mu_n)}.$$

Having determined the pressure where $\eta = 1$ from formula (4.35) and having substituted it into equation (4.33), we obtain

$$\left[\varkappa\tilde{h} + \frac{J_0(\mu_n)}{J_0'(\mu_n)}\right]\Omega_n^2 = \frac{\gamma^2\tilde{h}}{\alpha^2} \quad (n = 1, 2, 3, \ldots). \tag{4.44}$$

We shall limit ourselves to the cases where $\Omega^2 < \gamma^2/\varkappa\alpha^2$. This inequality satisfies nearly all the technical applications of the problem under consideration. On the basis of equation (4.44) we conclude that the roots μ_n of the Bessel functions must be imaginary.

Since α^2 is a positive number and Ω_n^2 is also a positive number for the conservative system, then from (4.43) it is possible to conclude that $\sigma_n < 0$ and $\alpha_n^2 > 0$. The solution of equation (4.41) where $\alpha_n^2 > 0$ may be consist of trigonometrical functions. With regard to conditions (4.36) and (4.37) we obtain

$$X_n(\xi) = \sin\alpha_n\xi.$$

The following values satisfy condition (4.36):

$$\alpha_n = \frac{(2n-1)\pi}{2} \quad (n = 1, 2, \ldots). \tag{4.45}$$

The following values satisfy condition (4.37)

$$\alpha_n = n\pi \quad (n = 1, 2, \ldots). \tag{4.46}$$

The numbers α_n have the same values as the dimensionless frequencies of the natural oscillations of a compressible column of liquid in a pipe with rigid walls.

The coefficients μ_n are the roots of equation (4.44). They may be determined numerically, if the frequency of natural oscillations Ω_n in equation (4. (4.44) is replaced by its expression from (4.43):

$$\Omega_n^2 = \frac{\mu_n^2}{a^2} + a_n^2. \tag{4.47}$$

We obtain

$$J_0(\mu_n)\left(\mu_n^2 + a^2 a_n^2\right) = J_0'(\mu_n)\left[\gamma^2 \tilde{h} - \varkappa \tilde{h}\left(\mu_n^2 + a^2 a_n^2\right)\right]. \tag{4.48}$$

The values a^2, γ^2, $\tilde{h}$, and κ characterize the parameters of the system and in each actual case are known, and, depending on the boundary conditions, the coefficient a_n may be calculated according to formulas (4.45) or (4.46). Only one eigen-value a_n will correspond to each value of the eigen-value μ_n. After μ_n is determined from equation (4.48) it is possible to calculate the frequency of the natural oscillations Ω_n according to formula (4.47). Since the eigen-values μ_n are imaginary, then $\Omega_n^2 < a_n^2$.

Dimensional ω_n and dimensionless Ω_n frequencies are connected by the relationship

$$\omega_n = \Omega_n \frac{a_0}{l},$$

where a_0 is the speed of sound in an undisturbed liquid. Having replaced the frequency Ω_n in this formula by its value from (4.47) we obtain

$$\omega_n = a_n \frac{a_0}{l} \sqrt{1 + \frac{\mu_n^2}{a^2 a_n^2}}.$$

We shall call the following value the equivalent speed of sound, corresponding to the n-th tone of oscillations:

$$a_{in} = a_0 \sqrt{1 + a_{in}^2}, \quad a_{in}^2 = \frac{\mu_n^2}{a^2 a_n^2}. \tag{4.49}$$

Then the frequency of the natural oscillations of a compressible liquid in an elastic pipe corresponding to the two-dimensional problem may be calculated

according to the usual formula

$$\omega_n = \alpha_n \frac{a_{tn}}{l}$$

with the only difference being that instead of the speed of sound a_0 in an undisturbed liquid it is necessary to take the equivalent speed of the liquid a_{tn}, which is less than a_0, since a_{tn}^2 is less than zero.

The equivalent speed of sound, determined by N. Ye. Zhukovskiy (4.32) does not depend on the number of the tone of oscillations, and the equivalent speed a_{tn} (4.49) depends on the number of the tone of oscillations.

In conclusion we will give a numerical example, from which it is possible to establish what refinements in accuracy in the equivalent speed of sound are introduced by formula (4.49) in comparisoh with formula (4.32). For purposes of calculation we shall assume $\kappa = 2.8$; $\tilde{h} = 0.05$; $\alpha = 0.05$, and $\gamma = 6$. Then on the basis of (4.32)

$$a_t^2 = 1,11; \quad a_t = 0,69a_0. \tag{a}$$

For a pipe closed from one end:

$$\alpha_n = \frac{(2n-1)\pi}{2}.$$

Where n = 1, 5, 10, and 20 we shall have, respectively

$$\alpha_{t1}^2 = -0,525; \quad \alpha_{t5}^2 = -0,54; \quad \alpha_{t10}^2 = -0,575; \quad \alpha_{t20}^2 = -0,652.$$

Then

$$a_{t1} = 0,69a_0; \quad a_{t5} = 0,68a_0; \quad a_{t10} = 0,65a_0; \quad a_{t20} = 0,59a_0. \tag{b}$$

For example, take a pipe with a length equal to 20 radii ($\alpha = 0.05$). The wavelength l of the first tone of oscillations for the pipe closed at one end is equal to $4l$, the wavelength of the fifth tone of oscillations is $0.44l$ or $8.8r_0$, the wavelength of the tenth tone is equal to $0.21l$, which is $4.2r_0$.

From a comparison of numerical calculations (a) and (b) it is apparent even for a comparatively short pipe ($\alpha \leq 0.05$), the equivalent speed of sound

a_{tn}, calculated with regard to the radial oscillations of the liquid, up to the fifth tone of natural oscillations inclusively, practically does not differ in the equivalent speed, calculated according to N. Ye. Zhukovskiy's formula. Hence it is possible to conclude that it is completely acceptable to consider unidimensional oscillations of liquid in pipes, connecting the tanks with the pumps. Instead of the propagation speed of sound in an undisturbed flow a_0, it is possible to take the equivalent speed of sound a_t, calculated according to N. Ye. Zhukovskiy's formula (4.32).

6. Calculation of the Elastic Properties of Sylphons

In order to compensate for variation in the length of pipelines and non-coaxial alignment of the flange at the bottom of the tank, the pump and the engine sylphons [16], short corrugated sections of pipe with very small axial and angular rigidities (Fig. 4.15), are attached at one or both ends of the pipelines between the tank and the pump. Due to the low rigidity a sylphon fills the function of a compensator. The length of the sylphon is small in

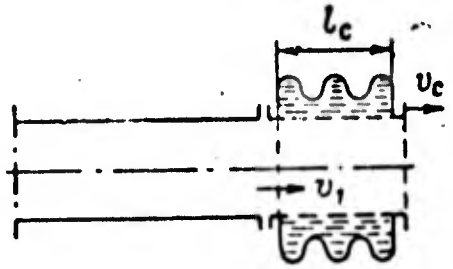

Figure 4.15

comparison with the length of the pipe, therefore we shall ignore wave processes within the sylphon, and consider the pressure at any point in the volume of liquid in the sylphon at a given moment of time to be equal.

The radial rigidity of a sylphon is considerably less than the radial rigidity of a pipe made of the same material and having the same wall thickness as the sylphon. In a scheme with a pipe we shall consider a sylphon to be a localized elastic unit (localized elasticity).

Variation in the volume of liquid in the sylphon depends on the variation l_c of the length of the sylphon and the pressure variation p_c within the sylphon (more precisely, pressure drop). In the general case, this relationship may be nonlinear.

Let the pressure of the liquid p_{c0}, the length of the sylphon l_{c0}, and the volume of the sylphon V_{c0} correspond to the understood motion of the flow of a liquid through a sylphon. In the case of longitudinal oscillations of the body and the liquid in the pipes the pressure p_c, the length of the sylphon l_c, and the volume of the sylphon V_c undergo small changes. Limiting ourselves to a consideration of only the main linear portions of the increment of the values names, we shall have

$$p_c = p_0 + dp_c,\ l_c = l_{c0} + dl_c,\ V_c = V_{c0} + dV_c.$$

It is possible to determine the increase in volume according to the formula

$$dV_c = \left(\frac{\partial V_c}{\partial l_c}\right) dl_c + \left(\frac{\partial V_c}{\partial p_c}\right) dp_c, \tag{4.50}$$

where the derivatives $\delta V_c/\delta l_c$ and $\delta V_c/\delta p_c$ must be calculated where $p_c = p_0$ and $l = l_{c0}$.

Increase in the volume of a sylphon takes place for two causes: 1) due to a change in the geometry of the sylphon from a displacement of one end of the sylphon in relation to the other. A gain in volume due to this cause increases with an increase in the ratio of the mean diameter of the sylphon and the diameter of the pipe; 2) as a consequence of a change in pressure with an unchanged distance between the ends.

We shall introduce two parameters, characterizing the geometrical and elastic properties of a sylphon [8]:

$$\lambda = \frac{1}{F_\tau}\left(\frac{\partial V_c}{\partial l_c}\right) - 1, \tag{4.51}$$

$$r = \frac{1}{F_\tau}\left(\frac{\partial V_c}{\partial p_c}\right),\ \tilde{r} = r\frac{a_0^2 \rho_0}{l},$$

where r and $\tilde{r}$ are the dimensional and dimensionless coefficients of the conductivity of a sylphon; λ is the dimensionless geometrical characteristic of the sylphon.

The dimensionless coefficients $\tilde{r}$ and λ are convenient for calculating the influence of the sylphon on the boundary conditions for the flow of a liquid in a pipe. We shall show this as applied to Fig. 4.15.

We shall differentiate equation (4.50) according to time and divide all terms of the equation by the cross-sectional area of the pipe F_T:

$$\frac{1}{F_T}\frac{dV_c}{dt}=\frac{1}{F_T}\left(\frac{\partial V_c}{\partial l_c}\right)\frac{dl_c}{dt}+\frac{1}{F_T}\left(\frac{\partial V_c}{\partial p_c}\right)\frac{dp_c}{dt}.$$

Having designated

$$\frac{1}{F_T}\frac{dV_c}{dt}=v_1,\quad \frac{dl_c}{dt}=v_c,$$

where v_1 is the deviation in the velocity of the liquid upon entering the sylphon; v_c is the displacement velocity of the right end of the sylphon (the left end is immobile), with calculation of formulas (4.51) we obtain

$$v_1=(1+\lambda)v_c+r\frac{dp_c}{dt}. \qquad (4.52)$$

Assuming in this equation the values of v_1, v_c, and p_c vary according to harmonic law with the frequency s, we obtain the following dimensionless dependence of the deviation of the velocity of the liquid upon leaving the pipe and the displacement velocity of the end of the sylphon and on the pressure deviation of the liquid in the sylphon:

$$\tilde{v}_1=(1+\lambda)\tilde{v}_c+i\tilde{s}\tilde{r}\tilde{p}. \qquad (4.52a)$$

The exit velocity of the liquid from the pipe is presented in the form of three components: ϑ_c — the displacement velocity of the end of the sylphon (the flow must fill the internal part of the sylphon having the diameter of the pipe), $\lambda\vartheta_c$ — the velocity necessary for changing the volume of the cross-hatched section of the sylphon (see Fig. 4.15), caused by a change in the distance between the ends; $is\tilde{r}\tilde{p}_c$ — the velocity necessary for changing the volume

of the cross-hatched section of the sylphon caused by pressure deviation in the sylphon. Equation (4.52a) is justified when $v_c \lesseqgtr 0$ and $p_c \gtreqless 0$. Where $v_c < 0$ and $p_c < 0$ the value of v_1 will be negative, therefore liquid from the sylphon will be crowded into the pipe.

The value $is\tau$ in equation (4.52a) can be considered to be the imaginary part of the complex conductivity z_2^*.

We shall use equation (4.52) below for calculating the influence of the elastic properties of sylphons on the dynamics of the flo/ of a liquid in the input mains.

7. Calculation of Elastic Displacement of Fuel Main Mountings

A common element in the construction of input mains is a unit in which the flow of the liquid undergoes significant changes—a turn in direction, change in cross-sectional area, and separation into several branches (Fig. 4.16).

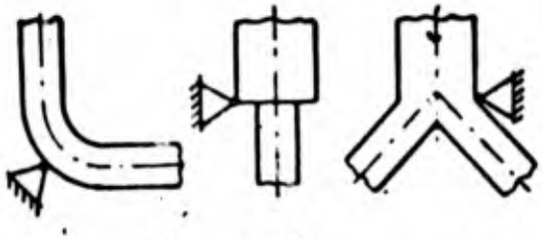

Figure 4.16

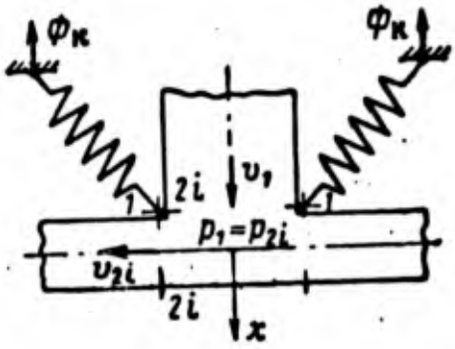

Figure 4.17

In these conditions supplementary pressure forces arise, under the influence of which elastic deformation of pipelines, mountings, and tank bottoms takes place. As a result of these variations the volume of the input main changes, which must be considered in analyzing the oscillations of the column of liquid. A characteristic example of such a unit is a collector for supplying fuel from one input main to several engines. A diagram of a collector is shown in Fig. 4.17. The input main (the cross-sectional area in front of the collector F_T)

divides into N branches, the weight of the column of liquid (from the collector to the free surface of the liquid in the tank) is received by the mounting (in Fig. 4.17 the mounting is provisionally depicted as springs) and transmitted to the rocket body. This same mounting receives the supplementary forces of the dynamic pressure of the liquid, acting on the collector.

Let us write an equation for the discharge of liquid through the collector. We assume the collector to be rigid and the volume of liquid filling to be incompressible. Then

$$v_1 = \frac{1}{F_т}\sum_{i=1}^{N} v_{2i}F_i + v_1(p_1) + v_1(\varphi_к).$$

Here v_1 is the flow speed deviation in the boundary section 1-1; v_{2i} is the flow speed deviation at the outlet from the collector into branch i; F_i is the cross-sectional area of branch i; $v_1(p_1)$ and $v_1(\varphi_k)$ are the flow speed deviation in section 1-1 caused by the displacement of the collector under the influence of the deviation p_1 and the oscillation of that section of the body from which the collector is suspended; $p_1 = p_{2i}$ is the pressure deviation in the collector.

The values $v_1(p_1)$ and $v_1(\varphi_k)$ are determined from the equation of motion of the collector as a mechanical system

$$m_к\ddot{x}_к = -k_к(x_к + \varphi_к) + F_1 p_1, \qquad (4.53)$$

where x_k is the displacement of the collector in the direction of the x-axis, reckoned from the understood position; k_k is the rigidity factor of the collector mounting in the direction of the x-axis, and m_k is the reduced mass of the collector and the column of liquid.

We assume that the pressure deviation and oscillations of the body take place according to harmonic law with the frequency ω:

$$p_1(t) = p_1 e^{i\omega t}, \quad \varphi_к(t) = \varphi_к e^{i\omega t}.$$

Then from equation (4.53) we obtain the following equations for the complex transmission ratios:

$$K[v_1,\ p_1]=i\omega\frac{F_T}{m_K\left(\omega_K^2-\omega^2\right)}, \tag{4.54}$$

$$K[v_1,\ \varphi_K]=-i\omega\frac{1}{1-\left(\frac{\omega}{\omega_K}\right)^2}, \tag{4.55}$$

in which ω_K is the frequency of the natural oscillations of the collector with the liquid.

We now write the equation for the discharge of liquid through the collector in the form

$$v_1=\sum_{l=1}^{\infty}K_l[v_1,\ v_{2l}]\,v_{2l}+K[v_1,\ p_1]\,p_1+K[v_1,\ \varphi_K]\,\varphi_K, \tag{4.56}$$

where

$$K_l[v_1,\ v_{2l}]=\frac{F_l}{F_T}.$$

Equation (4.56) expresses the coupling of the flow speed at the outlet from the input main into the collector with the flow speeds at the inlet to the individual branches and the displacement of the collector caused by oscillations of the rocket body and the pressure of the liquid in the collector.

8. Calculation of Additional Characteristics of Fuel Mains

We shall additionally examine several characteristic sections of fuel mains, including local sections with cavitating liquid, elements of the main possessing hydraulic resistance and hydraulic accumulators.

Cavitation of the liquid arises in those sections of the flow where the static pressure is less than the vapor pressure of the liquid and the equilibrium pressure of the gases dissolved in the fuel. The inlet to a centrifugal pump is usually such a section. There are constructions in which a screwpump or a jet ejector is located in front of the inlet to the pump in order to increase the cavitation reserve. In such constructions cavitation may arise in the jet ejectors or at the inlet to the screwpump.

A linearized equation of the state of a vapor-gas mixture may be put in the form

$$V_{vg} = -\kappa^{*}_{vg} p_{vg},$$

where V_{vg} is the deviation of the volume (from the stationary) of a vapor-gas mixture; p_{vg} is the pressure deviation; and k^{*}_{vg} is the proportionality factor. If the pressure increases ($p_{vg} > 0$) then the volume decreases ($V_{vg} < 0$).

In first approximation it is possible to represent a vapor-gas mixture in an input main in the form of localized elasticity. The relationship between the pressure deviaton p_{vg} and the velocity deviation v_{vg} of the flow of liquid in a pipe from the boundary with localized elasticity, on the basis of the preceeding equation has the form

$$v_{vg} = i\omega k_{vg} p_{vg} \tag{4.57}$$

where

$$k_{vg} = k^{*}_{vg}/F_{T}.$$

The localized hydraulic resistance in Fig. 4.18a is schematically depicted in the form of a grid. The grid is usually connected with some unit (including the pipe) and may perform oscillations relative to the flow at the velocity v_p. The pressure drop on the grid may be expressed by the formula

$$p_{1d} - p_{2d} = \xi \rho_0 \frac{v_d^2}{2},$$

where p_{1d} is the disturbed pressure of the liquid in front of the grid; p_{2d} is the disturbed pressure of the liquid behind the grid; ξ is the resistance factor of the grid; v_d is the disturbed flow speed of the liquid through the grid; and ρ_0 is the density of the liquid (we assume it to be constant). Deriving a linearization we obtain

$$p_2 = p_1 - \psi M(v - v_p) \tag{4.58}$$

where

$$\psi = \xi \rho_0 a_0;\ M = v_0/a_0;$$

p_1 is the pressure deviation in front of the grid; p_2 is the pressure deviation behind the grid; v_0 is the stationary flow speed; v is the flow speed deviation v_p is the velocity of grid oscillations in relation to the flow, in this case the positive direction of v_p and v is assumed to be equal.

If a smooth pipe of constant diameter performs oscillations along the flow, then these oscillations will not cause disturbance of the flow.

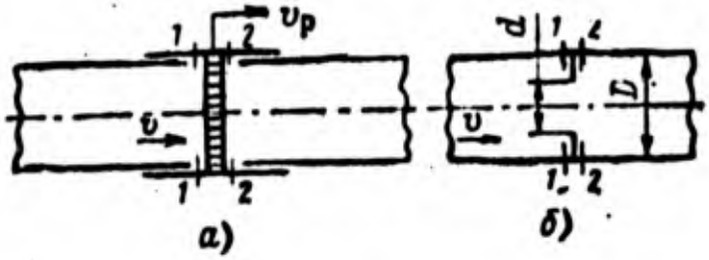

Figure 4.18

A delivery washer fixed in the pipe (Fig. 4.18b) causes 'reactive' resistance to the motion of the flow. In the case of motion through the delivery washer distorted streamlines are created in the flow and velocities appear which differ from the motion speed of the plane wave in a pipe without barriers. In the plane of the washer opening the greatest velocities appear at its edges. In addition to the kinetic energy of the plane wave of the flow an additional kinetic energy is greater here, which is communicated to a certain reduced mass m_{rw}, moving at an average velocity in the opening of the washer. On the basis of Newton's second law,

$$F_d(p_1 - p_2) = m_{rw} i\omega v_w. \qquad (4.59)$$

Here v_w is the mean deviation of the velocity of the liquid in the opening of the washer; ω is the frequency of oscillations; and $F_d = \pi d^2/4$. Since

$$v_w = v(D/d)^2,$$

where v is the deviation of the mean velocity of the plane wave of the flow in front of the washer (or after the washer), then replacing the velocity v_g in (4.59) by its expression, we obtain

$$p_2 = p_1 - i\omega a_{ш} v, \tag{4.60}$$

In this case the coefficient

$$a_{ш} = \frac{m_{т.ш}}{F_d}\left(\frac{D}{d}\right)^2.$$

The value of the reduced mass may be calculated according to the formula [11, 17]

$$m_{т.ш} = \frac{\varrho_0 F_d^2}{d f(d/D)},$$

where Foch's function is

$$f\left(\frac{d}{D}\right) \approx \frac{1}{1 - 1{,}47 d/D + 0{,}47 d^3/D^3}.$$

If the ratio d/D approaches unity, then the value of Foch's function will approach infinity, and the value of the reduced mass approaches zero. In a pipe without a washer localized 'reactive' resistance is absent.

Pressure drop also appears during the exit of liquid from the tank into the delivery main. Here, besides 'active' resistance (funnel damper and so forth), 'reactive' resistance also appears, caused by the scattering of a certain reduced mass of liquid. Deviation of pressure drop during the exit of liquid from the tank may be put in the form

$$p_1 = p_б - z_б v_1, \qquad z_б = \psi_б M + i\omega a_б. \tag{4.61}$$

The coefficient a_t, characterizing the reactive resistance during the exit of liquid from the tank, may be calculated on the basis of the following formulas [11, 17]

$$a_б = \frac{m_{пр.б}}{F_т}, \quad m_{пр.б} = \frac{\varrho_0 F_т^2}{4 r_0 f(r_0/R_1)},$$

$$f\left(\frac{r_0}{R_1}\right) \approx \frac{1}{1 - 1{,}47 r_0/R_1 + 0{,}47 r_0^3/R_1^3},$$

$$F_т = \pi r_0^2.$$

Here p_1 is the pressure deviation at the inlet to the pipe; p_t is the pressure deviation at the bottom of the tank; r_0 is the radius of the pipe; R_1 is the radius of the tank. In the expression for z_t the value $\psi_t M$ is the coefficient of active resistance during the exit of liquid from the tank.

Figure 4.19 presents diagrams of several hydraulic accumulators (hydraulic dampers) used to decrease the frequency of the natural oscillations of liquid in a delivery main. Diagram (a) is used on the fuel main, diagram (b) on the oxidizer main of the Titan-2 rocket, and diagram (c) on the oxidizer main of the first stage of one of the models of the Saturn-5 [2, 12].

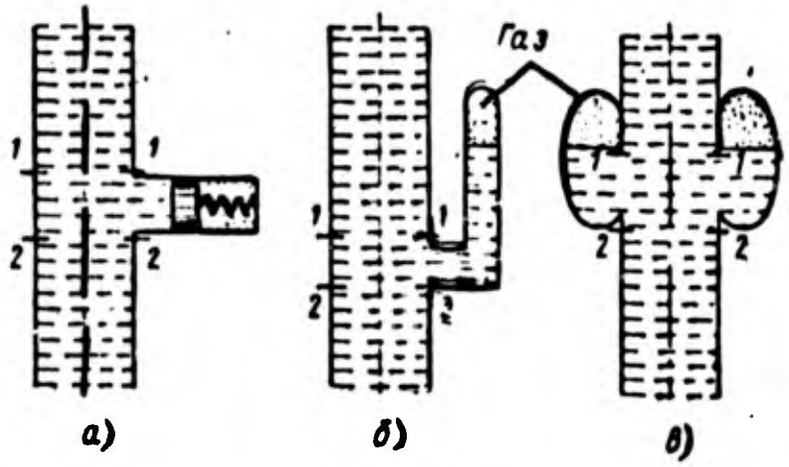

Figure 4.19

We shall examine the hydrodynamic properties of an accumulator with rigid walls, having assumed the amount and temperature of gas in the accumulator to be constant, and the liquid to be incompressible. We will also consider the liquid in the section of pipe between sections 1-1 and 2-2 to be incompressible.

If the pressure in section 1-1 increases by the value p in comparison with the stationary value, then the volume of gas decreases and the liquid flows from the pipe into the accumulator. The mean flow speed of the liquid going into the accumulator, relative to the cross-sectional area of the pipe F_T:

$$v_{ac} = i\omega(k_{ac}/F_T)p_{ac} \qquad (4.62)$$

where p_{ac} is the deviation of the gas pressure in the accumulator; k_{ac} is the proportionality factor between the deviations of volume and pressure in the accumulator; ω is the oscillation frequency. In diagram (a) the elasticity, along with the gas, creates a spring, therefore

$$v_{ac} = i\omega(F_p^2/kF_T)p_p$$

where F_p is the area of the piston; p_p is the pressure of the liquid on the piston; k is the proportionality factor between the deviation of force, acting on the piston, and the piston displacement. A certain pressure drop is necessary for dispersion of the liquid entering the accumulator so that

$$p_1 - p_{ac} = i\, m_r^* v_{ac} \tag{4.63}$$

where p_T is the pressure deviation of the liquid in the pipe in front of the accumulator; m_r^* is the coefficient of the reduced mass of liquid. Having replaced the value p_{ac} in equation (4.62) by its expression from (4.63), we obtain

$$v_{ac} = i\omega\alpha_{ac}^* p_T, \tag{4.64}$$

where

$$\alpha_{ac}^* = \frac{\frac{k_{ac}}{F_T}}{1 - \omega^2 m_r^* \frac{k_{ac}}{F_T}}. \tag{4.65}$$

In formula (4.65) the product $m_r^* k_{ac}/F_T$ is a value inverse to the square of the frequency of the natural oscillations ω_{ac}^2 of a certain oscillator consisting of a reduced mass of liquid and an elastic element (gas). Depending on the relationship of the frequency ω of the induced oscillations of the liquid in the pipe and the frequency ω_{ac} of the natural oscillations of the oscillator the coefficient α_{ac}^*, characterizing the reactive conductivity of the accumulator may be positive or negative. Where ω/ω_{ac} approahces 1 the coefficient α_{ac}^* approaches infinity, i.e., where the hydraulic accumulator is located the pipe is 'closed' in the acoustic sense. Equation (4.64) and formula (4.65) may also be applied to diagram (a), having assumed $k_{ac} = F_p^2/k$ in them.

If the walls of the hydraulic accumulator are considered to be elastic, then with an increase in the pressure the volume of liquid in the accumulator increases, not only due to compression of the gas, but also due to an increase in the volume of the accumulator. The mean flow speed of the liquid entering the accumulator, v_{ac}, relative to the cross-sectional area of the pipe, will consist of two parts: one part is caused by a change in the volume of gas, the other by a change in the volume of the accumulator. Then, instead of equation (4.62), we obtain

$$v_{ac} = i\omega\left(\frac{k_{ac}}{F_т} + \frac{k_{ут}}{F_т}\right) p_{ac}, \tag{4.66}$$

where the coefficient characterizing the elasticity of the accumulator wall is:

$$k_{ут} = \left(\frac{\partial V_{ac}}{\partial p}\right)_{p=p_0}.$$

Here V_{ac} is the volume of the entire accumulator and p_0 is the stationary pressure of the liquid in the pipe and accumulator.

Having replaced the pressure deviation p_{ac} in (4.63) by its expression from (4.66), we obtain equation (4.64), in which

$$a_{ac}^* = \frac{\frac{k_{ac} + k_{ут}}{F_т}}{1 - \omega^2 m_т^* \left(\frac{k_{ac} + k_{ут}}{F_т}\right)}. \tag{4.67}$$

The coefficient $m_т^*$, entering formulas (4.65) and (4.67), depends on the configuration of the accumulator, the mass of liquid in it, and the cross-sectional area of the pipe and, in these formulas, must have its own particular value for each accumulator.

The deviation of the mean velocity of liquid v_1 in section 1-1 (see Fig. 4.19) is connected with the deviation of the mean velocity v_2 in section 2-2 by a continuity equation which, in the presence of a hydraulic accumulator, has the form

$$v_1 = v_2 + v_{ac} \tag{4.68}$$

In first approximation it is possible to consider that the mean pressure of the liquid in section 1-1 is equal to the mean pressure in section 2-2. In more precise approximation it is possible to calculate the pressure drop caused by the change in the velocity of that mass of liquid which enters the accumulator. The velocity of the liquid entering the accumulator decreases from the value v_0 to practically zero. The pressure drop due to the change in velocity may be determined on the basis of the well-known theorem on change in momentum. Assuming disturbances taking place according to harmonic law with the frequency ω, we obtain

$$\frac{d}{dt}\left(F_T \varrho_0 \frac{v_{ac}}{i\omega} v_0\right) = F_T(p_2 - p_1)$$

or

$$p_2 = p_1 + (\varrho_0 v_0) v_{ac}. \tag{4.69}$$

This equation expresses the relationship between the mean pressure in sections 2-2 and 1-1 and the mean velocity v_{ac} of the flow of liquid in the accumulator relative to the area of the pipe F_T.

9. Forming Dynamic Flowcharts of Fuel Mains

In order to depict a dynamic flowchart we put the quadrupole equations (4.25) in the form

$$\begin{aligned} \tilde{p}_2 &= \tilde{v}_2 \cdot \operatorname{th} k + \tilde{p}_1 \frac{1}{\operatorname{ch} k}, \\ \tilde{v}_1 &= \tilde{v}_2 \cdot \operatorname{ch} k - \tilde{p}_2 \operatorname{sh} k, \end{aligned} \tag{4.70}$$

where $\tilde{p}_1$ and $\tilde{v}_1$ are the deviations of pressure and velocity at the inlet to the pipe; $\tilde{p}_2$ and $\tilde{v}_2$ are the deviations of pressure and velocity at the outlet from the pipe.

A delivery main usually has a complex structure, therefore it is convenient to combine its elements into a general flowchart according to the dimensional deviations of the flow parameters

$$p = a_{0.}^2 \varrho_0 \tilde{p}, \quad v = a_0 \tilde{v}$$

and the dimensional frequency of oscillations (4.18a)

$$\omega = s(a_0/l),$$

For the dimensional deviations of the flow parameters we shall write equations (4.70) by the complex transmission ratios

$$\begin{aligned} p_2 &= K[p_2,\ p_1]\,p_1 + K[p_2,\ v_2]\,v_2, \\ v_1 &= K[v_1,\ p_2]\,p_2 + K[v_1,\ v_2]\,v_2, \end{aligned} \tag{4.71}$$

where

$$K[p_2,\ p_1] = \frac{1}{\operatorname{ch}\omega\dfrac{l}{a_0}},$$

$$K[p_2,\ v_2] = -ia_0\varrho_0 \operatorname{tg}\omega\frac{l}{a_0},$$

$$K[v_1,\ p_2] = i\frac{1}{a_0\varrho_0}\sin\omega\frac{l}{a_0},$$

$$K[v_1,\ v_2] = \operatorname{ch}\omega\frac{l}{a_0}.$$

A dynamic flowchart of the quadrapole, expressing the relationship between the flow parameters at the inlet to the pipe and at the outlet from the pipe, on the basis of equation (4.71) has the form indicated in Fig. 4.20.

The harmonic properties of a sylphon built into the main, with the condition that the pressure of the liquid at any point in the sylphon is equal, are expressed by equation (4.52). In the case of dimensional deviations of the parameters we shall have

$$p_2 = p_1, \tag{4.72}$$

where

$$v_1 = K[v_1,\ p_2]\,p_2 + K[v_1,\ \Phi_c]\,\Phi_c,$$

$$K[v_1,\ p_2] = i\omega r; \quad K[v_1,\ \Phi_c] = i\omega(1+\lambda);$$

v_1 is the deviation of flow speed at the inlet to the sylphon; p_1 and p_2 is the pressure deviation of the liquid at the inlet to the sylphon and the oulet from the sylphon; ϕ_c is the amplitude of mechanical oscillations of the outlet section of the sylphon. A dynamic flowchart of a sylphon is shown in Fig. 4.21.

The relationship between the parameters of a flow passing through a localized hydraulic resistance of the type of a grid (see Fig. 4.18a) is determined according to equation (4.58), which we put in the form

$$p_2 = p_1 + K[p_2, v_1]v_1 + K[p_2, \phi_p]\phi_p,$$
$$v_1 = v_2, \tag{4.73}$$

where

$$K[p_2, v_1] = -\psi M; \quad K[p_2, \phi_p] = i\omega\psi M;$$

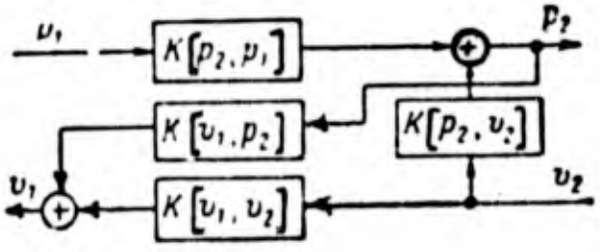

Figure 4.20

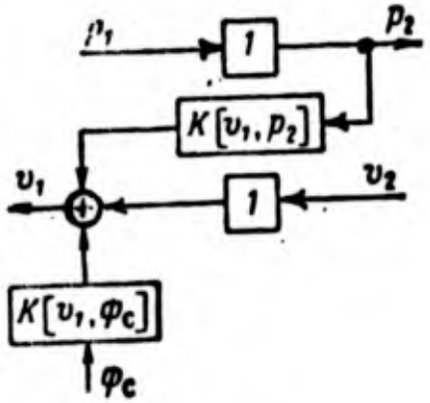

Figure 4.21

p_1, p_2, v_1, and v_2 are the deviation of pressure and velocity of the liquid in front of the grid and after the grid; ϕ_p is the amplitude of mechanical oscillations of the grid in relation to the flow. A dynamic flowchart, corresponding to equation (4.73) is given in Fig. 4.22a.

A dynamic flowchart of a delivery washer may be constructed according to equation

$$p_2 = p_1 + K[p_2, v_1]v_1,$$
$$v_1 = v_2, \tag{4.74}$$

where

$$K[p_2, v_1] = -i\omega a_m;$$

p_1, p_2, v_1, and v_2 are the deviation of mean pressure and mean velocity before the washer and after the washer. The diagram is given in Fig. 4.22b. A flow-chart for determining the pressure drop in the case of the exit of liquid from the tank is the same, but the complex transmission ratio (see equation (4.61)) will be different, namely:

$$K[p_2, v_1] = -(\psi_6 M + i\omega a_6).$$

Here p_2 is the pressure deviation of the liquid after the funnel damper.

On the basis of equations (4.64) and (4.68) the relationship between the pressure deviations p_1 and p_2 and the flow speed deviations v_1 and v_2 in the pipe before the hydraulic accumulator and after it may be put in the form

$$\begin{aligned} p_2 &= p_1, \\ v_1 &= v_2 + v_{ac}, \end{aligned} \tag{4.75}$$

where

$$v_{ac} = K[v_{ac}, p_2]\, p_2 = i\omega a_{ac}^{\bullet} p_2.$$

In equations (4.75) the pressure drop, determined by equation (4.69), is not considered. A dynamic flow diagram for a hydraulic accumulator is shown in Fig. 4.23a.

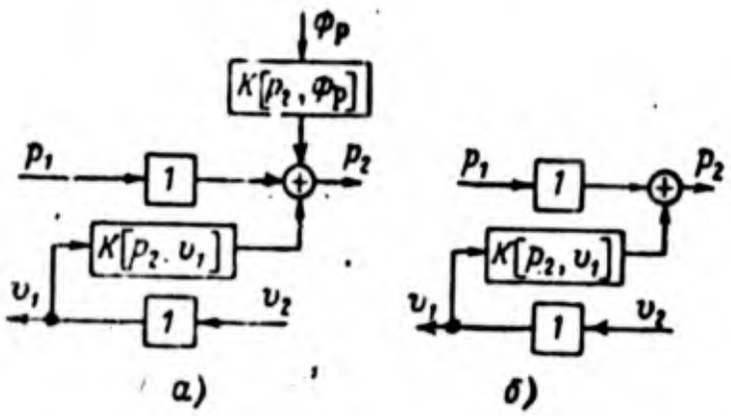

Figure 4.22

The section of the main with cavitating liquid at the inlet to the centrifugal pump in first approximation is presented in the form of localized elasticity. If the centrifugal pump performs oscillations according to the law $\phi\, e^{i\omega t}$ in

relation to the flow of liquid in the main, then with regard to equation (4.57) we obtain

$$p_2 = p_1,$$
$$v_1 = v_2 + K[v_1,\ p_2]\,p_2 + i\omega\varphi_н, \tag{4.76}$$

where p_1, v_1, p_2, and v_2 are the deviation of pressure and velocity before the localized elasticity and after it;

$$K[v_1,\ p_2] = i\omega k_{пг}.$$

A dynamic flowchart of the localized elasticity is given in Fig. 4.23b.

Figure 4.24a gives a dynamic flowchart of a collector, and a unit which is located at the outlet end of the delivery main, and therefore is a loading unit, is shown in Fig. 4.24b in the form of one block. This unit includes a centrifugal pump (turbine pump assembly), a pressure line and a combustion chamber. The complex conductivity of the loading unit is expressed by the complex transmission ratio $K[v_1, p_1]$, which we shall consider to be known.

It is not difficult to draw a dynamic flowchart of the entire delivery main from the flowcharts of the individual elements, shown in Fig. 4.20–4.24. It is convenient to draw the chart beginning with the delivery main element, which is an input unit. Then the output parameters of this element will be the input parameters for the following element, and so on up to the loading unit. A dynamic flowchart for the section of the main consisting of pipe I, sylphon II, and loading unit III (Fig. 4.25) is given in Fig. 4.26.

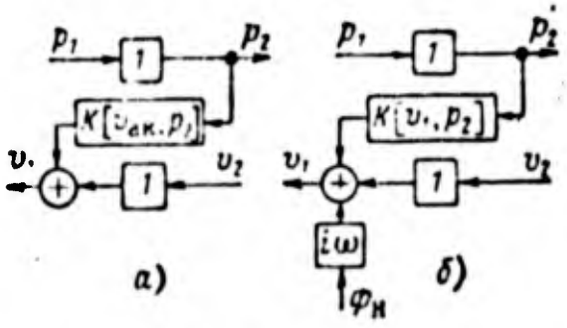

Figure 4.23

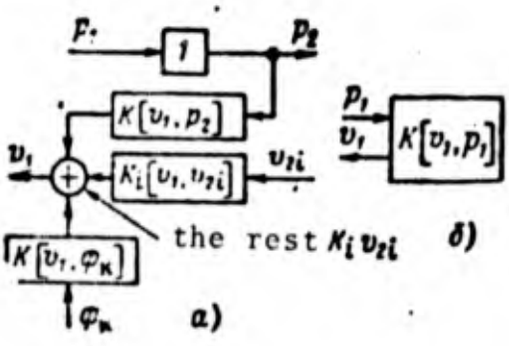

Figure 4.24

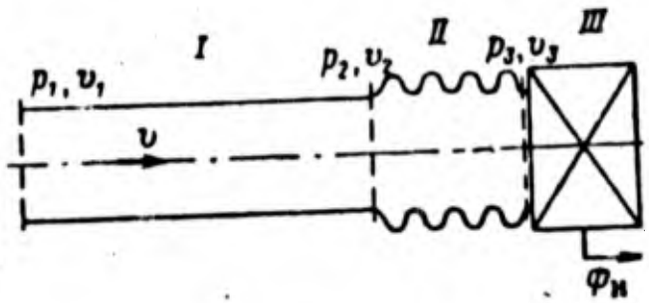

Figure 4.25

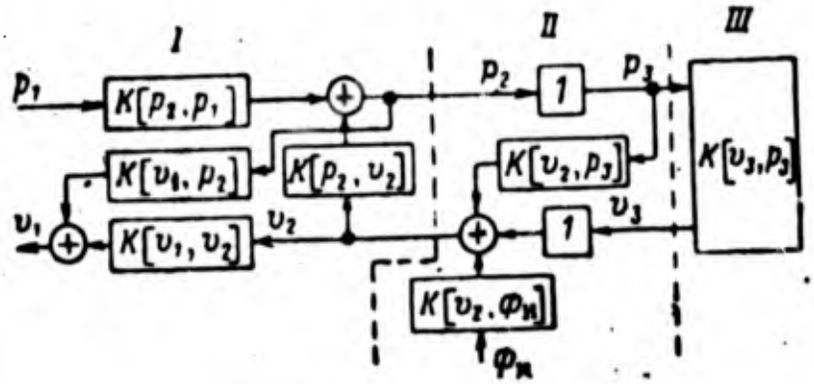

Figure 4.26

Let us now draw a dynamic flowchart for the delivery main, a diagram of which is shown in Fig. 4.27. Sections are drawn on the diagram which we shall provisionally consider to be the boundaries of the characteristic elements of the main. The initial section of the delivery main is located between sections 1 and 2, and further along the flow there are: a sylphon, a grid creating 'active' resistance, and a collector elastically suspended from the rocket body. One of the branches of the main is located between sections 5 and 6 and gas bubbles are indicated between sections 6 and 7, provisionally representing the cavitation region of the liquid; to the right of section 7 there is a unit, including the pump, a pressure line, and the combustion chamber. This unit may perform oscillations relative to the flow according to the law $\phi_p e^{i\omega t}$. At the outlet from the tank there is a funnel damper.

Oscillations of the collector do not directly influence pressure fall deviations on the grid, since the collector performs oscillations together with the grid. Pressure drop on the grid is transmitted only due to flow speed deviation at the inlet to branches of the main, going

from the collector to the engines. Velocity deviation, caused by the oscillation of the collector as a consequence of pressure fluctuations in it, as well as oscillations of its suspension point, is transmitted to the flow with the parameters p_2 and v_2. These characteristics are depicted on the dynamic flowchart, Fig. 4.28.

An engine, turbine pump assembly, and pressure line enter the loading unit for the delivery main. As applied to the diagram (see Fig. 4.28) deviations of pressure p_{7i} and velocity v_{7i} correspond to deviations of pressure and flow speed at the inlet to the pump. For each engine the relationship between deviations of pressure and flow speed in front of the pump must be completely determined and may be expressed by the complex impedance of the engine. In the general case this relationship may be put in the form

$$v_{1p} = K[v_{1p}, p_{1p}]p_{1p}, \tag{4.77}$$

where p_{1p} and v_{1p} are the deviation of pressure and flow speed at the inlet to the pump; $K[v_{1p}, p_{1p}]$ is the complex transmission ratio of the engine (in the given case the complex conductivity of the engine). The pressure deviation p_{1p} is determined by the dynamic properties of the delivery main. In order to determine the deviation, it is necessary to know the complex impedance of the engine. After the pressure deviation in front of the pump is determined, according to equation (4.77), it is possible to determine the flow speed deviation v_{1p} at the pump intake, and to find the pressure deviation in the combustion chamber according to the deviation of the rate of fuel feed into the engine.

The examples considered give a good presentation of the method of drawing dynamic flowcharts of fuel lines—the line is divided into individual typical elements, the dynamic properties of which are expressed by quadrapole equations, and then the flowchart of successively arranged quadrupoles are combined.

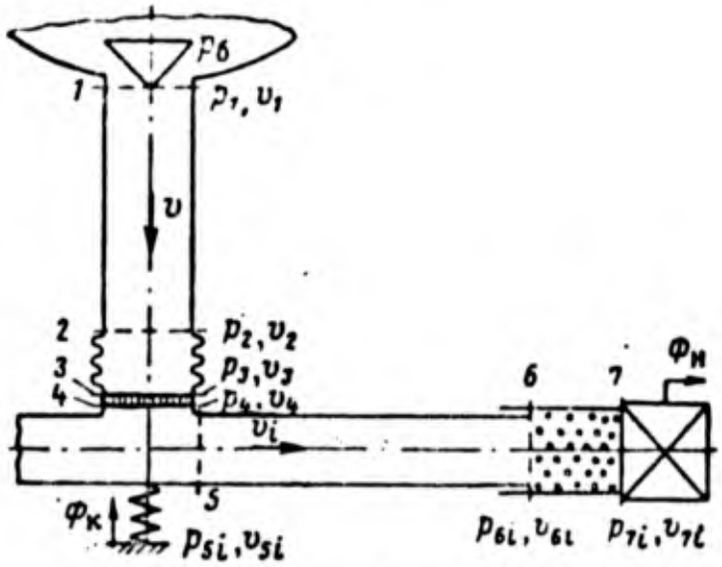

Figure 4.27

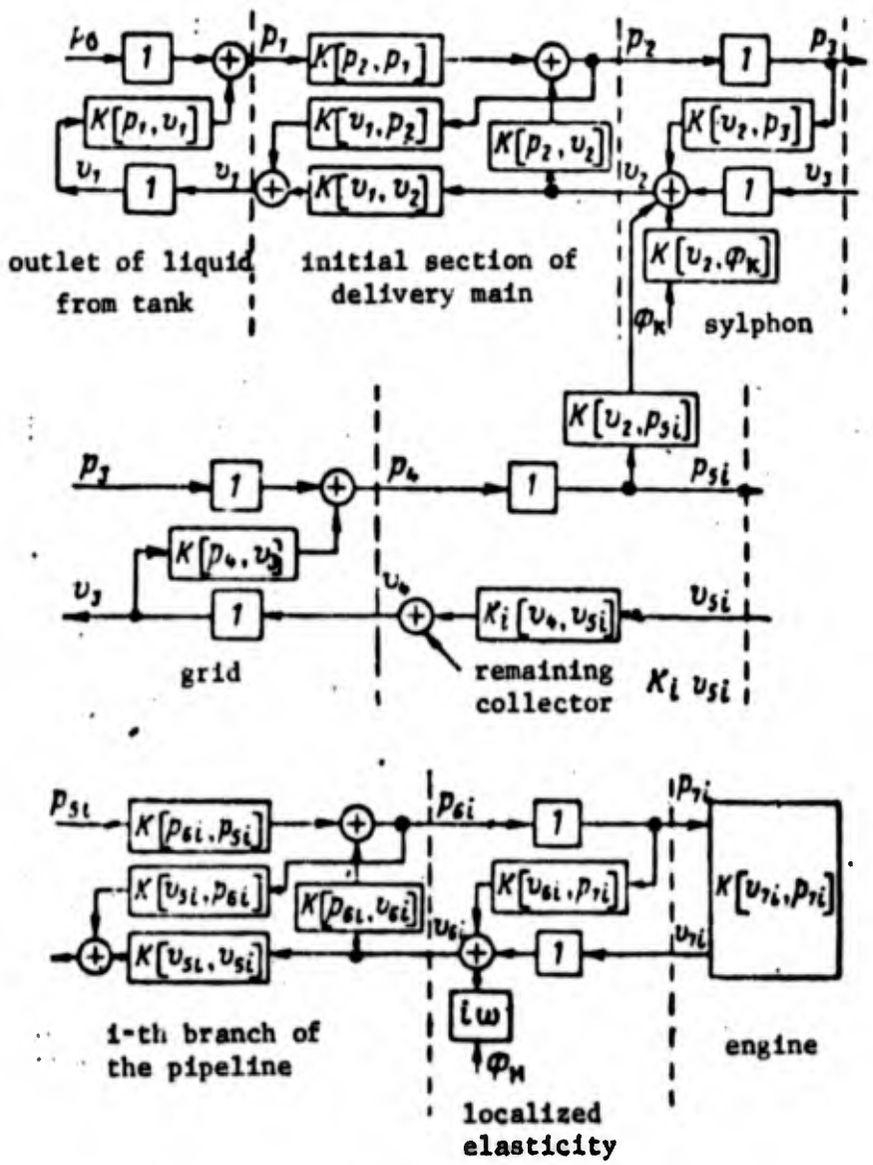

Figure 4.28

10. Induced Oscillations of the Liquid in Fuel Lines

From the active section of the trajectory the fuel in the delivery mains is subjected to the influence of different disturbances. Some disturbances are of a periodic nature and cause induced oscillations of the liquid. Among the most important periodic disturbances are: fluctuations in the pressure of liquid at the bottom of the tank, vibrations of fuel line mountings, caused by longitudinal oscillations of the rocket body, and fluctuations of pressure in the combustion chamber. Oscillations of a straight pipe along the flow of a liquid influence the flow due to friction on the walls. However, it is possible to ignore this effect due to its small size. Induced oscillations of a liquid, for example, in the delivery main, a diagram of which is given in Fig. 4.27, may arise under the influence of fluctuations in the pressure of the liquid on the bottom of a tank p_t, vibrations of the suspension point of the collector ϕ_k, and oscillations of the loading unit along the flow ϕ_p.

Induced oscillations in the delivery main cause fluctuations in the discharge of fuel through the pump and fluctuations in the fuel delivery to the combustion chamber. In a linear system the effect resulting from induced oscillations is determined as the geometrical sum of the induced oscillations caused by different external influences. If induced oscillations of pressure in front of the pump from any external influence, for example, fluctuation in pressure p_t, is presented in the form of a vector

$$p_{1p} = K^*[p_{1p}, p_t]p_t,$$

when the total pressure fluctuations in front of the pump in the case of longitudinal oscillation of the rocket will be determined as the sum of the vectors

$$p_{1н} = K^*[p_{1p}, p_б]p_б + K^*[p_{1p}, \phi_к]\phi_к + K^*[p_{1p}, \phi_p]\phi_p, \quad (4.78)$$

where $K^*[p_{1p}, p_б]$, $K^*[p_{1p}, \phi_к]$, $K^*[p_{1p}, \phi_p]$—

—the complex transmission ratios of the delivery main, characterizing fluctuations in the pressure of the liquid at the pump intake under the influence

of fluctuations in pressure at the bottom of the tank, vibrations of the suspension point of the collector, and vibrations of the pump along the flow (on Fig. 4.28 $p_{1p} = p_{yi}$).

Photographs of the vectors (amplitude-phase characteristics) of simple pipelines with resistances or localized elasticity on the ends are given in Figs. 4.9-4.13. For complex delivery mains, such as that shown in Fig. 4.27, it is useful to calculate the amplitude-phase characteristics on a digital computer using dynamic flowcharts for this purpose. The form of the amplitude-phase characteristic depends on the arrangement of the delivery main and the complex conductivity of the engine, which is expressed by the complex transmission ratio $K[v_{1p}, p_{1p}]$ (in Fig. 4.28 $v_{1p} = v_{7i}$).

Fig. 4.29 shows the amplitude-phase frequency characteristics of a delivery main $K[p_{ip}, p_t]$, which express the ratios of the pressure deviation in front of the pump to the pressure deviation at the bottom of the tank, depending on the oscillation frequency. The difference in characteristics is basically determined by the different properties of the complex admittances of the engine $K[\ _{1p}, p_{1p}]$, connected to the delivery main. At the frequency $\omega = \omega_1$ and $\omega = \omega_3$ the admittance of an engine is small, therefore the pressure deviation p_{1p} is great, and at the frequency $\omega = \omega_2$ the admittance of an engine is great and therefore the pressure deviation p_{1p} is small (Fig. 4.29a). The amplitude-phase characteristic, shown in Fig. 4.29b, does not have these properties.

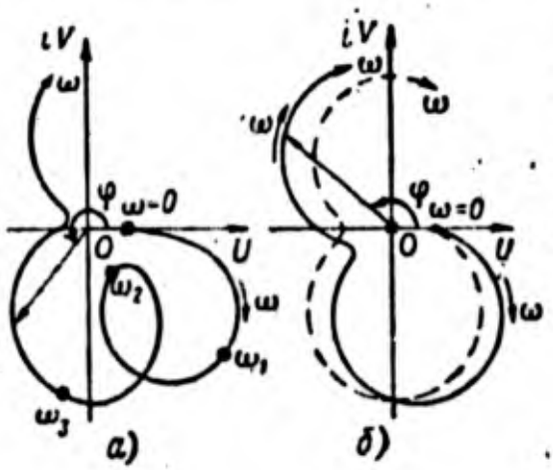

Figure 4.29

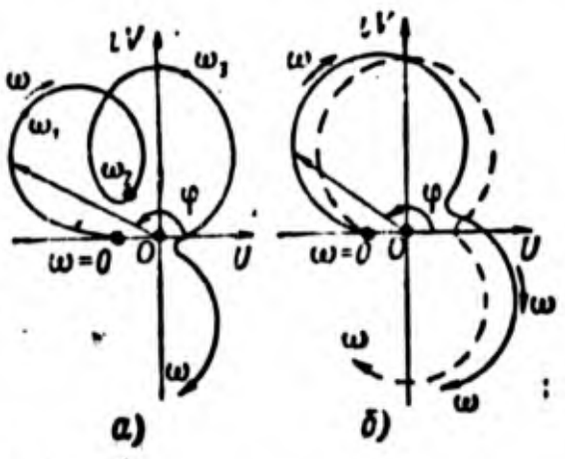

Figure 4.30.

The amplitude-phase characteristics $K[p_{1p}, \phi_p]$ of the same main is shown in Fig. 4.30. Disturbances are caused by pump vibrations. Resonance oscillations appear at the same frequencies as in the case where the pressure deviation p_p served as a disturbance. The characteristics begin from the negative real semi-axis. Displacement of the pump along the flow ($\phi_p > 0$) where $\omega = 0$ decreases the pressure in front of the pump ($p_{1p} < 0$).

A real fuel system or a model of one is used for an experimental of the dynamic characteristics of a fuel main. For example, a modified fuel system of a Titan-2 rocket engine, fixed on a stand, is shown in Fig. 4.31 [20]. A pulsator consisting of a piston and sylphon, placed in a hermetic casing, is installed on each main in front of the pump in order to excite induced oscillations. The amplitude of excitation is regulated by varying the radius of the tank. In order to equalize the flow in the pipe a pressure impulse, excited by the pulsator piston, enters a torus-shaped canal. The hydrodynamic properties of the engine are simulated by special devices which consist of the following items. Between the combustion chamber head and the gas generator inlet there are by-pass pipes, including Venturi cavitation pipes and control valves. The high-pressure fuel lines are so constructed that they can simulated the resistance and inertia of the flow of liquid, going from the pump to the combustion

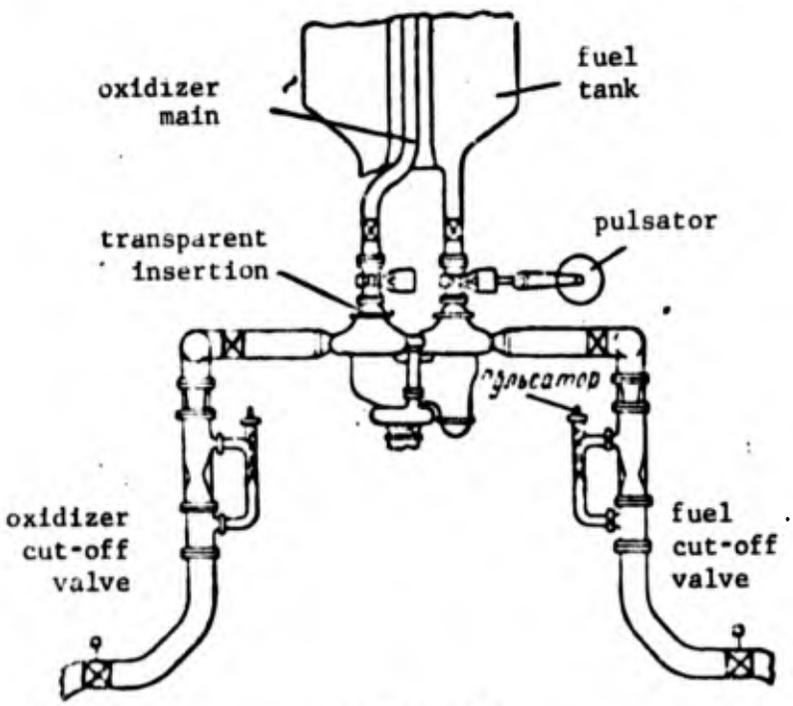

Figure 4.31

chamber. Moreover, the high-pressure line simulates the oxidizing track of the combustion chamber. The cavitation Venturi pipes with pulsators regulate the speed of the basic fuel flow and maintain the excess pressure, which simulates pressure in the combustion chamber.

It is possible to establish different cavitation reserves of the pumps by changing the boost pressure in the tanks and to determine the resonance frequencies and forms of the oscillations of liquid in the lines, corresponding to these cavitation reserves. It is possible to record the cavitation of liquid at the pump intake on motion picture film through a transparent insert. It is possible to obtain the values of the complex transmission ratios for different oscillation frequencies on this experimental set-up and to compare these data with the results of calculations.

References

1. Бетчелор Г. Г. Волны в суспензии газовых пузырьков в жидкости. — «Механика» (периодич. сб. переводов иностранных статей), М., «Мир», 1968, № 3.
2. Брамблетт, Ноулс, Сак. Исследование динамики кавитационных и напорных характеристик системы подачи двигателя J-2. — «Вопросы ракетной техники», 1967, № 5.
3. Гризодуб Ю. Н. Применение теории пассивных четырехполюсников к расчету распространения колебаний давления в разветвленных гидравлических системах авиадвигателей. — «Автоматика и телемеханика». Изд. АН СССР, 1950, т. XI, № 2.
4. Двухшерстов И. П. Гидравлический удар в трубах некруглого сечения и потоке жидкости между упругими стенками. Уч. записки МГУ, 1948, вып. 122, т. II.
5. Жуковский Н. Е. О гидравлическом ударе в водопроводных трубах. Полное собр. соч., т. VII. ОНТИ НКТП, 1937.
6. Карелин В. Я. Кавитационные явления в центробежных и осевых насосах. М., Машгиз, 1963.
7. Колесников К. С. Вынужденные колебания потока идеальной сжимаемой жидкости в однородной прямой трубе. Изв. АН СССР, ОТН, Механика и машиностроение, 1963, № 4.
8. Колесников К. С., Вынужденные колебания впрыска идеальной сжимаемой жидкости в камеру. Изв. АН СССР, ОТН, Механика и машиностроение, 1963, № 5.
9. Кочин Н. Е., Кибель И. А., Розе Н. В. Теоретическая гидромеханика, ч. I. М., Гостехиздат, 1955.
10. Ломакин А. А. Центробежные и пропеллерные насосы. М., Машгиз, 1950.

11. Нестеров В. С. ДАН СССР, М., «Наука», 1941, т. XXXI, № 9.
12. Раушенбах Б. В. Вибрационное горение. М., Физматгиз, 1961.
13. Роуз. Анализ продольной устойчивости ракет на жидком топливе. — «Вопросы ракетной техники», 1967, № 8.
14. Соболев С. Л. Уравнения математической физики. М., Гостехиздат, 1950.
15. Стретт Дж. (лорд Рэлей). Теория звука, т. II. М., Гостехиздат, 1950.
16. Феодосьев В. И., Синярев Г. Б. Введение в ракетную технику. М., Оборонгиз, 1960.
17. Фок В. А., ДАН СССР. М., «Наука», 1941, т. XXXI, № 9.
18. Чарный И. А. Неустановившееся движение реальной жидкости в трубах. М., Гостехиздат, 1951.
19. Radovcich N. A. Analytical Model for Missile Axial Oscillation Caused by Engine-Structure Coupling, AIAA, Unmanned Space-craft Meeting, Los Angeles, AIAA Publication, 1965.
20. Shupert T. Turbopump Transient Response Test Facilite and Program, J. Spacecraft, 1965, vol. 2, No. 5.
21. Worlund A. L., Glasgow V. L., Norman D. E., Hill R. D. The Reduction of Pogo Effects by Gas Injection, AIAA paper, 1966, No. 66—560.

Chapter 5

DYNAMIC PROPERTIES OF LIQUID PROPELLANT ROCKET ENGINES

1. A Liquid Propellant Rocket Engine as a Component of a Closed Oscillatory System

A liquid propellant rocket engine is the most complex component of the closed oscillatory system forming a rocket with a liquid propellant rocket engine. The dynamic processes in liquid propellant rocket engines have, for a long time, been the subject of theoretical and experimental studies, but due to the extreme complexity of these processes they have not been sufficiently studied up to the present time.

In the oscillations which arise in a rocket, the role of the engine may differ. If the operation of an engine is unstable and the pressure variations in the combustion chamber arise independently of the longitudinal oscillations of the rocket body, then the engine serves as a source of induced oscillations of the rocket body and its individual units. If the operation of the engine is stable, then the engine is a source of energy (booster) in a closed system, consisting of the rocket body, the fuel lines, and the engine. Induced oscillations of the fuel supply to the combustion chamber cause pressure fluctuations in the chamber and fluctuations in engine thrust. The dynamic properties of the engine as a source of energy may be expressed by the complex transmission ratios

$$p_к = K[p_к,\ p_{1op}]\,p_{1op} + K[p_к,\ p_{1fp}]\,p_{1fp},$$

where p_k is the deviation of gas pressure in the combustion chamber of the engine from a stationary value; p_{1op} and p_{1fp} are the deviation of oxidizer pressure and fuel pressure in front of the pump intakes.

Moreover, pressure oscillations in the combustion chamber cause oscillations of the bottom pressure p_{bp} (pressure on the stern section of the rocket body), which is connected with the pressure deviation in the combustion chamber through the complex transmission ratio

$$p_{bp} = K[p_{bp}, p_k]p_k.$$

For the fuel mains the engine is a loading unit and its dynamic characteristics influence the dynamics of the fuel main. The dynamic properties of the engine as a loading unit may also be expressed by complex transmission ratios, which have the value of complex admittances. For a two-component engine we will have:

$$v_{op} = K[v_{op}, p_{lop}]p_{lop} + K[v_{op}, p_{lfp}]p_{lfp},$$
$$v_{fp} = K[v_{fp}, p_{lfp}]p_{lfp} + K[v_{fp}, p_{lop}]p_{lop},$$

where v_{op} and v_{fp} are the flow speed deviation of the oxidizer and the fuel at the pump intakes. The complex transmission ratios $K[v_{op}, p_{lfp}]$ and $K[v_{fp}, p_{lop}]$ characterize the interconnection of the dynamic processes in the fuel mains, which are performed through the combustion chamber and the turbine pump assembly.

An engine of the simplest type, consisting only of basic units, may operate stably with permissible deviations of the parameters only in a narrow range of operating conditions and external disturbances. Therefore, in order to maintain operating conditions in addition to the basic units and the constant structural elements, automatic regulators are introduced into liquid propellant rocket engines. From the point of view of the static characteristics of liquid propellant rocket engines, maintaining a given operating condition of an engine is the task of the regulators. If, for example, it is necessary to provide for constant pressure in the combustion chamber, then in the case of a deviation of the actual pressure from the desired pressure, the regulator must automatically control the fuel supply and change the amount or proportion of fuel components entering the gas generator and combustion chamber. The dynamic properties of the regulator may be expressed by the following complex transmission ratio

$$\delta = K[\delta, p_k]p_k.$$

Here δ is a small displacement of the controlling member of the regulator.

The engine may also have a regulator for varying the operating conditions in correspondence with a flight plan. Such a regulator is usually called an

engine control regulator; the input value to the regulator may depend on the parameters of the rocket flight, the flight time, and so forth.

We shall assume the operating conditions of the engine to be stable and analyze its dynamic characteristics in the case of small deviations of the operating parameters from a certain stable (stationary) condition.

2. Component Parts of a Dynamic Model of a Liquid Propellant Rocket Engine

Liquid propellant rocket engines are divided into two basic groups according to the method of fuel delivery to the combustion chamber: engines with a turbopump feed system and engines with a displacer feed system. In the case of a displacer feed system the fuel components are displaced from the tanks into the combustion chamber under a gas pressure exceeding the pressure in the combustion chamber. In the case of a turbopump feed system the components of the fuel are delivered from the tanks to the pumps under low pressure, providing for pump operation without cavitation of the liquid. Increase in pressure and further fuel supply to the combustion chamber are provided for by turbopump assembly, which includes pumps and a gas turbine used to drive the pump.

Let us examine several models of liquid propellant rocket engines [13]. Fig. 5.1 shows a diagram of a liquid propellant rocket engine with displacer feed of the fuel component. Here 1 is a cylinder with high-pressure gas, 2 is a gas pressure regulator, 3 are shutoff valves, 4 is the oxidizer tank, 5 is the fuel tank, 6 are the main valves, 7 is the combustion chamber of the engine, G_{ox} and G_{fl} are the deflection of the oxidizer feed and the fuel feed into the combustion chamber of the engine.

Figures 5.2-5.4 show schematic diagrams of liquid propellant engines with turbine pump assemblies operating on the combustion products of the basic components. The diagrams differ only in the number and purpose of the regulators. On Fig. 5.2: 1 is the pressure regulator in the combustion chamber, 2 is the regulating unit of the regulator, 3 is a two-component gas generator, 4 is the oxidizer tank, 5 is the fuel tank, 6 is the fuel pump, 7 is the oxidizer pump,

8 is the turbine of the turbine pump assembly, 9 are the main valves, 10 is the combustion chamber, G_{og} and G_{gg} are the deflections of oxidizer feed and fuel feed into the gas generator.

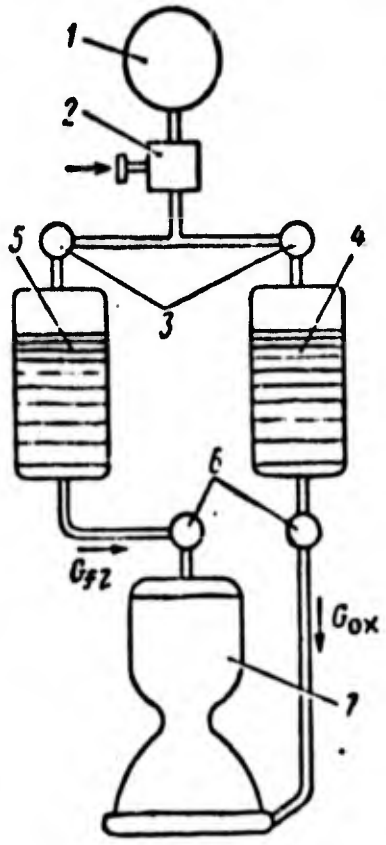

Figure 5.1

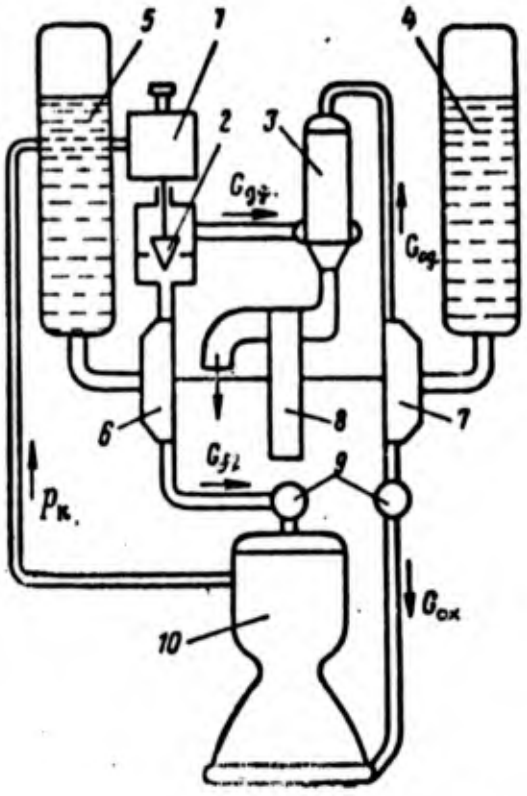

Figure 5.2

In the diagram given in Fig. 5.3, 1-10 designate the same items as in Fig. 5.2. However, in this diagram, besides a pressure regulator in the combustion chamber, there is a regulator of the proportion of components in the combustion chamber 11 with a regulating unit 12. Here 13 is a fuel feed gauge and 14 is an oxidizer feed gauge in the combustion chamber.

Fig. 5.4 shows a diagram with three regulators. In addition to the items designated on Fig. 5.3, here 15 is a regulator of the ratio of fuel components for the gas generator, 16 is the regulating member of this regulator, 17 is a sensor of fuel feed into the gas generator, and 18 is a sensor of oxidizer feed into the gas generator.

In fuel feed systems with a turbine pump assembly, the combustion process in gas generators operating on the basic fuel components is performed with a

significant excess or insufficiency of the oxidizer, as a consequence of which a large part of the chemical energy of the gas, expendable for driving the pumps of the turbine pump assembly, is not realized. In order to make subsequent use of this energy it is possible to complete the combustion of the gas in an afterburner chamber or directly in the combustion chamber of the engine. Liquid propellant rocket engines, in which after burning of this gas is performed in the combustion chamber, are called closed feed system engines.

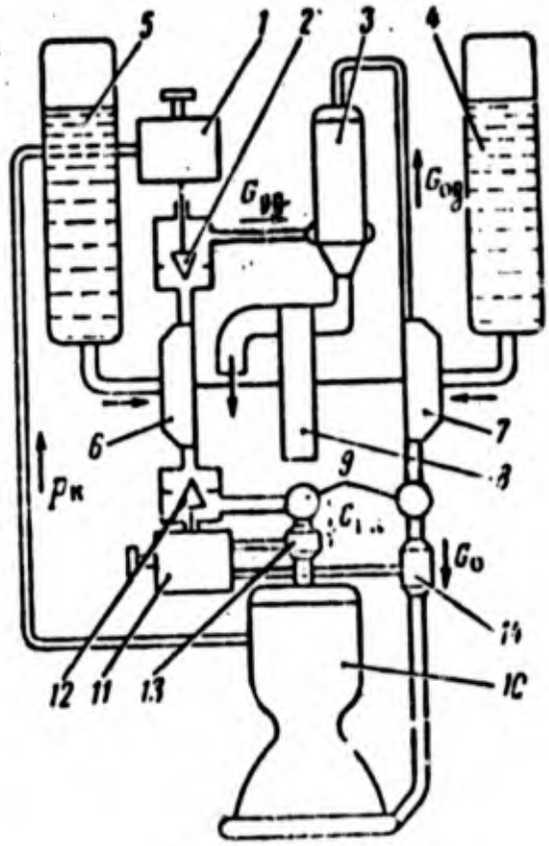

Figure 5.3

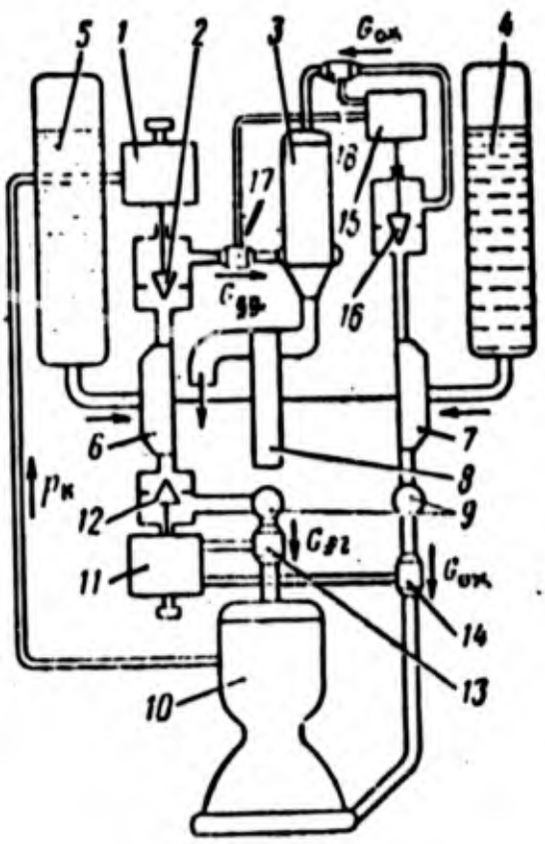

Figure 5.4

The liquid oxidizer and the fuel, and also the gas coming from the turbine with an excess or insufficiency of the oxidizer [13, 16], are fed into the combustion chamber of liquid propellant rocket engines with closed feed systems. It is possible to have an engine in which all the fuel (or all the oxidizer) passes through the turbine. In this case the liquid oxidizer (or the liquid fuel) and gas with an insufficiency (or excess) of the oxidizer enter the combustion chamber. Finally, it is also possible to have an engine where the entire volume of both the oxidizer and the fuel pass through the respective gas

generators and turbines before entering the combustion chamber. In this case gases of two compositions—one with an excess of fuel, and the other with an excess of oxidizer—are introduced into the combustion chamber and thoroughly burned in it. Mixing and burning a gas with a liquid fuel in a combustion chamber is called a heterogeneous process, and mixing and burning gas with gas is called an homogenous process.

As was indicated above, the combustion process in a gas generator takes place with a significant excess of one of the components of the fuel and, in practice, leads to high-temperature gasification of this component. The second component of the fuel (the additive) is only introduced in an amount necessary to provide for a given temperature of gasification.

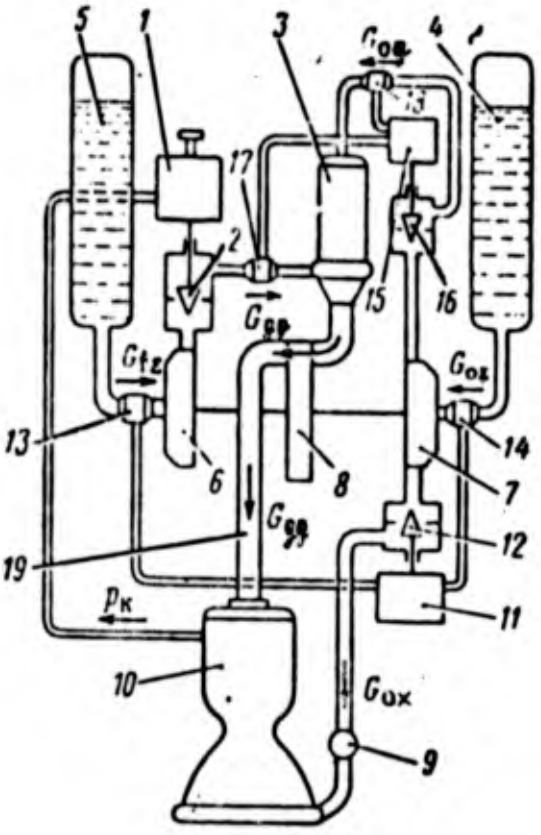

Figure 5.5

Figure 5.5 gives a schematic diagram of a liquid propellant engine with a closed feed system with a two component liquid gas generator, operating on the basic components. As is apparent, all the fuel is gasified in the gas

generator; the mixing and burning in the combustion chamber is heterogeneous. Three regulators are included in the diagram. Here 1-12 and 15-18 designate the same items as on Fig. 5.4; 13 is the total fuel feed ($G_{f\Sigma}$) deflection sensor; 14 is the total oxidizer feed ($G_{o\Sigma}$) deflection sensor; and 19 is the generator gas supply line into the combustion chamber.

The principal methods of regulating and controlling the engine to a significant degree depend on the method of feeding the engine and are determined by the purpose of the rocket.

An engine usually has several automatic control systems [12, 13]. Some parameters characterizing engine thrust are assumed as control variables for liquid propellant rocket engines. Usually, the systems for automatic control of the pressure in the combustion chamber and control of the ratio of fuel components are used, whereby the latter system is often provided for a liquid propellant gas generator. This is explained by the fact that under nominal combustion chamber conditions the basic thermodynamic characteristics of the combustion products (temperature T_k, gas constant R_k) vary very little. In a liquid propellant gas generator, operating on an excess of one of the components, the reverse picture is observed. Therefore, the requirements for a precise value of the coefficient of the component ratio in a liquid propellant gas generator are more rigid, since an insignificant change in this coefficient may cause a sharp change in the operating conditions of the turbine pump assembly and even to a burnout of the liquid propellant gas generator walls.

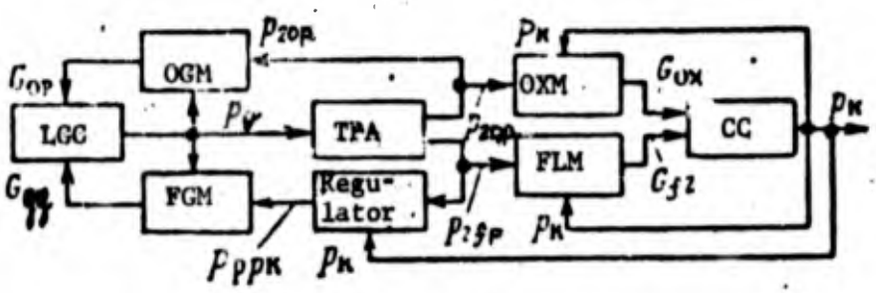

Figure 5.6

The amount of pressure at the pump intakes is also an important parameter for the reliable operation of liquid propellant rocket engines, therefore engines are provided with a system for controlling this pressure.

The range of a rocket basically depends on the ratio of the weight of the rocket at the end of the active section of flight to the launch weight. Therefore it is natural for a builder to try to decrease the amount of fuel in the tanks, which remains due to engine operation on an uncalculated ratio of components. In order to decrease residual fuel the rocket is provided with a system for controlling the levels of components in the tanks.

One of the possible methods of automatic pressure control in the combustion chamber is shown in Fig. 5.6. The basic interconnection between units of a liquid propellant rocket engine and a liquid gas generator are shown; pressure control in the combustion chamber is performed by means of varying the operating conditions of the turbine by varying the coefficient of the component ratio in the liquid gas generator. In this diagram: CC is the combustion chamber, OXM and FLM are the oxidizer main and fuel main of the combustion chamber, OGM and FGM are the oxidizer main and fuel main of the gas generator, p_k is the pressure deviation in the combustion chamber, G_{ox} and G_{fl} are the deflections of oxidizer feed and fuel feed into the combustion chamber, G_{og} and G_{gg} are the deflections of oxidizer feed and fuel feed into the liquid gas generator, p_{cr} is the pressure deviation at the regulator outlet, p_g is the gas pressure deviation at the gas generator outlet (at the turbine inlet), p_{2op} and p_{2fp} are the pressure deviations at the oxidizer pump outlet and at the fuel pump outlet.

A scheme for controlling coefficients of the fuel component ratio in the liquid gas generator is shown in Fig. 5.7. The regulator is attached to the fuel main and is designed to reduce the deviation of the coefficient κ, characterizing the ratio of components, to a minimum. Here $p_{r\kappa}$ is the pressure d deviation at the outlet from the component ratio regulator.

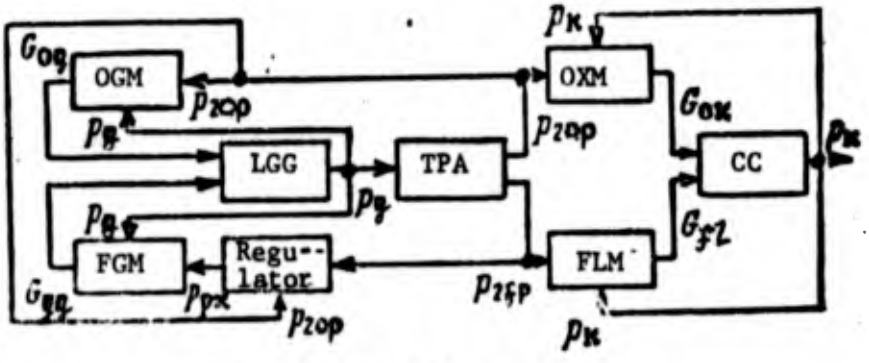

Figure 5.7

Figure 5.8 shows one of the simplified schemes for controlling the level of fuel components in the tank. Regulation of the proportional evacuation of the tanks is performed in the following way: the regulator determines the deviation of the levels of oxidizer and fuel H_0 and H_{fl} in the tanks and, depending on this deviation, varies the discharge of one of the components. In this diagram p_{rH} is the pressure deviation of the level of fuel components in the tanks at the outlet from the regulator.

One of the possible engine control schemes is given in Fig. 5.9.

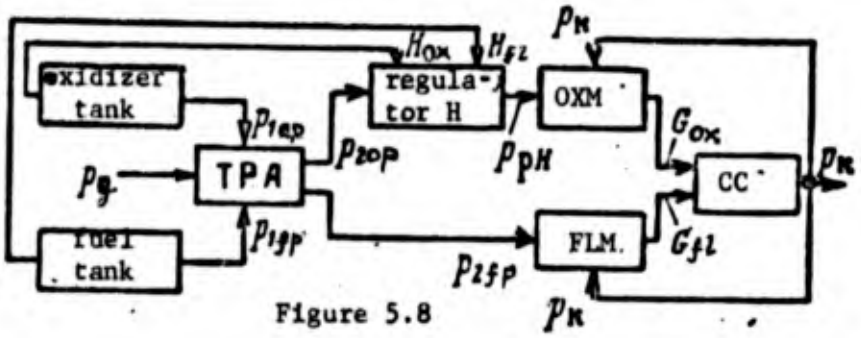

Figure 5.8

One of the possible engine control schemes is given in Fig. 5.9. This scheme includes a regulator of the fuel component ratio in the liquid gas generator (regulator κ), a regulator of the fuel component level H in the tanks (regulator H), a control system (CS), and a regulator for maintaining the apparent rocket velocity (ARV). A sensor, measuring the apparent rocket velocity v_{ap} signals the velocity to a calculator where the deviation of the velocity from the programmed velocity is calculated. A signal of misalignment is adjusted in the apparent rocket velocity, which changes the pressure in the combustion chamber (and therefore also the thrust). Fig. 5.9 shows such a system for pressure-charging the tanks using liquid propellant pressure accumulators (LPA); here (OGM) and (FMG) are the oxidizer and fuel mains going to the gas generators of the liquid propellant pressure accumulator.

It is characteristic for a liquid propellant rocket engine to have a large number of dynamic components, the interconnection of which is determined by the basic design of the engine.

The dynamic processes of the engine components are described by differential or algebraic equations, connecting the input and output coordinates of a

component, values characterizing the physical processes in the engine. In writing equations of perturbed motion we shall consider the deviation of coordinates and velocities to be small in comparison with their values in the case of a stationary power setting. This enables us to linearize the equations for the components of a liquid propellant rocket engine.

On the basis of an examination of schematic diagrams and control schemes, a liquid propellant rocket engine with a pump feed system may be divided into the following basic dynamic components:

— combustion chamber of the engine,
— gas generator,
— fuel pump,
— turbine,
— force mains for the combustion chamber,
— mains for the gas generator,
— regulators.

We shall now derive equations for the components of a liquid propellant rocket engine.

3. Equations for the Combustion Chamber and Gas Generator

The operating process of the combustion chamber of an engine includes atomization, mixture, and vaporization of fuel, combustion and expulsion of the combustion products from a nozzle.

There is always some irregularity in the combustion process in the combustion chamber. Variation in temperature, velocity, gas composition, and other parameters are also possible. There is always intense turbulence in the combustion chamber, which is one of the causes of the noise produced by an operating engine. A combustion process with small fluctuations is called practically regular, and a combustion process with large fluctuations is called irregular, although it is impossible to give precise definition of these terms.

We shall designate as low-frequency fluctuations those, the period of which is immeasurably greater than the propagation time of a pressure wave through the chamber. The operating in the combustion chamber is idealized in order to analyze low-frequency fluctuations [7]. The idealization is performed by substituting the process of gradual conversion of fuel into combustion products (atomization, heating, vaporization, diffusion, turbulent mixing, complex and diverse chemical reactions) by an abrupt process, whereby a particle of fuel does not give off a noticeable amount of energy and does not increase in volume until a certain moment of time, after which it is instantaneously converted into the end product of the product (Fig. 5.10). The time θ_0, which in the given case is equal for all particles of fuel, is called the conversion time (combustion lag time). Since the propagation time of a pressure wave along the chamber is immeasurably less than the period of the low-frequency oscillations, then wave processes in the chamber cannot be considered and it must be assumed that the pressure and temperature at all points of the chamber vary in time according to the same law.

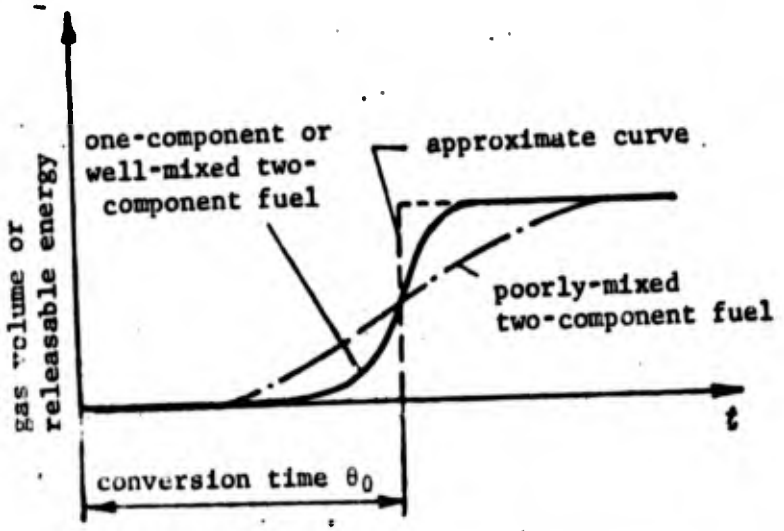

Figure 5.10

The process of the accumulation of gaseous products in the combustion chamber may be expressed by the following differential equation

$$V_к \frac{d\gamma_к}{dt} = G_к(t-\theta_0) - G_e, \qquad (5.1)$$

where V_k is the volume of the chamber; γ_k is the mean volumetric density of refuse products in the chamber; G_k is the deviation of secondary fuel supply into the chamber; G_e is the deviation of secondary gas exhaust from the chamber.

We shall consider the combustion products in the chamber to be an ideal gas, for which it is possible to write an equation of state in the form

$$p = \gamma_k RT, \tag{5.2}$$

where p is the pressure; R is the specific gas constant; T is the temperature.

In the case of a constant ratio of fuel components in the chamber, the temperature and specific gas constant of gaseous combustion products will be constant, and therefore after linearizing equation (5.1) where $RT = R_k^* T_k^* = \text{const}$ we obtain

$$\frac{d\gamma_k}{dt} = \frac{1}{R_k^* T_k^*} \frac{dp_k}{dt}, \tag{5.3}$$

Here the values R_k^* and T_k^* are determined for a constant ratio of components, corresponding to stable operating conditions of the engine.

The deviation of secondary gas exhaust from the chamber with the constants T_k^* and R_k^* can be considered to be proportional to the pressure deviation in the chamber T_k, i.e.,

$$G_e = \left(\frac{\partial G_e}{\partial p_k}\right)^* p_k = \left(\frac{\partial G_k}{\partial p_k}\right)^* p_k = \left(\frac{G_k}{p_k}\right)^* p_k. \tag{5.4}$$

Here, as before, the sign (*) denotes values corresponding to a stable power setting of the engine. In (5.4) it is calculated that $G_e^* = G_k^*$.

The deviation of secondary fuel supply into the chamber is composed of the deviations of oxidizer feed G_{ox} and fuel feed G_{fl}:

$$G_k = G_{ox} + G_{fl} \tag{5.5}$$

Replacing the value γ_k, G_e, and G_k in equation (5.1) by their expressions from (5.3)-(5.5), we obtain

$$\theta_k \frac{dp_k}{dt} + p_k = k_{ok} G_{ok}(t-\theta_0) + k_{gk} G_{gk}(t-\theta_0), \tag{5.6}$$

where

$$\theta_k = \frac{V_k p_k^*}{R_k^* T_k^* G_k^*}; \qquad k_{ok} = k_{gk} = \frac{p_k^*}{G_k^*};$$

$$G_k^* = G_{ok}^* + G_{gk}^*. \tag{5.7}$$

Here θ_k is the time constant (relaxation time) of the combustion chamber; k_{ox} and k_{fl} are the amplification coefficients of the combustion chamber for the discharge of oxygen and fuel.

Knowing the deviations of oxidizer feed and fuel feed into the chamber, it is possible to determine the pressure deviation in the chamber from equation (5.6). Equation (5.6) is obtained with the assumption that the values R_k^* and T_k^* are constant. Under this assumption the combustion chamber will possess the same dynamic properties as in the case of a one-component fuel. Pressure variation in such a chamber may be expressed by the total deviation of the fuel feed into the chamber.

We shall express the dynamic characteristics of the combustion chamber by complex transmission ratios. Since the deviation in the supply of fuel components into the chamber are assumed to be derived according to harmonic law with the frequency ω, then, considering the conversion time θ_0, we shall have [17]

$$G_{ok}(t-\theta_0) = G_{ok}(t)e^{-i\omega\theta_0} = G_{ok}e^{i\omega(t-\theta_0)}, \tag{5.8}$$

$$G_{gk}(t-\theta_0) = G_{gk}e^{i\omega(t-\theta_0)}.$$

Assuming, moreover, that

$$p_k(t) = p_k e^{i\omega t},$$

from equation (5.6) we obtain

$$p_k = K[p_k, G_{ok}]G_{ok} + K[p_k, G_{gk}]G_{gk}, \tag{5.9}$$

where

$$K[p_k, G_{ok}] = K[p_k, G_{gk}] = \frac{\left(\frac{p_k^*}{G_k^*}\right)e^{-i\omega\tau_k}}{1 + i\omega T_k}. \tag{5.10}$$

Deviation of the coefficient k of the ratio of components leads to a change in the gas temperature in the chamber, which, in turn, influences the pressure in the chamber and the secondary discharge of gas from the chamber. We shall write a differential equation in order to determine the pressure deviation in the combustion chamber with regard to the deviation of the coefficient of the ratio of components entering the chamber.

The discharge of gas from the combustion chamber is determined according to formula

$$G = A_k \frac{pF_{kp}}{\sqrt{RT}}, \tag{5.11}$$

where

$$A_k = \sqrt{k\left(\frac{2}{k+1}\right)^{\frac{k+1}{k-1}}}; \tag{5.12}$$

k is a polytropic exponent; g is the acceleration of the force of gravity; F_{kp} is the critical cross-sectional area of the nozzle; p is the pressure in the chamber; R, T are the specific gas constant and the temperature of the combustion products in the chamber.

Below we shall consider the value k to be a constant, i.e., k = const (A_k = const). Then formula (5.11) may be put in the form

$$G = \frac{pF_{kp}}{\beta}, \tag{5.13}$$

where β is a specific pressure pulse in the chamber. On the basis of (5.11) and (5.13)

$$\beta = \frac{1}{A_k}\sqrt{RT}. \tag{5.14}$$

The value β depends on the coefficient of the ratio of fuel components and gas pressure in the combustion chamber. This relationship may be expressed as

$$\beta = A\alpha^{a}p^{b}, \tag{5.15}$$

where A, a, b are certain constant coefficients of the chamber under consideration; α is a coefficient, depending on the ratio of fuel components and equal to the ratio of the actual coefficient of the ratio of component κ_{act} to the theoretical

$$\kappa_T = \left(\frac{G_{ok}}{G_{gk}}\right)_T.$$

Then

$$\alpha = \frac{1}{\kappa_T}\left(\frac{G_{ok}}{G_{gk}}\right)_{fact}. \tag{5.16}$$

Within the limits of the variation p = 20–200 gauge atmospheres and α = 0.6–0.92, the coefficients A, a, and b for certain fuel components have the following values:

for liquid oxygen (O_2) and kerosene

A = 163.55; a = -0.1322; b = 0.0128;

for liquid oxygen and liquid hydrogen (H_2)

A = 210.25; a = -0.2392; b = 0.0107.

Considering the relationship (5.15), the gas discharge from the combustion chamber is

$$G = G(p, \alpha) = \frac{F_{kp}}{A}\alpha^{-a}p^{1-b}. \tag{5.17}$$

We shall write the deviation of the gas discharge from the chamber in the form

$$G_c = \left(\frac{\partial G}{\partial p}\right)^{*} p_k + \left(\frac{\partial G}{\partial \alpha}\right)^{*} \alpha_k, \tag{5.18}$$

where α_k is the deviation of the coefficient α from its stable value α_k^{*}. On the basis of equation (5.16) we find

$$\alpha_k = \frac{1}{\kappa_T G_{gk}^{*}} G_{ok} - \frac{G_{ok}^{*}}{\kappa_T (i_{gk}^{*})^2} G_{gk}. \tag{5.19}$$

The values of the partial derivatives for the stable process may be calculated with regard to the relationship (5.17). We shall then have

$$\left(\frac{\partial i}{\partial p}\right)^{\circ} = \frac{F_{\kappa p}}{A}(1-b)(\alpha_{\kappa}^{-a}p_{\kappa}^{-b})^{\circ}, \tag{5.20}$$

$$\left(\frac{\partial i}{\partial \alpha}\right)^{\circ} = \frac{F_{\kappa p}}{A}(-a)(p_{\kappa}^{1-b}\alpha_{\kappa}^{-(1+a)})^{\circ}. \tag{5.21}$$

With regard to equation (5.19), relationship (5.18) may be put in the form

$$G_e = \frac{(1-b)F_{\kappa p}^{\circ}}{A(\alpha_{\kappa}^{a}p_{\kappa}^{b})^{\circ}}p_{\kappa} - \frac{aF_{\kappa p}p_{\kappa}^{\circ}}{z_T A G_{r\kappa}^{\circ}(\alpha_{\kappa}^{1+a}p_{\kappa}^{b})^{\circ}}G_{o\kappa}(t-\theta_0) + \tag{5.22}$$

$$- \frac{aF_{\kappa p}G_{o\kappa}^{\circ}p_{\kappa}^{\circ}}{z_T A G_{r\kappa}^{\circ 2}(\alpha_{\kappa}^{1+a}p_{\kappa}^{b})^{\circ}}G_{r\kappa}(t-\theta_0).$$

We find the time derivative from the volumetric density $d\gamma_k/dt$ from equation (5.2). Replacing the value RT in this equation by its value from equation (5.14) and bearing equation (5.15) in mind, we obtain

$$p = \gamma A_k^2 A^2 \alpha^{2a} p^{2b}. \tag{5.23}$$

Hence we find $\frac{d\gamma_{\kappa}}{dt} = -\frac{2a}{A_k^2 A^2}[p_{\kappa}^{1-2b}\alpha_{\kappa}^{-(1+2a)}]^{\circ}\frac{d\alpha_{\kappa}}{dt} + \frac{1-2b}{A_k^2 A^2}[p_{\kappa}^{-2b}\alpha_{\kappa}^{-2a}]^{\circ}\frac{dp_{\kappa}}{dt}$.

Replacing the deviation of the coefficient α_k here by its expression from (5.19), we obtain

$$\frac{d\gamma_{\kappa}}{dt} = \frac{1-2b}{A_k^2 A^2(p_{\kappa}^{2b}\alpha_{\kappa}^{2a})^{\circ}}\frac{dp_{\kappa}}{dt} -$$

$$- \frac{2ap_{\kappa}^{\circ}}{z_T A_k^2 A^2 G_{o\kappa}^{\circ}(p_{\kappa}^{2b}\alpha_{\kappa}^{1+2a})^{\circ}}\frac{d}{dt}G_{o\kappa}(t-\theta_0) +$$

$$+ \frac{2ap_{\kappa}^{\circ}G_{o\kappa}^{\circ}}{z_T A_k^2 A^2 G_{r\kappa}^{\circ 2}(p_{\kappa}^{2b}\alpha_{\kappa}^{1+2a})^{\circ}}\frac{d}{dt}G_{\kappa}(t-\theta_0). \tag{5.24}$$

We now return to equation (5.1). We replace the values G_e and $d\gamma_k/dt$ in it by their expressions from (5.22) and (5.24). We obtain

$$\theta_к \frac{dp_к}{dt} + p_к = k_{ок} G_{ок}(t-\theta_0) + k_{гк} G_{гк}(t-\theta_0) + \\ + k'_{ок} \frac{d}{dt} G_{ок}(t-\theta_0) + k'_{гк} \frac{d}{dt} G_{гк}(t-\theta_0). \tag{5.25}$$

The coefficients of this equation with regard to the fact that

$$\frac{F_{кр} p^*_к}{\beta^*} = G^*_к, \qquad A(a^a p^b)^* = \varphi^*,$$

are determined in the following way:

$$\theta_к = \frac{(1-2b) V_к p^*_к}{(1-b) A^2_к \beta^{*2} G^*_к},$$

$$k_{ок} = \frac{p^*_к}{(1-b) G^*_к} + \frac{a p^*_к}{\varkappa_т (1-b) G^*_{ок}},$$

$$k_{гк} = \frac{p^*_к}{(1-b) G^*_к} - \frac{a p^*_к G^*_{ок}}{\varkappa_т (1-b) G^{*2}_{гк}}, \tag{5.26}$$

$$k'_{ок} = \frac{2a V_к p^{*2}_к}{\varkappa_т (1-b) A^2_к \beta^{*2} G^*_{ок} G^*_к},$$

$$k'_{гк} = -\frac{2a V_к p^{*2}_к G_{ок}}{\varkappa_т (1-b) A^2_к \beta^{*2} G^{*2}_{гк} G^*_к}.$$

Bearing in mind that

$$R^*_к T^*_к = \varphi^{*2} A^2_к,$$

we may write formula (5.7) for the time constant of the combustion chamber in the form

$$\theta_к = \frac{V_к p^*_к}{A^2_к \beta^{*2} G^*_к}. \tag{5.27}$$

Since the coefficient b is small, the value of the time constant θ_k in equation (5.6) and in (5.7) is practically the same. Variation in the coefficient of the ratio fuel component has some influence on the value of the coefficients k_{ox} and k_{fl} and leads to a change in the structure of the differential equation. In comparison with (5.6) in the right member of equation (5.25) there

are additional terms proprotional to the time derivative from the deviations of fuel component feed into the combustion chamber.

The differential equation (5.25) for determining the pressure deviation in the combustion chamber with regard to the variation in the coefficient of the fuel component ratio κ has constant coefficients, depending on the volume of the chamber and the parameters of the stable operating process. Equation (5.25) is more precise than equation (5.6). However, if the ratio of fuel components in the stable operating condition is optimal, then calculation of the influence of small deviations of the coefficient κ cannot make noticeable improvements in accuracy. In such cases the dyanmic properties of the combustion chamber with low oscillation frequencies can be determined by the simpler equation (5.6).

Assuming the deviation in the supply of fuel components to the combustion chamber to be derived according to harmonic law with the frequency ω and assuming, moreover, the pressure deviation in the chamber to be also harmonic, from equation (5.25) we obtain

$$p_к = K[p_к, G_{ок}]G_{ок} + K[p_к, G_{гк}]G_{гк}, \tag{5.28}$$

where

$$K[p_к, G_{ок}] = \frac{(k_{ок} + i\omega k'_{ок})e^{-i\omega\delta_0}}{1 + i\omega\theta_к},$$
$$K[p_к, G_{гк}] = \frac{(k_{гк} + i\omega k'_{гк})e^{-i\omega\delta_0}}{1 + i\omega\theta_к}. \tag{5.29}$$

Knowing the deviations of oxidizer supply G_{ox} and fuel supply G_{fl} into the chamber, and the oscillation frequency ω, from equation (5.28) it is possible to determine the pressure deviation in the combustion chamber.

A gas generator does not usually operate with an optimal ratio of fuel components. In the first place this pertains to gas generators of liquid propellant rocket engines with closed feed, in which complete gasification of one of the components takes place. Even a small deviation in the supply of one of the components into the gas generator, in particular the supply of the additive,

causes a significant change in the temperature of the products of gasification. Therefore, in analyzing the dynamic properties of a gas generator one cannot be limited to equation (5.6).

A specific pressure impulse in a gas generator (5.14) can also be approximated by relationship (5.15), but the values of the coefficients a and b for a gas generator must be determined with regard to the pressure and coefficient κ of the ratio of fuel components for a gas generator in stable operation. Considering, as before, the polytropic exponent to be constant, we conclude that the differential equation for determining the pressure deviation in the gas generator p_g will have the same structure as equation (5.25). Therefore,

$$p_g = K[p_g, G_{og}]G_{og} - K[p_g, G_{gg}]G_{gg}, \tag{5.30}$$

where G_{ox}, G_{gg} are the deviations of oxidizer supply and fuel supply into the gas generator.

The complex transmission ratios of equation (5.30) can be determined by the values of the parameters of the stable process in a gas generator according to formulas analogous to (5.29) and (5.26). We obtain

$$K[p_r, G_{og}] = \frac{(k_{or} + i\omega k'_{og})\, e^{-i\omega\theta_{og}}}{1 + i\omega\theta_g},$$
$$K[p_r, G_{gg}] = \frac{(k_{rr} + i\omega k'_{gg})\, e^{-i\omega\theta_{og}}}{1 + i\omega\theta_g}. \tag{5.31}$$

Here

$$\theta_r = \frac{(1 - 2b_g) V_g p_g^*}{(1 - b_r) A_k^{2\beta_g^{**}} G_g^*},$$
$$k_{og} = \frac{p_g^*}{(1 - b_g) G_g^*} + \frac{a_g p_g^*}{\varkappa_T (1 - b_g) G_{og}^*},$$
$$k_{gg} = \frac{p_r^*}{(1 - b_g) G_g^*} - \frac{a_r p_r^* G_{or}^*}{\varkappa_T (1 - b_g) G_{gg}^{**}}, \tag{5.32}$$

$$k_{og}=\frac{2a_gV_gp_g^{**}}{x_T(1-b_g)A_k^2\beta_g^{**}G_{og}^*G_1^*},$$

$$k_{gg}=-\frac{2a_gV_gp_g^{**}G_{og}}{x_T(1-b_g)A_k^2\beta_g^{**}G_{gg}^{**}G_r^*}.$$

In formulas (5.31) and (5.32) the index 'g' designates the coefficient for the gas generator.

A schematic diagram of an engine combustion chamber is shown in Fig. 5.11. A schematic diagram for a gas generator will be the same, but replacement of the index 'k' by the index 'g'.

With the exception of starting and stopping regimes, engine thrust at a given altitude of flight is proportional to the pressure in the combustion chamber [13], therefore deviation of the thrust force P will be proportional to the pressure deviation in the combustion chamber p_k, i.e.,

$$P = k_{th}p_k, \tag{5.33}$$

where k_{th} is the coefficient of proportionality between the engine thrust and pressure in the combustion chamber.

With a change in the pressure in the pressure in the combustion chamber there will be a change in the pressure on the nozzle section and, consequently, the base pressure. The axial force acting on the rocket body changes due to the change in base pressure. .Not touching upon the essence of this complex phenomenon, we assume that the deviation in axial force, caused by the deviation in bas pressure, may be expressed using the complex transmission ratio

$$P_{bt} = K[P_{bt}, p_k]p_k. \tag{5.34}$$

The force P is transmitted to the rocket body through the engine frame, the force P_{bt} through the stern section.

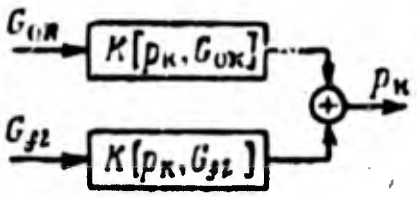

Figure 5.11

In engines with a closed feed system the expulsion of gas from the turbine through exhaust pipes creates a supplementary thrust. We shall consider the deviation in supplementary thrust of the exhaust pipes P_{sup} to be proportional to the deviation in gas pressure at the turbine outlet p_{2T}, i.e.,

$$P_{sup} = k_{TT} p_{2T}, \tag{5.35}$$

where the proportionality coefficient between the supplementary thrust and gas pressure deviation at the turbine outlet

$$k_{TT} = P^*_{sup}/p^*_{2T}; \tag{5.36}$$

P^*_{sup} and p^*_{2T} are the supplementary thrust and gas pressure leaving the turbine in stable operating condition.

4. Equations for the Turbine Pump Assembly

In order to derive equations it is useful to divide the turbine pump assembly into the following components: the flowthrough section of the turbine, the rotor, and the flowthrough sections of the pumps.

Let us consider a turbine pump assembly consisting of one turbine, a fuel pump and an oxidizer pump (see Figs. 5.2-5.5). The pressure at the pump outlet is determined according to the force characteristic of the centrifugal pump depending on the number of blade rotations, and the discharge of liquid passing through the pump in the case of a given pressure at the pump intake. In stable

operating conditions the force characteristic of the pump may be expressed by the following equation [12]:

$$p_{2p}^{*} - p_{1p}^{*} = a_p n^{*2} - b_p G_p^{*} n - c_p G_p^{*2}. \qquad (5.36)$$

where p_{2p}^{*}, p_{1p}^{*} are the pressure at the pump outlet and at the pump inlet; n^{*} is the number of blade rotations per minute; G_p^{*} is the discharge of the liquid through the pump; a_p, b_p, and c_p are the coefficients of the equation of the pump characteristics.

The equation for the force characteristic of the pump in deviation can be obtained on the basis of equation (5.36) with the addition of dynamic terms conditioned by the relative acceleration of liquid dw/dt in the entire volume of the pump and the acceleration of liquid transportation (du/dt)cos β in the volume of a blade, where w is the relative velocity, u is the peripheral (transportation) velocity and β is the angle between the directions of the relative and transportation velocities. We obtain

$$p_{2p} = p_{1p} + (2a_p n^{*} - b_p G_p^{*}) n - (b_p n^{*} + 2c_p G_p^{*}) G_p + T_n \frac{dn}{dt} - T_G \frac{dG_p}{dt} \qquad (5.37)$$

where n is the deviation of the angular velocity of the shaft of the turbine pump assembly; G_p is the deviation of the liquid discharge through the pump; T_n and T_G are coefficients characterizing the time constants of the flowthrough section of the pump. The last two terms in the right member of equation (5.37) express the pressure deviation at the pump outlet due to the transportation and relative accelerations of the liquid. The coefficients T_G and T_n can be determined according to the following formulas

$$T_G = \frac{1}{g} \int_{s_1}^{s_2} \frac{ds}{F(s)} \qquad (G_н = w\gamma F(s)),$$

$$T_n = \frac{\pi\gamma}{30g} \int_{s_1}^{s_2} r(s) \cos\beta\, ds \qquad \left(u(s) = \frac{\pi n}{30} r(s)\right).$$

Here s is a path along the flow; F(s) is the cross-sectional area of the flow; r(s) is the distance from the axis of rotation to an arbitrary point of the axis of the blade canal; (s_1, s_4) is a path along the flow from the beginning of the intake to the end of the outlet pipe; (s_2, s_3) is a path along the flow along the blade canal.

As a consequence of a change in the discharge of liquid through a pump there is a change in the torque, transmitted by the pump shaft, which for stable conditions may be written as [12]:

$$M_p^* = \frac{30 i_p^* (p_{2p}^* - p_{1p}^*)}{\pi n^* \gamma_p \eta_p^*}, \tag{5.38}$$

where η_p^* s the pump efficiency and γ_p is the specific gravity of the liquid.

Deviation in the pump efficiency may be expressed through the deviation in consumption G_p and the deviation of angular velocity n of the shaft

$$\eta_p = \left(\frac{\partial \eta_p}{\partial G_p}\right)^* G_p + \left(\frac{\partial \eta_p}{\partial n}\right)^* n. \tag{5.39}$$

On the basis of formula (5.38) with consideration of expressions (5.37) and (5.39) we find the deviation of the torque transmitted by the pump shaft:

$$M_p = k_{pG} G_p + k_{pn} n + k'_{pn} \frac{dn}{dt} - k'_{nG} \frac{dG_n}{dt}, \tag{5.40}$$

where

$$k_{pG} = M_n^* \left[\frac{1}{G_p^*} - \frac{1}{\eta_p^*}\left(\frac{\partial \eta_p}{\partial G_p}\right)^* - \frac{b_p n^* + 2c_n G_n^*}{p_{2n}^* - p_{1n}^*}\right],$$

$$k_{pn} = M_n^* \left[\frac{2a_p n^* - b_p G_p^*}{p_{2p}^* - p_{1p}^*} - \frac{1}{\eta_p^*}\left(\frac{\partial \eta_p}{\partial n}\right)^* - \frac{1}{n^*}\right], \tag{5.41}$$

$$k'_{pn} = M_p^* \frac{T_n}{p_{2p}^* - p_{1p}^*},$$

$$k'_{pG} = M_p^* \frac{T_G}{p_{2p}^* - p_{1p}^*}.$$

For an incompressible liquid and rigid fuel lines the deviation in liquid consumption through the pump is equal to the total of the deviation in the consumption of a component of the fuel, entering the combustion chamber and gas generator, i.e.,

$$G_p = G_k + G_g. \tag{5.42}$$

Let us determine the deviation in the torque of the turbine. We assume that there are no losses in the gas line between the gas generator and the turbine. The turbine torque is a function of the fuel consumption through the turbine, the angular velocity of shaft rotation, the efficiency of the gas (RT), and the ratio of gas pressures behind the turbine and in the gas generator. For stable operating conditions this function may be written in the form [12]

$$M_T^* = G_T^* \left[a_1(\nu_g) \beta_g - a_2 n - \frac{a_3(\nu_g) n^2}{\beta_g} - a_4(\nu_g) \frac{\beta_g^2}{n} \right]^*, \tag{5.43}$$

where

$$\nu_T^* = \frac{p_{2T}^*}{p_g^*}; \tag{5.44}$$

p^*_{2T} is the gas pressure behind the turbine; β^*_g is a specific pressure impulse in the gas generator; G^*_T is the gas consumption through the turbine; $a_1(\nu^*_g)$, $a_3(\nu^*_g)$, $a_4(\nu^*_g)$ are the coefficients depending on the value ν^*_g and the polytropic component which we shall assume to be constant; the coefficient a_2 = const.

We find the torque deviation

$$M_T = \left(\frac{\partial M_T}{\partial G_T}\right)^* G_T + \left(\frac{\partial M_T}{\partial n}\right)^* n + \left(\frac{\partial M_T}{\partial \beta_g}\right)^* \beta_g + \left(\frac{\partial M_T}{\partial \nu_g}\right)^* \nu_g \tag{5.45}$$

Here G_T is the deviation of gas consumption through the turbine; β_g and ν_g are the deviations from the stable values β^*_g and ν^*_g.

The values of the partial derivatives are found starting from the structure of equation (5.43):

$$\left(\frac{\partial M_T}{\partial G_T}\right)^{\circ} = \left[a_1(v_g)\beta_g - a_2 n - \frac{a_3(v_g)n^2}{\beta_g} - a_4(v_g)\frac{\beta_g^{\circ}}{n}\right]^{\circ},$$

$$\left(\frac{\partial M_T}{\partial n}\right)^{\circ} = -G_T\left[a_2 + \frac{2a_3(v_g)n}{\beta_g} - a_4(v_g)\frac{\beta_g^2}{n^2}\right]^{\circ},$$

$$\left(\frac{\partial M_T}{\partial \beta_g}\right)^{\circ} = G_T^{\circ}\left[a_1(v_g) + \frac{a_3(v_g)n^2}{\beta_r^2} - 2a_4(v_g)\frac{\beta_g}{n}\right]^{\circ}, \qquad (5.46)$$

$$\left(\frac{\partial M_T}{\partial v_g}\right)^{\circ} = G_T^{\circ}\left[\beta_g\left(\frac{\partial a_1}{\partial v_g}\right) - \frac{n^2}{\beta_g}\left(\frac{\partial a_3}{\partial v_g}\right) - \frac{\beta_r^2}{n}\left(\frac{\partial a_4}{\partial v_g}\right)\right]^{\circ}.$$

We shall express the deviations of ν_g and β_g by p_{2T} and p_g—the deviations of gas pressure behind the turbine and in the gas generator, and by α_g—the deviation of the coefficient α, characterizing the ratio of fuel components in the gas generator. Expressing the specific pressure impulse in the gas generator in the form (5.15),

$$\beta_g = A\alpha_g^a p_g^b,$$

we obtain

$$\nu_g = \frac{1}{p_g^{\circ}} p_{2T} - \frac{\nu_r^{\circ}}{p_g^{\circ}} p_g, \qquad (5.47)$$

$$\beta_g = a_g A(\alpha_g^{a_g-1} p_g^{b_g})^{\circ}\alpha_g + b_g A(\alpha_g^{a_r} p_g^{b_r-1})^{\circ} p_g.$$

The deviation of gas discharge through the turbine G_T and the deviation of the coefficient α may be determined from relationships analogous to (5.18) and (5.19).

$$G_T = \left(\frac{\partial G}{\partial \nu_g}\right)^{\circ}\nu_g + \left(\frac{\partial G}{\partial \alpha}\right)^{\circ}\alpha_g; \quad \alpha_g = \frac{1}{\varkappa_T G_{gg}^{\circ}} G_{0g} - \frac{G_{0r}^{\circ}}{\varkappa_T G_{gg}^{\circ 2}} G_{gg}. \qquad (5.48)$$

Finally, the turbine torque is

$$M_T = k_{T0r} G_{0g}(t-\tau_{0g}) + k_{Trr} G_{gg}(t-\tau_{0g}) + k_{T\,pg} p_g + k_{T\,p_{2T}} p_{2T} + k_{T\,n} n, \qquad (5.49)$$

where

$$k_{T0r}=\left(\frac{\partial M_T}{\partial G_T}\right)^{\circ}\left(\frac{\partial G_T}{\partial \alpha}\right)^{\circ}\frac{1}{\varkappa_T i^{\circ}_{gg}}+\left(\frac{\partial M_T}{\partial \beta_g}\right)^{\circ}\frac{a_g A\left(\alpha_g^{a_g-1}p_g^{b_g}\right)^{\circ}}{\varkappa_T i^{\circ}_{gg}},$$

$$k_{Trr}=\left(\frac{\partial M_T}{\partial G_T}\right)^{\circ}\left(\frac{\partial G_T}{\partial \alpha}\right)^{\circ}\frac{G^{\circ}_{0r}}{\varkappa_T G^{\circ\circ}_{rr}}-\left(\frac{\partial M_T}{\partial \beta_r}\right)^{\circ}\frac{a_r A\left(\alpha_r^{a_r-1}p_r^{b_r}\right)^{\circ}i^{\circ}_{0r}}{\varkappa_T G^{\circ\circ}_{rr}},$$

$$k_{T\,p_g}=\left(\frac{\partial M_T}{\partial \beta_g}\right)^{\circ}b_g A\left(\alpha_g^{a_g}p_g^{b_g-1}\right)^{\circ}-\frac{\nu^{\circ}_g}{p^{\circ}_g}\left[\left(\frac{\partial M_T}{\partial \nu_g}\right)^{\circ}+\left(\frac{\partial M_T}{\partial G_T}\right)^{\circ}\left(\frac{\partial G_T}{\partial \nu_g}\right)^{\circ}\right], \tag{5.50}$$

$$k_{T\,p_{2T}}=\frac{1}{p^{\circ}_g}\left[\left(\frac{\partial M_T}{\partial \nu_g}\right)^{\circ}+\left(\frac{\partial M_T}{\partial G_T}\right)^{\circ}\left(\frac{\partial G_T}{\partial \nu_g}\right)^{\circ}\right],$$

$$k_{T\,n}=\left(\frac{\partial M_T}{\partial n}\right)^{\circ}.$$

If the expulsion of gas from the turbine takes place through exhaust pipes, then the turbine usually operates on a super-critical pressure drop. In these conditions the ratio of pressure behind the turbine and in the gas generator is equal to the constant value ν^{*}_g. This same value is equal also to the ratio of pressure deviations

$$p_{2T}/p_g = \nu^{*}_g = \text{const}.$$

Therefore in the case of a super-critical pressure drop the value $p_{2T} = \nu^{*}_g p_g$, and equation (5.49) may be written in the form

$$M_T = k_{T0r}G_{0g}(t-\theta_{0r})+k_{Trr}G_{gg}(t-\theta_{0g})+ \\ +(k_{T\,p_g}+\nu^{*}_g k_{T\,p_{2T}})\,p_r+k_{T\,n}n, \tag{5.49a}$$

When gas from the turbine enters the combustion chamber of the engine, the turbine operates on a sub-critical pressure drop and the pressure deviation behind the turbine in this case will be the input coordinate for the turbine pump assembly.

The deviation of the angular velocity of the turbine pump assembly shaft is determined from the differential equation

$$\frac{\pi}{30} I \frac{dn}{dt} = M_T - M_{op} - M_{fp} \qquad (5.51)$$

Here I is the inertial moment of the turbine pump assembly shaft; M_{op} and M_{fp} are the deviations of the torques transmitted by the oxidizer pump and fuel pump shafts. These deviations are determined from equation (5.40). For example, for an oxidizer pump, with regard to equation (5.42), we shall have.

$$M_{op} = k_{op\,o}(G_{ok} + G_{og}) - k'_{op\,o}\frac{d}{dt}(G_{ok} + G_{og}) + k_{op\,n} n + k'_{op\,n}\frac{dn}{dt}. \qquad (5.52)$$

The coefficients of this equation are determined according to the formula (5.41) where it is necessary to add the letter 'o', besides n in the indexes to all the values. For a fuel pump, it is necessary to add the letter 'g' in the indexes in (5.40) and (5.41), and in equation (5.52) to replace the letter 'o' with the letter 'g'.

We now replace the values M_T, M_{op}, and M_{fp} in equation (5.51) by their expressions from (5.49) and (5.52). In this case we consider that the deviation of oxidizer consumption and fuel consumption through the pumps G_{og} and G_{gg} at the moment of time t corresponds to the deviation in oxidizer feed and fuel feed into the gas generator at the moment of time $(t-T_{ogM})$ and $(t-T_{fgM})$, where T_{ogM} and T_{fgM} are the relaxation times of the oxidizer main and the fuel main going to the gas generator. The differential equation for the deviation in angular velocity n of the turbine pump assembly shaft is now written in the form

$$T_T \frac{dn}{dt} + n = \frac{1}{B}\left[k_{T\,og} G_{og}(t - \theta_0 - T_{M\,og}) + k_{T\,gg} G_{gg}(t - \theta_0 - T_{M\,gg}) - \right.$$
$$- k_{op\,o}(G_{ok} + G_{or}) - k_{np\,o}(G_{gk} + G_{gg}) + k'_{op\,o}\frac{d}{dt}(G_{ok} + G_{og}) +$$
$$\left. + k'_{og\,o}\frac{d}{dt}(G_{gk} + G_{gg}) + k_{T\,p_r} p_r + k_{T\,p_{T2}} p_{T2}\right], \qquad (5.53)$$

where the time constant of the turbine is:

$$T_т = \frac{1}{B}\left(\frac{\pi}{30} I + k'_{вр\,n} + k'_{вд\,n}\right), \qquad (5.54)$$

$$B = k_{вр\,n} + k_{вд\,n} - b_{т\,n}.$$

Equations (5.37) for the oxidizer pump and the fuel pump and equation (5.53) determine the dynamic properties of the turbine pump assembly. For harmonic oscillations, the solution of these equations is given by the complex transmission ratios.

An equation for determining the pressure deviation at the oxidizer pump outlet has the form

$$p_{2ор} = K[p_{2ор}, p_{1ор}]\,p_{1ор} + K[p_{2ор}, n]\,n + K[p_{2ор}, G_{ок}]\,G_{ок} + K[p_{2ор}, G_{од}]\,G_{од} \qquad (5.55)$$

where

$$K[p_{2ор}, p_{1ор}] = 1,$$

$$K[p_{2ор}, n] = 2a_{ор}n^* - b_{ор}G^*_{ор} + i\omega T_{п\,о}, \qquad (5.56)$$

$$K[p_{2ор}, G_{ок}] = K[p_{2ор}, G_{од}] = -(b_{ор}n^* + 2c_{ор}G^*_{ор} + i\omega T_{0\,о}).$$

An equation for determining the pressure deviation at the outlet of the fuel pump p_{2fp} may be obtained from (5.55) and (5.56) with the substitution of the index 'o' by the index 'g'.

We write the formula for determining the deviation of the angular velocity n of the turbine pump assembly shaft (the equation for the turbine) in the form

$$n = K[n, G_{од}]\,G_{од} + K[n, G_{gg}]\,G_{gg} + K[n, G_{ок}]\,G_{ок} + K[n, G_{gк}]\,G_{gк} + K[n, p_g]\,p_g + K[n, p_{2т}]\,p_{2т}. \qquad (5.57)$$

Here

$$K[n, G_{од}] = \frac{k_{тод}e^{-i\omega'(\theta_0 + T_{м\,од})} - k_{вр\,0} + i\omega k'_{вр\,0}}{B(1 + i\omega T_т)},$$

$$K[n, G_{gg}] = \frac{k_{тgg}e^{-i\omega(\theta_0 + T_{м\,gg})} - k_{вg\,0} + i\omega k'_{вg\,0}}{B(1 + i\omega T_т)},$$

$$K[n, G_{ок}] = \frac{i\omega k'_{вр\,0} - k_{вр\,0}}{B(1 + i\omega T_т)}, \qquad (5.58)$$

$$K[n,\ G_{гк}]=\frac{i\omega k'_{нг\,G}-k_{нг\,G}}{B(1+i\omega T_г)},$$

$$K[n,\ p_г]=\frac{k_г p_г}{B(1+i\omega T_г)},$$

$$K[n,\ p_2]=\frac{k_г p_{2г}}{B(1+i\omega T_г)}.$$

A structural diagram of a turbine pump assembly is given in Fig. 5.12. The output coordinates are the pressure deviation at the outlet from the oxidizer pump p_{2op} and the fuel pump p_{2fp}, the input coordinates are the pressure deviation in front of the pump p_{1op} and p_{1fp}, the consumption deviation through the oxidizer pump and the fuel pump G_{ox} and G_{f1} and G_{og} and G_{gg}, the pressure deviations in the gas generator p_g and behind the turbine p_{2T}.

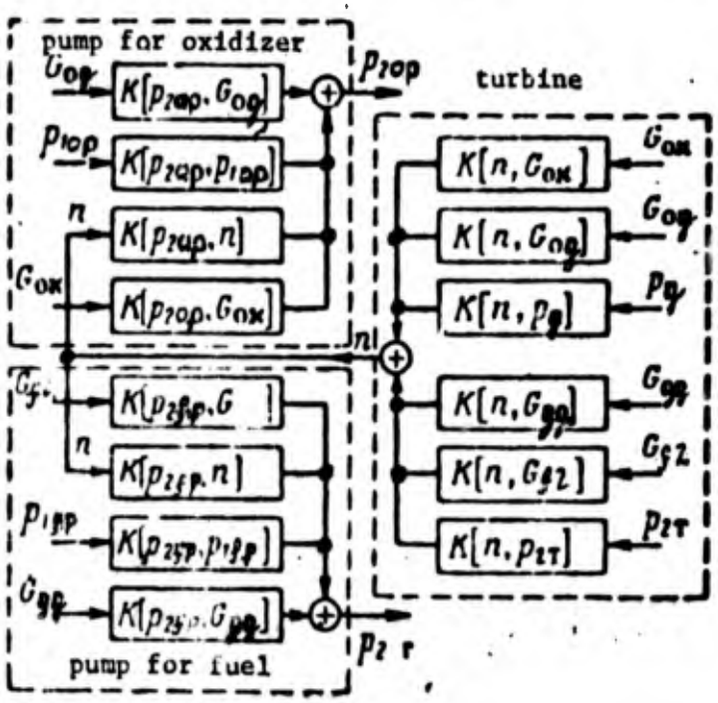

Figure 5.12

As was shown, the pressure deviation in front of the pump p_{1op} and p_{1fp} are determined from the analysis of the dynamics of the delivery mains, and the pressure deviation in the gas generator p_g, from the analysis of the dynamics of the gas generator. Deviation in discharge through the pump depends on the dynamics of the force mains of the combustion chamber and the gas generator.

5. Equations for the Force Mains and Regulators

The force mains between the pump and the combustion chamber of an engine (the cooling duct of the engine also enters the force main of one of the components), and also the force main going to the gas generator, are short and rigid. Therefore, in first approximation we shall ignore the compressibility of the liquid and the elasticity of the walls of the pipeline, and the flow parameters are lumped. In order to derive an equation for the motion of liquid along the mains, we shall make use of an energy balance equation which may be put in the following form for a main of constant cross-section F:

$$(pFv - p_2F_\phi v_2)\,dt = \left(\frac{G}{2g}v_2^2 - \frac{G}{2g}v^2\right)dt + \\ + \frac{\gamma}{g}lF\,dv + \xi_M\frac{G}{2g}v^2dt, \tag{5.59}$$

where p, v are the pressure and velocity of the liquid at the inlet to the main; p_2 and v_2 are the pressure and velocity of the liquid at the outlet from the main; F_ϕ is the area of the nozzle; d, l are the diameter and length of the main; G is the liquid consumption; ξ_M is the resistance coefficient of the main; γ is the specific gravity of the liquid.

The left member of equation (5.59) shows the variation in pressure energy, and the right member shows the variation in kinetic energy, energy expendable for accelerating the mass of liquid in the main, and energy expendable for overcoming the flow motion resistance.

In order to simplify equation (5.59) we use the continuity equation:

$$\gamma Fv = \gamma F_\phi v_2 = G. \tag{5.60}$$

Substituting the liquid consumption according to (5.60) into equation (5.59), instead of the values of v and v_2, we obtain

$$p - p_2 = \frac{1}{2g\gamma F_\phi^2}\left[1 + \xi_M\left(\frac{F_\phi}{F}\right)^2 - \left(\frac{F_\phi}{F}\right)^2\right]G^2 + \frac{1}{g}\frac{l}{F}\frac{dG}{dt}.$$

We derive a linearization of this equation and write a differential equation for the liquid consumption G in deviations in the form

$$T_{\text{м}}\frac{dG}{dt}+G=k_{\text{м}}(p-p_2), \tag{5.61}$$

where the time constant T_M and the amplification factor of the main k_M are equal to:

$$T_{\text{м}}=\frac{l}{gF}k_{\text{м}},$$
$$k_{\text{м}}=\frac{2g\gamma F_{\phi}^2}{2G^{**}\left[1+\xi_{\text{м}}\left(\frac{F_{\phi}}{F}\right)^2-\left(\frac{F_{\phi}}{F}\right)^2\right]}. \tag{5.62}$$

Equation (5.61) is identical for all mains, and only the values of the coefficients of the equation differ. For example, for the combustion chamber oxidizer main:

$$T_{\text{м к}}\frac{dG_{\text{ок}}}{dt}+G_{\text{ок}}=k_{\text{мок}}(p_{2\text{кр}}-p_{\text{к}}). \tag{5.63}$$

In this case it is necessary to substitute the respective parameters of the combustion chamber oxidizer main into the formulas (5.62). Then we obtain

$$T_{\text{мок}}=\frac{l_{\text{ок}}}{gF_{\text{ок}}}k_{\text{мок}},$$
$$k_{\text{мок}}=\frac{2g\gamma_{\text{ок}}F_{\phi\text{ок}}^2}{2G_{\text{ок}}^{**}\left[1+\xi_{\text{мок}}\left(\frac{F_{\phi\text{ок}}}{F_{\text{ок}}}\right)^2-\left(\frac{F_{\phi\text{ок}}}{F_{\text{ок}}}\right)^2\right]}. \tag{5.64}$$

For the gas generator oxidizer main (assuming a gas generator operating on the the basic components of the fuel),

$$T_{\text{мог}}\frac{dG_{\text{ог}}}{dt}+G_{\text{ог}}=k_{\text{мог}}(p_{2\text{кр}}-p_{\text{г}}), \tag{5.65}$$

where

$$T_{\text{мог}}=\frac{l_{\text{ог}}}{gF_{\text{ог}}}k_{\text{мог}},$$
$$k_{\text{мог}}=\frac{2g\gamma_{\text{ог}}F_{\phi\text{ог}}^2}{2G_{\text{ог}}^{**}\left[1+\xi_{\text{мог}}\left(\frac{F_{\phi\text{ог}}}{F_{\text{ог}}}\right)^2-\left(\frac{F_{\phi\text{ог}}}{F_{\text{ог}}}\right)^2\right]}. \tag{5.66}$$

The relationship between the deviation of oxidizer feed into the combustion chamber G_{ox} and the pressure deviations p_{2op} and p_k in the case of harmonic oscillations, on the basis of (5.63) is put in the form

$$G_{ox} = K[G_{ox},\ p_{2op}]\,p_{2op} + K[G_{ox},\ p_k]\,p_k, \tag{5.67}$$

where

$$K[G_{ox},\ p_{2op}] = \frac{k_{mox}}{1 + i\omega T_{mox}},$$
$$K[G_{ox},\ p_k] = -\frac{k_{mox}}{1 + i\omega T_{mox}}. \tag{5.68}$$

For the gas generator oxidizer main we obtain

$$G_{or} = K[G_{og},\ p_{2op}]\,p_{2op} + K[G_{og},\ p_g]\,p_g, \tag{5.69}$$

where

$$K[G_{og},\ p_{2op}] = \frac{k_{mog}}{1 + i\omega T_{mog}},$$
$$K[G_{og},\ p_g] = -\frac{k_{mor}}{1 + i\omega T_{mog}}. \tag{5.70}$$

Let us now examine flowcharts for several liquid propellant rocket engine regulators [12, 13]. The basic regulators of a liquid propellant rocket engine are the pressure regulator in the combustion chamber and the fuel component ratio regulator.

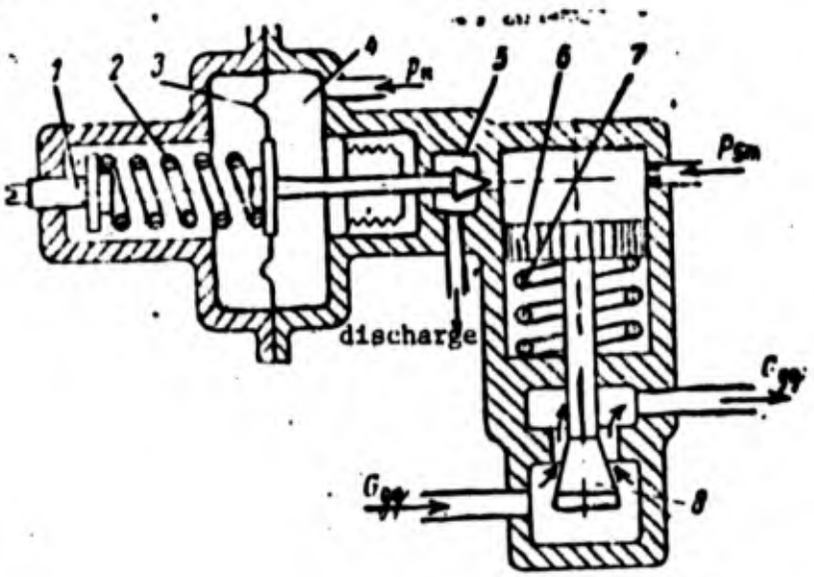

Figure 5.13

One of the possible designs for a pressure regulator in a combustion chamber with a hydraulic static servomotor is shown in Fig. 5.13. A liquid under the pressure p_c is supplied to feed the servomotor. Here 1 is the adjustment screw of the regulator, 2 is the sensing element spring, 3 is the sensing element membrane, 4 is the gas supply chamber from the combustion chamber, 5 is the control element of the servomotor, 6 is the servomotor piston, 7 is the servomotor spring, and 8 is the regulator control element.

As is apparent, an increase in pressure in the combustion chamber displaces the servomotor control element, which causes an increase in the cross-sectional area of the discharge opening, the pressure above the servomotor piston decreases and the consumption of one of the fuel components (in the diagram, the fuel) decreases. If such a regulator is present on the liquid gas generator line, then the turbine power decreases, the consumption of fuel components through the pump will decrease, and the pressure in the combustion chamber will drop.

Displacement of the servomotor control element depends on the pressure in the combustion chamber, the signal of regulator adjustment h, and pressure p_c. We shall consider the regulator adjustment to be unchanged, and the force from the pressure p_c on the servomotor control element to be independent of a small displacement of the control element. Then a small displacement y of the control element from the stable position will depend only on the pressure deviation in the combustion chamber p_k. Ignoring inertial forces, we obtain

$$p = -k_y p_k, \tag{5.71}$$

where k_y is the amplification factor of the servomotor control element, according to the gas pressure.

A small change in the pressure above the servomotor piston is proportional to a small displacement of the control element. Ignoring the change in pressure on the control element, we obtain an equation for determining small displacements δ of this element, whereby we must assume a positive displacement δ so that the deviation of the controlled value (in the given case G_{gg}) in the case of discharge from the regulator will be negative. We will then have

$$m\frac{d^2\delta}{dt^2}+h_\delta\frac{d\delta}{dt}+c\delta=-k_c'y, \tag{5.72}$$

where m is the mass of the piston and the control element; h_δ is the resistance coefficient; c is the stiffness factor of the spring; k_c' is the proportionality factor between the displacement of the control element and the deviation of the pressure force of the liquid on the piston.

With regard to relationship (5.71), we write equation (5.72) for determining small displacements δ in the form

$$T_{2p}^2\ddot{\delta}+T_{1p}\dot{\delta}+\delta=k_p p_k,$$

where

$$T_{2p}^2=\frac{m}{c};\quad T_{1p}=\frac{h_\delta}{c};\quad k_p=k_y k_c\quad\left(k_c=\frac{k_c'}{c}\right).$$

In the case of harmonic oscillations with the frequency ω small displacements δ can be determined by the complex transmission ratio

$$\delta=K[\delta,\ p_k]p_k, \tag{5.73}$$

where

$$K[\delta,\ p_k]=\frac{k_p}{1-T_{2p}^2\omega^2+i\omega T_{1p}}.$$

Usually T_{2p}^2 is a very small value and at low frequencies it is possible to assume $T_{2r}^2\approx 0$.

Deviation in the fuel supply to the gas generator G_{gg} is proportional to a small displacement of the control element

$$G_{rr}=-k_{p\delta}\delta\qquad(k_{p\delta}>0). \tag{5.74}$$

In Fig. 5.6 the output coordinate for the pressure regulator in the combustion chamber is the pressure deviation p_p. In this case

$$p_p = -k_p\delta + K[p_p,\ p_{2og}]\,p_{2og},$$

or

$$p_p = K[p_p,\ p_\kappa]\,p_\kappa + K[p_p,\ p_{2og}]\,p_{2og},$$

where

$$K[p_p,\ p_\kappa] = -k_p K[\delta,\ p_\kappa].$$

Figure 5.14 shows a possible design for a fuel component ratio regulator (κ) [13]. The regulator consists of a membrane sensory element and a static hydraulic servomotor. Here 1 is the membrane of the sensory element, 2 is the sensory element spring, 3 is the fuel supply chamber, 4 is the control element of the hydraulic servomotor, 5 is the servomotor piston, 6 is the servomotor spring, 7 is the control element, and 8 is the oxidizer supply chamber.

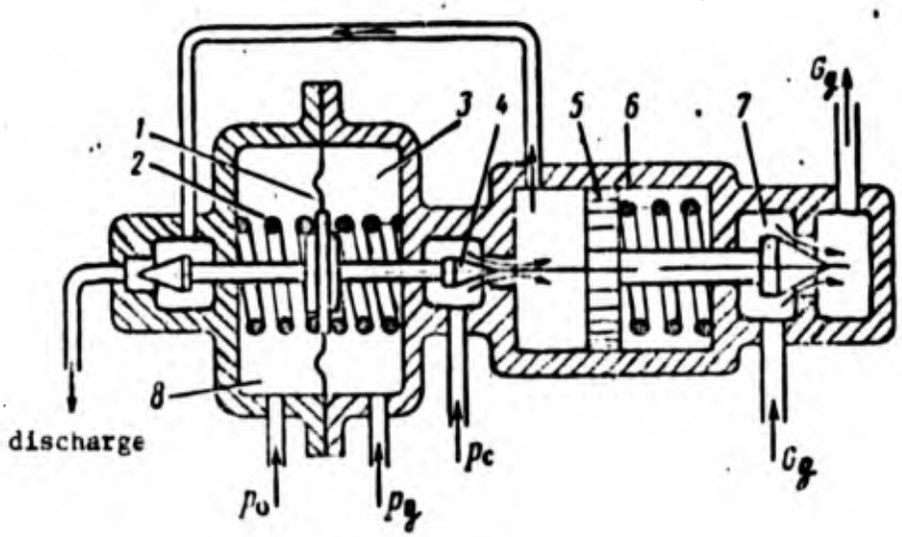

Figure 5.14

Regulator κ is attached to one of the fuel mains (in the given case, on the combustant main), going into the combustion chamber or the gas generator. On Fig. 5.7 regulator κ is shown to be included in the gas generator fuel main. The fuel and oxidizer pressures at the pump outlet are used as values, characterizing the consumption of fuel components. These pressures are equalized on the membrane. In the case of a deviation in the component ratio from the given ratio the membrane is deflected, which activates the hydraulic servomotor, and

the control element changes the fuel consumption in order to restore the given ratio of fuel components.

In order to derive an equation for small deflections δ of the control element, we use the same symbols as for equations (5.71)-(5.74). Small deflections y of the control element may be expressed by the relationship

$$y = -k_y(p_{2fp} - p_{2op}).$$

We write the equation for determining small deflections δ of the control element in the form

$$\delta = K[\delta,\ p_{2og}]\,p_{2og} + K[\delta,\ p_{2fg}]\,p_{2fg}, \tag{5.75}$$

where

$$K[\delta,\ p_{2fg}] = -K[\delta,\ p_{2op}] = \frac{k_{p\kappa}}{1 - T_{2p}^2\omega^2 + i\omega T_{1p}}, \tag{5.76}$$

$$\left(k_{p\kappa} = k_y k_c,\quad k_c = \frac{k_c'}{c}\right).$$

In Fig. 5.7 the output value of regulator κ is the pressure deviation $p_{p\kappa}$. On the basis of (5.72) and (5.75) we obtain

$$p_{p\kappa} = -k_{p\delta}\delta,$$
$$\delta = K[\delta,\ p_{2og}]\,p_{2og} + K[\delta,\ p_{2op}]\,p_{2op}.$$

In the scheme shown in Fig. 5.8, the regulator for the system controlling the level H of components in the tanks is included in the oxidizer force main of the combustion chamber. The output coordinate of the regulator is the pressure deviation p_{pH}, which may be determined from the formulas

$$p_{pH} = -K_{p\delta}\delta + K[p_{pH},\ p_{2op}]\,p_{2op},$$
$$\delta = K[\delta,\ H_0]\,H_0 + K[\delta,\ H_g]\,H_g,$$

where H_0 and H_g are the deviations of the oxidizer and fuel levels in the tanks.

6. Dynamic Scheme of Liquid Propellant Rocket Engines

The dynamic properties of the basic units of all liquid propellant rocket engines are expressed by identical linearized differential equations, the coefficients of which depend on the sizes of the unit and the parameters of stable operating conditions. The structure of the dynamic scheme of an engine depends on the method of feeding fuel components into the combustion chamber and on the engine control system. Let us now look at a dynamic scheme for a liquid propellant rocket engine with a turbine pump feed of fuel components.

We shall consider an engine, a schematic diagram of which is shown in Fig. 5.2. The gas generator operates on the basic components, and a regulator of the coefficients of the fuel component ratio is located on the fuel line of the gas generator; the control scheme is shown in Fig. 5.7. We cite the linearized differential equations for the individual units of the engine, obtained in the preceeding sections.

The equation for the combustion chamber

$$\theta_к \frac{dp_к}{dt} + p_к = k_{ок} G_{ок}(t-\theta_0) + k_{гк} G_{гк}(t-\theta_0).$$

The equations for the oxidizer and fuel mains of the combustion chamber

$$T_{мок} \frac{dG_{ок}}{dt} + G_{ок} = k_{мок}(p_{2ор} - p_к),$$

$$T_{мгк} \frac{dG_{гк}}{dt} + G_{гк} = k_{мгк}(p_{2ог} - p_к).$$

The equation for the gas generator.

$$\theta_г \frac{dp_г}{dt} + p_г = k_{ог} G_{ог}(t-\theta_0) + k_{гг} G_{гг}(t-\theta_0) +$$

$$+ k'_{ог} \frac{d}{dt} G_{ог}(t-\theta_0) + k'_{гг} \frac{d}{dt} G_{гг}(t-\theta_0).$$

The equations for the oxidizer and fuel main of the gas generator

$$T_{мог} \frac{dG_{ог}}{dt} + G_{ог} = k_{мог}(p_{2ор} - p_г),$$

$$T_{мгг} \frac{dG_{гг}}{dt} + G_{гг} = k_{мгг}(p_{рк} - p_г).$$

The equation for the regulator of the coefficient κ of the ratio of fuel components of the gas generator

$$T_{2р}^2 \frac{d^2 p_{рк}}{dt^2} + T_{1р} \frac{dp_{рк}}{dt} + p_{рк} = -k_{рк} k_{рк} (p_{2кг} - p_{2ар}).$$

The equations for the oxidizer and fuel pumps

$$p_{2ор} = p_{1ор} + (2a_{ор} n^* - b_{ор} G_{ор}^*) n + T_{nо} \frac{dn}{dt} -$$

$$-(b_{ор} n^* + 2c_{ор} G_{ор}^*)(G_{ок} + G_{ор}) - T_{Gо} \frac{d}{dt}(G_{ок} + G_{ор}),$$

$$p_{2ог} = p_{1ог} + (2a_{ог} n^* - b_{ог} G_{ог}^*) n + T_{nг} \frac{dn}{dt} -$$

$$-(b_{ог} n^* + 2c_{ог} G_{ог}^*)(G_{гк} + G_{гг}) - T_{Gг} \frac{d}{dt}(G_{гк} + G_{гг}).$$

The equation for the turbine (turbine pump assembly rotor)

$$T_т \frac{dn}{dt} + n = \frac{1}{B}[k_{тог} G_{ог}(t - \theta_0 - T_{мог}) + k_{тгг} G_{гг}(t - \theta_0 - T_{мгг}) -$$

$$- k_{ор\,G}(G_{ок} + G_{ор}) - k_{ог\,G}(G_{гк} + G_{гг}) +$$

$$+ k'_{ор\,G} \frac{d}{dt}(G_{ок} + G_{ор}) + k'_{ог\,G} \frac{d}{dt}(G_{гк} + G_{гг}) + k_{тр_г} p_г].$$

Figure 5.15 gives a structural diagram of the engine under consideration, a structural diagram of the turbine pump assembly is shown in Fig. 5.12. We assume that the turbine operates on a super-critical pressure drop, therefore the complex transmission ratio $K[n, p_{2T}] = 0$. The following are indicated in Fig. 5.15: 1- combustion chamber, 2,3- oxidizer and fuel mains of the combustion chamber, 4- gas generator, 5,6- oxidizer and fuel mains of the gas generator, 7- regulator of the coefficient κ of the fuel component ratio of the gas generator.

A large number of dynamic units, interconnected with numerous cross circuits, is characteristic for liquid propellant rocket engines. This may be seen in Fig. 5.15. The structure of the complex transmission ratios in Fig. 5.15 and Fig. 5.12 show the output and input coordinates for each dynamic unit of the engine.

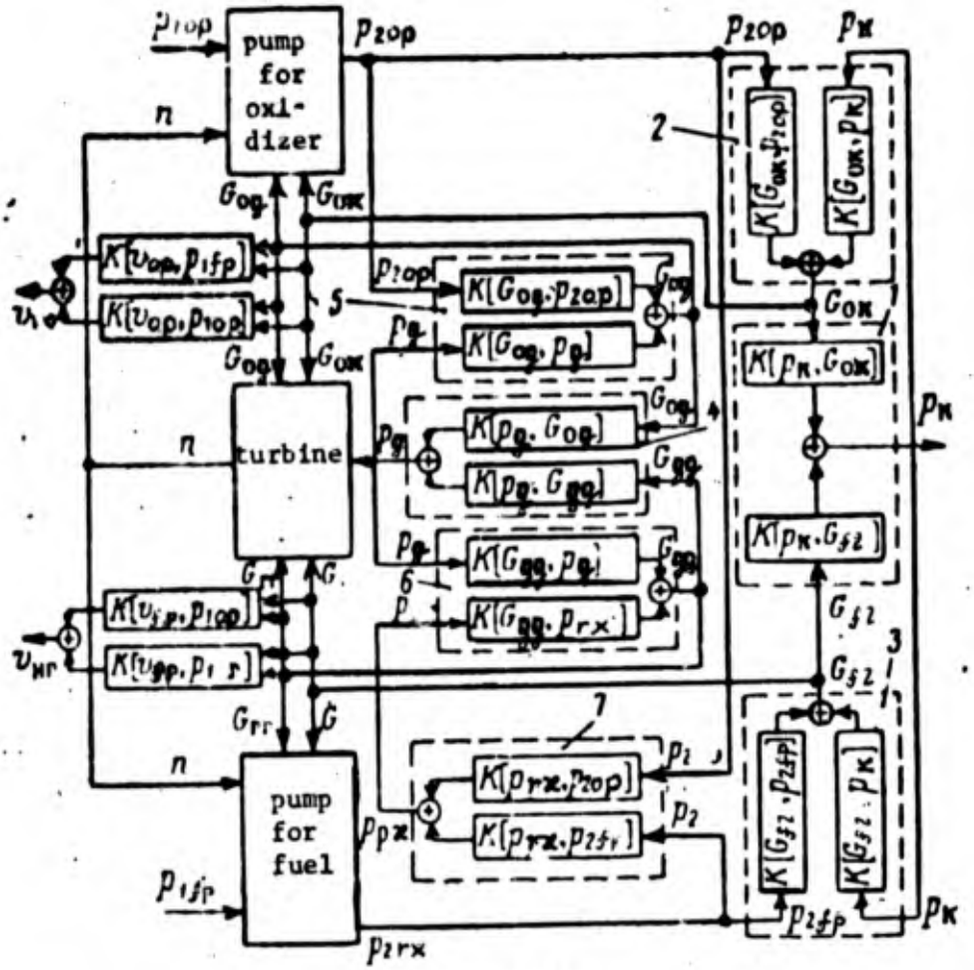

Figure 5.15

Deviation of the supply of oxidizer G_{ox} and fuel G_{fl} into the combustion chamber depends on the input coordinates—the pressure deviation at the outlet from the pumps p_{2op}; p_{2fl}, and pressure deviations in the combustion chamber p_k. Deviation of the supply of oxidizer G_{og} and fuel G_{gg} into the gas generator depends on the pressure deviation at the outlet from the oxidizer pump p_{2op}, pressure deviation at the outlet from the regulator p_{pk}, and pressure deviation in the gas generator p_g. Pressure deviation at the oxidizer pump outlet p_{2op} depends on the total deviation of oxidizer supply ($G_{ox} + G_{og}$), pressure deviation at the fuel pump outlet p_{2fl} depends on the total deviation in fuel supply ($G_{fl} + G_{gg}$), and the deviation of the rotational velocity n of the turbine pump assembly shaft depends on these same deviations in the supply of fuel components.

The input coordinates for the engine are p_{lop} and p_{lfl}—the pressure deviations at the inlet to the oxidizer and fuel pumps. The pressure deviation in the combustion chamber p_k is the output coordinate of the engine as an energy source.

The engine is, moreover, the loading unit for the delivery fuel main. The output coordinates of the engine as a loading unit will be v_{op} and v_{fl}, the velocity deviations of the fuel component at the inlet to the oxidizer and fuel pumps. These deviations are proportional to the deviations in oxidizer supply ($G_{ox} + G_{cg}$) and fuel supply ($G_{fl} + G_{gg}$). The velocity deviation v_{op} is conditioned not only by the pressure deviation p_{lop}, but it is also conditioned by the pressure deviation p_{lfl} through the combustion chamber and gas generator. The velocity deviation v_{fl} depends on the pressure deviation p_{lfl} and p_{lop}. The interconnection of the engine with the oxidizer and fuel delivery mains is shown in Fig. 5.16.

The liquid propellant rocket engine, a schematic of which is given in Fig. 5.5, has a closed feed system of fuel components. The entire fuel input is gasified in the gas generator and passes through the turbine ($G_{g\Sigma} = G_{gg} = G_{fl} = G_g$). The engine has three regulators: the pressure regulator on the fuel line, going into the gas generator, and the fuel component ratio regulator on the oxidizer line, going into the gas generator, and the fuel component ratio regulator on the oxidizer line, going into the combustion chamber. Fig. 5.17 gives a structural diagram of an engine (for a structural diagram of a turbine pump assembly see Fig. 5.12).

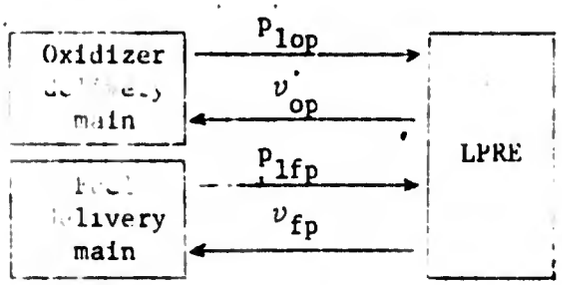

Figure 5.16

On Fig. 5.17: 1- combustion chamber, 2,3- oxidizer and fuel mains of the combustion chamber, 4- gas generator, 5,6- oxidizer and fuel mains of the gas generator, 7,8- fuel component ratio regulators of the gas generator and combustion chamber, 9- pressure regulator in the combustion chamber. The output coordinates of the engine as a loading unit for the delivery mains ν_{op} and ν_{fl} are not shown in Fig. 5.17.

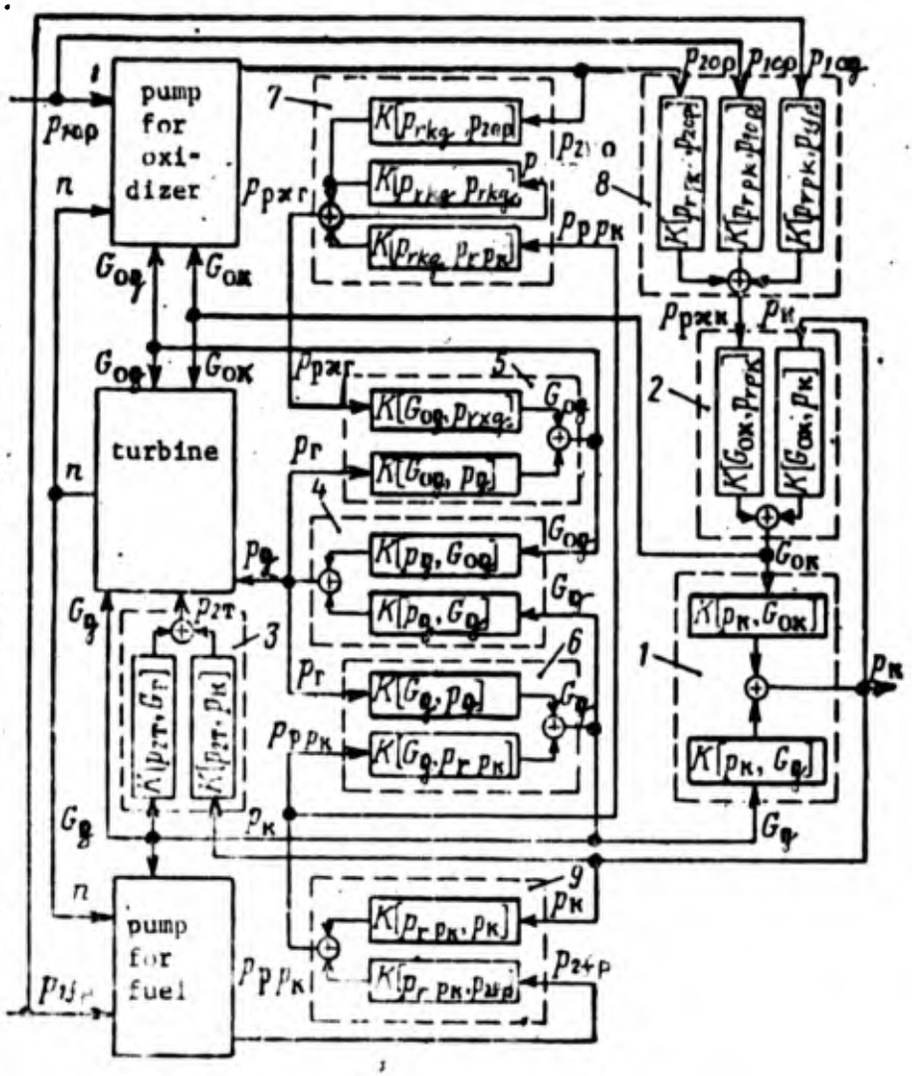

Figure 5.17

Linearized differential equations of individual units of the engine are structurally little different from equations for the corresponding units shown in Fig. 5.15. The basic difference is in the values of the coefficients and the input coordinates. The equations for the diagram in Fig. 5.17 may be put in the following form.

Equation for the combustion chamber

$$\theta_к \frac{dp_к}{dt} + p_к = k_{ок} G_{ок}(t-\theta_0) + k_{гк} G_{гк}(t-\theta_0).$$

Equation for the oxidizer main of the combustion chamber

$$T_{мок} \frac{dG_{ок}}{dt} + G_{ок} = k_{мок}(p_{гк} - p_к).$$

We shall consider that the gas pressure deviation in the main between the turbine and the combustion chamber is equal to the gas pressure deviation after the turbine, i.e., p_{2T}. Assuming the efficiency of the gas $(RT)^*_м$ to be constant, we obtain an equation for the accumulation of gas in this main

$$\frac{V_м}{(RT)^*_м} \frac{dp_{2т}}{dt} = G_г - G_{гк},$$

where G_g and G_{fl} are the weight deviation of gas going into the main and from the main into the combustion chamber.

The deviation of the gas injection pressure drop is

$$p_{2т} - p_к = \xi_ф \frac{G^*_{гк}}{\gamma g F^2_ф} G_{гк}.$$

The equation for the gas generator is

$$\theta_г \frac{dp_г}{dt} + p_г = k_{ог} G_{ог}(t-\theta_0) + k_{гг} G_г(t-\theta_0) +$$
$$+ k'_{ог} \frac{d}{dt} G_{ог}(t-\theta_0) + k'_{гг} \frac{d}{dt} G_г(t-\theta_0).$$

The equations for the oxidizer and fuel mains of the gas generator:

$$T_{мог} \frac{dG_{ог}}{dt} + G_{ог} = k_{мог}(p_{рег} - p_г),$$

$$T_{мгг} \frac{dG_г}{dt} + G_г = k_{мгг}(p_р p_к - p_г).$$

The equations for the oxidizer and fuel pumps:

$$p_{2но} = p_{1но} + (2a_{ор} n^* - b_{ор} G^*_{ор}) n + T_{но} \frac{dn}{dt} -$$

$$- (b_{ор} n^* + 2c_{ор} G^*_{ор})(G_{ок} + G_{ог}) - T_{Gо} \frac{d}{dt}(G_{ок} + G_{ог}),$$

$$p_{2нг} = p_{1нг} + (2a_{нг}n^* - b_{нг}G_г^*)\,n + T_{пг}\frac{dn}{dt} -$$

$$-(b_{нг}n^* + 2c_{нг}G_г^*)\,G_г - T_{Gг}\frac{dG_г}{dt},$$

The equation for the turbine (turbine pump assembly rotor):

$$T_т\frac{dn}{dt} + n = \frac{1}{B}[k_{тоg}G_{оg}(t - \theta_г - T_{моg}) + k_{тgg}G_g(t - \theta_0 - T_{мgg}) -$$

$$- k_{ор}\sigma(G_{ок} + G_{оg}) - k_{огG}G_г + k'_{ор}\sigma\frac{d}{dt}(G_{ок} + G_{оg}) +$$

$$+ k_{огG}\sigma\frac{dG_г}{dt} + k_{тр_g}p_g + k_{тр_{т2}}p_{т2}.$$

In the combustion chamber fuel component ratio regulator the pressure deviations at the oxidizer pump intake p_{1op} and the fuel pump intak p_{1fl} are equalized and in the gas generator fuel component regulator the pressure deviations of the oxidizer p_{pkg} and fuel p_{ppk} at the outlet from the pressure regulator in the combustion chamber are equalized. The pressure regulator in the combustion chamber acts upon the fuel main in front of the gas generator. For harmonic oscillations the equations for the regulators may be put in the form

$$p_{рнк} = K[p_{рнк},\ p_{2ор}]\,p_{2ор} + K[p_{рнк},\ p_{1но}]\,p_{1но} + K[p_{рнк},\ p_{1нg}]\,p_{1нg},$$

$$p_{рнg} = K[p_{рнg},\ p_{2ор}]\,p_{2но} + K(p_{рнг},\ p_{р р к}]\,p_{р р к} +$$

$$+ K[p_{рнг},\ p_{рнг}]\,p_{1нг},$$

$$p_{р\ р_к} = K[p_{р\ р_к},\ p_{2нg}]\,p_{2нg} + K[p_{р\ р_к},\ p_к]\,p_к.$$

It is necessary to note that structural models of liquid propellant rocket engines with closed feed systems have a larger number of internal connections between the units in comparison with structural models of liquid propellant rocket engines with closed feed systems. In a liquid propellant rocket engine with a closed feed system the entire delivery of one of the components is performed by the turbine, therefore the turbine in such an engine has significantly greater power than a turbine in an engine with a closed feed system. Therefore

the time constant of a turbine pump assembly for an engine with a closed feed system is less than that for an engine with an open system. Since in an engine with a closed feed system the gas enters the combustion chamber after the turbine, then the volume of the gas generator and the gas pressure in it is significantly greater than in the gas generator of an engine with a closed feed system.

On the basis of the structural diagram (see Fig. 5.17) it is possible to obtain an equation for determining the pressure deviation in the combustion chamber (the engine thrust deviation), expressed by the complex transmission ratios of the engine:

$$p_к = K[p_к,\ p_{1но}]\,p_{1но} + K[p_к,\ p_{1нг}]\,p_{1нг}$$

and equations for determining the velocity deviation of the fuel components at the oxidizer and fuel pump intakes:

$$v_{вр} = K[v_{вр},\ p_{1вр}]\,p_{1вр} + K[v_{вр},\ p_{1вг}]\,p_{1вг},$$
$$v_{вг} = K[v_{вг},\ p_{1вг}]\,p_{1вг} + K[v_{вг},\ p_{1вр}]\,p_{1вр}.$$

Hodographs of the complex transmission ratios (amplitude-phase characteristics) may be obtained by calculation or experimentally. Figure 5.18 shows

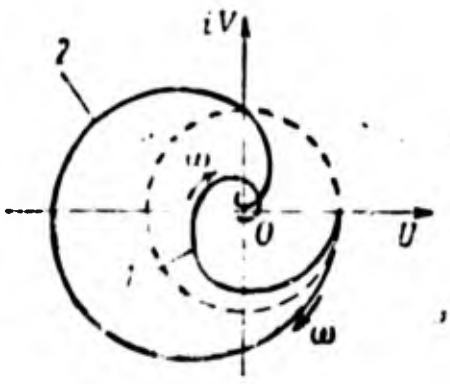

Figure 5.18

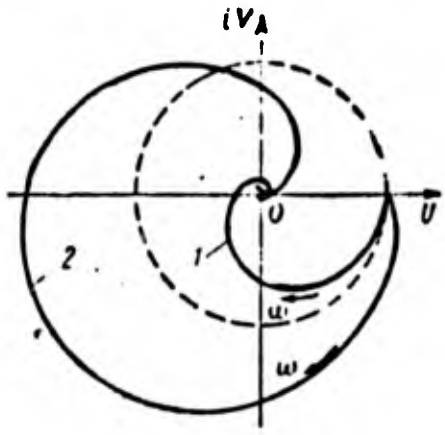

Figure 5.19

examples of hodographs of the complex transmission ratio $K[p_k, p_{lop}]$ of an engine with an open system (curve 1) and an engine with a closed feed system (curve 2). In the case of a deviation of the oxidizer flow rate through the

pump, the amplitude-phase characteristic of an engine with a closed feed system is similar to the amplitude-phase characteristic of an aperiodic unit with a lag. An engine with a closed feed system shows oscillatory properties and its amplitude-phase characteristic (curve 2) is similar to the amplitude-phase characteristic of an oscillatory component with a lag.

Figure 5.19 shows an example of hodographs of the complex transmission ratio $K[p_k, p_{lfp}]$ of an engine with an open feed system (curve 1) and an engine with a closed feed system (curve 2). The appearance of the hodographs is approximately the same, as in Fig. 5.18, however the amplification factors for an engine with a closed feed system are greater than for an engine with an open feed system.

An example of hodographs of the complex transmission ratio $K[v_{op}, p_{lop}]$, characterizing the dynamic properties of an engine as a loading unit, is shown in Fig. 5.20 (curve 1—for an engine with an open feed system, curve2—for an engine with a closed feed system). The appearance of these hodographs, as is

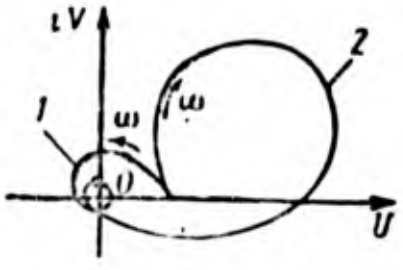

Figure 5.20

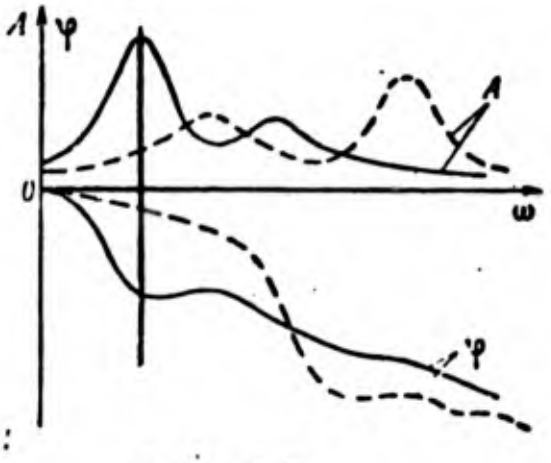

Figure 5.21

the case of hodographs of the complex transmission ratios $K[p_k, p_{lop}]$ and $K[p_k, p_{lfp}]$, may vary significantly depending on the variation in the dynamic properties of the combustion chamber, turbine pump assembly, gas generator, and regulators. For example, by selecting the dynamic properties of regulators it is possible to significantly change the amplitude-phase characteristics of an engine and thus to influence the stability of a closed system consisting of

a rocket, delivery mains, and engine. In Fig. 5.21 amplitude-frequency $A(\omega)$ and phase-frequency $\varphi(\omega)$ characteristics p_k/p_{1fp} are given for the same engine with different regulators.

7. Calculation of the Elasticity of the Walls of the Engine Head and the Combustion Chamber

The walls of the combustion chamber and the engine head possess a certain elasticity, the influence of which on the supply of fuel to the combustion chamber under certain conditions may be significant. The volume of the engine head and the cooling duct changes with a variation in pressure, therefore part of the fuel enters the combustion chamber with a certain lag.

The influence of the elasticity of the walls on the dynamics of the fuel supply to the chamber will be considered to be approximately in the range of the first frequency of natural oscillations, which may be determined, for e example, by Rayleigh's method.

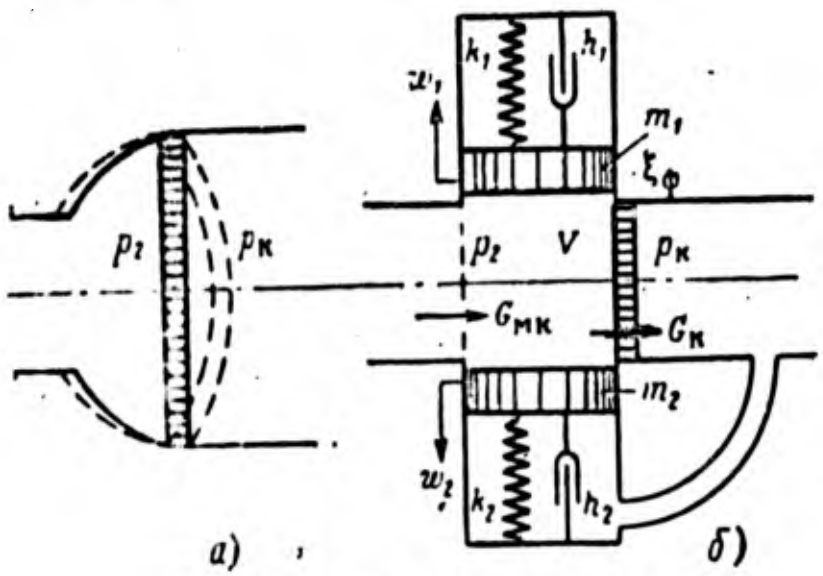

Figure 5.22

Let us now examine the engine head shown schematically in Fig. 5.22a. The external wall of the head is subjected only to the influence of pressure deviation of the liquid p_2, while the nozzle wall is acted upon from one side

by the pressure deviation of the liquid p_2, and from the other by the pressure deviation of gases in the combustion chamber p_k.

We shall represent the external and nozzle walls with two partial oscillatory systems:

1) we assume the nozzle wall to be absolutely rigid, and the external wall of the engine head in which the liquid is located will be considered to be elastic;

2) we assume the nozzle wall to be elastic, and the external wall of the head in this partial oscillatory system is assumed to be absolutely rigid.

As a result it is possible to represent the head by the dynamic model shown in Fig. 5.22b. Each partial oscillatory system consists of the piston mass m_1 and m_2, a weightless spring, and a damper.

We assume the areas of the pistons for both oscillatory systems to be equal to the area F_T of the pipe opening. The liquid, included in the small volume V, bounded by the pistons, the nozzle wall, and the outlet end of the pipe, will be considered to be incompressible. We select the rigidities k_1 and k_2 of the springs from the condition of the equality of the deviations in the volumes of the engine head and the dynamic model, caused by the static deviation of the pressure p_2 and p_k.

Let the frequencies of natural axisymmetrical oscillations of the first tone for each of the partial systems to be known, and we designate them, respectively, ω_I and ω_{II}. These same values must be equal to the frequencies of the natural oscillations of the dynamic model. An equation is provided for selecting the masses m_1 and m_2:

$$\omega_I = \sqrt{\frac{k_1}{m_1}}, \quad \omega_{II} = \sqrt{\frac{k_2}{m_2}}.$$

With the conditions assumed being fulfilled, the velocity deviation of the liquid in the pipe, appearing due to a change in the volume of the engine head under the influence of a deviation in the pressures p_2 and p_k, will be equal to the velocity deviation of liquid in a pipe, caused by piston displacements. We shall symbolize the piston displacements by w_1 and w_2 and write

equations for determining these displacements. We obtain

$$\ddot{w}_1 + 2\varepsilon_1\dot{w}_1 + \omega_1^2 w_1 = \frac{F_т}{m_1} p_2, \tag{5.77}$$

$$\ddot{w}_2 + 2\varepsilon_2\dot{w}_2 + \omega_{11}^2 w_2 = \frac{F_т}{m_2}(p_2 - p_к),$$

where ε_1 and ε_2 are the damping coefficients of the natural oscillations.

The relationship between the pressure deviation of the liquid p_2 and the pressure deviation of gases in the combustion chamber p_k may be put in the form

$$p_2 = p_к + \xi_ф \frac{G_к^*}{\gamma g F_ф^2} G_к, \tag{5.78}$$

where G_k^* is the supply of the fuel component into the chamber under stable operating conditions; G_k is the deviation of this value; $\xi_ф$ is the resistance coefficient of the nozzle; $F_ф$ is the area of the nozzle. The deviation in the discharge of the fuel component through the main between the pump and the engine chamber G_{MK} may be determined according to an equation analogous (5.61):

$$T_{мк} \frac{dG_{мк}}{dt} + G_{мк} = k_{мк}(p_{2к} - p_2), \tag{5.79}$$

where the time constant T_{MK} and the amplification coefficient k_{MK} of the main are equal to

$$T_{мк} = \frac{l}{gF_т} k_{мк},$$

$$k_{мк} = \frac{g\gamma F_т^2}{\lambda \frac{l}{d} G_{мк}^{*2}}.$$

Here λ is the resistance factor of the main.

We determine the deviation in the supply of a fuel component to the combustion chamber from a continuity equation, which we write in the form

$$G_к = G_{мк} + G_{w_1} + G_{w_2}, \tag{5.80}$$

where

$$G_{w_1} = -\gamma F_т \dot{w}_1, \quad G_{w_2} = -\gamma F_т \dot{w}_2. \tag{5.81}$$

From equations (5.77)-(5.81) it is possible to determine the deviation in the supply of a fuel component to the chamber G_k depending on the pressure deviation at the pump outlet p_{2p} and the pressure deviation of gases in the chamber p_k. We give the deviation of the discharges of the fuel component on the basis of (5.77) and (5.79) for harmonic oscillations in the form

$$\begin{aligned} G_{w_1} &= K[G_{w_1}, p_2]\, p_2, \\ G_{w_2} &= K[G_{w_2}, p_2]\, p_2 + K[G_{w_2}, p_к]\, p_к, \\ G_{мк} &= K[G_{мк}, p_{2н}]\, p_{2н} + K[G_{мк}, p_2]\, p_2, \end{aligned} \tag{5.82}$$

where

$$K[G_{w_1}, p_2] = -\frac{i\omega\gamma F_т^2}{m_1\left(\omega_1^2 - \omega^2 + i\omega 2\tau_1\right)},$$

$$K[G_{w_2}, p_2] = -K[G_{w_2}, p_к] = -\frac{i\omega\gamma F_т^2}{m_2\left(\omega_{11}^2 - \omega^2 + i\omega 2\tau_2\right)},$$

$$K[G_{мк}, p_{2н}] = -K[G_{мк}, p_2] = \frac{k_{мк}}{1 + i\omega T_{мк}}.$$

On the basis of equation (5.78) it is possible to determine the pressure deviation p_2 in the case of harmonic oscillations from the relationship

$$p_2 = K[p_2, p_к]\, p_к + K[p_2, G_к]\, G_к, \tag{5.83}$$

where

$$K[p_2, p_к] = 1,$$

$$K[p_2, G_к] = \xi_ф \frac{G_к^*}{\gamma g F_ф^2}.$$

On the basis of equations (5.80), (5.82), and (5.83) we can now draw a structural diagram (Fig. 5.23) for the oxidizer force main with regard to the elasticity of the engine head. To the deviations of the values p_{2p}, p_2, G_k, and G_{MK} we add the additional index 'o'.

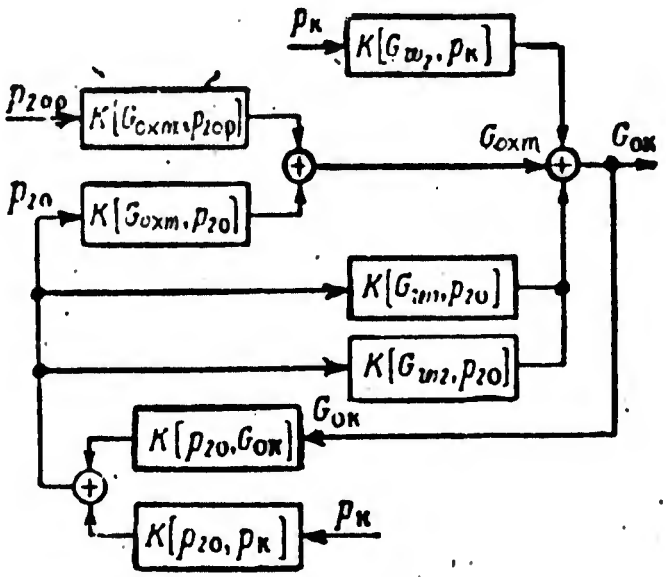

Figure 5.23

Calculation of the elasticity of the walls of the cooling duct is more complicated. The cooling duct has a curvilinear shape, variable cross-sectional area, variable wall thickness, and resistance distributed along the length. A determination of the elasticity of such a tract is usually connected with laborious numerical calculations. A change in the volume of the duct takes place under the influence of a pressure deviation of the liquid and a pressure deviation of the gases in the combustion chamber. If the possible phase conversions of the cooling component can be ignored, then a dynamic model of a cooling duct such as that shown in Fig. 22b can be assumed.

Calculation of the elasticity of the engine head and combustion chamber walls allows one to obtain more precise dynamic characteristics of the force main and thus to more precisely determine the dynamics of the engine. An additional feedback between the deviation of the fuel going to the combustion chamber and the pressure deviation of the gases is introduced into the dynamic

scheme. However, calculation of the elasticity of the walls gives a remarkable accuracy to the calculations at frequencies close to the frequencies of the natural oscillations of fuel in the elastic conduits and chambers of the engine. These frequencies are usually significantly higher than the lowest frequency of the natural longitudinal oscillations of the body of a large rocket and the lowest frequency of the natural oscillations of fuel in the long pipe between the tank and the pump. Therefore in analyzing the low frequency oscillations of large rockets the walls of the combustion chamber may be considered to be rigid. An analysis of oscillations with frequencies of several hundred cycles per second must be conducted with consideration of the elasticity of the engine walls.

8. Unstable Processes in Liquid Propellant Rocket Engines

Experience in testing liquid propellant rocket engines shows that under certain conditions the operation of the combustion chamber becomes unstable and periodic pressure oscillations arise in the chamber. Instability of the operating process in the chamber is a very unfavorable phenomenon, accompanied by intense engine vibrations and leading to mechanical failures of individual elements of the engine, burnthrough, and destruction of the chamber itself.

Observations have established that unstable conditions in the combustion chamber may be divided into two basic groups--low frequency instability (oscillations at frequencies up to 200-300 cps) and high frequency instability (oscillations at frequencies greater than 500-600 cps).

In the case of low frequency oscillations the wavelength significantly exceeds the dimensions of the combustion chamber, therefore it is possible to consider that the pressure change in different parts of the chamber takes place practically simultaneously. Low frequency oscillations appear as the result of the interaction of pressure oscillations in the combustion chamber with the fuel feed into the chamber or with the burning process.

In the case of high frequency oscillations the wavelength is commensurable with the dimensions of the combustion chamber, therefore pressure change in

various parts of the chamber takes place in correspondence with the propagation of the pressure wave throughout the chamber. High frequency oscillations therefore are often called acoustic. They are caused by the fuel feed into the combustion chamber and the burning process. The walls of the combustion chamber and the engine head participate in high frequency oscillations.

Structural diagrams of liquid propellant rocket engines (see Figs. 5.15 and 5.17) represent closed control systems with powerful energy sources (combustion chamber, gas generator) and a large number of feedbacks. Low frequency and high frequency pressure oscillations in the combustion chamber are auto-oscillations.

Let us examine several mechanisms for maintaining low frequency oscillations.

1. The interconnection of pressure oscillations of gases with the fuel feed into the combustion chamber. The combustion process is considered to be independent of the oscillations, i.e., θ_0 = const.

With a sudden increase in the pressure drop on the engine nozzles the rate of fuel feed into the combustion chamber will increase exponentially due to the time lag of the column of liquid. The time during which an error in this rate in relation to the new stable conditions decreases by e times is the relaxation time (time constant) of the fuel main T_M.

In the case of a sudden increase in pressure in the combustion chamber the excess gas and the excess pressure with it must also decrease exponentially with time, a characteristic of which is the time constant, or the relaxation time of the combustion chamber θ_k.

For engines the relaxation time of the chamber is between 0.001 and 0.01 seconds [7], for feed systems the relaxation time of the main, in general, is on the same order as the relaxation time of the chamber; however, the longer the main the greater the relaxation time, all other conditions being equal.

The mechanism for maintaining auto-oscillations under consideration was indicated by Karmand [22, 25]. It is based on the fact that the rate of fuel

feed into the chamber in relation to the injection pressure drop has a time lag on the order of the relaxation time of the fuel main T_{MK}, the combustion after fuel feed takes place with a lag equal to the conversion time θ_0, and the equilibrium pressure in the chamber is established with a lag on the order of the relaxation time of the chamber θ_k. That such a mechanism for maintaining auto-oscillations is possible may be qualitatively indicated by the following discussion.

Let us assume that fluctuations of pressure from the nominal value arise in the combustion chamber. As a result the injection pressure drop will also fluctuate, passing through a minimum with the maximum pressure in the chamber and vice versa. The rate of fuel feed will also vary, but with a time lag on T_{MK} in relation to the injection pressure drop. The conversion of the fuel present into gas fuel will follow with a time lag on θ_0. The phase shift between the minimal value of the rate of gas fuel formation (burning rate) and the maximal amount of pressure in the chamber approximately corresponds to the total relaxation time of the main and the conversion time $(T_{MK} + \theta_0)$.

On the other hand, the influence of oscillations of the burning rate (the establishment of equilibrium pressure) appears in the chamber with a lag equal to the relaxation time of the chamber θ_k. If the total of the two relaxation times $(T_{MK} + \theta_k)$ and the conversion time θ_0 is approximately equal to the half period of the oscillations, then a decrease in the influence of burning on the amount of pressure in the chamber appears at the moment when the pressure in the chamber will pass through a minimum and vice versa. The oscillations which have arisen will be intensified. The relative position of the oscillation curves of different parameters, corresponding with the above considerations, is shown in Fig. 5.24. Thus, an approximate condition of instability is that the total $(T_{MK} + \theta_k + \theta_0)$ must be on the order of the half period of the oscillations.

The quantitative relationships of the parameters determining the boundary of instability may be obtained from the equations for the combustion chamber and the fuel mains. For example, for a single-component engine we will have

$$\theta_к \frac{dp_к}{dt} + p_к = k_к G_к (t - \theta_0),$$

$$T_{мк} \frac{dG_{мк}}{dt} + G_{мк} = - k_{мк} p_к.$$

The characteristic equation of this system may be put in the form

$$\theta_к T_{мк} r^2 + (\theta_к + T_{мк}) r + 1 + k_к k_{мк} e^{-r\theta_0} = 0.$$

Since at the boundary of instability r = iω then, having separated the real and imaginary parts, we obtain

$$1 + k_к k_{мк} \cos \omega\theta_0 - \theta_к T_{мк} \omega^2 = 0,$$

$$(\theta_к + T_{мк})\omega - k_к k_{мк} \sin \omega\theta_0 = 0.$$

From these equations it is possible to determine the relationship between the parameters of the system θ_k, T_{MK}, θ_0, k_k, and k_{MK} and the oscillation frequency ω at the boundary of instability. The best conditions for the appearance of instability will be where $\theta_0 \approx T_{MK} + \theta_k$. Where $_0$ is much less than $T_{MK}+\theta_k$ the system is stable. If we assume that $\theta_0 \approx T_{MK} + \theta_k = 0.005$ sec (which gives the correct order of magnitude), then the frequency of auto-oscillations will be approximately 50 cps.

2. The interconnection of gas pressure oscillations with the burning process. It is considered that the fuel feed into the combustion chamber is constant, therefore this aspect of instability is usually called intra-chamber instability. The mechanism of intra-chamber instability was examined by Krokko [7] and is based on the fact that the conversion time in oscillatory conditions is also a fluctuating value.

Let us assume that in unstable conditions, as in stable conditions, the conversion time decreases with an increase in pressure and increases with a decrease in pressure. With an increase or decrease in the conversion time the burning process will respectively expand or contract in time. Consequently, the maximum speed of combustion products leaving the burning zone will correspond to the maximum negative value of the derivative $d\theta_0/dt$ and, conversely, to the

minimum speed of combustion products leaving the burning zone will correspond to the maximum positive value of the derivative $d\theta_0/dt$. Thus, oscillations in gas pressure cause oscillations in the speed of combustion products leaving the burning zone through a change in the conversion time. The resulting oscillations in the burning rate must lag behind the oscillations in the conversion time by one-quarter, as shown in Fig. 5.25. The influence of oscillations in the burning rate on the pressure in the chamber appears, as before, with a lag on the order of the relaxation time of the chamber.

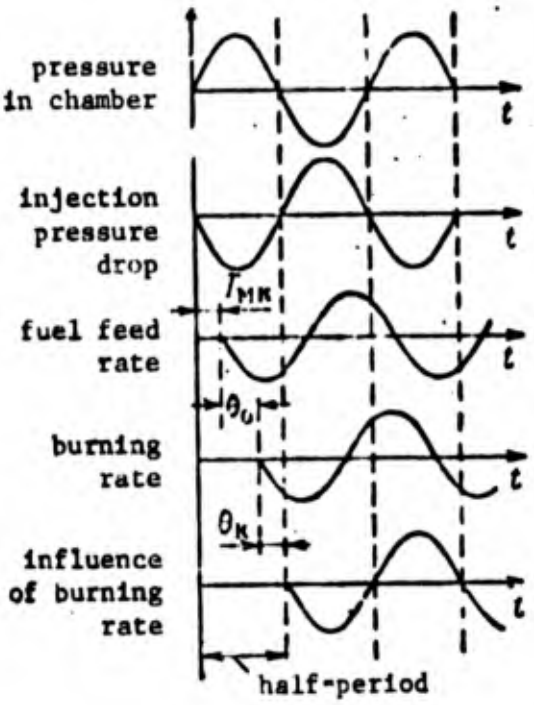

Figure 5.24

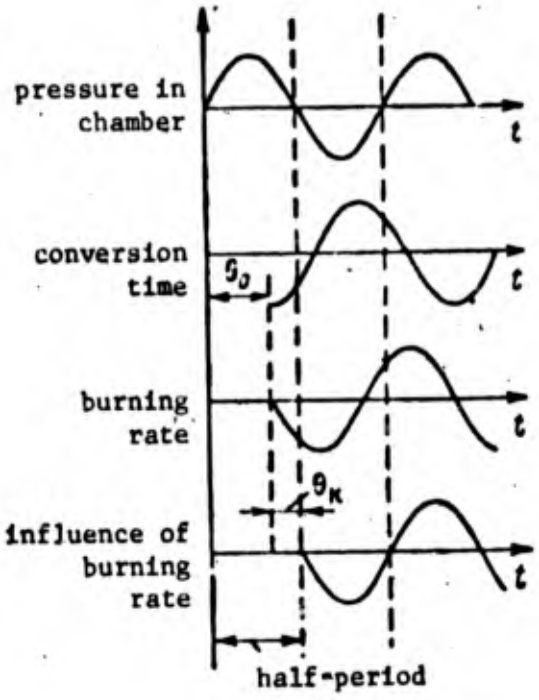

Figure 5.25

If this effect corresponds in phase with the pressure oscillations in the chamber (see Fig. 5.25) then the most favorable conditions are created for self-excitation of oscillations. The frequency range in the case of intrachamber instability will be the same as in paragraph 1.

3. The interconnection of gas pressure oscillations with wave oscillations of fuel in a long pipeline. Let, for example, the length of the pipeline be 5 m and the equivalent speed of sound in the liquid be 600 m/s. If the pipe is considered to be open at both ends, then the wavelength of the first tone of the natural oscillations of the liquid in the pipeline will be 10 m, and the oscillation frequency will be 60 cps. For a pipe closed at both ends, the

frequency of the first tone of natural oscillations will be two times smaller. This is exactly the order of frequencies corresponding to low-frequency auto-oscillations.

The mechanism of auto-oscillations with regard to wave processes in fuel mains in many respects corresponds with the mechanism described in paragraph 1. Let us clarify it with the aid of Fig. 5.26. We assume that pressure oscillations with the same frequency arise in the fuel main and the combustion chamber, whereby when the fuel pressure in the front of the nozzles increases, the gas pressure in the chamber decreases. In this case the most favorable conditions for fluctuations in the fuel feed rate arise. If the sum of the conversion time and the relaxation time of the chamber ($\theta_0 + \theta_k$) will be equal to half the period of the natural oscillations of the liquid in the pipeline, then the pressure in the chamber will be in counterphase to the pressure in front of the nozzles and the most favorable conditions for oscillations of fuel feed into the chamber will be maintained.

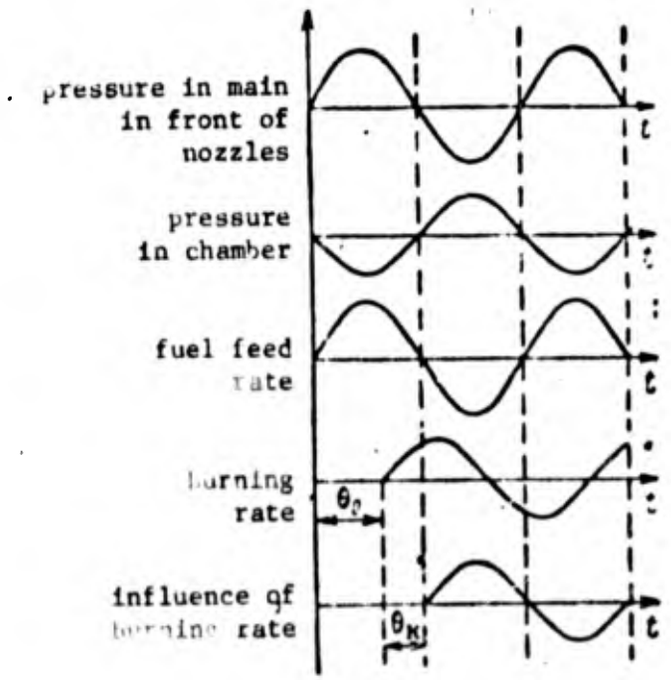

Figure 5.26

The following qualitative conclusions may be drawn from an examination of low-frequency oscillations: in order to suppress oscillations it is necessary to increase the resistance of the nozzle, to lower the conversion time $_0$, and to increase the relaxation time of the chamber $_k$. It is possible to lower the time $_0$ by improving atomization and by intensification of the burning process; it is possible to increase the time $_k$ by means of increasing the volume of the combustion chamber.

As was already noted, in the case of high-frequency (acoustic) oscillations, in view of the smallness of the oscillatory period, the pressure at each moment of time is different in neighboring points. The spatial distribution of pressure, density, and other parameters in the combustion chamber in the case of stable oscillations may be characterized by standing waves (the form of the oscillations). The standing waves may be longitudinal and transverse. Standing waves characterize the distribution of pressure along the combustion chamber. Fig. 5.27 shows longitudinal pressure waves for the first and second tones of the oscillations. Transverse waves characterize the pressure distribution in the transverse direction, whereby the pressure in the longitudinal direction remains constant. Transverse oscillations may be tangential and radial. Tangential forms of oscillations are indicated in Fig. 5.28a; the presence of a junction diameter is characteristic for cross-sectional tangential oscillations. Radial forms of oscillations are shown in Fig. 5.28b; the presence of junction areas in a cross-section is characteristic for radial oscillations.

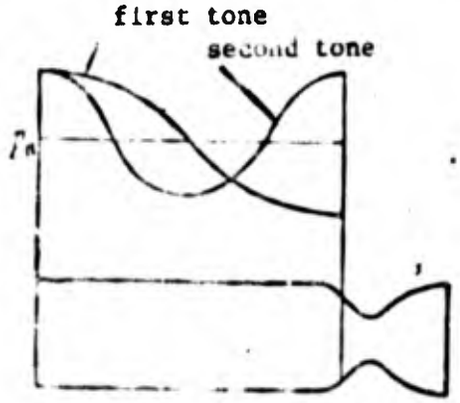

Figure 5.27

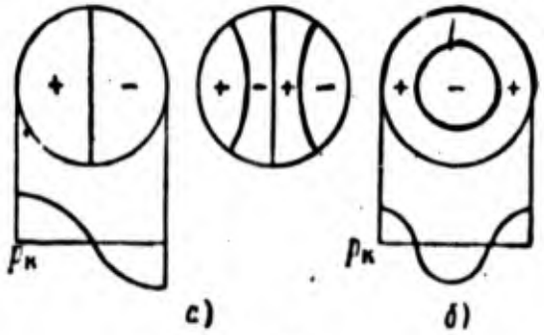

Figure 5.28

The frequencies of natural longitudinal acoustic oscillations of the first tone may be approximately determined according to the formula

$$\omega = a/2l_k$$

where a is the speed of sound in the combustion chamber; l_k is the length of the combustion chamber. The value of a may be calculated according to the formula

$$a = \sqrt{kgRT} = \frac{p}{A\rho}\sqrt{kg}.$$

The frequency of the first tone of radial and tangential oscillations [16] is:

$$\omega_{rad} = 1.22\frac{a}{2r_к}, \quad \omega_{tan} = 0.586\frac{a}{2r_к}.$$

Here r_k is the radius of the combustion chamber. As is seen, in the case of comparatively short combustion chambers ($r_k \sim l_k$) tangential oscillations of the first tone have the lowest frequency.

The mechanisms of non-damping high-frequency oscillations are based on these same phenomena of the interaction of gas pressure oscillations in the combustion chamber with oscillations of fuel feed into the chamber or with the burning rate (conversion rate), as in the case of low-frequency oscillations. However, temporal relationships are necessary but insufficient for the development of high-frequency oscillations. A favorable spatial location of the burning zone is still necessary. Historically, the importance of the spatial distribution of energy in the case of burning is not new. Farraday first mentioned it in 1818 and in 1878 the phenomenon of 'singing flames' was examined by Rayleigh.

If the burning process is concentrated near a junction surface, then oscillations of the corresponding type will be dampened, since they are not in a condition to excite the energy sufficient for maintaining them. The burning process may have great influence on pressure oscillations only in the case if the burning zone is located where the amplitude of pressure oscillations is great. Oscillations of the burning rate and the liberation of energy in these regions will immediately influence the pressure in this zone, intensifying the oscillatory process. The probability of the appearance of such a type of oscillations is the greatest when combustion in the ideal case is concentrated on the surface, where the amplitude of pressure oscillations is maximum. In this

connection the distribution of fuel feed along a cross-section of the nozzle wall has great significance. In refs. [11, 18] it is noted that for combustion sensitive to pressure variation, tangential forms of oscillations are stabilized with a decrease in the flowrate on the periphery of the nozzle wall. An increase in fuel feed in the center of the nozzle wall leads to destabilization of radial forms of oscillations. The optimal zone of fuel feed is from 0.42 to 0.61 of the combustion chamber radius.

Elastic axisymmetrical oscillations of the nozzle wall, as in the case of longitudinal oscillations of the entire engine, cause a change in the pressure in front of the nozzle and, consequently, deviation of the fuel feed into the chamber. 'Nodes' are formed on fuel jets, whereby the 'nodes' are synchronized on all nozzles [10] in the case of the first tone of oscillations of the nozzle head. Vibrations of the nozzle wall cause synchronized modulation of the fuel flow, oscillations of the flame front, and oscillations of pressure. In case of a specific mixture of phases the interaction of gas dynamics and elastic oscillations may lead to the formation of a single oscillatory system—to auto-oscillations.

If antisymmetrical elastic oscillations of the nozzle wall arise, for example oscillations with one junction diameter, then in this case modulation of the fuel feed will enable the appearance of transverse forms of oscillations of the gases in the combustion chamber.

The basic conditions for removing high-frequency oscillations are the following: disruption of the resonance ratio of the time θ_0, θ_k, and T_{MK}, and eliminating the favorable spatial disposition of the combustion zone. These conditions may be obtained by means of expanding the combustion process in time and in space and by changing the acoustic properties of the combustion chamber.

Let us now turn to an examination of the longitudinal stability of the rocket, and in this case we shall consider the engine operation to be stable.

References

1. Белтран, Франкель. Предсказание неустойчивости зон в жидкостном ракетном двигателе. — «Ракетная техника и космонавтика», 1965, № 3.

2. Брамблетт, Ноулс, Сак. Исследование динамики кавитационных и напорных характеристик системы подачи двигателя J-2. — «Вопросы ракетной техники», № 5, 1967.

3. Гор, Кэррол. Динамика регулируемого двухкомпонентного жидкостного ракетного двигателя с насосной системой подачи. — «Вопросы ракетной техники», 1957, № 5.

4. Гуров А. Ф. Расчеты на прочность и колебания в ракетных двигателях. М., «Машиностроение», 1966.

5. Квасников А. В. Теория жидкостных ракетных двигателей, М., Судпромгиз, 1959.

6. Колесников К. С. Низкочастотная неустойчивость номинального режима жидкостного ракетного двигателя. — ПМТФ, М., «Наука», 1965, № 2.

7. Крокко Л., Чжен Синь-И. Теория неустойчивости горения в жидкостных ракетных двигателях. М., ИЛ, 1958.

8. Крокко, Грей, Габри. Теория неустойчивости горения в жидкостных ракетных двигателях и ее экспериментальная проверка. — «Вопросы ракетной техники», 1960, № 9.

9. Крокко Л., Харье Д., Рирдон Д. Поперечные высокочастотные колебания в жидкостных ракетных двигателях. — «Ракетная техника и космонавтика», 1962, № 3.

10. Маккормак. Движущий механизм высокочастотной неустойчивости горения в камере ЖРД. — «Вопросы ракетной техники», 1965, № 4.

11. Макклур, Кентрелл, Харт. Теоретический анализ влияния характеристик форсуночной головки на неустойчивость горения в жидкостных ракетных двигателях. — «Ракетная техника и космонавтика», 1966, № 1.

12. Махин В. А., Присняков В. Ф., Белик Н. П. Динамика жидкостных ракетных двигателей. М., «Машиностроение», 1969.

13. Мелькумов Т. М., Мелик-Пашаев Н. И., Чистяков П. Г., Шпуков А. Г. Ракетные двигатели. М., «Машиностроение», 1968.

14. Мошкин Е. К. Динамические процессы в ЖРД. М., «Машиностроение», 1964.

15. Мэрфи, Осборн. Исследование продольной неустойчивости в камерах сгорания ракетных двигателей.—«Вопросы ракетной техники», 1966, № 2.
16. Основы теории и расчета жидкостных ракетных двигателей. Под ред. В. М. Кудрявцева М., «Высшая школа», 1967.
17. Попов Е. П. Динамика систем автоматического регулирования М., Гостехиздат, 1954.
18. Рирдон, Макбрайд, Смит. Влияние распределения расходонапряженности на устойчивость горения. — «Ракетная техника и космонавтика», 1966, № 3.
19. Тзян Г. Автоматическое регулирование процесса горения в ракетных двигателях. — «Вопросы ракетной техники», 1953, № 3.
20. Хаммер, Агоста. Распространение продольных колебаний в жидкостных ракетных двигателях. — «Ракетная техника и космонавтика», 1964, № 11.
21. Шевяков А. А. Автоматика авиационных и ракетных силовых установок. М., «Машиностроение», 1965.
22. Gunder D. F., Friant D. R. Stability of Flow in a Rocket Motor, J. Appl. Mech., 1950, vol. 17.
23. Reardon F. H., An Investigation of Transverse Mode Combustion Instability in Liquid. Propellant Rocket Motors, Princeton Univ. Aeronautical Engineering Rept. 550 (June, 1961).
24. Sabersky R. H., Effect of Wave Propagation in Feed Lines on Low-frequency Rocket Instability, Jet. Propulsion, 1954, vol. 24.
25. Summerfield M. A., A Theory of Unstable Combustion in Liquid Propellant Rocket System, J. Amer. Rocket Soc., 1951, vol. 21, No. 5.
26. Wick R. S. The Effect of Vehicle Structure on Propulsion System Dynamics and Stability, Jet. Propulsion, 1956, vol. 26, No. 10.

Chapter 6

DYNAMIC SCHEMES AND STABILITY

1. Dynamic Schemes

The properties of the individual members of the system are examined in Chapters 3-5. We shall include them in the general dynamic schemes. As a function of the structure of the discharge lines and the number of engines, the dynamic schemes of closed systems differ.

A consolidated block diagram of a common rocket with a two-component liquid fuel engine composed of physical members is presented in Fig. 6.1. Here 1 is the combustion chamber, 2 is the rocket body, 3 is the fuel line, 4 is the oxidant line.

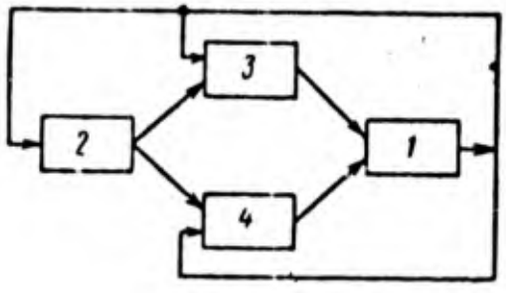

Figure 6.1

Longitudinal oscillations of the rocket body produce pressure oscillations in the fuel line and, consequently, oscillations in the supply line into the combustion chamber. In the chamber pressure oscillations arise which affect the fuel lines and the rocket body. This is a closed system.

Equations of perturbed motion of the rocket body in the direction of the longitudinal axis are presented in Chapter 3 in two variants. In the first variant the perturbed longitudinal oscillations of the body are in the form of a series composed of the eigen-functions:

$$u(x, t)=u_{\text{ц}}(t)+\sum_{n=1}^{\infty} f_n(x)\,q_n(t), \tag{6.1}$$

where u_M are the oscillations of the center of mass of the rocket; $f_n(x)$ is the form of the characteristic oscillations of the bodies; $q_n(t)$ is the generalized coordinate.

In examining the dynamic schemes we shall assume that the turbine pump assembly is rigidly attached to the combustion chamber, therefore the coefficients of the form of the characteristic oscillations of the turbine pump assembly and the engine are equal, i.e., $f_{np} = f_{ne}$. We shall not consider the deviation of the additional thrust of the exhaust nozzles of the turbine (for an open system of engine feeding) and the deviation of the ground pressure in the first approximation.

When expression (6.1) is used, the generalized coordinates of forced oscillations may be determined from the differential equations (3.70).

Let a rocket have one engine and a perturbation of the liquid in one discharge line significantly larger than in the other. On this basis in the right members of equation (3.70) we shall calculate the deviation of pressure p_{1p} only before one pump. Taking into account formulas (3.71), (3.73), and (5.33), the equations of forced oscillations of the body may be presented in the form

$$\begin{aligned} \ddot{u}_M &= \frac{1}{m}\left[-k_{1e}p_k(t) + F_T p_{1p}(t)\right], \\ \ddot{q}_n + 2\xi_n\omega_n\dot{q}_n + \omega_n^2 q_n &= \frac{1}{m_n}\left[-k_{1e}f_{ne}p_k(t) + F_T f_{np}p_{1p}(t)\right], \end{aligned} \tag{6.2}$$

where m is the rocket mass; m_n is the reduced mass of the rocket; F_T is the area of the longitudinal section of the low-pressure turbodrive.

The minus sign is placed before the deviation of pressure p_k in the combustion chamber because in equations (6.2) the translation of the body in the direction from the top of the rocket to the tail section is taken as positive.

For steady-state harmonic oscillations with frequency ω

$$\begin{aligned} p_k(t) &= p_k e^{i\omega t}, \quad p_{1k}(t) = p_{1k}e^{i\omega t}, \\ u_M(t) &= u_M e^{i\omega t}, \quad q_n(t) = q_n e^{i\omega t} \end{aligned}$$

and the solution of equations (6.2) may be expressed as the complex transmission numbers

$$u_м = K[u_м, p_к]\, p_к + K[u_м, p_{1р}]\, p_{1р},$$
$$q_n = K[q_n, p_к]\, p_к + K[q_n, p_{1р}]\, p_{1р}, \tag{6.3}$$

where

$$K[u_м, p_к] = \frac{k_{тл}}{m\omega^2}, \quad K[u_м, p_{1р}] = -\frac{F_т}{m\omega^2},$$
$$K[q_n, p_к] = -\frac{k_{тл} f_{nл}}{m_n\left(\omega_n^2 - \omega^2 + i2\xi_n\omega_n\omega\right)}, \tag{6.4}$$
$$K[q_n, p_{1р}] = \frac{F_т f_{nм}}{m_n(\omega^2 - \omega^2 + i\omega 2\xi_n\omega_n)}.$$

In the second variant the forced longitudinal oscillations of the body are expressed by the complex function

$$u(x, t) = \varphi(x, \omega)e^{i\omega t} = -A_к(x, \omega)e^{i\varphi_к(x,\omega)}k_{тл}p_к e^{i\omega t} + \\ + A_м(x, \omega)e^{i\varphi_м(x,\omega)}F_т p_{1м}e^{i\omega t}. \tag{6.5}$$

Using the complex transmission numbers we may write the expression for the complex function in the form

$$\varphi = K[\varphi, p_к]\, p_к + K[\varphi, p_{1р}]\, p_{1р}. \tag{6.6}$$

Here

$$K[\varphi, p_к] = -A_к(x, \omega)k_{1к}e^{i\varphi_к(x,\omega)},$$
$$K[\varphi, p_{1р}] = A_р(x, \omega)F_т e^{i\varphi_р(x,\omega)}. \tag{6.7}$$

In the first variant when the forced oscillations of the body are expressed in the form of a series (6.1), the rocket body in the dynamic scheme presents a certain number of parallel blocks with complex transmission numbers (6.4). In the second variant for each external influence $p_к$, $p_{1р}$ the body is formed from one block in the dynamic scheme (6.6).

The deviation of pressure entering the pump $p_{1р}$ depends upon the structure of the discharge line. We shall assume that the structure of the discharge

line corresponds to the diagram shown in Fig. 4.25. The dynamic scheme of this line is presented in Fig. 4.26. The interconnection of the deviation of pressure p_1 and the deviation of velocity v_1 leaving the tank is shown in Fig. 4.28. The inlet coordinates for the discharge line are the deviation of the pressure of the liquid leaving the tank p_t, depending upon the longitudinal oscillations of the body. The longitudinal oscillations of the body induce also translation of the engine together with the pump relative to the current of the liquid ($\Phi_A = \Phi_B$). Therefore the longitudinal oscillations act upon the flow of the liquid in the lines through the deviation of the pressure of the liquid leaving the tank and through the motion of the engine together with the pump relative to the current. If the discharge line has the structure shown in Fig. 4.27, then the longitudinal oscillations of the rocket body act upon the current of the liquid in the line also through the motion of the collector.

We shall assume that the pressure of the gases on the surface of the liquid in the tank during the oscillations of the rocket body remain constant and the deviation of the pressure going out of the tank arises only as a consequence of the oscillations of the bottom of the tank. Neglecting the formation of waves on the free surface of the liquid in the tank, in the first approximation we may assume that the deviation of the pressure is equal to the force of inertia of the liquid head

$$p_6 = -\varrho_0 H \varkappa \frac{d^2 u_6(t)}{dt^2}.$$

Here ρ_0, H are the density and height of the liquid head in the tank; $u_t(t)$ is the motion of the bottom of the tank (where it is joined to the tube) during longitudinal oscillations of the body; κ is a certain dimensionless coefficient depending upon the shape of the oscillations of the bottom.

For harmonic oscillations with a frequency ω

$$p_6 = \varrho_0 H \varkappa \omega^2 \left(u_\tau + \sum_{n,s} f_{nsj} q_n \right), \qquad (6.8)$$

where f_{nsj} is the coefficient of the form of the oscillations of the bottom of the tank, equal to the coefficient of the form of the oscillations of the mass of the mechanical oscillator m_{sj} for the n-th tone of oscillations of the body. The index j corresponds to the number of the tank (j = A, b), the

index s shows the number of the mechanical oscillator corresponding to the oscillations of the liquid in an elastic tank.

When the forced longitudinal oscillations of the body are expressed as a complex function (6.5), then the deviation of the pressure of the liquid leaving the tank may be written in the form

$$p_6 = \varrho_0 H \chi \omega^2 \sum_s \phi_{sj}, \tag{6.9}$$

where ϕ_{sj} is the value of the complex function for the mass of the mechanical oscillator m_{sj}.

If the frequencies ω_n of the characteristic oscillations of the body are not close to one another, then for an analysis of the stability of the closed system in the frequencies close to ω_n, we may confine ourselves to oscillations only of the first tone of the oscillations of the body with the generalized coordinates q_n. Then instead of (6.8) we shall have

$$p_6 = \varrho_0 H \chi \omega^2 \sum_s f_{nsj} q_n. \tag{6.10}$$

If the frequencies ω_{sj} of the characteristic oscillations of the mechanical oscillators are not close to one another, then for determination of the deviation of the pressure of the liquid p_t and frequencies close to ω_{sj}, we may consider only one s-th tone of oscillations of the liquid in the elastic tank (the s-th mechanical oscillator).

We shall determine the deviation of the velocity v_2 leaving the tube caused by the motion of the pump and the bottom of the tank. Let us assume that the front end of the low-pressure tube is rigidly attached to the bottom of the tank. Then

$$v_2 = i\omega(1 + \lambda)\phi_n - \lambda i\omega \sum_s \phi_{sj},$$

where ϕ_n is the value of the complex function for the pump; λ is the geometric characteristic of the bellows. Or

$$v_2 = K[v_2,\ \phi_p]\phi_p + \sum_s K[v_2,\ \phi_{sl}]\phi_{sl}, \tag{6.11}$$

where

$$K[v_2,\ \phi_p] = i\omega(1+\lambda),$$
$$K[v_2,\ \phi_{sl}] = -i\omega\lambda.$$

When the forced oscillations of the body are expressed in the form of the sum of the oscillations by the eigen function, then for a calculation for only one tone of the oscillations of the body we shall have

$$v_2 = K[v_2,\ q_n]q_n. \tag{6.12}$$

where $$K[v_2,\ q_n] = i\omega\left[(1-\lambda)f_{np} - \lambda\sum_{(s)} f_{nsl}\right].$$

The deviation of velocity v_2 caused by a change in the volume of the bellows and the vapor-gas mixture as a consequence of the deviation of the pressure $p_2 = p_{1p}$ may be determined from the equation

$$v_2 = i\omega(k_{vg} + r)p_{1p}, \tag{6.13}$$

where k_{vg}, r are the coefficients of conductivity of the vapor-gas mixture and the bellows.

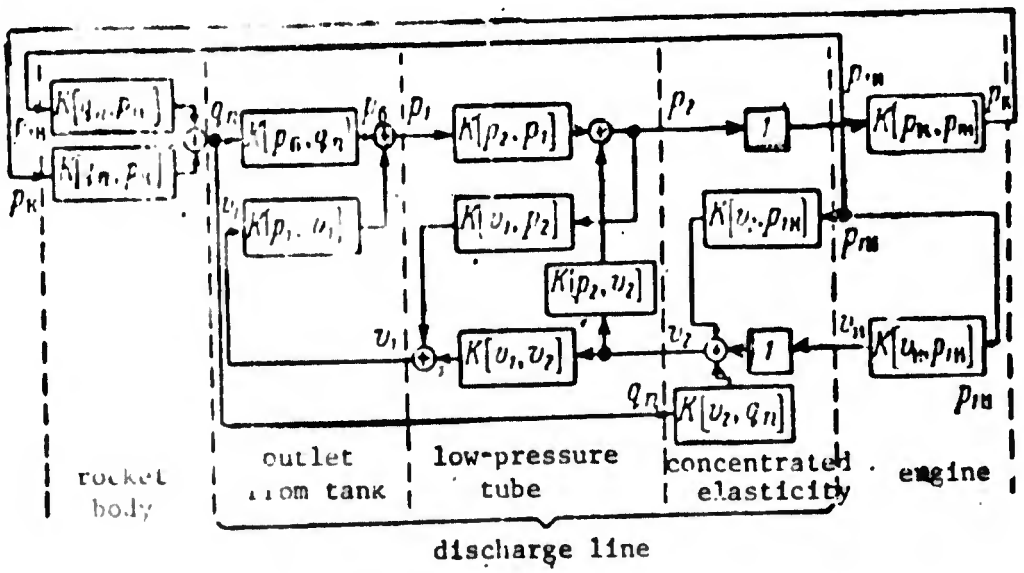

Figure 6.2

The dynamic scheme of the closed system with the discharge line only for one component is presented in Fig. 6.2. The dynamic properties of the engine as a force unit are expressed by the complex transmission number $K[p_k p_{lp}]$, as a load carrying unit they are expressed as the complex transmission number $K[v_p, p_{lp}]$. These complex transmission numbers may be obtained on the basis of the diagrams of Figs. 5.15 and 5.17. The diagram of Fig. 6.2 is presented taking into account only one tone of the oscillations of the body.

A dynamic scheme with two discharge lines is presented in Fig. 6.3. The discharge lines are not shown, only the inlet and outlet coordinates for them are shown.

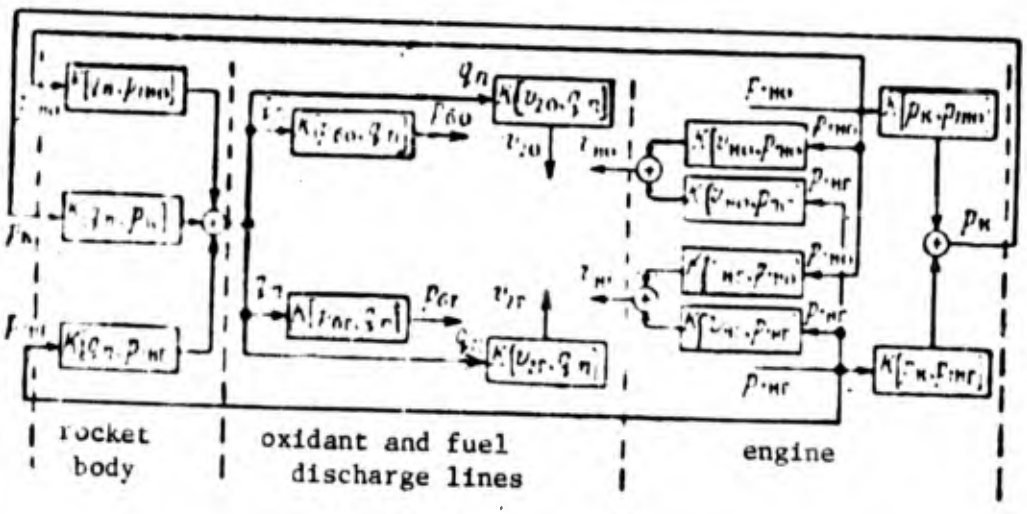

Figure 6.3

As a consequence of the oscillations of the liquid in the elastic tanks, the frequencies of the characteristic oscillations, two or more tones of the body may sometimes be close. In these conditions, in an analysis of the stability of motion, one should take into consideration simultaneously several tones of the elastic oscillations of the rocket body. As a consequence of the deviation of the pressure in the chamber p_k and upon entering the pump p_{lpo}, p_{lpf} in each tone of the oscillations of the body it is evaluated separately, and the deviations of pressure of the liquid leaving the tanks of the oxidant and the fuel p_{to}, p_{tf} and the velocity deviation of the current v_{2o}, v_{2f} should be summated from each tone of the oscillations of the body. For two tones

of oscillations with generalized coordinates q_n and q_m, the diagram of interaction of the body with the discharge line is shown in Fig. 6.4.

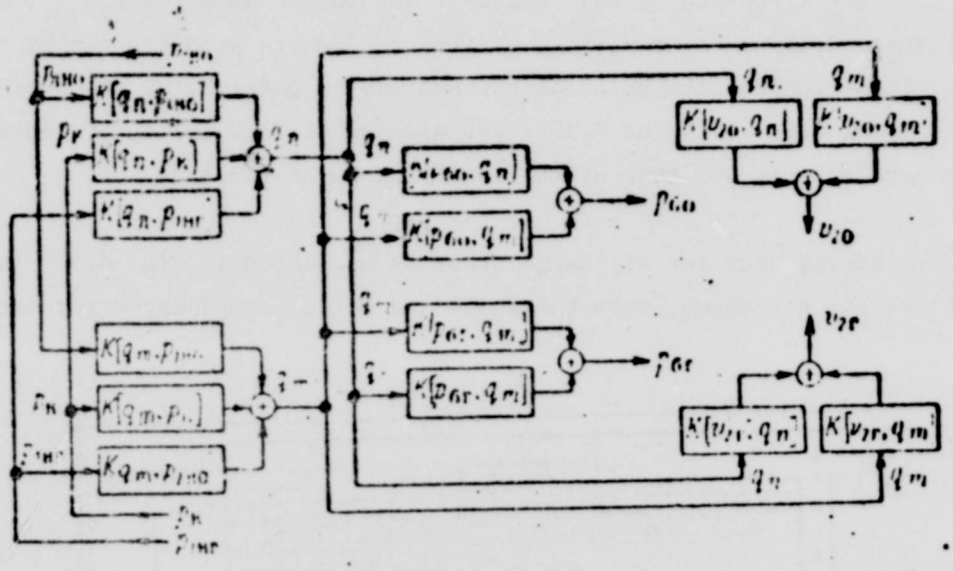

Figure 6.4

If it is necessary to simultaneously calculate more than two tones of the body oscillations, then the dynamic scheme in which the longitudinal oscillations of the body are expressed in the form (6.1) becomes very cumbersome. This deficiency may be eliminated if the longitudinal oscillations of the body are expressed by the complex function (6.5). The complex function (x, ω) considers all tones of the oscillations.

In calculating the longitudinal oscillations of the body in the form (6.5) the oscillations of the characteristic sections are determined separately--the bottom of the tank, the collectors, the engine with the turbopump unit, from each action of the pressures p_k, p_{lop}, p_{lpf}. The oscillations of the bottom of the tanks of the oxidant and the fuel are determined to the values of the complex functions ϕ_{so}, ϕ_{sf} for the masses of the mechanical oscillators

$$\phi_{so} = \sum_s \phi_{s\,o}, \quad \phi_{sg} = \sum_s \phi_{s\,1}.$$

The deviation of the velocities v_{2o} and v_{2f} in accordance with (6.11) is equal to the sum of the deviations due to the oscillations of the pumps and the bottom of the tanks. A diagram of the interaction of the body with the

discharge lines is shown in Fig. 6.5. The deviation of the pressure of the liquid leaving the tank is connected to the oscillations of the bottom of the tank by the scale coefficient

Here the indexes 'o' and 'f' correspond to the parameters of the tanks of the oxidant and the fuel.

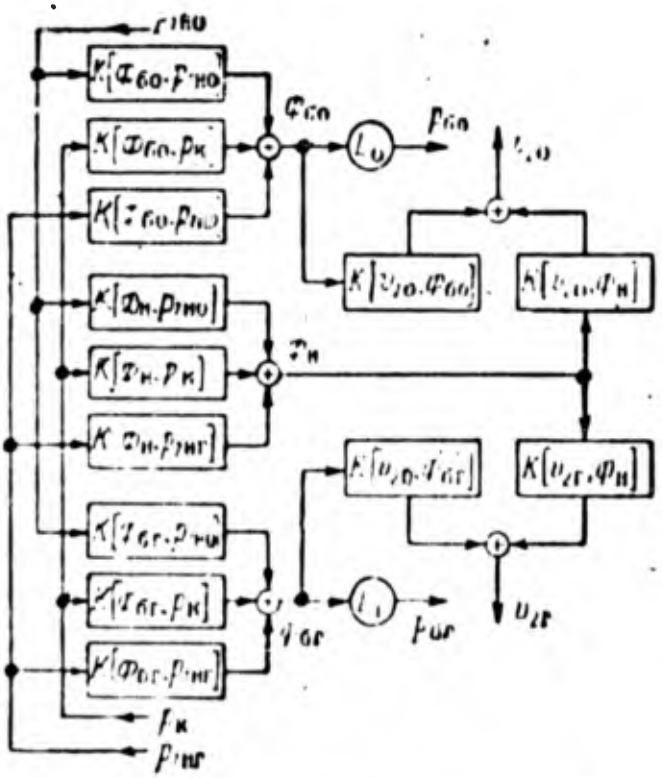

Figure 6.5

In large carrying rockets a package of several engines is generally used which engines are suspended to the body from one or several branches. The structure of the discharge line, for example, may be analogous to that shown in Fig. 4.27. The discharge line has a collector, from which the separate branches of the lines to the engine proceed. Each engine has a turbopump unit. The action of the oscillations of the rocket body on the current of the liquid in the lines is caused by oscillations in the bottom of the tanks, the collectors, and the pumps of the engine relative to the flow of the liquid.

In Fig. 6.6 a structural diagram is presented of a closed system with two engines; in the diagram is shown the discharge line only for one fuel component. The structure of the line corresponds to Fig. 4.27 but without hydraulic resistance distributed between sections 3 and 4. The initial segment of the discharge line is connected through a bellows and collector, from which proceeds two lines to the engine. For an expression of the dynamic properties of the initial segment of the discharge line and each branch, quadrapoles are used, the complex transmission numbers of which are composed according to rules expounded in Chapter 4. The pressure in the collector and the bellows are assumed to be the same, i.e., $p_2 = p_c$. The same quantity is equal to the pressure entering both branches of the discharge lines $p_{31} = p_{32} = p_c$.

The perturbation of the flow of the liquid in the discharge tube rises by the oscillations in the bottom of the tank $[p_t, q_n]$, the collector $[v_2, q_n]$, and the engines $[v_{41}, q_n]$ and $[v_{42}, q_n]$ relative to the flow. The complex transmission numbers are determined by formulas analogous to (6.10) and (6.12), taking into account the specific interaction of the end sections of the sylphons. The complex transmission numbers for the concentrated elasticities $K[v_{41}, p_{51}]$ and $K[v_{42}, p_{52}]$ are determined from equations analogous to (6.13). Besides the connections between the separate members of the dynamic system shown in Figs. 6.2 and 6.6, connections may exist between the rocket body and the regulator of the engine. These connections may be traced to the regulators shown in Fig. 5.13 and 5.14. If, for example, the pressure of the axis of the regulator κ of the ratio of pure components (see Fig. 5.14) coincides with the axis of the rocket, then the longitudinal oscillations of the body will induce oscillations of the control element 4 and the regulating organ 7, as a consequence of which oscillations arise in the discharge of the fuel. These oscillations may cause instability of the closed system.

Under certain circumstances, a connection may arise between the longitudinal oscillations of the rocket and the transverse oscillations. Such a connection may arise as a consequence of the presence of significant asymmetrically distributed masses in the body of the rocket, and as a consequence of the fact that the sensitive elements of the system of angular stabilization may react on the longitudinal oscillations of the rocket.

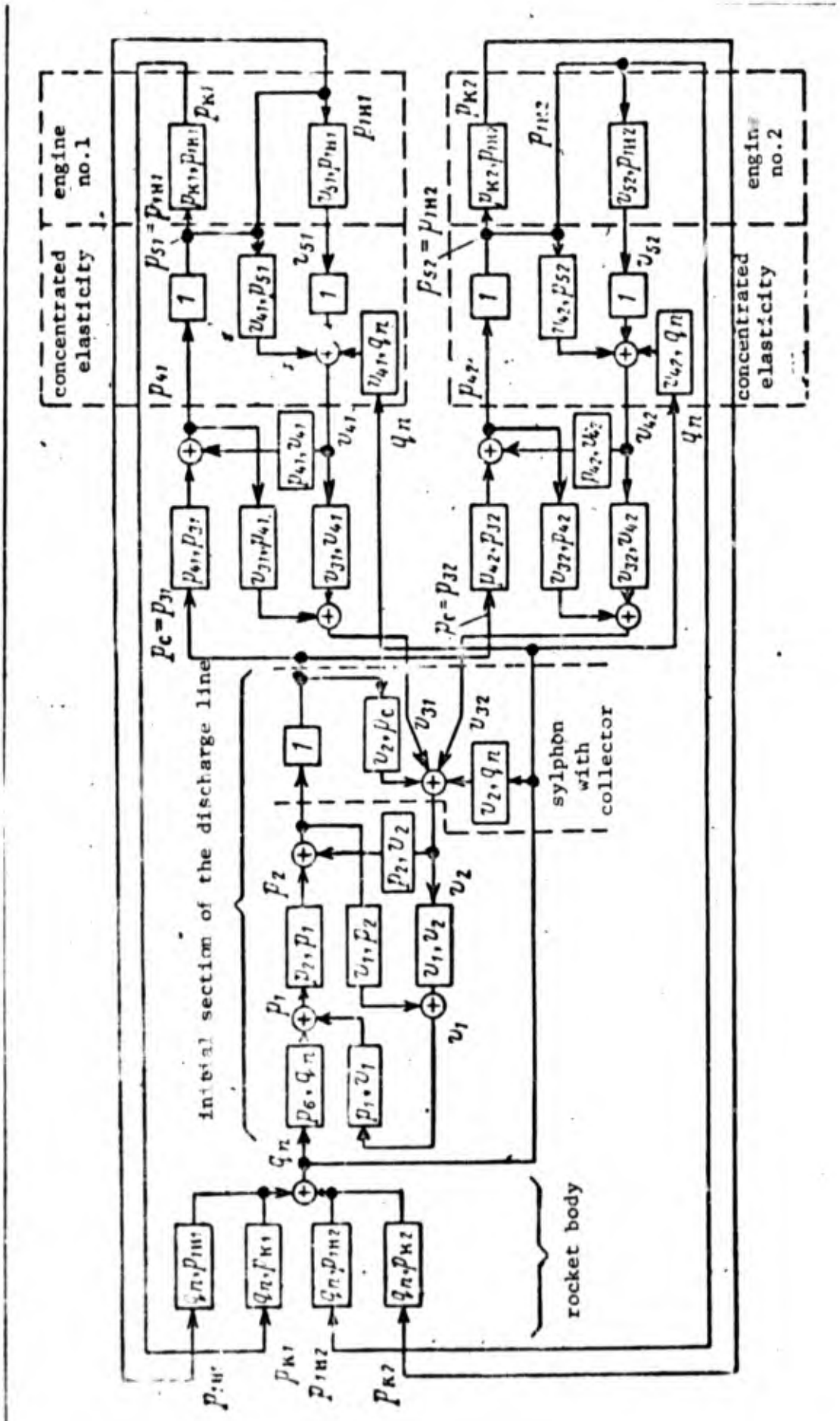
engine no.1
concentrated elasticity
engine no.2
concentrated elasticity
initial section of the discharge line
sylphon with collector
rocket body

Figure 6.6

The fuel injection system of the tanks in the presence of feedback by the pressure of the gas in the tanks and by the regulator forms an independent dynamic system. This system, generally speaking, is connected to the longitudinal oscillations of the body, because during the oscillations of the body the volume is changed and, consequently, the pressure of the gas in the tanks. In Fig. 6.7 is presented the diagram of the injection fuel feeding of the tanks of the Atlas rocket. The injection system consists of a tank with compressed helium (1), a heat exchanger (2), regulators (3), which regulate the discharge of the helium in each fuel tank during the operation of the engine in relation to changes of pressure in the gas cushion, the injection tubes (4), and the lines (5) of the measurement of the pressure of the gas in the tank. The injection systems of the oxidant tank and the fuel tank are identical in structure. The line for measuring the pressure of the gas is a tube of small diameter in which the discharge of the gas in steady-state conditions is almost always equal to zero. This line accomplishes the feedback of pressure between the gas cushion in the tank and the regulator.

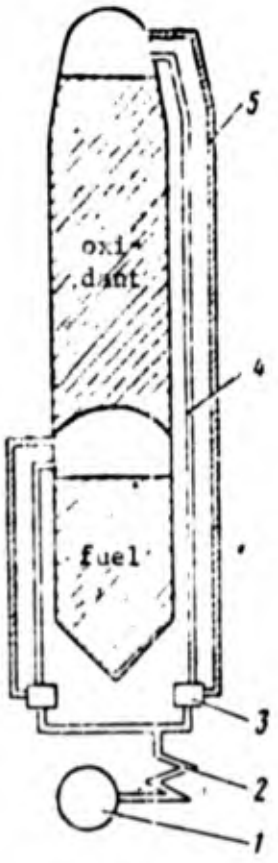

Figure 6.7

In Fig. 6.8 a block diagram of the injection system of one of the tanks of the Atlas system is shown, consisting of physical members. The basic oscillating member of the injection system is the vapor tank. During the oscillations of the gas supplied to the tank, the pressure of the gas changes on the free surface of the liquid. If it is assumed that the free surface of the liquid moves in the same way as the mass m_s of the mechanical oscillator, then taking into account resistance, the equation of the forced oscillations of the mass m_s relative to the force ring may be written in the form

$$m_s\ddot{q}_s + h_s\dot{q}_s + (k_V + k_s)q_s = p_{gt}F_t, \tag{6.14}$$

where q_s is the motion of the mass m_s relative to the force ring of the lower bottom of the tank; k_V is the rigidity of the spring, depending upon the volume of the gas cushion; h_s, k_s are the coefficients of the friction and the rigidity of the spring of the mechanical oscillator; p_{gt} is the deviation of the gas in the tank; F_t is the effective area of the tank.

On the basis of equation (6.14) the motion is

$$q_s = K[q_s, p_{gt}]p_{gt}.$$

The deviation of the pressure of the gas in the tank depends upon the change of the volume of the gas cushion, determined through the generalized coordinates q_s and upon the discharge of the gas through the injection tube:

$$p_{gt} = K[p_{gt}, q_s]q_s + K[p_{gt}, G_{gt}]G_{gt}.$$

Here G_{gt} is the deviation of the mass flow rate of the gas discharge through the injection tube. This deviation is determined by the properties of the injection tube and depends upon the deviations of the pressure of the gas p_{gt} in the tank and the pressure p_p leaving the regulator

$$G_{gt} = K[G_{gt}, p_p]p_p + K[G_{gt}, p_{gt}]p_{gt}.$$

If it is assumed that the deviation of the pressure leaving the regulator is proportional to the deviation of the pressure p_M transmitted to the regulator by the pressure measuring line, then we may write

$$p_p = K[p_p,\ \rho_м]\, p_м.$$

The dynamic properties of the pressure measuring line are expressed by the equation

$$p_м = K[p_м,\ p_{газ}]\, p_{газ}.$$

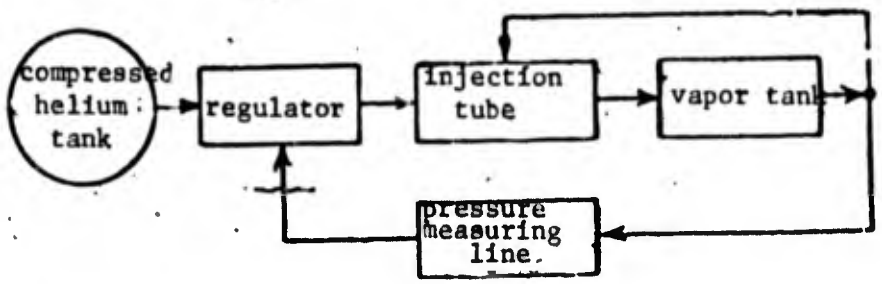

Figure 6.8

If we assume that from the oscillations of the pressure of the gas arise oscillations of the entire rocket body, then the equation for the forced oscillations of the n-th tone of the body will have the form

$$m_n\ddot{q}_n + h_n\dot{q}_n + k_n q_n = \sum_{s=1}^{s^0}\sum_{(j)} p_{гб\,j} F_{б\,j} f_{nsj}.$$

2. Stability Evaluation by the D-Partition Method

As was already shown, in a closed system consisting of the rocket body, the discharge lines, and the liquid fuel engine, auto-oscillations may arise. In spite of the fact that many parameters of the system are functions of time, the velocity of their change is sufficiently small in comparison with the period of the examined oscillations, therefore an analysis of stability in a specific moment of time may be conducted, assuming the parameters of the system to be constants. For an evaluation of the stability, let us examine a non-linear quasi-stationary model of a system.

Let us examine the dynamic scheme of Fig. 6.2. To ensure sufficiently smooth results, we shall express the dynamic properties of the discharge line

and the engine, assuming certain simplifying assumptions, which we shall give in the course of our study.

We shall write the equation for the generalized coordinate of the n-th tone of oscillations of the body in the form

$$\ddot{q}_n + 2\xi_n\omega_n\dot{q}_n + \omega_n^2 q_n = \frac{1}{m_n}\left[F_r p_{1p}(t) - k_{r\kappa} p_\kappa(t)\right] f_{n\kappa}. \tag{6.15}$$

For low-frequency oscillations, we shall consider the engine with the open system of feeding in the first approximation as a simple statistical member. Instead of the complex transmission numbers $K[p_k, p_{1p}]$ and $K[v_p, p_{1p}]$ in this case we shall use the simplest functions. For the engine as an amplifying member

$$p_k = kp_{1p}. \tag{6.16}$$

For the engine as a loading unit interesting to us, we shall obtain a relation from the pressure transmission equation

$$p_{1p} - p_k = \xi_e \rho_0 v_p^* v_p.$$

Substituting in this equation the quantity p_k by its expression from (6.16), we get a formula for determining the deviation of velocity of the liquid through pump

$$v_p = z_e^* p_{1p}, \tag{6.17}$$

where the coefficient of conductivity of the engine is

$$z_n = \frac{1-k}{\xi_n \rho_0 v_n^*}.$$

The deviation of the pressure of the liquid leaving the tank is

$$p_t = -hq_n, \tag{6.18}$$

where

$$h = \rho_0 H \times \sum_{(s)} f_{nsj}.$$

The pressure deviation p_1 going into the tube is somewhat smaller than the deviation of pressure p_t as a consequence of the losses in overcoming local resistance and the acceleration of a certain mass of liquid. On the basis of equation (4.61) we obtain

$$p_1 = p_6 - \dot{z}_6 v_1 - a_6 \dot{v}_1, \tag{6.19}$$

where

$$\dot{z}_6 = z_6 \varrho_0 v_1.$$

We now turn to the equation describing the motion of the liquid in the low-pressure turbodrive. In the first approximation, we assume the turbodrive to be rigid, and the liquid to be incompressible. We shall assume that between the low-pressure turbodrive and the inlet into the pump (into the engine) there is a concentrated elasticity in the form of a sylphon and a vapor-gas mixture.

Since the liquid is incompressible, then we shall consider the acceleration of all particles of liquid to be identical, i.e., $\dot{v}_1 = \dot{v}_2$. We obtain

$$p_1 - p_2 = \varrho_0 l \dot{v}_2, \tag{6.20}$$

where l is the length of the turbodrive.

We determine the deviation of the deviation of the pressure of the liquid in the turbodrive due to a change in the volume of the concentrated elasticity as a consequence of the deviation of the pressure, on the basis of equation (6.13)

$$v_{2_{упр}} = k_{упр} \dot{p}_{1_н} \quad (\dot{k}_{упр} = k_{пр} + r). \tag{6.21}$$

We determine the deviation of the velocity of the liquid in the turbodrive due to the motion of the engine relative to the flow of the liquid, taking into account the function (6.12)

$$v_{2q_n} = k_{q_n} \dot{q}_n, \tag{6.22}$$

where

$$k_{q_n} = (1+\lambda) f_{nn} - i \sum_{(s)} f_{nsj}.$$

So that the system of equations describing the motion of the liquid in the dischage lines will be complete, it is necessary to add one more relation connecting the deviation of pressures of the flow of the liquid in sections up to and after the concentrated elasticity:

$$v_2 = v_{2ynp} + v_{2q_n} + v_n. \tag{6.23}$$

Excluding from equations (6.15)-(6.23) all of the variables except p_{1p} and q_n, we obtain the equation for the closed system

$$\ddot{q}_n + 2\xi_n\omega_n\dot{q}_n + \omega_n^2 q_n = -k^* p_{1p}, \tag{6.24}$$

$$\ddot{p}_{1p} + 2\xi_T\omega_1\dot{p}_{1p} + \omega_T^2 p_{1p} = -(a\ddot{q}_n + b\dot{q}_n),$$

where

$$\omega_T^2 = \frac{1 + \xi_6^* z_1^*}{k_{ynp}(a_6 + \varrho_0 l)},$$

$$\xi_1 = \frac{\xi_T}{\omega_T}, \quad 2\xi_T = -\frac{z_1^*}{k_{ynp}} + \frac{\xi_6^*}{a_6 + \varrho_0 l},$$

$$a = -\frac{k_{q_n}}{k_{ynp}} + \frac{h}{k_{ynp}(a_6 + \varrho_0 l)}, \tag{6.25}$$

$$b = \frac{\xi_6^* k_{q_n}}{k_{ynp}(a_6 + \varrho_0 l)},$$

$$k^* = \frac{1}{m_n}(kk_{re} - F_1) f_{ne}.$$

Thus the system investigated leads to two harmonic oscillators, one of which (the body of the rocket) has the frequency of the characteristic oscillations ω_n, and the other (the low-pressure turbodrive with the engine as the loading unit) has a frequency ω_T.

The characteristic oscillations of the liquid in the lines are oscillations of an incompressible liquid head in the elastic element which is the vapor-gas mixture (and the syiphons). The frequency of these oscillations changes with an increase in k_k, which is the coefficient of conductivity of the concentrated elasticity and the mass of the oscillating liquid $(a_t + \rho_0 l)$. The

relative damping coefficient ξ_T of the characteristic oscillations of the liquid in the low-pressure turbodrive depends upon the coefficient of conductivity of the engine z_e^* and the coefficient of active resistance ξ_t^* in the outlet of the tank.

The maximum value of the amplification coefficient k* for the first oscillator will be for the frequency $\omega \approx \omega_n$, and for the second—for the frequency $\omega \approx \omega_T$. When the approximation is satisfied $\omega_n \approx \omega_T$ in the frequency $\omega \approx \omega_n \approx \omega_T$ the coefficient of amplification of the system reaches the maximum value and herein arises the most suitable condition for the loss of stability. For nearly equal conditions the coefficient of amplification is larger as the coefficient of the form of the characteristic oscillations of the engine with the turbopump unit and the bottom of the tank is larger. A structural diagram of the closed system is shown in Fig. 6.9.

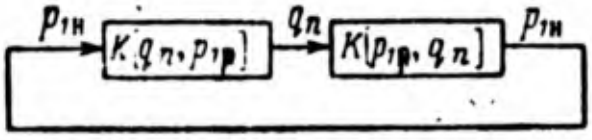

Figure 6.9

We shall now evaluate the stability of the system. In the limit of stability the system oscillates harmonically. We shall assume $q_n(t) = q_n e^{i\omega t}$ and $p_{1p}(t) = p_{1p} e^{i\omega t}$ and we shall place these expressions in (6.24). After excluding the variables q_n and p_{1p} and separating the real and imaginary parts, we find the connection between the parameters of the system and the frequency of the oscillations ω in the limit of stability:

$$\begin{aligned} 4\xi_n^2\omega^2\xi_n\omega_n\omega_T - (\omega_n^2 - \omega^2)(\omega_T^2 - \omega^2) &= k^* a\omega^2, \\ \xi_n\omega_n(\omega_T^2 - \omega^2) + \xi_T\omega_T(\omega_n^2 - \omega^2) &= \frac{1}{2} bk^*. \end{aligned} \tag{6.26}$$

From these two equations may be excluded the frequency of the oscillations ω and the relation between the parameters of the system at the limit of stability may be found; thereupon, the boundary of stability may be established in the plane of any two parameters of the system while the rest of the parameters are held constant.

It is suggested by S. M. Nathanson [7] that an evaluation be conducted of the stability of the system by means of comparing the quantities of the relative damping coefficient, for example ξ_n^0 of ξ_T^0, in which the system is in the limit of stability with real values of the relative coefficient ξ_n or ξ_T. In this case the criterion for evaluating the stability of the system is sufficiently simple: if $\xi_n^0 < \xi_n$, then the system is stable, if $\xi_n^0 > \xi_n$, then the system is unstable.

Solving equations (6.26) for the quantities $\xi_n^0\omega_n$ and ω_n^2, we obtain

$$\xi_n^0\omega_n = k^* \frac{a\frac{\xi_T}{\omega_T} + \frac{b}{2\omega_T^2}\left[1-\left(\frac{\omega}{\omega_T}\right)^2\right]}{\left[1-\left(\frac{\omega}{\omega_T}\right)^2\right]^2 + 4\xi_T^2\left(\frac{\omega}{\omega_T}\right)^2}. \tag{6.27}$$

$$\omega_n^2 = \omega^2\left\{1 - k^* \frac{a\left(\frac{\omega}{\omega_T}\right)^2\left[1-\left(\frac{\omega}{\omega_T}\right)^2\right] + 2\frac{\xi_T}{\omega_T} b\left(\frac{\omega}{\omega_T}\right)^2}{\left[1-\left(\frac{\omega}{\omega_T}\right)^2\right]^2 + 4\xi_T^2\left(\frac{\omega}{\omega_T}\right)^2}\right\}. \tag{6.28}$$

Calculations show that in many cases the quantity of the first component in the brackets of expression (6.28) is significantly smaller than one, as a consequence of which the frequency of the oscillations in the limit of stability practically coincides with the frequency of the characteristic oscillations of the rocket body. Therefore a determination of the quantity ξ_n^0 in the limit of stability may be conducted by equation (6.27), obtaining in it $\omega = \omega_n$.

Since the quantities ω_n^2, k*, a, and b change in the flight process, then at different moments of time the values of the coefficient ξ_n^0 also change. From expression (7.27) it is evident that the quantity ξ_n^0 has a maximum value at $\omega \approx \omega_T$, therefore, as has already been noted, the best condition for instability is created when the value of the frequencies of the characteristic oscillations of the rocket body and the liquid head in the low-pressure turbodrive coincide. Knowing the value of the coefficients ξ_T and ω_T, which practically do not change in the flight process, and the coefficients k*, a, b, ω_n in different moments of the flight time $\bar{t}$, it is possible according to equation

(6.27) to calculate for these moments of time the quantities ξ_n^0 in the limit of stability and compare them with the real values of the coefficients ξ_n.

As an illustration, in Fig. 6.10 the results are presented graphically of the calculation of $\xi_n^0\gamma_n$, where $\gamma_n = \omega_n/(\omega_n)_0$, and $(\omega_n)_0$ are the values of the frequencies of the characteristic oscillations of the body at the beginning as a function of the dimensionless flight time $\bar{t}$ for a certain hypothetical rocket. The calculation is conducted for four different ratios of the frequencies of characteristic oscillations $\gamma_T = \omega_T/(\omega_n)_0 = 0.9; 1.1; 1.4; 2.0$. In the lower part is shown the dependence taken for the calculation $\gamma_n(\bar{t})$, and the values of $\gamma_n(\bar{t})$ are shown by the same horizontal lines. In the upper part the slope condition is presented for the line of the real coefficient $\xi_n\gamma_n$ of the rocket body. From a simultaneous observation of the upper and the lower part it is evident that the areas of instability are in the range of frequencies where ω_n and ω_T have close values. For sufficiently small values of frequencies of the characteristic oscillations of the liquid in the lines ($\omega_T \ll \omega_n$), and also in the case $\omega_T \gg \omega_n$, the system is stable throughout the entire flight time.

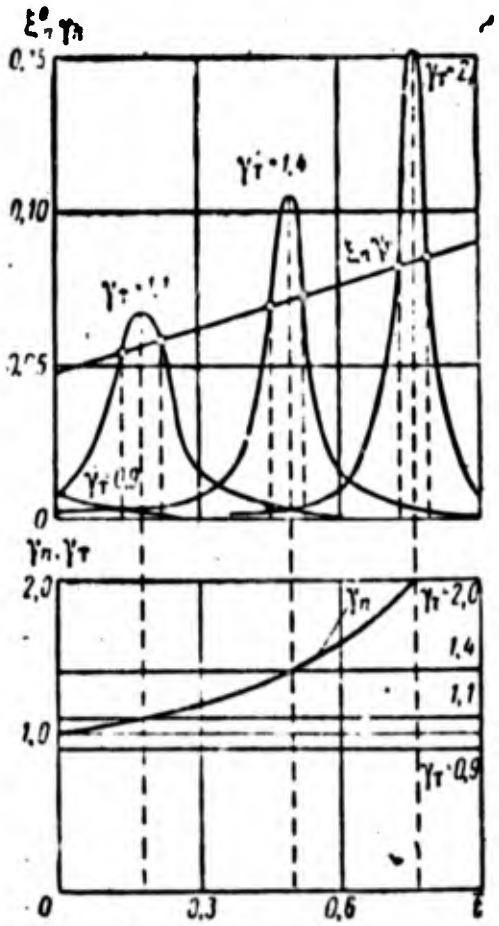

Figure 6.10

The quantity of the relative coefficient of damping ξ_n^0 in the limit of stability for $\omega = \omega_n = \omega_T$ may be determined from equation (6.27)

$$\xi_n^0 = \frac{k^* a}{4\xi_T \omega_n^2}.$$

Substituting in this equation the quantity k* and a for their expressions from (6.25), we obtain

$$\xi_n^0 = \frac{kk_{Te} - F_T}{4\xi_T \omega_n^2 k_{упр} m_n} \times$$

$$\times \left\{(1+\lambda) f_{ne}^2 + f_{ne} \sum_{(s)} f_{nsl} \times \right.$$

$$\left. \times \left[\frac{(1+\lambda)\varrho_0 H\varkappa}{a_6 + \varrho_0 l} - \lambda\right]\right\}. \quad (6.29)$$

From this equation it is evident that if the coefficient of the form of the characteristic oscillations of the engine with the turbopump unit $f_{ne} = 0$ (the external force is applied to the body in the joining section), then $\xi_n = 0$ and for $\xi_n > 0$ the system is always stable. The circuit in Fig. 6.9 is, as it were, broken and a closed system comes into existence.

When the coefficient of the form of the characteristic oscillations of the bottom of the tank f_{nt} is equal to zero, i.e., $\sum_{(s)} f_{nsj} = 0$, then $p_t = 0$, but the system remains closed. Oscillations of the body act on the flow of the liquid in the low pressure turbodrive through the motion of the engine with the turbopump unit relative to the current ($f_{ne} \neq 0$). From equation (6.29) it is evident that the possibility of losing the stability is increased if $f_{ne} \sum_{(s)} f_{nsj} > 0$ and decreases if $f_{ne} \sum_{(s)} f_{nsj} < 0$, in comparison with the case where $\sum_{(s)} f_{nsj} = 0$. The quantity of the relative coefficient of damping ξ_n^0 in the limit of stability is inversely proportional to the relative coefficient of damping ξ_T of the liquid in the low-pressure turbodrive. Therefore the more the pressure differential in the nozzle characterized by the coefficient z_e^*, the less the value will be of the quantity ξ_n^0 in the limit of stability.

Now we shall conduct an evaluation of the stability of a dynamic system shown in Fig. 6.2 with a more complete calculation of the properties of the discharge line. We shall assume the liquid in the turbodrive to be compressible and all of the turbodrive to be elastic. From the physical content of the problem of stability it follows that for the coincidence of frequencies ω_n and ω_T there is no significance to the form of elasticity determining the frequency of these characteristic oscillations of the liquid in the discharge line. Therefore calculation of the compressibility of the liquid and the elasticity of the walls of the tube, along with a calculation of the concentrated elasticity before the inlet of the pump, insures a more accurate determination of the frequency of the characteristic oscillations of the liquid and consequently more exact quantitative ratios of the parameters of the system in the limit of stability.

In the limit of stability of the system the ratios between the deviation of pressures p_1 and p_2 and the deviation of velocities v_1 and v_2 for the flow

of the liquid in the tube, on the basis of equation (4.71), may be written in the form

$$p_2=\frac{1}{\operatorname{ch}\Omega}\,p_1-i(a_0\varrho_0\operatorname{tg}\Omega)v_2,$$
$$v_1=i\left(\frac{1}{a_0\varrho_0}\sin\Omega\right)p_2+\operatorname{ch}\Omega v_2, \tag{6.30}$$

where the dimensionless frequency of the oscillations of the liquid in the tube is

$$\Omega=\omega\frac{l}{a_0},$$

where a_0, ρ_0 are the velocity of sound and the density of the liquid in the unperturbed flow.

The dynamics of the remaining members of the system are as before expressed by equations (6.16)-(6.19) and (6.21)-(6.23). We shall assume that the reactants upon entering the tube is equal to zero ($\alpha_t = 0$). Then from equations (6.17)-(6.19), (6.21)-(6.23), and (6.30) for the condition where $p_2 = p_{1p}$, the dependence between the deviations p_{1p} and q_n for the discharge line in the limit of stability may be written in the form

$$p_{1p}(X(\omega)+iY(\omega))=\left[\frac{h\omega^2}{\operatorname{ch}\Omega}+\omega k_{q_n}a_0\varrho_0\operatorname{tg}\Omega-i\omega\xi_6^*k_{q_n}\right]q_n, \tag{6.31}$$

where

$$X(\omega)=1+\xi_6^*z_A^*-\omega k_{\text{упр}}a_0\varrho_0\operatorname{tg}\Omega,$$
$$Y(\omega)=\frac{\xi_6^*}{a_0\varrho_0}\,\frac{\sin\Omega}{\operatorname{ch}\Omega}+\omega\xi_6^*k_{\text{упр}}+a_0\varrho_0z_A^*\operatorname{tg}\Omega. \tag{6.32}$$

The function X(ω) expresses the active part of the oscillating member, Y(ω) expresses the dissipative part. The quantity of the frequency of the characteristic oscillations of the liquid Ω_n in the low-pressure turbodrive is significantly well determined from the condition X = 0. We obtain

$$\operatorname{tg}\Omega_n=\frac{1+\xi_6^*z_A^*}{\Omega_n a_T^*}\qquad\left(a_T^*=\frac{a_0^2\varrho_0}{l}\,k_{\text{упр}}\right). \tag{6.33}$$

This formula has the same sense as the analogous on page 137 [Russian text], illustrated graphically in Fig. 4.5.

Using (6.31) and the first equation of (6.24), we obtain the following relation of the parameters of the system and the frequency of oscillations in the limit of stability:

$$(\omega_n^2 - \omega^2) X(\omega) - 2\xi_n \omega_n \omega Y(\omega) = -k^* \left[\frac{h\omega^2}{\operatorname{ch} \Omega} + \omega k_{q_n} a_0 \varrho_0 \operatorname{tg} \Omega \right],$$

$$(\omega_n^2 - \omega^2) Y(\omega) + 2\xi_n \omega_n \omega X(\omega) = k^* \omega \xi_0^* k_{q_n}.$$

If these equations are solved for the quantities $\xi_n^0 \omega_n$ and ω_n^2, we obtain

$$\xi_n^0 \omega_n = \frac{k^*}{2} \frac{\xi_0^* k_{q_n} X(\omega) + \left(\frac{h\omega}{\operatorname{ch} \Omega} + k_{q_n} a_0 \varrho_0 \operatorname{tg} \Omega \right) Y(\omega)}{X^2(\omega) + Y^2(\omega)}, \tag{6.34}$$

$$\omega_n^2 = \omega^2 \left[1 - k^* \frac{\left(\frac{h}{\operatorname{ch} \Omega} + \frac{k_{q_n} a_0 \varrho_0}{\omega} \operatorname{tg} \Omega \right) X(\omega) - \frac{\xi_0^* k_{q_n}}{\omega} Y(\omega)}{X^2(\omega) + Y^2(\omega)} \right]. \tag{6.35}$$

Since, as in the case of incompressibility of the liquid and rigid tube walls, the second term in the square brackets of equation (6.35) in many practical cases is significantly less than 1, therefore the frequency of the oscillations in the limit of stability practically practically coincides with the frequency of the characteristic oscillations of the body. Inserting into equation (6.34) $\omega = \omega_n$, we may determine the quantity ξ_n^0 in the limit of stability. The dependence $\xi_n^0(\bar{t})$, as in the case of an incompressible liquid, has a sharply expressed maximum, when the frequency of the characteristic oscillations of the body is close to the frequency of the characteristic oscillations of the liquid in the discharge line, i.e., when

$$\omega_n = \Omega_n \frac{a_0}{l},$$

where Ω_n is the root of the equation (6.33).

We shall use the D-partition method to evaluate the stability of a dynamic system including two discharge lines (see Fig. 6.3). We shall assume that the crossover connection of the discharge lines is weak, therefore for simplification we shall assume that

$$K[v_{op}, p_{1og}] = 0, \quad K[v_{og}, p_{1op}] = 0.$$

For definiteness we shall assume the structure of the discharge lines of the oxidant and the fuel lines to be the same and corresponding to the diagram shown in Fig. 6.2. For each line the complex transmission number may be obtained using equation (6.31):

$$K[p_{1op}, q_n] = \frac{\omega[Q_o(\omega) + iR_o(\omega)]}{X_o(\omega) + iY_o(\omega)},$$
$$K[p_{1og}, q_n] = \frac{\omega[Q_r(\omega) + iR_r(\omega)]}{X_r(\omega) + iY_r(\omega)}, \tag{6.36}$$

where for the oxidant line

$$Q_o(\omega) = \left(\frac{h\omega}{\mathrm{ch}\,\Omega} + k_{q_n} a_0 Q_0 \mathrm{tg}\,\Omega\right)_o,$$
$$R_o(\omega) = -(\xi_0 k_{q_n})_o.$$

The quantities $X_0(\omega)$ and $Y_0(\omega)$ are determined by formulas (6.32), in which it is necessary to insert the corresponding parameters of the oxidant line. The quantitites $Q_f(\omega)$, $R_f(\omega)$, $X_f(\omega)$, $Y_f(\omega)$ are determined by the identical formula by means of inserting in them the fuel line parameters.

In the presence of fuel and oxidant lines, instead of equation (6.16), we shall have

$$p_u = k_o^* p_{1op} + k_g^* p_{1og}.$$

Then for the body of the rocket we obtain

$$q_n[(\omega_n^2 - \omega^2) + i\omega 2\xi_n\omega_n] = k_o^* p_{1op} + k_r^* p_{1og}, \tag{6.37}$$

where

$$k_o^* = \frac{1}{m_n}(k_o k_{1q} - F_{1o}) f_{na},$$
$$k_r^* = \frac{1}{m_n}(k_r k_{1q} - F_{1r}) f_{na}.$$

The structural diagram of the closed system with two discharge lines is presented in Fig. 6.11.

The equation of the closed system in the limit of stability may be written in the form

$$K[q_n, p_{1ap}]K[p_{1ao}, q_n]+K[q_n, p_{1ag}]K[p_{1gg}, q_n]=1.$$

Inserting in this equation, instead of the complex transmission number, their expression from (6.36) and (6.37) and separating the real and imaginary parts, we obtain

$$\begin{aligned} k_o^*\omega(Q_oX_g-R_oY_g)\omega+k_g^*\omega(Q_rX_o-R_rY_o)=(\omega_n^2-\omega^2)(X_gX_o-Y_gY_o)-\\ -2\omega\xi_n\omega_n(Y_rX_o+Y_oX_r), \end{aligned} \tag{6.38}$$

$$\begin{aligned} k_o^*\omega(Q_oY_g+R_oX_g)+k_g^*\omega(Q_rY_o+R_gX_o)=\\ =(\omega_n^2-\omega^2)(Y_gX_o+Y_oX_r)+2\omega\xi_n\omega_n(X_rX_o-Y_gY_o). \end{aligned}$$

These equations as in (6.26) may be solved relative to any parameters interesting us, in particular $\xi_n^0\omega_n$ and ω_n^2 and may determine the quantity of the relative coefficient of damping ξ_n^0 in the limit of stability. If the frequencies of the characteristic oscillations of the liquid in the turbodrive of the oxidant and the fuel (ω_{To}, ω_{Tf}) are not close, then the maximum values of the quantity of the relative coefficient of damping ξ_n^0 in the limit of stability corresponds to the moment of flight time when the frequency of the characteristic oscillations of the body is close to ω_{To} or ω_{Tf}. On this basis instead of the dynamic diagram with two discharge lines, we may examine two dynamic schemes, in each of which there is only one discharge line—an oxidant or a fuel line. Of greatest importance is the moment of flight time when the frequency of the characteristic oscillations of the first tone of the body ω_1 coincides or is close with one of the frequencies ω_{To} or ω_{Tf}.

The analytical equation (6.38) for the relationship of the parameters of the system and the frequency of the oscillations in the limit of stability are very cumbersome, and to evaluate them in general form is rather tedious. In particular this relates to the complex dynamic systems in which the engine may not be considered a simple statistical member. It is advisable to conduct an evaluation of the stability of such complicated systems by other methods, in paritcular, by the methods of the theory of automatic regulation.

3. Stability Evaluation by the Frequency Characteristic Method

Let us examine at first the dynamic system of Fig. 6.2. Combining the discharge line with the engine as the load unit in one member with the complex transmission number $K[p_{op}, q_n]$, we obtain the structure of the dynamic system shown in Fig. 6.12. We shall consider the member with these complex transmission numbers as stable. We shall convert the two-circuit system of Fig. 6.12 to a one-circuit system, the stability evaluation of which is simplest to conduct using the Nyquist criterion. A structural diagram of the single-circuit system is shown in Fig. 6.13. Here

$$K^*[q_n, p_{1p}] = K[q_n, p_{1p}] + K[q_n p_k] K[p_k, p_{1p}]. \qquad (6.39)$$

The essence of the method of frequency characteristics is comprised in the fact that it is necessary in any point to break the circuit, construct a phase-amplitude frequency characteristic of the closed circuit (Nyquist diagram), and on the basis of the Nyquist criterion conduct an evaluation of the stability of the closed system. Since the construction of phase-amplitude characteristic of a closed circuit amounts to the addition or multiplication of vectors of the complex transmission numbers of the separate members in the specified values of frequency ω, these vectors may be predetermined by calculation or by experiment by methods with the required accuracy without any sort of substantial simplifying assumptions. This is certainly a worthwhile method, especially in the cases where reliable phase-amplitude characteristics of certain members of the system may be obtained only from experimental results.

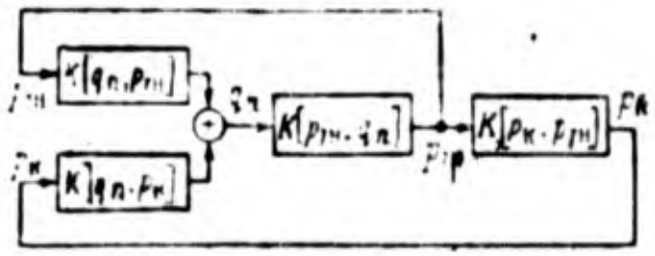

Figure 6.12

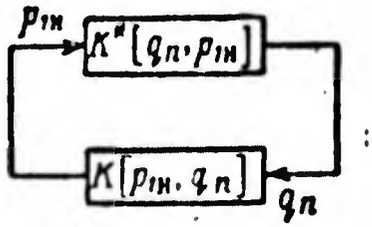

Figure 6.13

We shall write an equation of the phase-amplitude characteristic of the closed circuit in the form

$$W(i\omega)=U(\omega)+iV(\omega)=$$
$$=K[p_{1\beta}, q_n]K^*[q_n, p_{1\beta}]=A(\omega)e^{i\varphi(\omega)}. \quad (6.40)$$

Taking into account the equation (6.39) this equation of the phase-amplitude characteristic of the closed circuit may through the vector of the complex transmission number of the initial members of the system (see Fig. 6.12) be written in the form

$$W(i\omega)=[A_{qp_\kappa}A_{p_\kappa p_\beta}\exp i(\varphi_{p_\beta q_\kappa}+\varphi_{p_\kappa p_\beta})+A_{qp_\beta}e^{i\varphi_{p_\beta}}]A_{p_\beta}e^{i\varphi_{p_\beta}}, \quad (6.41)$$

where the vectors of the complex transmission numbers of the individual members have the value:

$$A_{qp_\beta}e^{i\varphi_{qp_\beta}}=K[q_n, p_{1\beta}],$$
$$A_{qp_\kappa}e^{i\varphi_{qp_\kappa}}=K[q_n, p_\kappa].$$
$$A_{p_\kappa p_\beta}e^{i\varphi_{p_\kappa p_\beta}}=K[p_\kappa, p_{1\beta}], \quad (6.42)$$
$$A_{p_\beta q}e^{i\varphi_{p_\beta q}}=K[p_{1\beta}, q_n].$$

Here and later the dynamic coefficients of amplification A_{qp_n}, A_{qp_k}, ... and the phase characteristics φ_{qp_n}, φ_{qp_k} are functions of the frequency ω.

The formulas for the complex transmission numbers characterizing the dynamic properties of the rocket body may be obtained on the basis of equation (6.15)

$$K[q_n, p_{1\beta}]=\frac{F_\tau f_{n\beta}}{\omega_n^2-\omega^2+i2\omega\xi_n\omega_n},$$

$$K[q_n, p_\kappa]=\frac{-k_\tau f_{n\kappa}}{\omega_n^2-\omega^2+i2\omega\xi_n\omega_n}.$$

The form of the phase-amplitude characteristics of the rocket body are presented in Fig. 6.14a, b. These are characteristics of the general oscillations of the members with damping. The broken lines show the characteristics for the phase where the coefficient of the form of the characteristic oscillations of the motor is $f_{ne} < 0$. In Fig. 6.14c, d, the possible phase-amplitude

characteristics of the discharge line and the engine are presented. As a function of the design of the discharge line and its parameters, and also of the design and the parameters of the engine, the form of these characteristics may change to a significant degree.

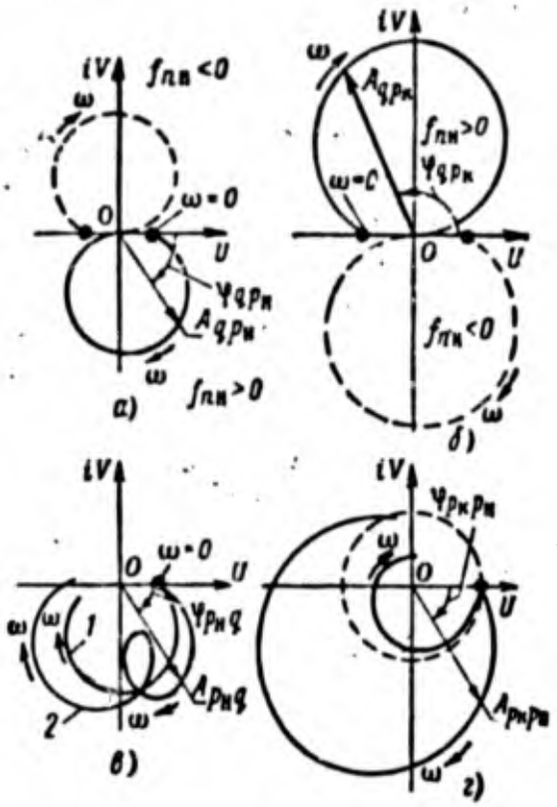

Figure 6.14

Performing the addition and multiplication of vectors in the range of frequencies in which we are interested agreeable to equation (6.41) and reproducing the obtained results graphically, we obtain the Nyquist diagram (Fig. 6.15). Curve 1 corresponds to a system in which the frequency of the characteristic oscillations of the rocket body is close to the frequency of the characteristic oscillations of the liquid in the discharge line. Both members of this system (see Fig. 6.13) are stable, and inasmuch as curve 1 intersects the real axis once to the right of the point C(1, i0), this closed system is unstable.

Curve 2 corresponds to the system in which the frequency of the characteristic oscillations of the liquid in the discharge line is significantly lower

than the frequency of the characteristic oscillations of the body. The maximum dynamic coefficient of amplification of the closed circuit is less than one, the phase-amplitude characteristic may not intersect the real axis right of the point C(1, i0), and the closed system is stable.

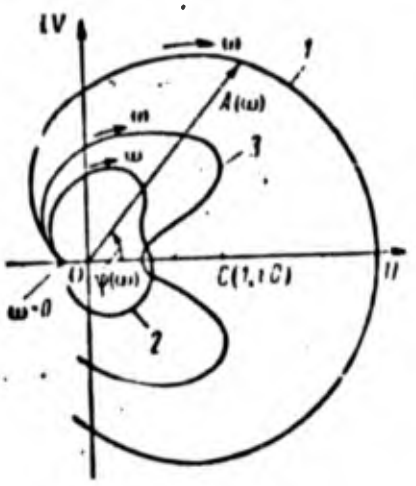

Figure 6.15

Curve 3 characterizes the dynamic properties of a closed circuit when the frequency of the characteristic oscillations of the body and the liquid in the discharge line are close to each other, however by the dynamic characteristics of the regulators of the engine in the range of these frequencies, it was possible to significantly reduce the coefficient of amplification of the engine and thus ensure the stability of the closed system.

The equation of the phase-amplitude characteristic of the closed system is simpler when the vector $A_{qp_n} e^{i\varphi_{qpn}}$ may be neglected in comparison with the product of the vectors $A_{qp_k} A_{p_kp_n} \exp i(\varphi_{qp_k} + \varphi_{p_kp_n})$. For such a closed circuit, for the phase-amplitude and phase-frequency characteristics, the equations are

$$A(\omega) = A_{qp_k} A_{p_kp_p} A_{p_pq},$$

$$\varphi(\omega) = \varphi_{qp_k} + \varphi_{p_kp_p} + \varphi_{p_pq}.$$

As seen from Fig. 6.15, for a certain frequency $\omega = \omega_n$ the equation

$$\varphi(\omega_n) = \varphi_{qp_k} + \varphi_{p_k p_n} + \varphi_{p_n q} = 0,$$

will be satisfied.

The closed system will be unstable if

$$A(\omega_n) = A_{qp_k} A_{p_k p_n} A_{p_n q} > 1.$$

The best conditions for such a situation are those when the frequency of the characteristic oscillations of the liquid in the discharge line coincides with the frequency of the characteristic oscillations of the body. From an analysis of the dependence of the coefficients A_{qp_k}, $A_{p_k p_n}$, $A_{p_n q}$ upon the parameters of the system, it is possible to make a definite conclusion on the influence of the stability of the system of such parameters as ξ_n, ξ_T, f^2_{ne}, $f_{ne}\sum_{(s)} f_{nsj}$, etc. These conclusions were formulated in a foregoing section.

We shall now obtain an equation for the phase-amplitude characteristics of the dynamic system with two discharge lines (see Fig. 6.3). If we neglect the interaction of the liquid with the lines through the engine and combine each discharge line in the engine as a load unit in a separate member with a complex transmission number $K[p_{ipf}, q_n]$ then the dynamic scheme of the closed system will consist of two parallel circuits (Fig. 6.16). The complex transmission numbers $K^*[q_n, p_{lop}]$, $K^*[q_n, p_{lfp}]$ may be obtained from equation (6.39), in which the quantity p_{lp} for the oxidant line must be subatituted for the quantity p_{lop}, and for the fuel line, for the quantity p_{lfp}.

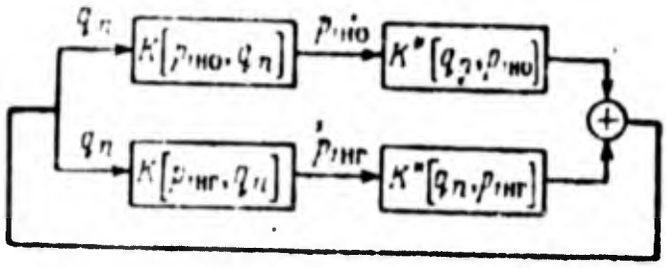

Figure 6.16

Disrupting the system, as shown in Fig. 6.16, we write the equation for the phase-amplitude characteristic of the open circuit in the form

$$W(i\omega) = A(\omega)e^{i\varphi(\omega)} =$$

$$= A_{p_1 p_0 q} e^{i\varphi_{r_0 p_0 q}} \left[A_{q p_k} A_{p_k p_{\alpha p}} \exp i(\varphi_{q p_k} + \varphi_{p_k p_{\alpha p}}) + \right.$$

$$\left. + A_{q p_p} e^{i\varphi_{q p_0 p}} \right] + A_{p_{0g} q} e^{i\varphi_{p_{\alpha g} q}} \left[A_{q p_k} A_{p_k p_{\alpha g}} \exp i(\varphi_{q p_k} + \varphi_{p_k p_{0g}}) + \right.$$

$$\left. + A_{q p_{0g}} e^{i\varphi_{q p_{0g}}} \right].$$

Here the notation used is analogous to the notation in (6.41) and (6.42).

4. The Role of Feedback

According to the data of laboratory experiments, during the operation of liquid fuel rocket engines, the pulsations of the thrust are studied even when the closed system (the rocket body, the fuel lines, and the engine) are stable. These pulsations arise from processes transpiring in the engine. Thus the inducement of the pulsations is a property inherent in the operational processes of a liquid fuel rocket engine.

The thrust pulsation P of the engine may be characterized by the function of spectral density $S_p(\omega)$ and the dispersion of the deviation of the engine thrust

$$\sigma_p^2 = \int_{-\infty}^{\infty} S_p(\omega)\, d\omega.$$

In the active part of the flight, the rocket as a closed system experiences action of thrust pulsations of the engine, which are outside of the closed system. The pulsations cause forced longitudinal elastic oscillations of the body and oscillations of pressure in the fuel line. The rocket itself during the flight time experiences feedback due to the oscillations of the rocket body and the liquid in the fuel line. The feedback as a function of the amplification coefficient and the phase relationships may have a great significance and, as was shown, in a closed system instability may arise.

In Fig. 6.17a, the influence of engine thrust pulsations on the closed system is shown. Here, $W(i\omega)$ is the phase-amplitude frequency characteristic

of the closed circuit consisting of the rocket body, the fuel lines, and the engine; P_{fi} is the external influence on the closed system of engine thrust fluctuations, not depending upon the oscillations of the body and the pressure in the fuel lines (for example, in laboratory experiments); P_{etx} are the fluctuations in engine thrust located in the closed system (leaving the member); P_{ex} are the thrust fluctuations acting on the rocket body during flight (entering the member). The relations between the fluctuations are expressed by the known formulas

$$P_{вх} = P_{вн} + P_{вых},$$
$$P_{вых} = P_{вх} W(i\omega).$$

Considering the fluctuation of the force as stationary, we shall obtain a relation between the function of the spectral density $S_{ex}(\omega)$ of the thrust fluctuations acting upon the body and the function $S_{fi}(\omega)$ of the thrust fluctuation in laboratory experiments:

$$S_{вх}(\omega) = S_{вн}(\omega) \frac{1}{|1 - W(i\omega)|^2}.$$

We shall determine in a certain cross-section x the deviation of the longitudinal overload of the rocket n_x caused by the action of thrust fluctuations upon the closed system. Studying

$$W(i\omega) = W_k(i\omega) W_{ey}(i\omega)$$

where $W_k(i\omega)$, $W_{ey}(i\omega)$ are the phase-amplitude characteristics of the rocket body and the engine apparatus (the engine and the fuel lines), we obtain a structural diagram of the system shown in Fig. 6.17b. Here the engine apparatus plays the role of feedback relative to the rocket body.

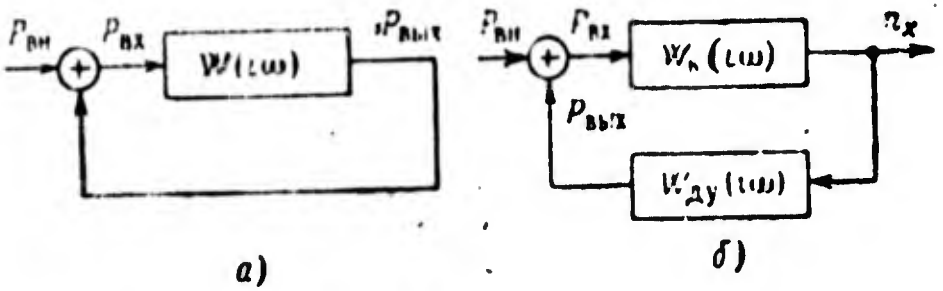

а) *б)*

Figure 6.17

Since the spectral density of an arbitrary process in the output of a linear system is equal to the spectral density of the external action on its inlet multiplied by the square of the modulus of the frequency characteristic of this system then the spectral density of deviation of the longitudinal overload is

$$S_n(\omega) = S_{вх}(\omega)\,|W_к(i\omega)|^2.$$

Keeping in mind the relation between $S_{ex}(\omega)$ and $S_{fi}(\omega)$ we obtain an expression for the dispersion of the deviation of the longitudinal overload

$$\sigma_n^2 = \int_{-\infty}^{\infty} S_n(\omega)\,d\omega = \int_{-\infty}^{\infty} S_{вн}(\omega)\,\frac{|W_к(i\omega)|^2}{|1 - W(i\omega)|^2}\,d\omega.$$

The transmission band determined by the frequency characteristic of the rocket body is small, therefore in the limits of this band it may be assumed that the function S_{fi} = const. Then

$$\sigma_n^2 \approx S_{вн} \int_{-\infty}^{\infty} \frac{|W_к(i\omega)|^2}{|1 - W(i\omega)|^2}\,d\omega.$$

If the body had no feedback, then the dispersion of the deviation of the longitudinal overload would be

$$\sigma_n^2 \approx S_{вн} \int_{-\infty}^{\infty} |W_к(i\omega)|^2\,d\omega.$$

In a frequency range close to the frequency of the characteristic oscillations of the body, the quantity $|1 - W(i\omega)|$ may be less than 1, and the dispersion of the longitudinal overload of the body for feedback would be larger than without feedback. For harmonic external action P_{fi} the ratio of the deviation of the longitudinal overload will be equal to

$$\frac{(n_x) \text{ for feedback}}{(n_x) \text{ without feedback}} = \frac{P_{ex}}{P_{fi}} = \frac{1}{1 - W(i\omega)}.$$

Feedback produces an increase in the deviation of the longituinal overload; it, as it were, decreases the deformation coefficient of the body.

Thus, in a range of frequencies of characteristic oscillations of the body in the active part of the flight, even in the case of stability, large oscillations of the longitudinal overload may arise and slowly dampen the transition processes arising for example during the firing of the engine.

The amplitude of the oscillations of the longitudinal overload should be restricted. For pilotted ships complying with NASA* technical specifications, it should not be more than 0.2-0.25.

In the Titan-2 rocket, for example, in the nose cone area of the rocket the amplitude of the oscillations of the longitudinal overload reached unity and were reduced after the installation of hydraulic dampers to $A_n = 0.18$. (Ekspress-Informatsiya RKT, No. 24, 1964.) In the spacecraft Apollo 6 in the 126-th second of flight the amplitude of the longitudinal overload was observed to be $A_n \approx 0.7$ at a frequency $\omega = 5.5$ Hz. This is about five times greater than at the beginning of the flight (Ekspress-Informatsiya RKT, No. 30, 1968).

5. Methods of Insuring Stability

In order that the dynamic system may be practically stable it is necessary first of all that in the flight process the frequencies of the characteristic longitudinal oscillations of the body do not coincide with the frequencies of the characteristic oscillations of the liquid in the discharge line. Both the rocket body and the liquid in the discharge line have a complete spectrum of characteristic oscillations. The frequencies of the characteristic oscillations of the liquid in the discharge line depend upon the length of the line and the elasticity of its walls, the compressibility of the liquid, and the presence of the vapor-gas mixture (the concentrated elasticity) before the inlet in the pump. These frequencies during the flight process remain constant if the parameters of the concentrated elasticity do not change. The frequencies of the characteristic oscillations of the body change in the flight process,

increasing smoothly in proportion to the discharge of the fuel from the tank. It is most important that the frequencies of the characteristic oscillations of the lower tone of the body and the liquid in the lines do not coincide. Since the line for one of the fuel components is generally significantly longer than the line for the other component, then it is most probable that the frequency of the characteristic oscillations of the liquid in the long discharge line may coincide with the lower frequency of the characteristic oscillations of the body.

If during the flight process at any moment of time these frequencies approach each other, then the dynamic properties of the discharge line should change in such a way that the frequency of the characteristic oscillations of the liquid in the line decrease or, on the contrary, increase. It is possible to increase the frequency of the characteristic oscillations of the liquid in the line primarily by a decrease in the coefficient of conductivity of the concentrated elasticity k_{cc}. For this it is necessary to increase the pressure of injection into the tank and thus improve the cavitational characteristic of the pump. An increase in the rigidity of the sylphons also leads to a decrease in the coefficient k_{cc}, but in a significantly lesser degree than a decrease or a complete elimination of the volume of the vapor-gas mixture.

It is possible to decrease the frequency of the characteristic oscillations of the liquid in the discharge line by several methods. A hydraulic accumulator (a damper of longitudinal oscillations) may be installed in the discharge lines (preferrably in the pump inlet). The hydraulic accumulator reduces the frequency of the oscillations and in this regard possesses the properties of a concentrated elasticity. Several diagrams of hydraulic diagrams are presented in Fig. 4.19. This method is somewhat feasible and reliable but has the deficiency that the hydraulic accumulator increases the rate of the rocket structure.

A significant in the frequency of the characteristic oscillations of the liquid may be attained if the tube of circular cross-section is exchanged for a tube of a non-circular cross-section. In Chapter 4, for example, it was shown that in a tube with a cross-section in the form of an ellipse the reduced

velocity of sound and consequently the frequency of the characteristic oscillations of the liquid is less than in a circular tube. The frequency of oscillations is decreased even more if the tube has large longitudinal corrugations. The use of a tube of a non-circular cross-section does not increase the structural weight of the rocket, but planning the durability and preparation technique of such tubes is more complicated than for tubes of circular cross-section.

As one of the methods of decreasing the frequency of the characteristic oscillations of the flow of the liquid in the line, a blast in the flow of an insignificant amount of insoluble gas may be used. As was shown in Chapter 4, the presence of a small quantity of insoluble gas in the flow of liquid insures a significant decrease in the reduced velocity of sound.

In a decrease of the pressure feeding of the tank, the cavitational characteristics of the pump get worse, a volume of vapor-gas mixture is formed or significantly increases, as a result of which the frequency of the characteristic oscillations of the liquid in the line decreases. But this method is least acceptable since when the cavitational characteristics get worse, the coefficient of useful action of the pump is decreased.

From the data of the analysis it follows that the stability of motion of the system may be increased by raising the coefficient of resistance of the line. One of the methods in this direction is an increase in the transmission pressure in the engine nozzles.

For insuring the stability of the dynamic system, engine regulators may also be used. This in particular relates to the scheme in which the engine has a closed feeding system. The working process of the engine with such a system of feeding at low frequencies has vibratory properties. By means of a selection of the characteristics of the regulators, it is possible to change the frequency range in which the engine has the maximum coefficient of amplification, and succeed in significantly changing the phase characteristic of the engine in the necessary direction.

6. Examples of Instability Formation

As follows from works [9, 12], in the rockets Titan-2 and Atlas, during the flight tests longitudinal instability was observed which was afterwards eliminated by various construction methods. In determining the instability by calculation methods a simplified mathematical model of this system was used in these works, which insured satisfactory agreement of the results of calculated data with experimental data. The basic simplifying assumptions are correct for an engine with an open feeding system. We shall present the mathematical model of the system used in works [9, 12].

The equation for the generalized coordinate q_n of the oscillations of the body may be written in the form

$$\ddot{q}_n + 2\xi_n\omega_n\dot{q}_n + \omega_n^2 q_n = \frac{1}{m_n}\left[-k_{\tau\kappa}p_\kappa(t) + \sum_{\substack{j=0\\ j=\tau}} F_{\tau j}p_{1pj}\right] f_{n\kappa} \qquad (6.43)$$

where the indices j = o, j = f correspond to the lines and (tanks) of the oxidant and fuel.

Each fuel line consists of three members: the low-pressure tube (the discharge line), the pump, and the high-pressure tube (the delivery line). The deviation of pressure in the bottom of the tank may be calculated by the formula

$$p_{6j}(t) = -\varrho_{0j}H_{j\kappa}f_{n6j}\ddot{q}_n, \qquad (6.44)$$

where f_{ntj} is the coefficient of the form of the characteristic oscillations of the bottom of the tank determined taking into account one basic tone of the oscillations of the liquid in the tank.

The compressible liquid in the elastic low-pressure tube is schematized in form of a certain elastic rod with an equivalent modulus of elasticity E_e. In the front end of the rod a pressure deviation p_{tj} acts; the lower end of the rod rests upon a spring imitating a concentrated elasticity in the inlet of the pump.

Since the force of the pressure of the spring on the rod is equal to the sum of the forces of the inertia of the rod, the equation for determining the generalized coordinate q_r of the forced oscillations of the rod (the liquid in the tube) may be written in the form

$$\ddot{q}_{rj} + 2\xi_{rj}\omega_{rj}\dot{q}_{rj} + \omega_{rj}^2 q_{rj} = \\ = \frac{-\rho_{0j}F_{Tj}\dot{v}_{2j}(t)}{m_{rj}}\int_{l_{1j}}^{0} f_{rj}\,dx + \frac{p_{0j}F_{Tj}f_{rj}(0)}{m_{rj}}, \tag{6.45}$$

where ξ_{rj}, ω_{rj}, m_{rj}, f_{rj} are the relative coefficient of damping, the frequency of the characteristic oscillations, the reduced mass, and the form of the characteristic oscillations of the r-th tone of the rod on the spring, wherein $f_{rj}(l_{1j}) = 1$; $v_{2j}(t)$ is the deviation of the velocity of the liquid leaving the tube (for $x = l_{1j}$); F_{Tj} is the area of the cross-section of the tube.

The pressure of the liquid going out of the tube may be considered as the stress in the end of the elastic rod by the formula

$$p_{2j}(t) = -E_{0j}q_{rj}\left(\frac{df_{rj}}{dx}\right)_{x=l_{1j}}. \tag{6.46}$$

We shall assume that $p_{2j} = p_{vgj} = p_{1pj}$, where p_{vgj} is the deviation of the pressure of the vapor-gas mixture.

The deviation of velocity of the liquid going out of the tube may be determined from the equation of discontinuity

$$v_{2j}(t) = v_{pj}(t) + f_{np}\dot{q}_n + v_{vgj}, \tag{6.47}$$

where v_{pj} is the deviation of velocity of the liquid through the pump; v_{vgj} is the deviation of the velocity of the liquid going out of the tube due to the concentrated elasticity. On the basis of (4.57)

$$v_{vgj} = K[v_2, p_{1pj}]\,p_{1pj} = k_{vgj}\dot{p}_{1pj}. \tag{6.48}$$

We shall consider the velocity of the shaft of the turbopump assembly unit to be constant. Then the deviation of pressure in the outlet of the pump may be determined from equation

$$p_{2pj}=\left[1+\left(\frac{\partial H_{pj}}{\partial p}\right)^{\circ}\right]p_{1pj}+\left(\frac{\partial H_{pj}}{\partial v_{p}}\right)^{\circ}v_{pj}, \qquad (6.49)$$

where H_{pj} is the pressure of the liquid going out of the pump.

We shall assume the high-pressure tube to be rigid, and the liquid in the tube to be incompressible. Taking into account the inertia of the liquid and the resistance of the tube, including the resistance of the nozzle, the equation of the motion of the liquid in the high-pressure tube may be written in the form

$$p_{2pj}(t)-p_{k}(t)=l_{2}\rho_{0j}\dot{v}_{kj}(t)+\xi_{j}\rho_{0j}v_{kj}^{\circ}v_{kj}(t); \qquad (6.50)$$

where $v_{kj}(t)$ is the deviation of the velocity of the incoming liquid in the combustion chamber ($v_{kj}=v_{pj}$); ξ_{j} is the coefficient of resistance of the tube and the nozzle head.

We shall assume the combustion chamber to be a simple aperiodic member, and we may write the equation for the deviation of pressure in the combustion chamber in the form

$$\theta_{k}\dot{p}_{k}+p_{k}=\sum_{(j)}k_{kj}\rho_{0j}F_{\tau j}v_{kj}, \qquad (6.51)$$

where k_{kj} is the coefficient of amplification of the chamber according to the discharge of the j-th component.

Equations (6.43)-(6.51) give a mathematical model of a closed system. A structural diagram with one fuel line is shown in Fig. 6.18. It is not difficult to obtain expressions for complex transmission numbers of the members on the basis of equations (6.43)-(6.51).

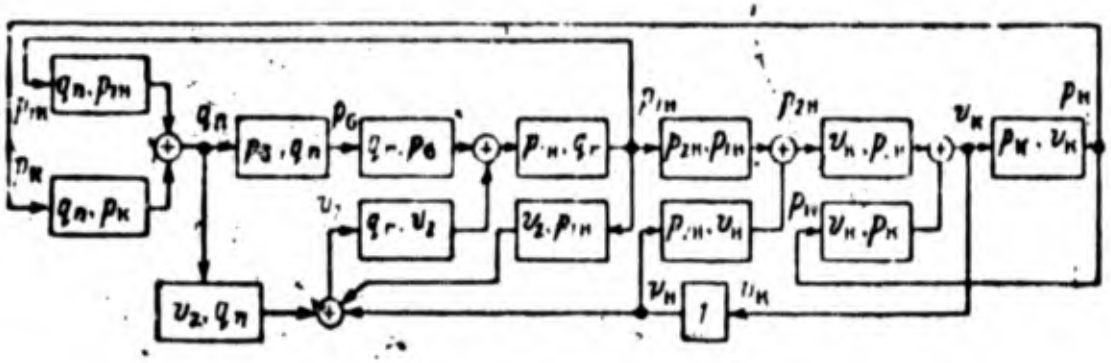

Figure 6.18

An evaluation of the stability of the system may be conducted by means of a determination of the trajectory roots $z = \varepsilon + i\omega$ of the characteristic equation of the closed system. In Fig. 6.19 results are presented of a calculation of the roots of the characteristic equation for the Titan-2 rocket [9]. The graph shows the change in roots corresponding to the first and second tones of the oscillations of the rocket as a function of flight time. The instability of the rocket in the frequency of the first tone of oscillations of its body is theoretically assumed to be approximately between 105 and 140 seconds of flight. Approximately the same data were obtained in the telemetric measurements at the time of the first flight tests of the Titan-2 rocket. In Fig. 6.20 a graph is shown of the axial overload n_x obtained in flight tests [12]. The oscillations began at a moment of time $t \approx 100$ seconds and reached the maximum at the moment of time $t \approx 120$ seconds and stopped at the end of the flight. The oscillations had an almost sinusoidal character with the frequency changing during the time of flight from 10 to 15 Hz. The amplitudes of the oscillations of the pressure are charcterized by the data cited in Table 6.1 obtained as a result of a simulation according to equations (6.43)-(6.51) in conditions of a restricted amplitude of oscillations of the body and during flight tests.

In order to give the system stability, on the low-pressure turbodrive in front of the inlet of the pump, a spring-hydraulic damper was installed. A diagram of the turbodrive with the damper is shown in Fig. 6.21a; the phase-amplitude characteristic of the turbodrive with the damper in the condition that the liquid is incompressible is presented in Fig. 6.21b. The damper reduces the oscillations in the inlet of the pump and, as it were, breaks the

circuit between the fuel line and the engine. The rigidity of the spring of the damper is selected such that the least modulus of the phase-amplitude

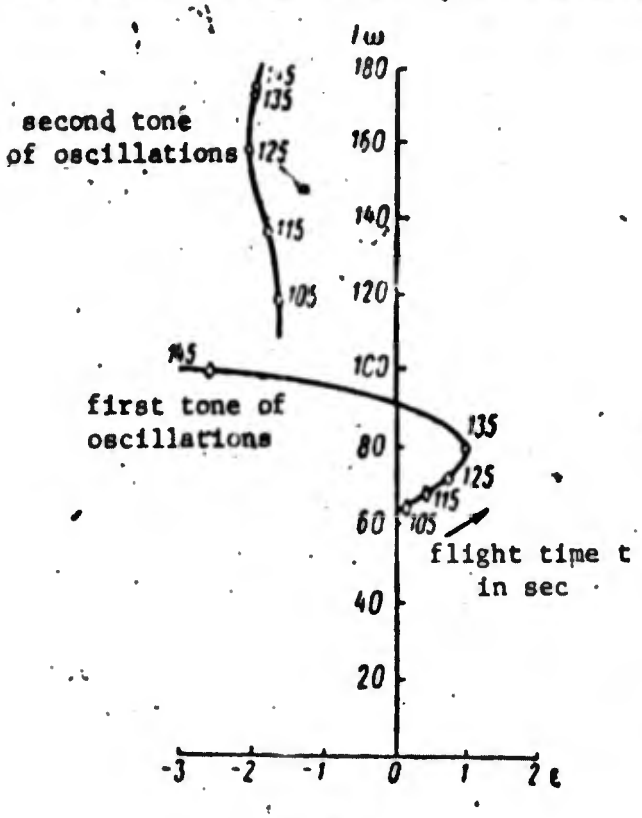

Figure 6.19

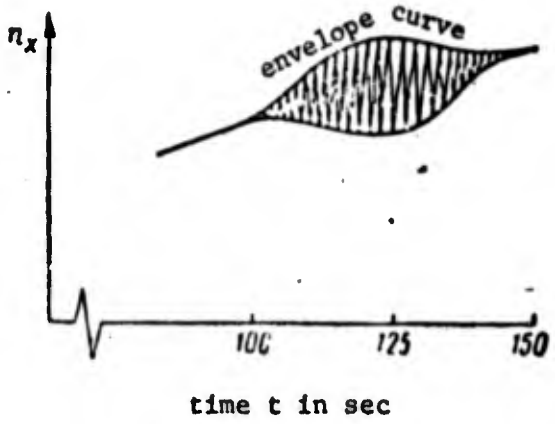

Figure 6.20

characteristic of the turbodrive and the damper will be at the frequency equal to the frequency of the charcteristic oscillations of the body. For a long turbodrive a calculation of the rigidity of the spring of the damper should be conducted taking into account the compressibility of the liquid and the concentrated elasticity in the end of the turbodrive.

In Fig. 6.22 results are presented of a determination of the trajectory of the roots $z = \varepsilon + i\omega$ of the characteristic equation for the first two tones of oscillations of the Atlas rocket. The roots are calculated for two values of the relative damping coefficient: $\xi = 0.01$ and $\xi = 0.02$. As is evident, for very small coefficients of damping, each tone of oscillations in different moments of time may become unstable.

Table 6.1

Pressure deviation kg/cm²	Calculated data of mathematical model	Data of rocket flight tests
$p_к$	3,5	4,3
$p_{бо}$	1,62	1,9
$p_{1но}$	10,26	9,6
$p_{2но}$	10,54	12,66
$p_{бг}$	0,84	0,7
$p_{1нг}$	0,91	1,12
$p_{2нг}$	7,03	8,44

For the interval of time before the separation of the stages of the rocket the relative coefficient of damping for the first tones of oscillations were determined in the time of the longitudinal dynamic tests and amounted to ξ = = 0.01–0.03.

In the flight time of the Atlas rocket in the last few seconds before separation of the stages, longitudinal instability arises by the first tone of oscillations of the body, but the amplitude of oscillations does not reach a substantial quantity [9].

In Fig. 6.23 are presented the phase-amplitude frequency characteristics of the closed circuit of the injection system of the tanks of the Atlas rocket for the moment of launching the rocket (the place of closing the system is shown by the wavy line in Fig. 6.8). The curve a is the phase-amplitude characteristic of tank injection of the fuel for the disconnected oxidant tank system.

With the change of frequency from zero to plus infinity the curve intersects the real axis once right of the point C(1, i0) clockwise. Since all members of the closed circuit (see Fig. 6.8) are stable, the fuel tank injection system (for the disconnected system of the oxidant tank) will be unstable at a frequency of ~40/sec, which is equal to the first tone of the characteristic oscillations of the rocket.

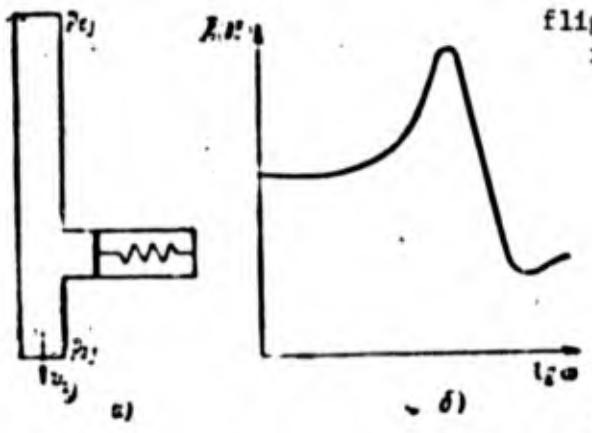

Figure 6.21

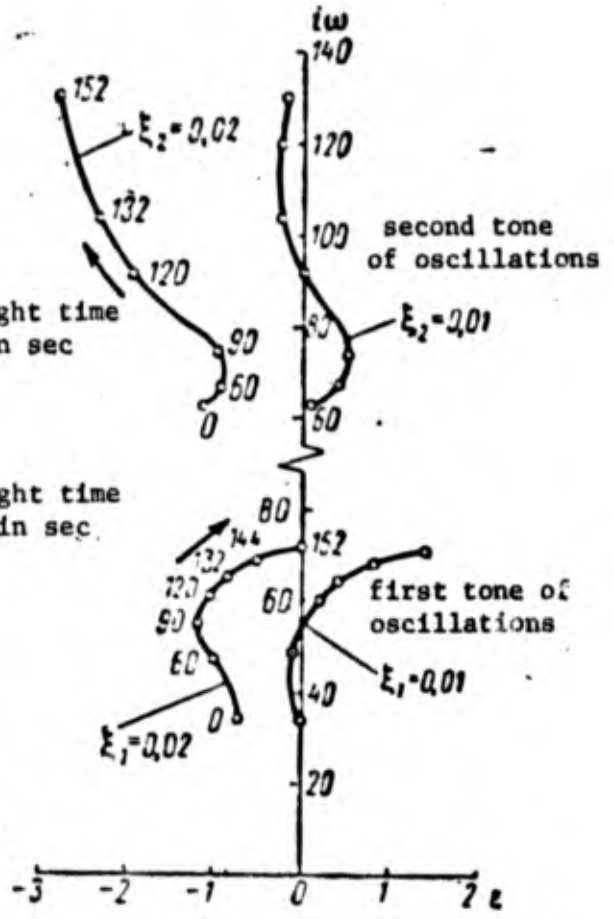

Figure 6.22

Curve b is a frequency characteristic of the closed circuit of the oxidant tank injection system; it is assumed that the fuel tank injection system at this time is not operating. For a change of frequency from zero to plus infinity the curve intersects the real axis right of the point C(1, i0) two times in opposite directions. Therefore the system will be stable.

As noted in work [9], from a simultaneous analysis of the stability of both systems of injection it is established that the system is unstable at a

frequency of approximately 14 per second, and at a frequency of 40 per second, the system is at the limit of stability. The results of analogous calculations for different moments of time after launching showed that the system becomes more stable. The limit of stability is reached in the fifth second, after which the stability of the system increases. This is explained by an increase in the volume of gas levels and a corresponding decrease in the coefficient of amplification of the pressure deviation p_{ft} of the gas in the tank. The results of a calculation confirm the rocket flight test results [9].

Particularly great attention is paid to the study of the dynamic characteristics of the cosmic rocket system Saturn-5/Apollo [8]. The system consists of four stages: S-1, S-2, S-3, S-4, and a lunar exploration module connected to one another successively. In NASA's Langley Research Center for investigating longitudinal oscillations of the Saturn-5 rocket, a dynamic scheme was developed and a physical dynamically similar model of the system was made at a scale of 1:10. For studying the dynamic properties of the rocket construction an elastic mass model was used, the basic construction principles of which are the same as for the model shown in Fig. 3.1. In a one-dimensional mathematical model, the tank is considered as an isotropic one-dimensional shell which is deformed by the action of oscillations of the liquid; the distribution of the liquid pressure in the oscillations process is similar to the hydrostatic distribution. The one-dimensional model has 28 degrees of freedom.

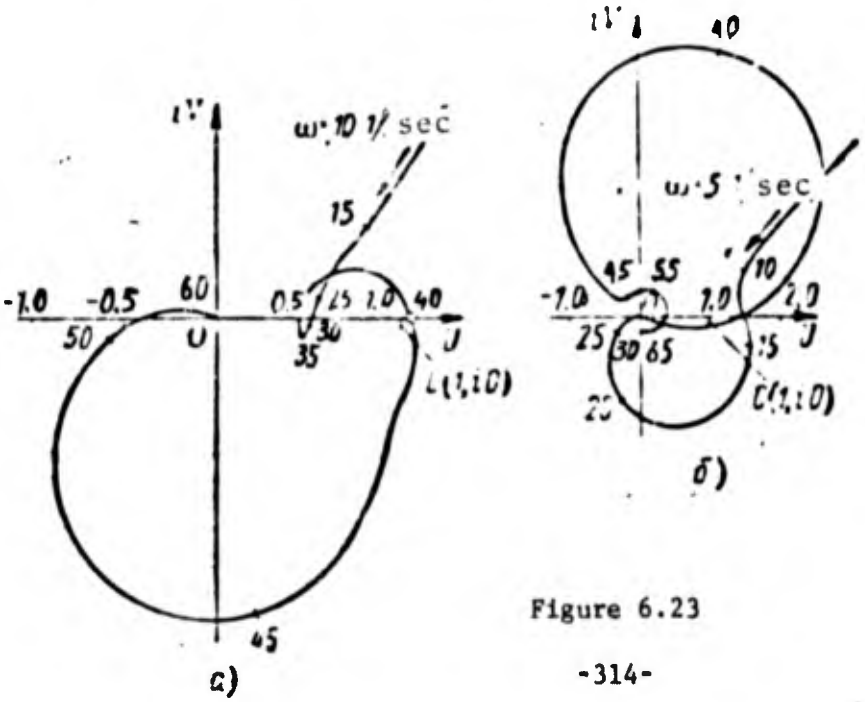

Figure 6.23

In a two-dimensional mathematical model, the theory of orthotropic axi-symmetrical shells is used, taking into account the longitudinal and radial oscillations of the shell and the liquid. The two-dimensional model possesses 75 degrees of freedom. For a solution of the system of differential equations the Rayleigh-Ritz method is used, in which the mixing function is taken in the form of stepped series.

The force construction of the physical dynamically similar model of the system in basic outline is an exact geometrically similar copy of the actual structure. The length of the model is approximately 11 meters, the diameter of the first stage is approximately 1 meter. The elements of the structure situated above the transition of the lunar expedition module cone are geometrically similar to the prototype, but differ in respect to construction and the use of materials. The model of the lunar expedition module is similar only by the mass, the position of the center of mass, inertia, and suspension. For an imitation of the fuel in the S-1 stage and the liquid oxygen in all stages, water was used. For imitating the liquid hydrogen in the S-2 and S-4 stages, foam plastic beads were used, having a density of approximately 60 kg/m^3. The pressure of all tanks was accomplished by nitrogen at a pressure of 0.7 atmospheres.

For the test the physical model was suspended with a specially constructed system consisting of four symmetrically arranged tables attached above to a rigid supporting girder. The length and the diameter of the cables was selected so that the frequency of the oscillations of the rocket model as a solid body would be less than the frequency of the first tone of this elastic oscillation. The perturbation of the physical model was conducted through a dynamometer and the pivots of the central motor. The dynamometer was used a sensitive element in the servosystem with electrodynamic vibrators for supporting the indicated amount of perturbation.

In Table 6.2 are presented frequencies ω per second of the characteristic oscillations of the Saturn-5 rocket, calculated for one-dimensional and two-dimensional mathematical models and also the experimental data obtained on the dynamically similar physical model of the scale 1:10. The calculated and

experimental data correspond to the starting moment of the rocket and the moment of complete fuel combustion in the S-1 stage.

Table 6.2

Tone of Oscillations	Start			Complete Fuel Combustion		
	Experimental data of the physical model	Calculated data of the mathematical model		Experimental data of the physical model	Calculated data of the mathematical model	
		1-dimen.	2-dimen.		1-dimen.	2-dimen.
First	30.9	37.5	31.4	51.1	54.5	56.1
Second	40.2	39.3	40.7	69.5	71.1	72.0
Third	56.4	56.4	59.1	-	74.1	75.8
Fourth	71.3	71.1	74.0			

In Fig. 6.24 are presented for comparison the forms f_n of the characteristic oscillations of the first four tones, corresponding to the starting moment of the rocket. The results of calculations for the one-dimensional model are shown by the solid lines and the darkened spots; and the results of calculations of the two-dimensional model are shown by the broken lines. The darkened spots show the value of the forms of the characteristic oscillations of the center of mass of liquid in the tank. The experimental data are presented in the light circles showing the values of the forms od the characteristic oscillations of the separate points of the longitudinal axis of the rocket body.

Basically, a good coincidence was obtained of experimental and calculated data for the one-dimensional mathematical model. An exception was the first tone of oscillations in the starting condition, when the motion of the liquid mass in the oxidant tank of the first stage went out of phase with the body. Calculations of the two-dimensional mathematical model produced for this condition a good coincidence with experimental data.

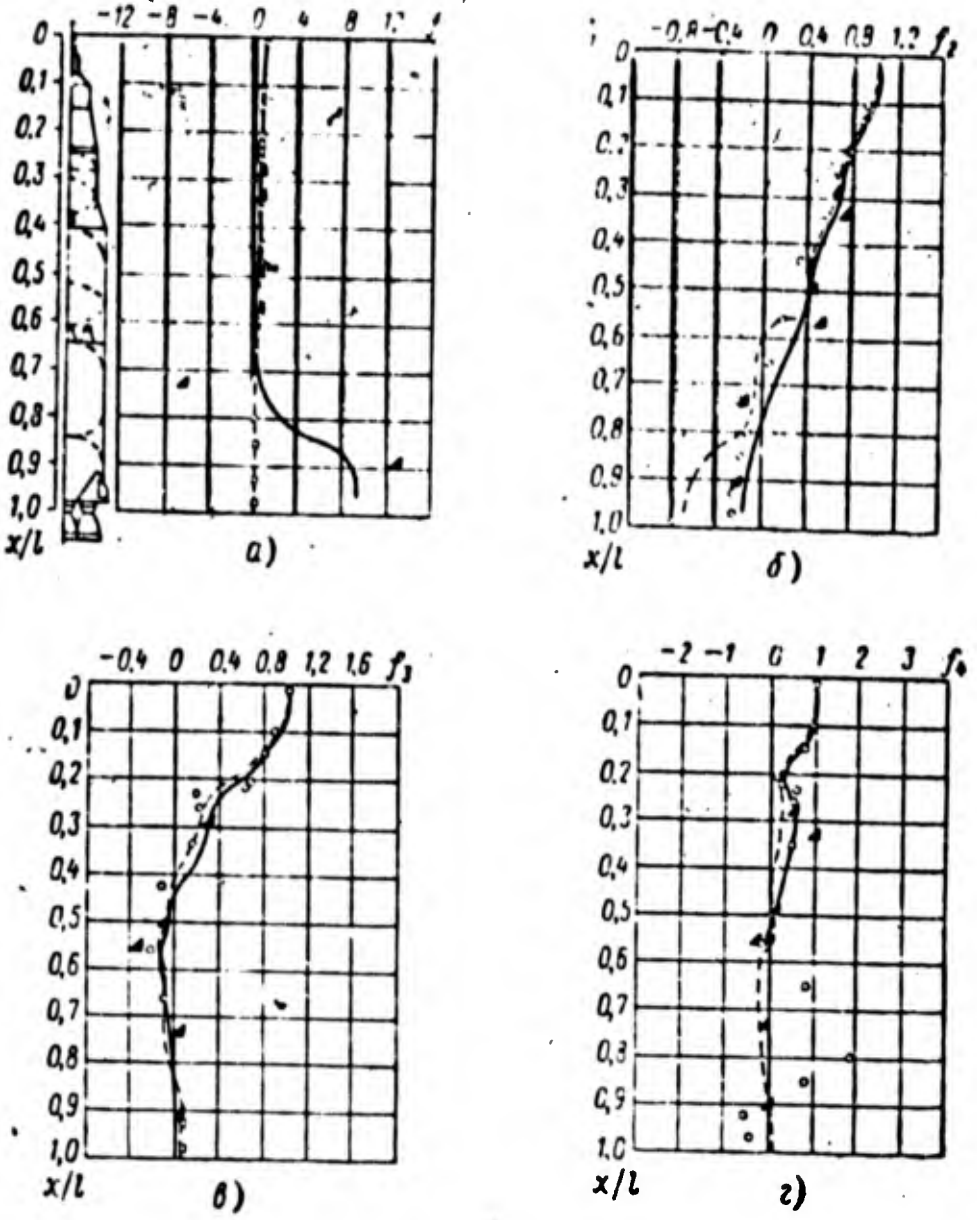
-12 -8 -4 0 4 8
0 0,1 0,2 0,3 0,4 0,5 0,6 0,7 0,8 0,9 1,0
x/l
а)
-0,8 -0,4 0 0,4 0,8 1,2
0 0,1 0,2 0,3 0,4 0,5 0,6 0,7 0,8 0,9 1,0
x/l
б)
-0,4 0 0,4 0,8 1,2 1,6
0 0,1 0,2 0,3 0,4 0,5 0,6 0,7 0,8 0,9 1,0
x/l
в)
-2 -1 0 1 2 3
0 0,1 0,2 0,3 0,4 0,5 0,6 0,7 0,8 0,9 1,0
x/l
г)

Figure 6.24

References

1. Гор, Кэррол. Динамика регулируемого двухкомпонентного жидкостного ракетного двигателя с насосной системой подачи. — «Вопросы ракетной техники», 1957, № 5.

2. Колесников К. С. Низкочастотная неустойчивость номинального режима жидкостного ракетного двигателя. — ПМТФ, М., «Наука», 1965, № 2.

3. Крегер, Бекхэм. Моделирование динамики ракеты на огневом стенде. — «Вопросы ракетной техники», 1966, № 8.

4. Крокко Л., Чжень Синь-И. Теория неустойчивости горения в жидкостных ракетных двигателях. М., ИЛ, 1958.

5. Маккена, Уолкер, Виньe. Совместные колебания двигателя и конструкции ракеты на жидком топливе. — «Вопросы ракетной техники, 1966, № 1.

6. Мошкин Е. К. Динамические процессы в ЖРД. М., «Машиностроение», 1964.

7. Натанзон М. С. Влияние собственной частоты колебаний жидкости в топливоподающем тракте на продольную устойчивость корпуса ракеты. Изв. АН СССР, Энергетика и транспорт, 1969, № 3.

8. Пинсон, Монард, Рейни. Исследование продольных колебаний ракеты-носителя «Сатурн-5». — «Вопросы ракетной техники», 1968, № 5.

9. Роуз. Анализ продольной устойчивости ракет на жидком топливе. — «Вопросы ракетной техники», 1967, № 5.

10. Стенн. Влияние акустического давления и скорости на низкочастотную неустойчивость. — «Ракетная техника и космонавтика». 1967, № 5.

11. Iwanicki L. R., Fontaine R. J., Sensitivity of Rocket Engine Stability to Prapellant Feed Systems Dynamics. AIAA Paper, No. 558, 1965.

12. Makkena K. J., Walker J. H., Winje R. A., A Model for Studying the Coupled Engine-Airframe Longitudinal Instability of Liquid Rocket Systems, AIAA, Aerospace Sci. Meeting, January, 1964.

13. Radovcich N. A., Analytical Model for Missile Axial Oscillation Caused by Engine-Structure Coupling, AIAA Unmanned Spacecraft Meeting, Los Angeles, 1965.

14. Rubin Sh., Longitudinal Instability of Liquid Rockets Due to Propulsion Feedback (POGO), AIAA Paper, No. 65—223, 1965.

DISTRIBUTION LIST

Organization		Nr Cys
AIR FORCE		
E053	AF/INAKA	1
E017	AF/RDGC - AFSC	1
E018	AF/RDGC - SAMSO	1
E404	AEDC	1
E408	AFWL	1
E410	ADTC	1
E413	ESD	2
E427	RADC	1
E429	SAMSO	1
	FTD	
	CCN	1
	NIA/PHS	2
	NIIR	15
	NIT	1
	PDT/PHE	15
	PDYA	3
	LNA	1
	PDSE/McAllister	2
	PDTA/Kaminski	1
	GALE/Purdue	1

Organization		Nr Cys
DISTRIBUTION DIRECT TO RECIPIENTS		
	DDC	12
A205	DMATC	1
A210	DMAAC	2
B344	DIA/DS-4C	5
C043	SURG GEN	1
C509	BALLISTIC RES LABS	1
C513	PICATINNY ARSENAL	1
C523	HARRY DIAMOND LAB	1
C535	AVIATION SYS COMD	1
C557	USAIIC	1
C591	FSTC	7
C619	MIA REDSTONE	1
D008	NISC	1
D217	NAVWPNSCEN	1
D220	ONR	1
H300	USAICE (USAREUR)	1
P005	AFC	2
P055	CIA/CRS/ADD/SD	5
R085	NASA (ATCS-T)	1
	OTHER GOVERNMENT AGENCIES	
	FAA	1